



UNIVERSITY OF SASSARI

LIFE SCIENCES AND BIOTECHNOLOGIES

Director: Prof. Leonardo Sechi

**PARKINSON'S DISEASE AND VESICULAR
TRAFFICKING: FROM MOLECULAR PATHOLOGICAL
MECHANISM TO A THERAPEUTIC OPTION**

PHD STUDENT:

Milena Fais

TUTOR:

Prof.Ciro Iaccarino

INDEX

1. INTRODUCTION.....	3
1.1 PARKINSON'S DISEASE.....	4
1.2 TREATMENTS	6
<i>Levodopa</i>	<i>6</i>
<i>COMT Inhibitors</i>	<i>8</i>
<i>MAO-B Inhibitors.....</i>	<i>8</i>
<i>DA Receptor Agonists.....</i>	<i>8</i>
<i>Anticholinergics.....</i>	<i>8</i>
<i>Amantadine.....</i>	<i>9</i>
<i>Cannabis</i>	<i>9</i>
1.3 ETIOLOGY	10
1.3.1 ENVIRONMENTAL FACTORS	10
1.3.2 GENETIC FACTORS.....	12
<i>α-Synuclein: SNCA (PARK1-PARK4)</i>	<i>12</i>
<i>PARKIN (PARK2)</i>	<i>16</i>
<i>Ubiquitin carboxyl-terminal esterase L1: UCHL-1 (PARK5).....</i>	<i>16</i>
<i>PTEN-induced kinase 1: PINK-1 (PARK6)</i>	<i>17</i>
<i>DJ-1 (PARK7).....</i>	<i>17</i>
<i>Leucine Rich Repeat kinase 2: LRRK2 (PARK8)</i>	<i>18</i>
1.4 EXOCYST COMPLEX	24
1.5 LRRK2, VESICULAR DYNAMICS AND RECEPTOR TRAFFICKING.....	27
1.6 SINAPTIC VESICLE GLYCOPROTEIN 2A (SV2A)	30
1.7 LEVETIRACETAM (LEV)	31
2. RESULTS.....	34
2.1.....	35
RESULT 1: GENERATION OF STABLE CELL LINES EXPRESSING THE GFP REPORTER UNDER THE CONTROL OF STRESS INDUCIBLE PROMOTERS.	35
Materials and Methods	40
2.2.....	42
RESULT 2: LEVETIRACETAM TREATMENT AMELIORATES LRRK2 PATHOLOGICAL MUTANT PHENOTYPE	42
2.3.....	45

RESULT 3: LRRK2 MODULATES THE EXOCYST COMPLEX ASSEMBLY BY INTERACTING WITH SEC8	45
2.4	48
RESULT 4: PARKINSON'S DISEASE-RELATED GENES AND LIPIDE ALTERATION	48
3. CONCLUSIONS	51
4. REFERENCES	57

1. INTRODUCTION

1.1 PARKINSON'S DISEASE

Parkinson's disease (PD) is the second most common neurological disorder described for the first time in the 1817 by James Parkinson in "An essay on the on the shaking palsy". PD is mainly characterized by death of dopaminergic neurons in the Substantia Nigra pars compacta (SNpc) which neurons form the nigrostriatal pathway, this results in a decrease in dopamine levels¹.

The cell bodies of nigrostriatal neurons located in the SNpc, project primarily to the putamen and normally contain substantial amounts of neuro-melani. Loss of these neurons produces the classic gross neuropathological finding of SNpc depigmentation. At the onset of PD symptomatology, roughly 80% of DA in the putamen is depleted, and 60% of SNpc dopaminergic neurons have already been lost. Mesolimbic dopaminergic neurons, whose cell bodies reside adjacent to the SNpc in the Ventral Tegmental Area (VTA), are much less affected in PD. The two primary efferent fiber projections of the VTA are the mesocortical and the mesolimbic pathways, which correspond to the prefrontal cortex and nucleus accumbens respectively and consequently there is significantly less DA depletion in these neurons¹. (Figure 1)

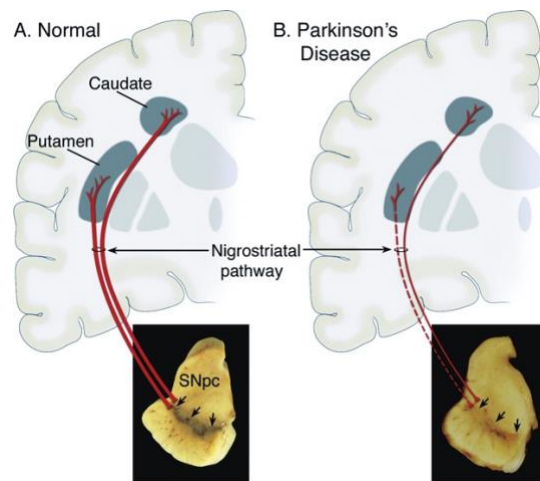


Figure 1: Schematic representation of the differences between the normal nigrostriatal pathway (A) and in Parkinson's disease (B)

The trend of PD incidence is increasing. Some studies have shown a 118% increase in cases from 1990 to 2015, counting about 6.2 million affected people, and it is estimated that around 2040 this number will increase to 12 million, mainly due to fact that the disease is clearly related to the increase in longevity.²

Aging is the first risk factor for the disease development, and, in fact, with advancing age, the prevalence of PD increases tenfold between the ages of 50 and 80³.

PD is usually associated with a Lewy bodies, cytoplasmic inclusions formed by alpha-synuclein and lipid aggregates which together with motor symptoms suggest the final diagnosis of the disease⁴.

Bradykinesia, muscular rigidity, dystonia, resting tremor or postural instability are the first requisite for the diagnosis⁵. Usually, before motor symptoms, are present non-motor symptoms like disturbances in autonomic function, sensory symptoms, sleep, cognitive and psychiatric disturbances⁴.

1.2 TREATMENTS

Currently, targeted surgical therapies such as gene therapy, neural transplantation, and nanotechnology are very promising, but need further consideration of safety and efficacy in animal models before moving into clinical trials. However, the surgical treatment called DBS (Deep Brain Stimulation) provides a significant improvement in the motor symptoms of Parkinson's disease and relief from the motor complications of pharmacological treatments⁶.

Pharmacologic treatments with regard to Parkinson's disease target motor symptoms only. These primarily include dopaminergic and non-dopaminergic therapies. Dopaminergic drugs, used for decades, now include levodopa or levodopa plus, catechol-O-methyl transferase (COMT) inhibitors, dopa-decarboxylase inhibitors (DDC-I), monoamine oxidase type B (MAO-B) inhibitors, and DA agonists and non-dopaminergic drugs.

Levodopa

DA is synthesized from L-3,4-dihydroxyphenylalanine (L-dopa) resulting from the hydroxylation of tyrosine. This pathway leads to the synthesis of DA in its first stage and finally to the synthesis of other catecholamines, such as norepinephrine and adrenaline, by the action of L-amino acid aromatic decarboxylase⁷.

In 1970, after several studies, the US Food and Drug Administration approved Levodopa as a treatment for PD⁷.

Levodopa is the most potent drug for the treatment of motor symptoms of PD. Levodopa is actively absorbed in the proximal small intestine

where it is metabolized by L-amino acid aromatic decarboxylase (AADC), for this reason the treatment is combined with an AADC inhibitor such as carbidopa⁸.

However, there is about a 40% chance of developing motor complications after about 6 years of levodopa treatment⁹.

Pulsatile stimulation, because of the short half-life and rapid catabolism of DA, leads to intermittent delivery to dopamine receptors¹⁰.

Formulation of levodopa and DDC-I (benserazide and carbidopa are currently used) may reduce peripheral levodopa degradation and consequently DAergic side effects¹¹.

Several new levodopa formulations, such as IPX066, have been developed to optimize the plasma concentration of Levodopa, most of which are able to reduce the withdrawal time and frequency of levodopa use, or increase the time of intake without troublesome dyskinesias¹².

Several methods of administration such as continuous intestinal and subcutaneous infusion and inhalable formulation are currently being developed¹².

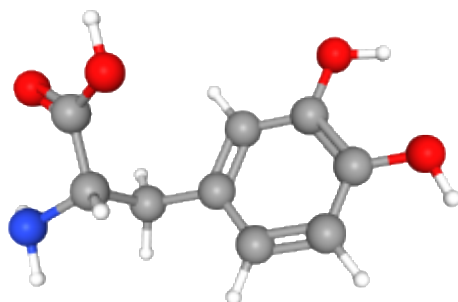


Figure 2: Levodopa 3D structure (<https://pubchem.ncbi.nlm.nih.gov/compound/6047>)

COMT Inhibitors

COMT is an enzyme involved in the peripheral metabolism of levodopa. Its inhibitors are always used in triple combination with levodopa and carbidopa. Entacapone may lead to improved motility; Stalevo[®], a tablet consisting of LD/CD and entacapone, may provide a more stable plasma level of levodopa and persistent stimulation of DA receptors in the striatum; Nebicapone, a COMT inhibitor apparently more effective than entacapone, is in phase 3 clinical trials¹².

MAO-B Inhibitors

MAO-B are essential in DA metabolism in the brain, in fact it can be used as monotherapy especially in the early stage of the disease or in combination with levodopa. Selegiline, the first MAO-B inhibitor used in PD, has been shown to delay the need for levodopa treatment by slowing the progression of PD¹³.

DA Receptor Agonists

DA receptor agonists are commonly used drugs for PD but cause many adverse effects that include hypotension, hallucinations, nausea, vomiting, compulsive shopping, compulsive shopping, and hypersexuality¹⁴.

Anticholinergics

Anticholinergic drugs such as trihexyphenidyl, benztropine are often used in the treatment of tremors although the clinical use of

anticholinergics is limited due to the obvious adverse effects, which far outweigh even the therapeutic benefits¹².

Amantadine

Amantadine, developed as an antiviral drug, it was discovered by accident that is capable of improving parkinsonian symptoms, especially balance and gait¹².

Cannabis

Cannabis could be an alternative therapy for PD since in a small controlled study, 30 minutes after smoking cannabis, there was a significant reduction in tremor, bradykinesia and rigidity, but still requires verification through further studies¹⁵.

1.3 ETIOLOGY

Both environmental and genetics factors play a critical role in the pathogenesis of PD.

1.3.1 ENVIRONMENTAL FACTORS

The first evidence for the involvement of external factors in PD development was provided by the parkinsonism induced by the neurotoxin 1-methyl-4-phenyl-1,2,3,6-tetrahydropyridine (MPTP)¹⁶. The toxin is capable of triggering metabolic reactions that culminate in the neuronal death¹⁷.

The structure of MPTP is similar to that of meperidine produced as a byproduct in the process of 1-methyl-4-phenyl-propionoxy-piperidine synthesis. In vivo experiments show that once this toxin is injected it is capable of crossing the blood-brain barrier (BBB) and reaching the central nervous system (CNS) probably due to its lipophilicity. In the CNS, the enzyme monoamine oxidase type B (MAO-B) secreted by astrocytes converts MPTP to 1-methyl-4-phenyl-2,3-dihydropyridine, an intermediate metabolite, and subsequently to 1-methyl-4-phenylpyridinium (MPP⁺), the final toxic metabolite. MPP⁺ which is the active neurotoxin is a polar compound and as such cannot cross the BBB, indicating that it acts at the cellular level.

MPP⁺ selectively enters noradrenergic (NE) and dopaminergic (DA) neurons by transporters, NE transporter and DA transporter (DAT), respectively. In the NE/DA nerve cell, MPP⁺ is able to form a complex with neuromelanin in the axoplasm that is transported by the vesicular monoamine transporter type 2 (VMAT-2) and stored in synaptosomal

vesicles. MPP⁺ accumulates in synaptosomal vesicles to the point where cell death of nigrostriatal DA neurons occurs in the SNpc and striatum¹⁸. MPP⁺ is also capable of inhibiting respiratory chain complex 1 in mitochondria by inducing a decrease in the expression of anti-apoptotic proteins, such as Bcl2. Stabilization of the electron transport chain and blockage of ATP synthesis increases the production of reactive oxygen species (ROS) leading to the opening of mitochondrial transition pores. As a result, cytochrome C is released from the mitochondrion and forms a complex with pro-caspase-9 and apoptosis protease activation factor-1. The formed complex activates caspase-9 and downstream caspases resulting in apoptosis and ultimately nigrostriatal DA cell death in the SNpc and striatum¹⁸.

Epidemiological studies on the relationship between PD, rural life and farm works have suggested the importance of pesticides as a significant cause of the disease¹⁹. Paraquat, Rotenone and several dithiocarbamates and organochlorines exposure, active or passive, are associated with manifestation of the disease²⁰.

Rotenone is an organic molecule originally thought to be non-toxic to humans but now, it is well established that it is a mitochondrial toxin able to inhibit Complex I of the electron transport chain²¹ causing neurodegeneration of dopaminergic neurons²².

Exposure to Paraquat herbicide causes an increase of alpha-synuclein level in mice and aggregate formation²³. Moreover, mice treated with injections of Paraquat shown a loss of dopaminergic neurons in SNpc, strongly supporting the conclusion that Paraquat induces the dopaminergic degeneration typically observed in PD²⁴.

Interestingly, Rotenone and Paraquat molecules have a chemical structure similar to MPTP²⁵.

Recent studies are focusing on a new class of household pesticides like Pyrethroids. Preliminary results suggest that Pyrethroids are capable of increasing dopamine transporter-mediated uptake²⁶ thus causing indirect apoptosis of dopaminergic cells²⁷.

1.3.2 GENETIC FACTORS

Until 1997, PD was considered a disease purely caused by environmental factors; while the discovery of mutation in SNCA, encoding alpha-synuclein, allowed to highlight heritable components²⁸. After that many other genes are identified to be cause of PD²⁹.

Among them, mutations in SNCA and LRRK2 are associated at autosomal dominant forms of PD while PARKIN, PINK1 and DJ1 mutations are typical of autosomal recessive forms²⁹.

α-Synuclein: SNCA (PARK1-PARK4)

SNCA gene has been mapped in 4q21- q22 region³⁰ and encodes at least four different α -synuclein isoforms through alternative splicing Isoforms. The isoforms composed of fewer amino acids have a higher aggregation potential leading to the formation of amyloid fibrils³¹.

In 1997 Polymeropoulos et al. identified, through linkage analysis in an Italian family and three Greek families, the A53T point mutation implicated in the disease.³²

In the same year Spillantini et al. discovered that Lewy bodies, characteristic of PD, are mainly composed of α -synuclein aggregates. In particular, they stained tissue sections of the Substantia Nigra with a

specific serum against α -synuclein and they obtained a strong staining in Lewy bodies demonstrating the high content of α -synuclein³³.

Following this discovery, two further point mutations, A30P and E46K, were identified, as well as duplications and triplications of the SNCA gene although these mutations are rare in familial forms of autosomal dominant PD³⁴.

Currently several mutations in SNCA such as A18T, A29S, A30P, A30G, E46K, G51D, H50Q, A53E, A53T, and A53V have been linked to familial parkinsonism in addition to triplication and duplication of the SNCA gene locus. Triplication and duplication are of particular interest since strongly demonstrate that overexpression of α -synuclein alone can lead to disease³⁵.

Moreover, post-transcriptional mechanisms acting on SNCA transcripts, such as the use of alternative start sites and variable UTR lengths are associated with PD³⁵.

α -synuclein is a protein (14kD) expressed at presynaptic terminals in the brain and it is characterized by a lysine-rich amphipathic amino terminal, an acidic carboxylic terminal, and a central region that contains a highly hydrophobic motif including amino acid residues (NAC domain)³⁶.

The frequent form of α -synuclein is thought to be monomeric and is found in the cytoplasm of neuronal cells, whereas under pathological conditions α -synuclein is thought to form oligomers. Spontaneous conversion of soluble unfolded α -synuclein monomers into aggregates leads to accumulation of α -syn in neurons³⁵. Although α -synuclein physiological function is still cryptic, α -synuclein seems to play a critical role of modulating neuronal stability by acting on presynaptic signaling and vesicular trafficking³⁷. The physiological role of α -synuclein seems

related to lipid and membrane proteins interactions to regulate synaptic plasticity and neurotransmitter release.

The most important partners of α -syn, are the soluble N-ethylmaleimide-sensitive factor (NSF) receptor attachment proteins (SNAREs), which represent the most important mediators in vesicle trafficking and membrane fusion. Cooperation between α -syn proteins and SNAREs allows careful regulation of synaptic plasticity and neurotransmitter release³⁵.

α -syn helps stabilize the SNARE complex, which mediates SV fusion with the presynaptic plasma membrane (PM) during neurotransmission, by binding directly to the N-terminal domain of VAMP2 through a short sequence in its C-terminal domain (residues 96-100). The SNARE complex is composed of the target-SNARE (t-SNARE) Syntaxin-1 and SNAP25 (synaptosome associated protein-25) located on the PM and the vesicular-SNARE (v-SNARE) synaptobrevin2/VAMP2 located in membrane vesicles³⁵.

Many studies have reported that α -synuclein within LBs undergoes several posttranslational modifications, including phosphorylation, cross-linking, ubiquitination, nitration, and truncation; it is very likely that these modifications play an important role in regulating α -synuclein aggregation and toxicity in vivo. Phosphorylation at residue S129 (pS129) and its possible implication on α -synuclein-induced neurodegeneration are of particular interest. Indeed, while a large accumulation of pS129 has been observed in the brains of patients with synucleinopathies, under normal conditions only a small fraction of α -synuclein is constitutively phosphorylated at S129 in the brain. These results support the hypothesis that phosphorylation at S129 could play an important role

in the control of normal α -synuclein functions, as well as neurotoxicity, regulating its aggregation, and LB formation.³⁸

A substantial portion of α -synuclein in cells is associated with the mitochondrial and synaptic vesicles membrane and it is subject to phosphorylation by membrane-associated kinases, the G protein-coupled receptor kinases (GRKs). A crucial role of membrane-associated α -synuclein phosphorylation is the regulation of neurotransmitter uptake, particularly dopamine³⁸. Recently, overexpression of Polo-like kinase 2 (PLK2), the major kinase responsible for α -synuclein phosphorylation in the brain, has been shown to increase α -synuclein turnover through the autophagic degradation pathway, a cellular process unique to the synuclein (α - and β -synuclein). The PLK2-mediated clearance of α -synuclein represents a new opportunity for the development of therapeutic strategies for the treatment of PD that aim to reduce, specifically, toxic levels of α -synuclein³⁸.

Further studies showed that the unphosphorylated α -synuclein peptide interacts primarily with proteins related to mitochondrial electron transport whereas the phosphorylated peptide has more affinity for some cytoskeletal proteins and presynaptic proteins implicated in synapse transmission and vesicle trafficking³⁸. The C-terminal region of α -synuclein has been shown to be involved in the interaction with the Rab GTPase (Rab8a), a small guanine nucleotide-binding protein implicated in the coordination of vesicle trafficking³⁸. Phosphorylation at S129 promotes α -synuclein binding to Rab8a and modulates Rab8a-mediated α -synuclein toxicity. These observations suggest that pS129 might serve as a molecular switch to control the interaction of α -synuclein with different protein partners and thereby modulate its functions³⁸.

PARKIN (PARK2)

Parkin is a large gene in the human genome, mapping 1.38Mb and composed in 12 exons³⁹. Parkin gene is organized in an N-terminal ubiquitin like domain (Ub1), and four zinc-coordinating RING like domains (RING0, RING1, IBR, RING2)⁴⁰.

Mutations in parkin gene are one of the genetic causes of autosomal recessive early onset PD⁴¹.

Parkin is widely expressed throughout the brain and has multiple neuroprotective functions, such as maintaining of the ubiquitin-proteasome system and mitochondrial metabolism⁴². Indeed, parkin plays an essential role in ubiquitin-mediated degradation of misfolded or damaged proteins and removal of dysfunctional mitochondria through mitophagy⁴².

Parkin functions as an E3-ubiquitin ligase that is involved in monoubiquitylation and multiple monoubiquitylation as well as polubiquitylation⁴².

Ubiquitin carboxyl-terminal esterase L1: UCHL-1 (PARK5)

UCHL1 (PARK5) stands for ubiquitin carboxy-terminal hydrolyase L1 that already suggests a function of the protein. The I93M mutation in this gene has been identified in PD affected members of a single family of German origin. Whether UCHL1 is indeed a causative or susceptibility gene is still unclear. Remarkably, loss of UCHL1 function leads to neurodegeneration in mice⁴³.

UCHL-1 is an enzyme present at high levels in the brain and its function could be related to the recycling of polymeric ubiquitin and its conversion into monomeric units. Mutations in the PARK5 gene causes a reduction

in the enzymatic activity of UCHL-1 causing an alteration in proteasome activity⁴⁴.

PTEN-induced kinase 1: PINK-1 (PARK6)

PINK-1 is a 581 amino acid ubiquitous protein and most of the mutations identified are located in the kinase domain, pointing the importance of PINK1 enzymatic activity in the pathogenesis of PD⁴⁵.

PINK1 is a Ser/Thr protein kinase localized at mitochondrial level. PINK1 has been identified as a ubiquitin kinase that activates Parkin in response to mitochondrial dysfunction.

Studies in drosophila with PINK1 or Parkin deficiency have shown a very similar phenotype: they present morphological abnormalities of mitochondria in muscle and gonadal cells and muscle degeneration. These observations indicate that Parkin and PINK1 may be on the same mitochondrial signaling pathway⁴⁶.

Furthermore, it has been shown that the mutant phenotype of PINK1-deficient drosophila can be rescued by Parkin overexpression demonstrating that Parkin acts downstream of PINK1. The PINK1-Parkin axis is linked to early-onset PD, as demonstrated by its discovery through disease-causing mutations. Nevertheless, it remains unclear whether it is involved in sporadic PD⁴⁶.

DJ-1 (PARK7)

The DJ-1 gene contains eight exons on chromosome 1p36 and encodes for a 189-amino acid protein, spans 24 Kb, and is conserved and ubiquitously expressed. Normally, the wild-type DJ1 protein is a homodimer, is distributed intracellularly between nucleus or cytoplasm,

and can increase in response to endogenously produced reactive oxygen species (ROS), most probably through activation of nicotinamide adenine dinucleotide phosphate (NADPH) oxidase⁴⁷. In fact, the oxidative modification of Cys106 of DJ1 has been suggested to allow DJ-1 to act as a sensor of cellular redox homeostasis and to participate in cytoprotective signaling pathways in the cell. All these results support the idea that oxidative stress is an essential factor in PD pathogenesis⁴⁷.

Leucine Rich Repeat kinase 2: LRRK2 (PARK8)

The PARK8 locus was first identified in a large Japanese family affected by autosomal dominant parkinsonism. Subsequent studies showed that the original family had a mutation in the leucine-rich repeat kinase 2 (LRRK2) gene^{48,49,50}.

Shortly thereafter, mutations in LRRK2 gene were found to have a significant impact in familial and sporadic PD, and hundreds of nonsense or missense genetic variations in the LRRK2 locus have been identified⁴⁹. Approximately 100 mutations in this gene have been discovered, but only six have been strongly associated with the disease: G2019S, R1441C/G/H, Y1699C, and I2020T⁵¹ (Figure 3).

G2019S and R1441C are the prevalent mutations and are responsible for up to ~30% of inherited PD cases in certain populations, and up to 2.5-10% of sporadic PD cases, respectively⁴⁸.

The penetrance range of the G2019S mutation increases from 17% at age 50 years to 85% at age 70 years while the R1441C mutation has been shown to have lower penetrance⁴⁸.

LRRK2 is a 286-kDa protein composed of seven sequential domains: armadillo repeat motif (ARM), ankyrin repeat (ANK), leucine-rich repeat

(LRR), ras-of-complex (ROC), C-terminal of ROC (COR), kinase (KIN), and WD40 domains.³⁹

The Armadillo repeat motif (ARM) domain is organized in 3 α -helices and is composed by a repeated 42 amino acids. The armadillo domain is an actor for several protein interactions⁵³.

The ankyrin repeat (ANK) domain is composed of seven ankyrin repeats, each of which forms two antiparallel helices followed by a beta hairpin loop, which stack together to form a curved structure in the ankyrin repeat domain. Ankyrin repeats are found in both eukaryotic proteins and bacterial, including transcription factor cytoskeletal proteins, signaling proteins, and cell cycle regulators⁵⁴.

Thirteen LRRs were identified in LRRK2 that form a β -strand followed by an α -helix. The helices align side by side to form an arc structure classified as an LRR domain. LRR domains can interact with different proteins through binding to their extended solvent-accessible surface⁵⁵.

The WD40 domain of LRRK2 is composed of seven WD40 repeats. It is possible that the seven-bladed helix forms a rigid structure useful for reversible interaction with proteins. WD40 domains are common in proteins that have different functions, including the G β subunit of heterotrimeric G proteins, protein phosphatase subunits, cytoskeletal assembly proteins transcriptional regulators, RNA processing complexes, and proteins involved in vesicle formation and trafficking⁵⁵.

Recent studies have shown that the WD40 domain is required both to stabilize the LRRK2 dimer and to modulate the LRRK2 kinase activity but the role of this domain in the physiological and pathological function of LRRK2 has not yet been fully elucidated. Piccoli et al. analyzed protein-protein interactions conferred by the LRRK2 WD40 domain finding that the LRRK2 WD40 domain is able to bind to synaptic vesicles (SVs)

contributing to the accumulation of evidence suggesting that LRRK2 serves as a scaffold protein linking vesicle trafficking and the cytoskeleton⁵⁶.

Although progress has been made in elucidating the structure of LRRK2 and its bacterial homolog, the ROCO proteins^{57,58} the molecular details regarding domain assembly and their functional roles remain unknown due to the lack of a high-resolution structure of LRRK2 as a whole⁵².

LRRK2 has two distinct enzymatic activities: it is a serine-threonine kinase capable of both autophosphorylating and phosphorylating a select group of heterologous substrates; it performs GTPase activity, which is mediated by the Roc domain⁵⁹.

Disease-associated variants, especially the most common pathogenic variant, LRRK2 G2019S, are located in the central catalytic core of LRRK2 and could lead to increased kinase activity. Furthermore, elevated LRRK2 activity has been found in PD patients with variants related to other disease-related genes or even without known genetic causes, suggesting that LRRK2 contributes to the pathogenesis of PD⁶⁰.

The precise function of LRRK2 is still unknown but the presence of multiple enzymatic domains and protein-protein interaction domains suggests that LRRK2 is involved in several cellular functions. However, several studies of PD-related mutant forms and LRRK2 knock out animals have suggested the involvement of LRRK2 in neurite outgrowth, cytoskeleton maintenance, vesicular trafficking, protein degradation, and the immune system⁶¹.

LRRK2 is a protein that is present in both the cytosol and the plasma membrane in monomeric or dimeric form. It has been shown that the LRRK2 dimer is concentrated in the membrane, whereas the monomer is present in significant amounts in the cytoplasm. The LRRK2 dimer despite

being less abundant is more active than the monomer⁶².

The identification of endogenous substrates of LRRK2 kinase has been intensively studied. After identifying moesin, a cytoskeletal actin-binding protein, as a substrate of LRRK2, it was discovered that LRRK2 may autophosphorylate itself at the S910 and S935 sites and the phosphorylations are essential for the binding of 14-3-3 proteins⁶³

Mapping of the phosphosites by mass spectrometry showed at least 74 phosphorylation sites on the isolated LRRK2 protein, and the phosphorylation sites include a majority of serines (59%), followed by 37% threonines and some tyrosines (4%)⁶⁴.

Experimental data confirm that 60% of LRRK2 phosphorylation sites are autophosphorylation sites while 36% are heterologous. The remaining 4% of sites have been identified as both autophosphorylation and PKA phosphorylation sites (threonine 833, serine 1443, and serine 1444^{65,66,67}).

Observing the distribution of phosphorylated residues throughout the LRRK2 protein, an important phosphorylation cluster can be seen between the ANK and the LRR domain at serines S860, S910, S935, S955, S973, and S976 for the most studied sites. Different findings support the idea that these sites are mainly phosphorylated by kinases other than LRRK2. The importance of heterologous phosphorylation sites for LRRK2 function was reinforced by the findings that 14-3-3 binding to LRRK2 is dependent on S910 and S935 phosphorylation and that LRRK2 phosphorylation levels at heterologous phosphorylation sites influence the subcellular distribution of LRRK2⁶⁴. Up to date, S1292 is considered the main LRRK2 autophosphorylation site and in fact, different studies have evidenced that the inhibition of LRRK2 kinase activity induces both decreased phosphorylation levels at S1292 (directly) and at the

constitutive sites (indirectly).

In addition to autophosphorylation, it was found that LRRK2 also phosphorylates different proteins. For instance, LRRK2 phosphorylates tubulin-associated protein Tau suggesting that LRRK2 might modulate microtubule stability through regulation of Tau phosphorylation. Other proteins such as p53, p53, eIF4E-BP, akt1, endophilinA, and ASK1 have been suggested as LRRK2 kinase substrates, although it remains unclear whether they are physiological substrates or not.

The development of cellular and biochemical assays, specific LRRK2 kinase inhibitors and phospho-substrate-specific antibodies have been very useful to verify LRRK2-mediated phosphorylation of endogenous proteins. Using these approaches, several members of the Rab GTPase family have been identified as likely endogenous LRRK2 kinase substrates⁶⁸.

Rab proteins are part of the superfamily of small Ras-like GTPases and up to date, 66 different Rab genes have been identified in the human genome. They function as molecular switches in the regulation of intracellular membrane trafficking in all eukaryotic cells by alternating between GTP and GDP bound states. The GTP bound conformation is usually considered "active" form that interacts with downstream specific effector proteins⁶⁹.

Rab proteins are stably prenylated on one or two cysteine residues at the C-terminus by geranylgeranyl transferases after binding to REPs (Rab escort proteins). When bound the membrane, Rab proteins are activated by the exchange of GDP for GTP, via guanine nucleotide exchange factors (GEFs). GTP is subsequently hydrolyzed to GDP thus allowing recognition of Rab proteins by a GDP dissociation inhibitor (GDI) that retrieves Rabs from membranes to sequester them in the cytosol⁷⁰.

Each Rab targets an organelle and specifies a transport step along endocytic, exocytic, and recycling pathways as well as crosstalk between these pathways. Interactions with multiple effectors allow Rabs to control membrane budding and transport vesicle formation as well as vesicle movement along the cytoskeleton and membrane fusion in the target compartments. Rab proteins are valuable regulators of signal transduction, cell growth, and differentiation. Altered Rab expression and/or activity have been studied in several diseases including cancer, neurological disorders and diabetes⁷¹.

Rab GTPases were initially discovered in brain tissue but were then found in all eukaryotic cells. Regulation of membrane trafficking processes by Rab GTPases depends on interactions with effector proteins such as coating proteins (COPI, COPII, and clathrin), motor proteins (kinesins and dyneins), tethering complexes (EEA1, Golgins, the exocyst complex, and the HOPS complex), and SNAREs. Especially in neurons, these interactions are required to regulate protein and lipid trafficking for the maintenance of cellular morphology and synaptic function⁷².

Upon activation, LRRK2 phosphorylates its auto-phosphorylation sites and roughly 14 different Rab GTPases: Rab3A/B/C/D, Rab5A/B/C, Rab8A/B, Rab10, Rab12, Rab29, Rab35 and Rab43⁷⁰.

Rab29 functions differently from other Rab proteins because it interacts with the ankyrin (ANK) domain of LRRK2. It allows localization of LRRK2 to the trans-Golgi network or to the lysosome and activates its kinase activity⁶⁸. Moreover, LRRK2 pathogenic mutants Y1699C and R1441G/C that promote GTP binding are more easily recruited to the Golgi and activated by Rab29 than LRRK2 WT. Mutations that prevent LRRK2 from interacting with both Rab29 and GTP inhibit phosphorylation of a group of highly studied biomarker phosphorylation sites (Ser910, Ser935,

Ser955, and Ser973)⁷³

Rab GTPases regulate vesicle trafficking and recent studies suggesting that LRRK2 may be a regulator of such vesicle trafficking. Another vesicle trafficking regulator VPS35 modulates the kinase activity of LRRK2; the PD-associated pathogenic mutation, VPS35 D620N, increases LRRK2-mediated phosphorylation of Rab proteins⁷⁴, suggesting that Rab29 and VPS35 perform an upstream regulatory function of LRRK2 while Rab8/10/12/35 are downstream targets of LRRK2.

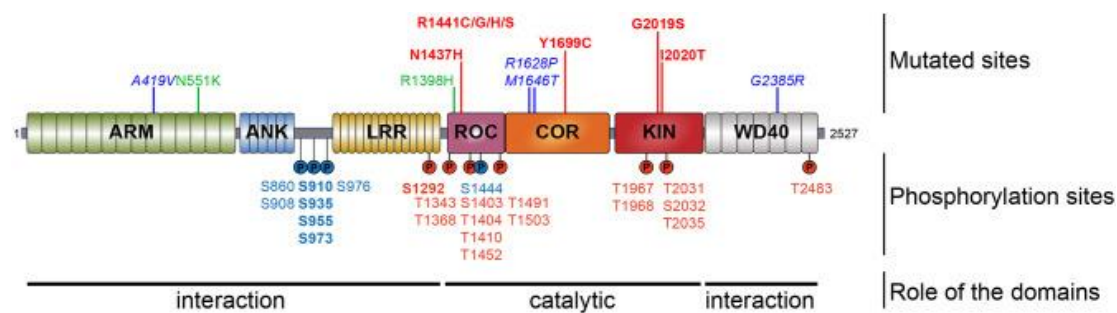


Figure 3: Schematic representation of the domains of LRRK2. Mutations implicated in disease development are shown at the top while phosphorylation sites are indicated at the bottom⁶⁴.

We recently found that LRRK2, particularly the kinase domain, interacts with Sec8, a subunit of the exocyst complex.

1.4 EXOCYST COMPLEX

The exocyst complex is an evolutionarily conserved multisubunit protein complex primarily implicated in binding secretory vesicles to the plasma membrane and it is composed of eight single-copy subunits: Exo70, and Exo84 and Sec3, Sec5, Sec6, Sec8, Sec10, Sec15¹.

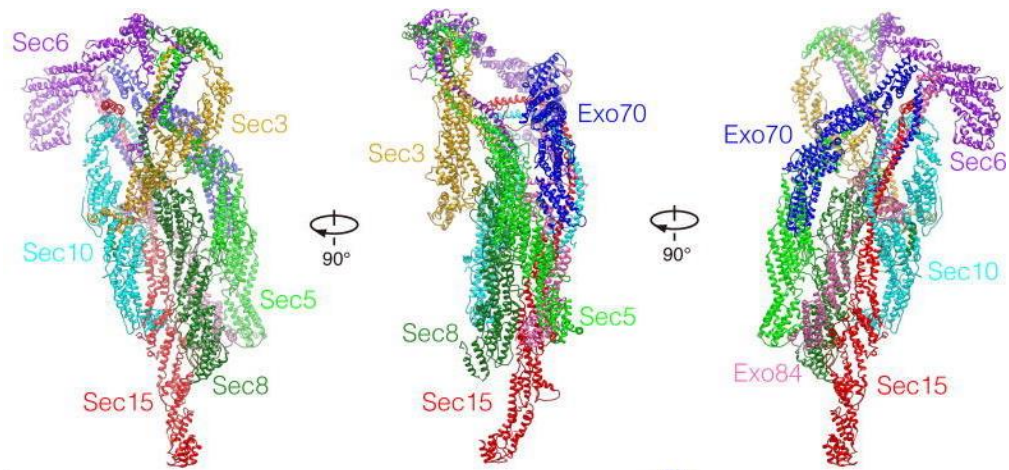


Figure 4: The model of the exocyst complex.⁷⁶

Different studies have shown that several members of the exocyst complex are able to interact with SNARE members or SNARE-interacting proteins and these interactions are thought to precede vesicle priming, a process mediated by SNAREs, t-SNAREs on the plasma membrane and v-SNAREs on the vesicle membrane, to attach vesicles to the target membrane and ultimately to induce lipid fusion⁷⁷.

Because vesicle binding precedes fusion, temporal and spatial control of exocytosis in cells can be accomplished through exocyst regulation. Exocyst subunits have been found to be direct targets of a number of GTPases and kinases, such as Rab, Rho, and Ral⁷⁵.

The first reported interaction between the exocyst and small GTPases was between yeast Sec15 and the exocytic Rab protein Sec4. This interaction could mediate exocyst recruitment to secretory vesicles as well as assembly of the complex. In mammalian cells, however, Sec15 has been shown to interact with Rab11, which is involved in the generation of vesicles from the trans-Golgi network (TGN) or recycling endosomes for subsequent delivery to the plasma membrane⁷⁵.

Although the exocyst complex was first discovered for its primary function in exocytosis, afterwards it has been involved in many biological

processes such as cell migration, primary ciliogenesis, cytokinesis, and autophagy⁷⁵.

Riefler et al. identified sec8 as binding partners of postsynaptic density protein-95 (PSD-95)⁷⁸. PSD-95 plays a crucial role in synapse development, and recent studies suggest that PSD-95 expression enhances excitatory synapse maturation, postsynaptic clustering, and glutamate receptor activity⁷⁸.

PDZ domains of PSD-95 play a role in the localization of PSD-95 and binding partners to neuronal synapses. Sec8, contains a C-terminal consensus sequence for binding to PDZ. Sec8 binds to PDZ1-2 of PSD-95, and this binding can be competitive with a peptide that binds to PDZ1 and PDZ2 at the peptide binding site⁷⁸. Indeed, binding of sec8 may also compete with the cytosolic PSD-95 interacting protein (Cypin) for binding to PSD-95, suggesting that cypin may act to decrease PSD-95 localization by disrupting the sec8/PSD-95 interaction⁷⁸.

In addition to their role in anchoring and regulating receptors at synapses, PDZ proteins are also involved in early events of receptor protein assembly, processing and delivery⁷⁹.

The exocyst is thought to direct intracellular membrane vesicles to their fusion sites with the plasma membrane, and exocyst proteins are often concentrated at sites of rapid membrane addition, such as the growth cone of a neuron⁷⁹.

SAP102, a member of the membrane-associated guanylate kinase (MAGUK) family of PDZ proteins, has a wider and more abundant distribution in the cytoplasm than PSD-95. SAP102 may interact with NMDARs during delivery to synapses and function as the preferred partner of NMDARs at immature synapses, whereas PSD-95 may be the preferred partner at mature synapses⁷⁹.

Sec8 is capable of binding directly to the PDZ domain of MAGUK proteins and forming a complex containing NMDAR (N-methyl -D-aspartate receptors)⁷⁹.

Despite its importance in exocytosis, the molecular mechanisms elucidating the role of the exocyst in exocytosis are still largely unknown. Chernyshova et al. demonstrate that exo70 and sec8 subunits of the exocyst complex associate with the intracellular domain of NCAM140. Deficiency of NCAM (neural cell adhesion molecule) results in decreased tyrosine phosphorylation and altered targeting of the exocyst to growth cone membranes. Compartmentalized exocytosis and neurite outgrowth are inhibited in NCAM-deficient neurons and in wild-type neurons transfected with mutant Sec8 deficient for phosphorylation. These observations indicate a direct exocyst-dependent link between NCAM at the cell surface and delivery of new plasma membrane at surface in NCAM-induced neurite outgrowth⁸⁰.

In addition, loss of function of exo84 and sec-8 causes defects in proximal dendritic arborization leading to accumulation of RAB-10-positive intracellular vesicles⁸¹.

These results suggest a crucial role for the Rab10 GTPase and the exocyst complex in controlling vesicle transport from secretory and/or endosomal compartments that is required for dendritic growth⁸¹.

1.5 LRRK2, VESICULAR DYNAMICS AND RECEPTOR TRAFFICKING

Vesicular trafficking from the presynaptic pool depends on the presence of LRRK2 as an integral part of the presynaptic protein complex. Piccoli et al. identified the presynaptic proteins NSF, subunits of the AP-2

complex, SV2A, synapsin and syntaxin 1, as well as actin, as a protein complex interacting with LRRK2⁸².

NSF catalyzes the release of the SNARE complex (SNAP-25, synapsin 1, and Vamp) and enables the first step of the endocytic cycle^{83,82}, while the clathrin complex constitutes a major pathway for recycling SV from the membrane to the resting pool (RP)⁸⁴.

Control of SV storage and mobilization in the readily releasable pool (RRP) depends on the glycoproteins of synaptic vesicles SV2A and SV2B, whereas synapsins are thought to immobilize SV in the (RP) by relegating the vesicles to the actin cytoskeleton⁸². Experiments conducted by Piccoli et al. using knock-out models suggest that LRRK2 performs its main function at the presynaptic site and may serve as a molecular hub/scaffold that coordinates both storage and mobilization of SVs. Accordingly, analysis of vesicle movement showed that SVs in siLRRK2 neurons were characterized by greater spatial freedom. Thus, while under basal conditions the lack of LRRK2 might confer vesicles a greater likelihood of contacting the membrane and fusing, it might also affect the organization of the presynaptic machinery, thereby compromising the mobilization of SVs required during high activity⁸².

The role of LRRK2 in multiple aspects of vesicle trafficking is described primarily through its interaction with trafficking proteins such as endophilin A, Rab7, Rab7L1, and members of the GTPase dynamin superfamily. Studies in *Drosophila* have revealed specific LRRK2 roles in synaptic vesicle recycling, retromer trafficking, and lysosomal positioning. LRRK2 phosphorylates endophilin A (at S75), a protein required for endocytosis of synaptic vesicles and it appears that phosphorylation of endo A mediates its release from newly formed vesicles and then subsequent dephosphorylation allows further binding

to the presynaptic membrane and thus any disruption of this tightly coordinated phosphorylation/dephosphorylation cycle prevents vesicle recycling⁸⁵.

Migheli et.al with their studies highlighted an important cellular function of LRRK2 in the regulation of vesicle trafficking dynamics and dopamine receptor trafficking. They have in fact demonstrated that in neuronal cells that the presence of the LRRK2G2019S pathological mutant results in increased levels of extracellular dopamine. In addition, the LRRK2 mutant affects dopamine D1 receptor levels on the membrane surface in neuronal cells or animal models. Ultrastructural analysis of PC12-derived cells expressing the mutant LRRK2-G2019S shows an altered distribution of intracellular vesicles. These results indicate the key role of LRRK2 in controlling vesicle trafficking in neuronal cells⁸⁶.

Alteration in dopamine receptor distribution or signaling have been evidenced by other independent groups. For instance, Beccano-Kelly and others analysing adult LRRK2 overexpressing mice have shown that they exhibit clear alterations to D2-receptor-mediated short-term synaptic plasticity, behavioral hypoactivity and impaired recognition memory. Western blot analysis of striatal lysates evidences a significant increase in DRD2 levels with a parallel increase in DARPP32 and pT34-DARPP32 (activated form of DARPP32) protein level indicating an over-activation of D2-dependent pathway in LRRK2 over-expressing mice⁸⁷. The over-activation of DRD2 in LRRK2 G2019S transgenic mice inhibiting the striatal glutamatergic transmission was further confirmed by Tozzi and others⁸⁸.

Moreover, LRRK2 regulates dopamine receptor activation in the striatal projection neurons (SPN). In these neurons, LRRK2^{-/-} mice show a significant and abnormal phosphorylation in S845 of GluR1 in response

to dopamine receptor DRD1 activation likely due to an over-activation of PKA activity. Notably, LRRK2 R1441C missense mutation expression also induces excessive PKA activity in the SPNs strongly leading to similar pathological phenotype⁸⁹.

All these findings, further supported by the low expression level of LRRK2 in dopaminergic neurons, strongly suggest the hypothesis that LRRK2 pathological mutants may determine a dysregulation at striatal level (likely by an alteration of dopamine receptor pathways) that in turn affect the dopaminergic neuron physiology.

Mutant LRRK2 was further shown to delay EGFR receptor degradation. EGFR degradation is a classical assay to evaluate degradative pathway of membrane receptors upon internalization due to agonist binding. In this cellular assay, mutant LRRK2 significantly delays the EGFR degradation mainly affecting the late endosomes trafficking in a RAB7 dependent mechanism⁹⁰.

1.6 SINAPTIC VESICLE GLYCOPROTEIN 2A (SV2A)

SV2 are integral membrane proteins present on all synaptic vesicles and consists of a small gene family composed of three isoforms, designated SV2A, SV2B, and SV2C. SV2A is the most widely distributed isoform, being almost ubiquitous in the CNS, as well as being present in endocrine cells. SV2B is brain-specific, with a wide but not ubiquitous distribution, and SV2C is a minor isoform in the brain⁹¹.

Given their ubiquitous presence in synaptic vesicles, it has been proposed that SV2s may transport a shared vesicle constituent, such as calcium or ATP⁹¹.

It is postulated that SV2 regulates the exocytosis modulating the release of neurotransmitters and proteins in an action potential-dependent manner from nerve terminals without altering the morphology or number of synaptic vesicles⁹².

SV2A, in particular, interacts with the presynaptic protein synaptotagmin, which is considered the main calcium sensor for regulating calcium-dependent exocytosis of synaptic vesicles and may influence synaptotagmin function but it is likely possible that SV2A has multiple functions⁹¹.

In vivo studies showed that animals lacking SV2A suffer severe seizures and die within 3 weeks demonstrating that SV2A is implicated in seizure control⁹².

SV2A is the molecular target in the brain for Levetiracetam (LEV), a drug commonly used in epilepsy therapy in human. The correlation between SV2A binding and drug potency suggests that LEV modulates one or more of the functions of SV2A⁹¹.

Furthermore, some studies show that overexpression of SV2A causes abnormal neurotransmission that can be rescued by treatment with levetiracetam⁹³.

1.7 LEVETIRACETAM (LEV)

LEV ((S)-2-(2-Oxopyrrolidin-1-yl)butanamide) (commercial name Keppra)) belongs to a group of pyrrolidone compounds derived from piracetam⁹⁴.

LEV was studied in models of epilepsy because piracetam had shown efficacy in treating photoparoxysmal responses and myoclonus⁹⁴.

LEV is considered a second-generation antiepileptic drug (AED) that is

approved for clinical use as monotherapy and may also be used for adjunctive treatment of patients with seizures. LEV has favorable characteristics, including a low interaction potential, a short elimination half-life, and has neither active metabolites nor major adverse effects on cognition⁹⁵.

The identification of the SV2A protein of synaptic vesicles as the binding site in the brain for LEV is an important finding not only for the elucidation of antiepileptic mechanism of action of LEV, but also for future drug discovery/development of new treatment for both epilepsy and other neurological disorders⁹¹.

Although the exact mechanism of action of the drug is currently debated, recent studies have proposed that LEV possesses remarkable neuroprotective properties in non-epileptic and epileptic disorders. Experimental evidence suggests that LEV may be considered not only an antiepileptic drug but also neuroprotective and hyperalgesic⁹⁵.

Hanon et al. reported that LEV induced significant neuroprotection in the rat models of focal cerebral ischemia⁹⁶ while Wang et al. observed that administration of a certain concentration of LEV in clinically relevant animal models was neuroprotective against traumatic brain injury⁹⁷.

Kilicdag et al. found that administration of LEV after hypoxic ischemia was responsible for a significant decrease in the number of apoptotic cells in the hippocampus and cerebral cortex compared with the placebo-treated group⁹⁸.

Marcotulli and colleagues have analyzed the effect of LEV on the level and distribution of presynaptic proteins in rat cerebral cortex. In this experimental model, the expression of several vesicle proteins is altered upon LEV treatment and LRRK2 is part of this protein network. It is reasonable to hypothesize that SV2A and LRRK2 are both involved in

modulating vesicle dynamics, although the molecular mechanisms are still unknown⁹⁹.

2. RESULTS

2.1

Result 1: Generation of stable cell lines expressing the GFP reporter under the control of stress inducible promoters.

The first aim of my research was to screen a large number of molecules with epigenetic activity to evaluate possible neuroprotective properties in Parkinson's disease.

Parkinson's disease is the second most frequent neurodegenerative disease after Alzheimer's and to date no drug is able to stop the course of disease, but the available treatments allow only to control the motor symptoms.

This project was supported by PON Dottorati Innovativi con caratterizzazione industriale. Title: "Sviluppo pre-clinico di farmaci epigenetici per il trattamento della Malattia di Parkinson" Code: DOT1329971.

The project was performed in collaboration with Epi-C (Epigenetic Compounds), a biotech company that studies and develops compounds capable to modulate epigenetic modifications. The Epi-C is interested to use these compounds in different pathological context ranging from cancer to neurological diseases. In fact, the proposed project aims to develop and screen compounds with significant neuroprotective properties in PD context. The screening of the compounds can be realized in an automated manner using a robotic platform at the company Epi-C. For any high throughput screening of specific compounds is necessary to have an easy "read-out" usable in a robotic platform. An easy "read-out" are cellular systems that expresses fluorescent probes, easily detectable by automated platforms, which vary according to the state of cellular health. For this reason, I generated a cellular model that

expressed the GFP under the control of the stress-sensitive promoter of DNA damage-inducible transcript 3, also known as C/EBP homologous protein (CHOP) gene¹⁰⁰. CHOP is a transcriptional factor belonging to CCAAT/enhancer-binding protein (C/EBP) family. Interestingly, CHOP is ubiquitously expressed, and its promoter is activated by a variety of stimuli such as mitochondrial stress, amino acid starvation, neurological diseases or neoplastic diseases as well as by pathogenic microbial or viral infections¹⁰⁰. Due to the large variety of upstream regulatory pathways and the very low expression level under physiological conditions, CHOP promoter was an ideal candidate to drive the expression of reporter genes to generate cell systems useful as read-out for high throughput screening.

The CHOP promoter was cloned upstream of GFP by restriction enzyme digestion and subsequent ligase (Figure 5).

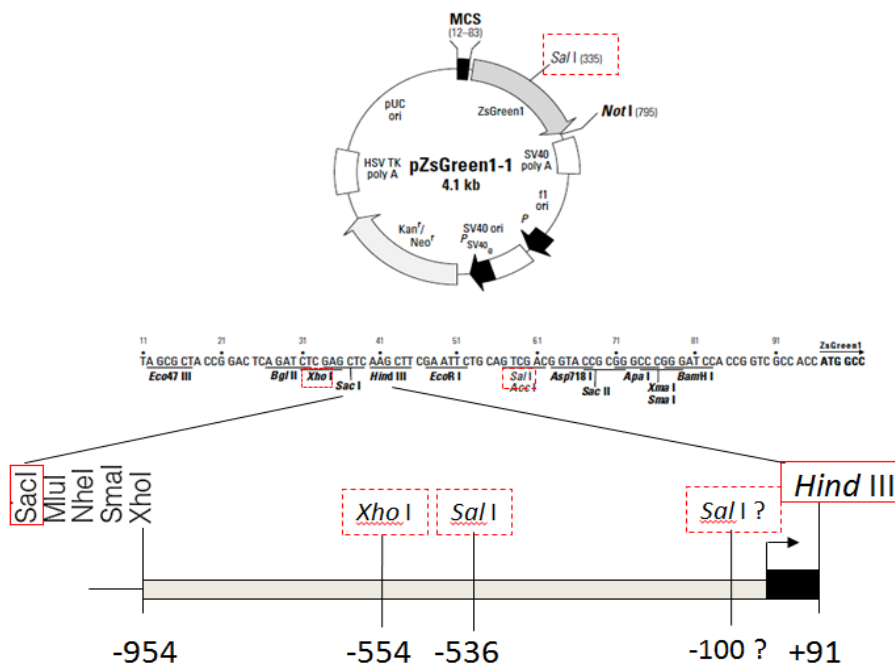


Figure 5: Plasmid map with the indication of restriction sites used for cloning

The obtained plasmid was transfected into SH-SY5Y lines and after roughly four weeks of selection, individual cell clones were obtained. Clone screening was performed evaluating the fluorescence emitted, both by a multi-plate reader (Victor- Multilabel Plate Reader) and by confocal microscope, following treatment with sodium arsenite at various concentrations to induce the cellular stress (Figure 6A and C). The GFP protein was also evaluated by western blot (Figure 6B)

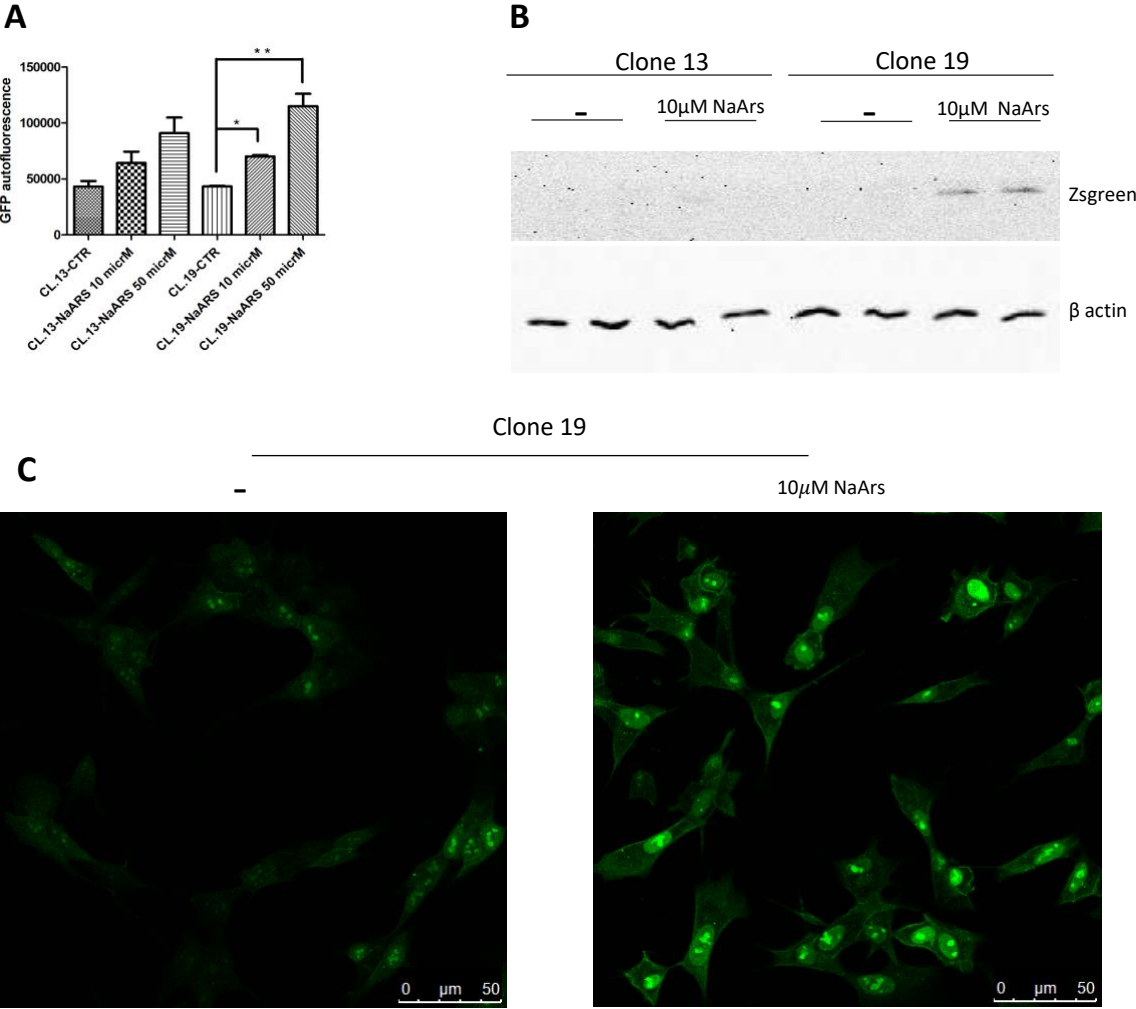


Figure 6: Comparison between clone 13 and clone 19 in GFP expression following treatment with sodium arsenite at two concentrations. A) Auto-fluorescence quantification of SH-SY5Y-GFP cells (clone 13 and 19) treated or not by sodium arsenite as indicated measured by multi-plate reader. B) SHSY5Y cells treated as previously described were lysed and analysed by Western blot using ZsGreen antibody for GFP and β-actin as control for equal number of cells. C) Analysis of SHSY5Y-GFP (clone 19) fluorescence by confocal microscope after sodium arsenite treatment.

Clones that showed the lowest basal level of GFP and the best induction of GFP after treatment with toxic stimuli were expanded and frozen in liquid nitrogen.

The clone 19 has shown the best features to be used as read-out.

To characterize SHSY5Y-GFP cells in a Parkinson's disease context, we used recombinant adenovirus expressing the pathological alpha-synuclein mutant A53T. Synuclein is the major constituent of Lewy bodies, and pathological mutations in this gene are responsible of familial forms of Parkinson's disease. Synuclein A53T expression induced by viral transduction resulted in a significant increase in GFP expression assessed both by reading with the Victor-Multilabel Plate Reader (data not shown) and by confocal microscopy analysis (Figure 7).

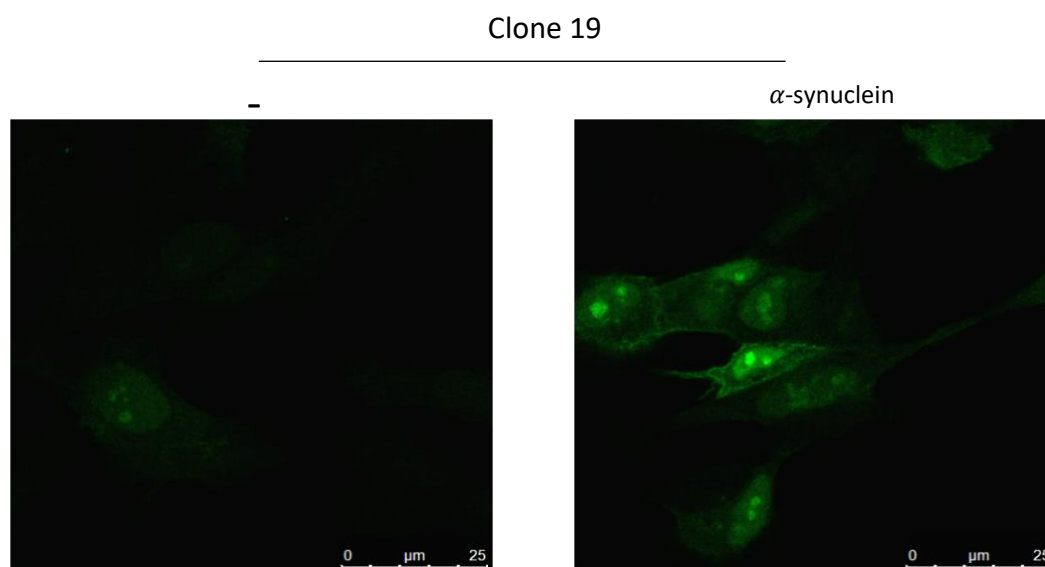


Figure 7: Analysis of GFP fluorescence in SHSY5Y GFP (clone 19) cells by confocal microscope after transduction by α -synuclein A53T.

From the analysis of obtained experimental data, the SH-SY5Y-CHOP-GFP cells have proven suitable to be able to highlight neurotoxic stress and represent a valuable "read-out" for the screening of epigenetic molecules with neuroprotective action.

The generated line has been sent to Epi-C in Naples for the screening of molecules with neuroprotective activity.

Materials and Methods

SHSY5Y stably expressing GFP

Human neuroblastoma SHSY5Y cells were grown in DMEM/F12 (Dulbecco's Modified Eagle Medium/F-12 Nutrient Mixture, Gibco), 10% FBS (fetal bovine serum, Gibco) at 37°C and 5% CO₂.

40% confluent cells in 6 cm plates were transfected by pZsGreen1-1-CHOP promoter plasmid already present in our laboratory.

Transfections were performed with LTX (Lipofectamine LTX Reagent, Life Technologies) according to the datasheet. After 4h with transfection reagent, cells were grown in a normal medium. The selection was performed in the presence of 400µg/mL of G418 and 200µg/mL of hygromycin B (Gibco).

Individual clones expressing antibiotic resistance were picked after 15 days of selection, moved in a 96 well plate and maintained in the selective medium.

When the cells reached confluence, they were screened for GFP expression upon toxic stimulus.

Stable clones screening by multiplate reader, confocal microscopy and Western blot

Multi plate reader: Cells were grown in 24 well, after 24h of sodium arsenite treatment, fluorescence was read at 500-570nm. The results were compared with the negative control.

Confocal microscopy analysis: Cells were grown in cover glass and treated by sodium arsenite or transduced by α -synuclein. After 24h the

cells were fixed by 4% of paraformaldehyde and permeabilized with 0,2% Triton X-100/PBS. Cells were incubated for 5 minutes with DAPI and washed by PBS 1X- tween 0,05% and PBS 1X. Cells were analysed by Leica TCS SP5 confocal microscope with LAS lite 170 image software.

Western blot analysis: equal amounts of protein extracts resolved by standard sodium dodecyl sulfate-polyacrylamide gel electrophoresis. Samples were electroblotted onto nitrocellulose membranes (Thermo Scientific). Membranes were incubated with 3% skim milk in 1X PBS-Tween 0.05% with the indicated antibody: anti-ZsGreen (632474 1:1000 Clontech) and anti-beta-actin (A5441 1: 5000 Sigma-Aldrich) for 16 hours at 4°C. Peroxidase-conjugated goat anti-mouse IgG antibody (1:2500 Millipore Corporation) or peroxidase-conjugated goat anti-rabbit IgG antibody (1:5000 Millipore Corporation) were used to detect immunocomplexes by enhanced chemiluminescence (ECL-start, Euroclone).

Characterization of SHSY5Y- GFP cells in a Parkinson's disease context by transduction with A53T-expressing adenovirus

40% of SHSY5Y-GFP cells were seeded in cover glass. 24h later cells were trasduced by adenoviral particles in DMEM F12 (without serum) for 90 minutes. Finally, 10% of FBS was added and the cells were kept in culture for other 48 hours.

2.2.

Result 2: Levetiracetam treatment ameliorates LRRK2 pathological mutant phenotype

As highlighted in the introduction, many experimental evidences suggest that LRRK2 may be part of and regulate a complex protein network that modulates vesicle dynamics/traffic. For instance, the main putative LRRK2 phosphorylation targets are a subset of RAB proteins that play a prominent role in the control of trafficking of vesicles, of different origin, inside the cells. Moreover, our research group and others have demonstrated a significative role of LRRK2 in the control of membrane receptor dynamics in neuronal experimental models. Based on these considerations, we were interested in some specific chemical compounds able to modulate the vesicle trafficking to explore the possibility to use them to block/impair the LRRK2 pathological effects. In particular, we focused our attention on Levetiracetam (LEV), a drug widely used in human therapy for the treatment of epilepsy as extensively discussed in the Introduction. Interestingly, SV2A protein is the binding site of LEV into the brain and, as demonstrated by Piccoli et al (see introduction), LRRK2 and SV2A belong to the same protein network in neuronal cells.

Binding of LEV to SV2A has been shown to reduce neuronal firing by modulating vesicle trafficking, although the molecular mechanism has not yet been defined. Moreover, as discussed in the Introduction, LEV has a significant neuroprotective activity in different experimental models.

To understand the relationship that might exist between LRRK2 and SV2A and, more important, to evaluate any LEV neuroprotective effect in LRRK2 toxicity we set up three different experimental models:

a) Primary neurons from WT or LRRK2 G2019S BAC transgenic mice (in collaboration with prof. Elisa Greggio, University of Padua, Italy).

b) PC12 cells expressing the dox-inducible G2019S LRRK2 mutant.


c) SH-SY5Y stably expressing DRD2 (Dopamine Receptor D2) transduced by recombinant adenovirus expressing LRRK2 G2019S.

As demonstrated by the following PDF paper we were able to demonstrate that LEV may partially, but significantly, rescue the LRRK2 pathological effect in terms of neurite outgrowth in primary neurons and PC12 cells and in terms of DRD2 trafficking in SH-SY5Y cells. In particular, I mainly dealt with the analysis by western blot of β -tubulin expression in the presence or absence of LEV treatment.

Our data support the idea that LEV may represent a valuable neuroprotective compound for PD treatment, especially for PARK8 patients.

SHORT COMMUNICATION

Levetiracetam treatment ameliorates LRRK2 pathological mutant phenotype

Mauro Rassa¹ | Alice Biossa² | Manuela Galioto¹ | Milena Fais¹ | Paola Sini¹ |
Elisa Greggio² | Giovanni Piccoli³ | Claudia Crosio¹ | **Ciro Iaccarino¹** 

¹Department of Biomedical Sciences,
University of Sassari, Sassari, Italy

²Department of Biology, University of
Padova, Padova, Italy

³Department of Cellular, Computational and
Integrative Biology, University of Trento,
Trento, Italy

Correspondence

Ciro Iaccarino, Department of Biomedical
Sciences, University of Sassari, via Francesco
Muroni 25, 07100 Sassari, Italy.
Email: ciaccarino@uniss.it

Funding information

Fondazione Banco di Sardegna, Grant/
Award Number: 2014.0489; PRIN 2015,
Grant/Award Number: 2015LFPNMN_005;
Regione Sardegna, Grant/Award Number:
CRP-78083; PON 2014-2020, Grant/Award
Number: CCI2014IT16M2OP005

Abstract

Mutations in leucine-rich repeat kinase 2 (LRRK2) are the most common genetic cause of Parkinson's disease (PD). The LRRK2 physiological and pathological function is still debated. However, different experimental evidence based on LRRK2 cellular localization and LRRK2 protein interactors suggests that LRRK2 may be part and regulate a protein network modulating vesicle dynamics/trafficking. Interestingly, the synaptic vesicle protein SV2A is part of this protein complex. Importantly, SV2A is the binding site of the levetiracetam (LEV), a compound largely used in human therapy for epilepsy treatment. The binding of LEV to SV2A reduces the neuronal firing by the modulation of vesicle trafficking although by an unclear molecular mechanism. In this short communication, we have analysed the interaction between the LRRK2 and SV2A pathways by LEV treatment. Interestingly, LEV significantly counteracts the effect of LRRK2 G2019S pathological mutant expression in three different cellular experimental models. Our data strongly suggest that LEV treatment may have a neuroprotective effect on LRRK2 pathological mutant toxicity and that LEV repositioning could be a viable compound for PD treatment.

KEYWORDS

Levetiracetam, LRRK2, Parkinson's disease, SV2A

1 | INTRODUCTION

Approved by the US Food and Drug Administration in the 1999, levetiracetam (LEV) is a widely used drug for the treatment of partial and generalized epilepsy. In contrast to the common antiepileptic compounds, which preferentially bind to voltage-gated sodium channels in their inactive conformation, LEV binds the integral transmembrane protein SV2A, localized on both synaptic dense-core vesicles and small clear vesicles containing neurotransmitters and almost ubiquitously expressed in the different areas of central nervous system (CNS).¹ Up to date, although the clear involvement in seizure control, the SV2A physiological role

is far from being understood. Among the functions proposed, calcium-dependent exocytosis, neurotransmitter loading/retention in synaptic vesicles, synaptic vesicle priming and transport of vesicle constituents are the most robust (for review, see Ref.²). A possible molecular mechanism by which SV2A controls vesicle dynamics is via the interaction with synaptotagmin 1.³ The SV2A role in the seizure control is further confirmed by the analysis of SV2A knockout mice. A large proportion of SV2A knockout mice die immediately after birth and the surviving knockout soon develop frequent seizures that lead to premature death.⁴ Primary neurons from SV2A knockout mice present synapses that are ultrastructurally indistinguishable from the wild-type mice.⁴ Interestingly,

This is an open access article under the terms of the Creative Commons Attribution License, which permits use, distribution and reproduction in any medium, provided the original work is properly cited.

© 2019 The Authors. *Journal of Cellular and Molecular Medicine* published by John Wiley & Sons Ltd and Foundation for Cellular and Molecular Medicine.

alteration in vesicle trafficking seems a common feature shared by different PD causative genes.⁵ Mutations in the leucine-rich repeat kinase 2 gene (LRRK2, PARK8) are the most frequent genetic causes of Parkinson's disease, reaching up to 40% in some ethnic groups, that is Ashkenazi Jewish and North African Arab Berbers.⁶ Although LRRK2 physiological and pathological function is largely debated, different lines of evidence have pointed out an important role of LRRK2 in the control of vesicle trafficking that in turn may explain the different cellular dysfunctions ascribed to mutant LRRK2 expression.⁷⁻⁹

Interestingly, Marcotulli and colleagues have analysed the effect of LEV on presynaptic proteins level and distribution in the rat cerebral cortex.¹⁰ In this experimental model, the expression of different vesicular proteins is modified upon LEV treatment and LRRK2 is part of this protein network.¹⁰ In addition, SV2A was pulled down from adult mouse brain lysates by the LRRK2 WD40 domain¹¹ suggesting a their involvement to common cellular pathways.

Based on the previous considerations, it is reasonable to speculate that SV2A and LRRK2 are both involved in the modulation of vesicle dynamics, although the molecular mechanisms are still unknown. Whether LRRK2 and SV2A have a functional interaction and more important whether they have an opposite or synergistic biological effect remain to be explored. To test this hypothesis, we have evaluated the ability of LEV to affect the LRRK2 cellular effects in different experimental models.

2 | MATERIAL AND METHODS

2.1 | Primary cortical neurons and neurite measurement

Experimental procedures involving the use of animals were approved by the Italian Ministry of Health (licence 318/2013-B and licence 1041/2016-PR). C57BL/6 LRRK2 wild-type (WT) and LRRK2 G2019S BAC mice were obtained from Jackson Laboratory [B6.Cg-Tg(Lrrk2*G2019S)2Yue/J]. Housing and handling of mice were done in compliance with national guidelines. Primary neurons were prepared from brain cortex as previously described.⁷ Neurons were transfected with 1 µg of GFP plasmid at 3 days in vitro (DIV) using Lipofectamine 2000. Starting from DIV3, neurons were treated with 5 µmol/L LEV every 48 hours, fixed in 4% paraformaldehyde at DIV 7 and then processed for immunofluorescence. The mouse anti-tubulin III (clone 2G10, 1:500 Sigma) was used as a neuronal marker. Fluorescent images of GFP-positive neurons were acquired using the epifluorescent microscope Leica 5000B with a 40× objective. Exposure settings for the GFP channel were kept constant across images and experiments. Each microscope field includes one single neuron. The images were taken by a blinded operator, and the total sum of all traced neurites was performed on GFP images using NeuronJ with a total of ≈ 20 neurons analysed/genotype/condition. Any type of GFP-transfected cortical neurons was selected for the analysis.

2.2 | PC12-G2019S differentiation and analysis

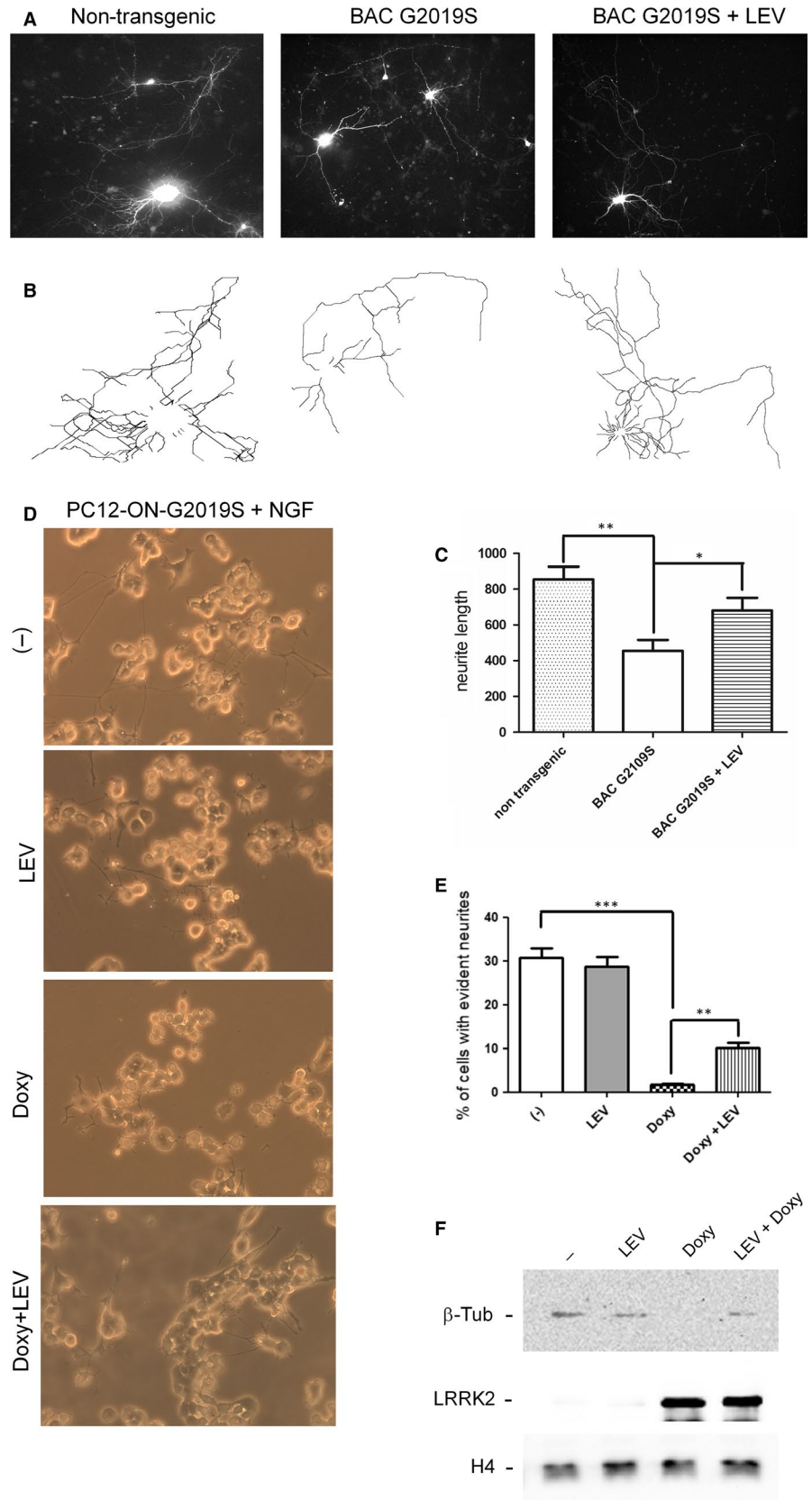
PC12 cells stably expressing doxycycline (dox) inducible LRRK2 G2019S mutant¹² were grown in DMEM-F12, 10% Fetal Bovine Serum (FBS) at 37°C. For differentiation experiment, the cells were plated at low density (5% of confluence) on a cover glass, previously treated with poly-L-lysine solution for 1 hour. The differentiation was performed growing the cells in 1% FBS in the presence of 100 ng/mL of NGF for 6 consecutive days, adding new medium containing NGF each 48 hours. Doxycycline (0.2 µmol/L) and LEV (10 µmol/L) were added together with NGF and replaced every 48 hours in the same experimental conditions. At the end of the experimental procedure, the differentiated cells were fixed with 4% paraformaldehyde/PBS and analysed by phase-contrast microscopy. For Western blot analysis, the cells were plated on 24 multiwell culture plates in the same experimental conditions. The cells were lysed by Laemmli buffer, and the protein extracts were normalized by histone 4 (H4) or beta-actin levels.

2.3 | SH-SY5Y transduction, immunofluorescence and Western blot

SH-SY5Y cells stably expressing dopamine receptor D2 carrying a Flag epitope (SH-SY5Y-DRD2)⁷ were grown in DMEM-F12, 10% Fetal Bovine Serum (FBS) at 37°C. Cell transduction and immunofluorescence experiments were performed as previously published.⁷ Briefly, the cells were grown on a cover glass and transduced by adenoviral particles (10-30 pfu/cell) in DMEM-F12. 48 hours after transduction, the cells were fixed with 4% paraformaldehyde/PBS and permeabilized with 0.1% Triton X-100. Cells were incubated with primary antibodies: anti-LRRK2 (1:500 Mjff2 c41-2 epitomics), anti-Flag (1:2500 Sigma-Aldrich) and anti-SV2A (HPA007863 1:500 Sigma-Aldrich) and then incubated with secondary antibodies: Goat Secondary Antibody Alexa Fluor® 488 or Alexa Fluor® 647 (Life Technologies). The cells were analysed by Leica TCS SP5 confocal microscope with LAS lite 170 image software.

Western blot analysis was performed as previously described.⁷ Briefly, equal amounts of protein extracts were resolved by standard sodium dodecyl sulphate-polyacrylamide gel electrophoresis. Samples were electroblotted onto Protran nitrocellulose (GE Healthcare Life Sciences). Membranes were incubated with 3% low-fat milk in 1X PBS-Tween 0.05% solution with the indicated antibody: anti-Myc (clone 9E10 1:5000 Sigma-Aldrich), anti-Flag (F3165 1:2500 Sigma-Aldrich), anti-beta-actin (A5441 1:5000 Sigma-Aldrich), anti-histone H4 (SAB4500313 1:1000 Sigma-Aldrich), anti-β3-Tubulin (4466 1:1000 Cell Signaling), anti-SV2A (HPA007863 1:1000 Sigma-Aldrich) for 16 hours at 4°C. Goat antimouse immunoglobulin G (IgG) peroxidase-conjugated antibody (1:2500 Millipore Corporation) or goat anti-rabbit IgG peroxidase-conjugated antibody (1:5000 Millipore Corporation) were used to reveal immunocomplexes by enhanced chemiluminescence (Pierce Biotechnology).

FIGURE 1 Analysis of LEV effect on neurite branching on primary cortical neurons or PC12 cells expressing LRRK2 G2019S. A-B, Primary neurons from BAC G2019S LRRK2 transgenic animals were transfected at DIV3 with GFP and then treated with 5 $\mu\text{mol/L}$ LEV from DIV3 to DIV7. At DIV7, the cells were fixed and the neurite extension was measured analysing the GFP expression by confocal microscope (B). C, Quantification of data obtained in (B). The data represent the sum of total length of neurites/neuron in two independent replicates and are represented as mean \pm SD. * $P < .05$; ** $P < .01$; *** $P < .001$. One-way ANOVA test and Bonferroni's post-test were used. D, PC12 cells stably expressing dox-inducible LRRK2 G2019S were treated for 6 d with NGF in the presence or absence of dox or dox + LEV. E, Quantification of data obtained in (D). The data represent the numbers of cells clearly showing neurite extensions in three independent replicates and are represented as mean \pm SD. ** $P < .01$; *** $P < .001$. One-way ANOVA test and Bonferroni's post-test were used. F, PC12-G2019S cells treated as previously described were lysed and analysed by Western blot using specific antibodies for the indicated proteins (anti- β 3-tubulin, anti-Myc antibody for LRRK2). Histone H4 serves as controls for equal number of cells



2.4 | Statistical analysis

The results are presented as means \pm SD of at least $n = \geq 3$ independent cultures. Statistical evaluation was conducted by

one-way ANOVA test and Bonferroni's post-test or Student's *t* test as indicated. Values significantly different from the relative control are indicated with an asterisk. * $P < .05$; ** $P < .01$; *** $P < .001$.

3 | RESULTS

3.1 | Effect of LEV on the inhibition of neurite outgrowth due to LRRK2 G2019S expression in primary neurons and in PC12 cells

Primary neurons from WT or LRRK2 G2019S BAC transgenic mice were prepared and transfected with GFP to fill the cell and trace the neurite branching and length. The LEV concentration to be used in the assay was established by MTS assays. At 5 $\mu\text{mol/L}$ of LEV, no significant toxic effect was detected (data not shown). At DIV3 and DIV5, the primary neurons were treated with 5 $\mu\text{mol/L}$ LEV and subsequently analysed at DIV7. As shown in Figures 1,2A-B-C, the G2019S expression determines a significant reduction in neurite length compared with WT primary neurons, as previously reported.⁷ Of note, LEV treatment significantly ameliorates the neurite shortening phenotype of G2019S neurons (Figures 1,2A-B-C).

To confirm the data obtained on primary neurons, we used a different experimental model: PC12 cells expressing the dox-inducible G2019S LRRK2 mutant.¹² The cells were treated with NGF to induce neuronal differentiation in the presence or absence of dox. As illustrated in Figure 1D-E, roughly 30% of PC12-G2019S show significant neurite outgrowth after 6 days of NGF treatment. The concomitant expression of G2019S mutant, by doxycycline treatment, determines a strong reduction in neurite outgrowth (roughly 1%-2% of cells). The LEV addition partially, but significantly, increases the neurite outgrowth (roughly 10% of cells) (Figure 1D-E). No effect of LEV was visible in PC12-G2019S cells without dox treatment. To further validate the differentiation process, we used the β -tubulin marker. In a preliminary experiment, we have evaluated the β -tubulin expression level in PC12-G2019S cells. The β -tubulin protein was almost undetectable in our experimental conditions (data not shown). Then, we performed the same

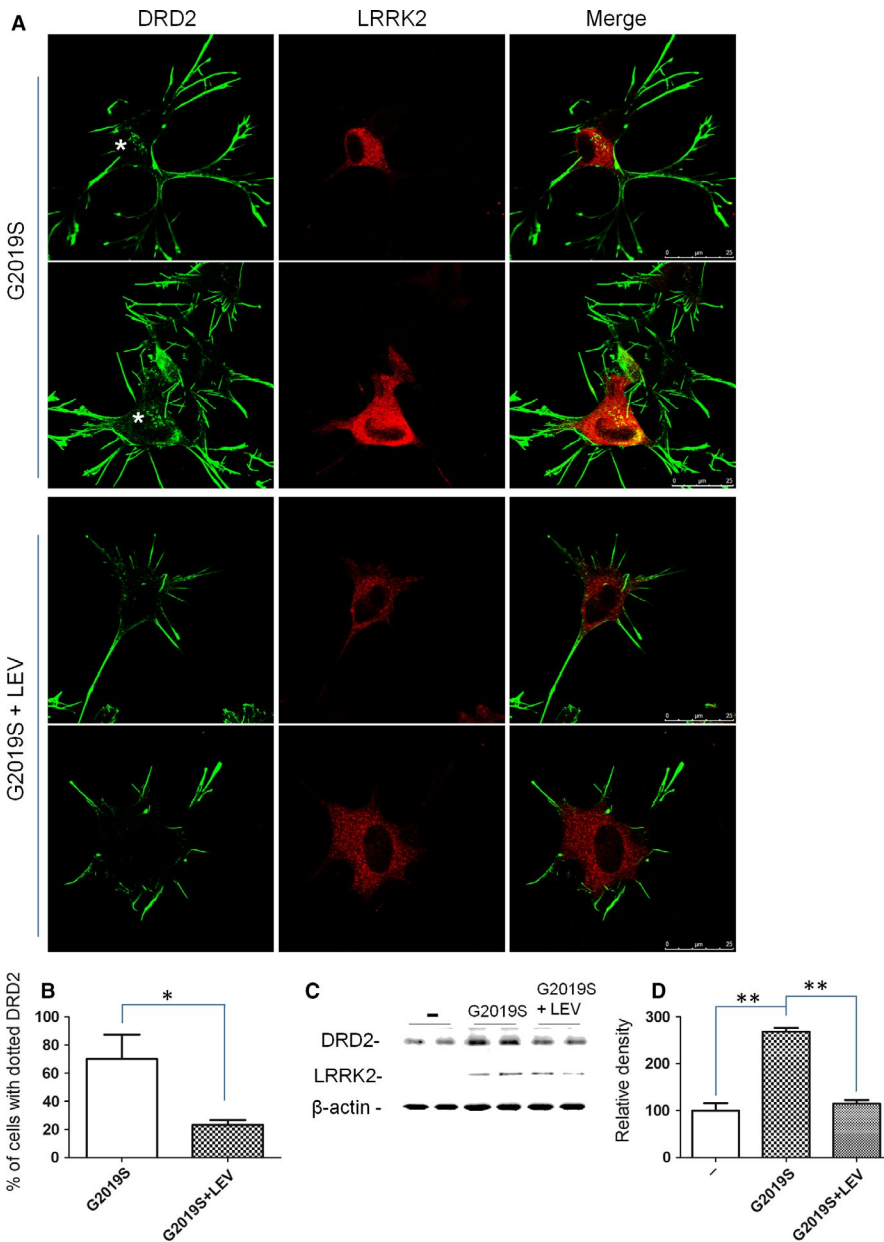


FIGURE 2 Analysis of LEV effect on DRD2 localization and level in the presence of LRRK2 G2019S. A, SH-SY5Y cells stably expressing Flag-tagged DRD2 were transfected by LRRK2 G2019S and treated or not for 48 h with LEV. The cells were fixed and incubated with different primary antibodies (anti-Flag for DRD2 and anti-LRRK2 antibody). The asterisk indicates the DRD2 in the Golgi areas. Scale bars = 25 μm . B, Quantification of data obtained in (A). The data represent the mean \pm SD. * $P < .05$; Student's t test was used. C, Cells treated as previously described were lysed and analysed by Western blot using specific antibodies for the indicated proteins (anti-Flag for DRD2 and anti-Myc antibody for LRRK2). β -actin serves as controls for equal loading of samples. D, Quantification of data obtained in (C). The data represent the mean \pm SD; ** $P < .01$. One-way ANOVA test and Bonferroni's post-test were used

differentiation protocol, and at the end of the procedure, the cells were lysed and normalized to histone H4 level as indicator of the same number of cells. As indicated in Figure 1F, the PC12-G2019S cells express a significant level of β 3-tubulin upon NGF treatment (with or without LEV) that is almost undetectable in the same cells treated with doxycycline. The simultaneous LEV administration in the doxycycline-treated cells partially rescues the β 3-tubulin expression (Figure 1F).

3.2 | Effect of LEV on DRD2 accumulation in Golgi areas due to LRRK2 G2019S expression

We have recently demonstrated that LRRK2 is implicated in the regulation of dopamine receptor trafficking. In particular, the expression of LRRK2 pathological mutant affects the dopamine receptor D2 (DRD2) localization,⁷ determining a significant receptor accumulation into the Golgi areas. Taking advantage of this experimental model, we have evaluated the LEV effect on the DRD2 localization in the presence of LRRK2 G2019S mutant. In a preliminary experiment, we have evaluated the LEV effect on DRD2 protein level and localization. No effect of 48 hours of LEV treatment was visible in SH-SY5Y stably expressing DRD2 (SH-SY5Y-DRD2) (data not shown). Then, the SH-SY5Y-DRD2 was transduced by recombinant adenovirus expressing G2019S, treated or not with LEV and analysed 48 hours later. As previously reported,⁷ the cells expressing the G2019S show an important accumulation of DRD2 into the Golgi areas and this phenotype is significantly rescued by LEV treatment (Figure 2A-B). The result is further confirmed by the analysis of DRD2 protein accumulation (Figure 2C-D) as in Ref⁷. To further validate these results, we have analysed possible SV2A alteration by LEV treatment both at protein level (Western blot) and localization (immunofluorescence) without detecting any significant difference (data not shown).

4 | DISCUSSION

The binding to SV2A protein is responsible for the antiepileptic action of LEV, a compound largely used in human therapy. Whether LEV binding is reducing or enhancing SV2A physiological function is largely unknown. Of note, the absence of SV2A protein in knockout animals results in the development of frequent seizures, suggesting an agonistic rather than an antagonistic effect of LEV on SV2A. Different lines of evidence indicate that both LRRK2 and SV2A are involved in common protein network^{10,11} that modulate the vesicle trafficking/dynamics. Moreover, alteration in vesicle trafficking seems a common feature shared by different PD causative genes.⁵ Here, we show using three different experimental models (primary neurons, PC12 cells and SH-SY5Y) that LEV is able to significantly revert the LRRK2 G2019S-associated pathological effects. Interestingly, LEV attenuates rotenone-induced toxicity in a rat model of PD,¹³ and in human, LEV treatment leads to an improvement in memory performance in patient with amnesic mild

cognitive impairment (aMCI).¹⁴ In the past, LEV has been tested in the control of levodopa-induced dyskinesia (LID) and, based on the conflicting results, for the International Parkinson and Movement Disorder Society the efficacy conclusion is 'insufficient evidence' although there are no safety concerns.¹⁵ Importantly, different side effects have been associated with LEV treatment or discontinuation. Among them, drowsiness, weakness, infection, loss of appetite and changes in behaviour and mood, including increased risk of suicide, are the most frequent. Some of these adverse effects were partially reduced by brivaracetam a new SV2A ligand with higher affinity compared with LEV. Although our research is far from the clinical application, our data support the idea that LEV repositioning may represent a valuable neuroprotective compound for PD, especially for PARK8 patients, that deserves future investigations.

ACKNOWLEDGEMENTS

This work was supported by Fondazione Banco di Sardegna (grant number 2014.0489), Regione Sardegna (grant number CRP-78083) and PRIN 2015 (2015LFPNMN_005). P.S and MF are supported by PhD fellowship granted by PON 2014-2020 (CCI2014IT16M2OP005).

CONFLICT OF INTEREST

The authors confirm that there are no conflicts of interest.

AUTHORS' CONTRIBUTIONS

RM, BA, FM and PG carried out the experiments. IC wrote the manuscript with support from CC and GE. IC, CC, GE and PG conceived and planned the experiments. SP and GM contributed to sample preparation. RM, B.A, IC, CC., GE and PG contributed to the interpretation of the results. All authors provided critical feedback and helped shape the research, analysis and manuscript.

ORCID

Ciro Iaccarino  <https://orcid.org/0000-0003-1619-7146>

REFERENCES

- Lynch BA, Lambeng N, Nocka K, et al. The synaptic vesicle protein SV2A is the binding site for the antiepileptic drug levetiracetam. *Proc Natl Acad Sci USA*. 2004;101:9861-9866.
- Bartholome O, Van den Ackerveken P, Sánchez Gil J, et al. Puzzling Out Synaptic Vesicle 2 Family Members Functions. *Front Mol Neurosci*. 2017;10:148.
- Kaempfer N, Kochlamazashvili G, Puchkov D, et al. Overlapping functions of stonin 2 and SV2 in sorting of the calcium sensor synaptotagmin 1 to synaptic vesicles. *Proc Natl Acad Sci USA*. 2015;112:7297-7302.
- Janz R, Goda Y, Geppert M, Missler M, Südhof TC. SV2A and SV2B function as redundant Ca²⁺ regulators in neurotransmitter release. *Neuron*. 1999;24:1003-1016.

5. Sheehan P, Yue Z. Deregulation of autophagy and vesicle trafficking in Parkinson's disease. *Neurosci Lett*. 2019;697:59-65.
6. Healy DG, Falchi M, O'Sullivan SS, et al. Phenotype, genotype, and worldwide genetic penetrance of LRRK2-associated Parkinson's disease: a case-control study. *Lancet Neurol*. 2008;7:583-590.
7. Rassu M, Del Giudice MG, Sanna S, et al. Role of LRRK2 in the regulation of dopamine receptor trafficking. *PLoS ONE*. 2017;12:e0179082.
8. Beccano-Kelly DA, Volta M, Munsie LN, et al. LRRK2 overexpression alters glutamatergic presynaptic plasticity, striatal dopamine tone, postsynaptic signal transduction, motor activity and memory. *Hum Mol Genet*. 2015;24:1336-1349.
9. Matikainen-Ankney BA, Kezunovic N, Mesias RE, et al. Altered development of synapse structure and function in striatum caused by Parkinson's disease-linked LRRK2-G2019S mutation. *J Neurosci*. 2016;36:7128-7141.
10. Marcotulli D, Fattorini G, Bragina L, Perugini J, Conti F. Levetiracetam affects differentially presynaptic proteins in rat cerebral cortex. *Front Cell Neurosci*. 2017;11:389.
11. Piccoli G, Condliffe SB, Bauer M, et al. LRRK2 controls synaptic vesicle storage and mobilization within the recycling pool. *J Neurosci*. 2011;31:2225-2237.
12. Migheli R, Del Giudice MG, Spissu Y, et al. LRRK2 affects vesicle trafficking, neurotransmitter extracellular level and membrane receptor localization. *PLoS ONE*. 2013;8:e77198.
13. Erbas O, Yilmaz M, Taskiran D. Levetiracetam attenuates rotenone-induced toxicity: a rat model of Parkinson's disease. *Environ Toxicol Pharmacol*. 2016;42:226-230.
14. Bakker A, Krauss GL, Albert MS, et al. Reduction of hippocampal hyperactivity improves cognition in amnesic mild cognitive impairment. *Neuron*. 2012;74:467-474.
15. Fox SH, Katzenschlager R, Lim S-Y, et al. International Parkinson and movement disorder society evidence-based medicine review: update on treatments for the motor symptoms of Parkinson's disease. *Mov Disord*. 2018;33(8):1248-1266.

SUPPORTING INFORMATION

Additional supporting information may be found online in the Supporting Information section at the end of the article.

How to cite this article: Rassu M, Bioss A, Galioto M, et al. Levetiracetam treatment ameliorates LRRK2 pathological mutant phenotype. *J Cell Mol Med*. 2019;23:8505–8510. <https://doi.org/10.1111/jcmm.14674>

2.3

Result 3: LRRK2 modulates the exocyst complex assembly by interacting with Sec8

To understand how LRRK2 may participate in the modulation of vesicular trafficking, we focused our attention on another prominent actor in the vesicle trafficking pathway: Sec8. The starting point of this research project was the identification of Sec8 as specific interactor of LRRK2 by a GST-pull down approach (see attached PDF). Sec8 is a member of exocyst complex composed of eight different proteins (see Introduction). The exocyst complex is an evolutionarily conserved multisubunit protein complex primarily implicated in binding secretory vesicles to the plasma membrane. Although the exocyst complex was first discovered for its primary function in exocytosis, afterwards it has been involved in many biological processes such as cell migration, primary ciliogenesis, cytokinesis, and autophagy.

Interestingly, exocyst and Rabs, including Rab8 and Rab10, which are two targets of LRRK2 phosphorylation, are part of the same protein complex that couples the generation of secretory vesicles in donor compartments to their docking and fusion.





In the following PDF article, we subcloned three different LRRK2 domains (LRR, kinase, or WD40 domain) in frame with GST to generate GST-LRR, GST-Kinase, or GST-WD40 constructs. These proteins (GST-LRR, GST-WD40, or GST-Kinase) were used in GST pulldown experiments with mouse brain protein extracts. The LRRK2 binding protein were separated by SDS-PAGE and identified by mass spectrometry. Interestingly, the GST-Kinase domain specifically associated with a protein of approximately 110 kD. Mass spectrometry analysis identified this protein

as Sec8. The specificity of LRRK2/Sec8 interaction was confirmed in different experimental models and confirmed in mouse brain extracts at physiological protein expression levels. Interestingly, the LRRK2 overexpression determines an increase in exocyst complex formation and this increase is ablated by the treatment with a specific LRRK2 kinase inhibitor.

Finally, it was interesting to note that the overexpression of Sec8 can significantly rescue the inhibition in differentiation due to the expression of LRRK2 G2019S.

Article

LRRK2 Modulates the Exocyst Complex Assembly by Interacting with Sec8

Milena Fais¹, Giovanna Sanna¹, Manuela Galioto¹, Thi Thanh Duyen Nguyen¹, Mai Uyên Thi Trần¹, Paola Sini¹, Franco Carta², Franco Turrini^{2,3}, Yulan Xiong^{4,5,†}, Ted M. Dawson^{4,5,6,7}, Valina L. Dawson^{4,5,7,8}, Claudia Crosio¹ and Ciro Iaccarino^{1,*}

- ¹ Department of Biomedical Sciences, University of Sassari, 07100 Sassari, Italy; faismilena@gmail.com (M.F.); sanna.posta@gmail.com (G.S.); galioto@uniss.it (M.G.); nguyenthahduyen88@gmail.com (T.T.D.N.); uyenthimai@gmail.com (M.U.T.T.); sinipaoladrop@gmail.com (P.S.); ccrosio@uniss.it (C.C.)
- ² Nurex Srl, 07100 Sassari, Italy; franco.cart@nurex.it (F.C.); francesco.turrini@unito.it (F.T.)
- ³ Department of Oncology, University of Turin, 10126 Turin, Italy
- ⁴ Neuroregeneration and Stem Cell Programs, Institute for Cell Engineering, Johns Hopkins University School of Medicine, Baltimore, MD 21205, USA; yxiong@uchc.edu (Y.X.); tdawson@jhmi.edu (T.M.D.); vdawson@jhmi.edu (V.L.D.)
- ⁵ Department of Neurology, Johns Hopkins University School of Medicine, Baltimore, MD 21205, USA
- ⁶ Department of Pharmacology and Molecular Sciences, Johns Hopkins University School of Medicine, Baltimore, MD 21205, USA
- ⁷ Solomon H. Snyder Department of Neuroscience, Johns Hopkins University School of Medicine, Baltimore, MD 21205, USA
- ⁸ Department of Physiology, Johns Hopkins University School of Medicine, Baltimore, MD 21205, USA
- * Correspondence: ciaccarino@uniss.it; Tel.: +39-079-228610
- † Present Address of Yulan Xiong: Department of Neuroscience, University of Connecticut School of Medicine, Farmington, CT 06030, USA.



Citation: Fais, M.; Sanna, G.; Galioto, M.; Nguyen, T.T.D.; Trần, M.U.T.; Sini, P.; Carta, F.; Turrini, F.; Xiong, Y.; Dawson, T.M.; et al. LRRK2 Modulates the Exocyst Complex Assembly by Interacting with Sec8. *Cells* **2021**, *10*, 203. <https://doi.org/10.3390/cells10020203>

Academic Editors: Michele Morari and Paolo Calabresi

Received: 28 October 2020

Accepted: 18 January 2021

Published: 20 January 2021

Publisher's Note: MDPI stays neutral with regard to jurisdictional claims in published maps and institutional affiliations.

Abstract: Mutations in LRRK2 play a critical role in both familial and sporadic Parkinson's disease (PD). Up to date, the role of LRRK2 in PD onset and progression remains largely unknown. However, experimental evidence highlights a critical role of LRRK2 in the control of vesicle trafficking, likely by Rab phosphorylation, that in turn may regulate different aspects of neuronal physiology. Here we show that LRRK2 interacts with Sec8, one of eight subunits of the exocyst complex. The exocyst complex is an evolutionarily conserved multisubunit protein complex mainly involved in tethering secretory vesicles to the plasma membrane and implicated in the regulation of multiple biological processes modulated by vesicle trafficking. Interestingly, Rabs and exocyst complex belong to the same protein network. Our experimental evidence indicates that LRRK2 kinase activity or the presence of the LRRK2 kinase domain regulate the assembly of exocyst subunits and that the over-expression of Sec8 significantly rescues the LRRK2 G2019S mutant pathological effect. Our findings strongly suggest an interesting molecular mechanism by which LRRK2 could modulate vesicle trafficking and may have important implications to decode the complex role that LRRK2 plays in neuronal physiology.

Keywords: LRRK2; Sec8; exocyst complex; Parkinson's disease



Copyright: © 2021 by the authors. Licensee MDPI, Basel, Switzerland. This article is an open access article distributed under the terms and conditions of the Creative Commons Attribution (CC BY) license (<https://creativecommons.org/licenses/by/4.0/>).

1. Introduction

Mutations in the leucine-rich repeat kinase 2 gene (LRRK2, PARK8) are the most frequent genetic causes of Parkinson's disease, reaching up to 40% in some ethnic groups such as Ashkenazi Jewish and North African Arab Berbers [1]. These LRRK2 pathological mutations are autosomal dominant and PD patients carrying the LRRK2 mutations are clinically and neuropathologically indistinguishable from idiopathic patients [2,3]. LRRK2 belongs to the Roco superfamily of proteins, which constitutes a novel multi-domain family of Ras-like G-proteins. LRRK2 is a large multidomain protein consisting of armadillo

repeats (ARM), ankyrin repeats (ANK), leucine-rich repeats (LRR), Ras of complex (Roc), C-terminal of Roc (COR), kinase, and WD40 domains [4]. LRRK2 mutations are high frequent around the central catalytic core of the protein, two mutations are found in the Roc domain, one in the COR domain and two in the kinase domain. In addition, two variants that act as risk factors for sporadic PD have been identified, one in the COR domain and one in the WD40 repeats [4].

Despite the apparent clinical association between LRRK2 mutations and PD, it remains enigmatic how LRRK2 pathological mutations may contribute to disease onset and progression. Different experimental evidence suggests that LRRK2 has a functional role in the vesicle trafficking control, and alteration in synaptic vesicle trafficking seems a common pathological mechanism in PD [5,6]. In fact, many LRRK2 protein interactors belong to protein families involved in the regulation of vesicle trafficking (among them Rab5 [7], Rab7 [8], Rab7L [9,10], Sec16A [11], a subset of Rabs [12], endoA [13]) or of cytoskeleton dynamics that in turn may modulate vesicle trafficking [14–17]. Since one of the first deep analyses by Piccoli et al. in 2011 where LRRK2 controls synaptic vesicle storage and mobilization within the recycling pool [18], hundreds of different publications have underlined the role of LRRK2 vesicle trafficking. Mutant LRRK2s alter endocytosis by the phosphorylation of DNAJC6 (auxilin) [19], synaptojanin1 [19], endoA [13], or Rab5b [7] and modulate vesicle dynamics via aberrant phosphorylation of NSF [20] or different Rab family proteins. Recently, a significant reduction in synaptic vesicle number and a greater abundance of clathrin-coated vesicles were observed in a mouse line expressing tetracycline-inducible LRRK2 G2019S in catecholaminergic neurons, [21]. We have previously demonstrated that LRRK2 modulates dopamine receptor trafficking [22,23]. LRRK2 mutations dramatically modify the excitatory synaptic activity with a fourfold increase in sEPSC frequency in the dorsal striatal spiny projection neurons altering the shape of postsynaptic structures into striatum [24]. Moreover, in G2019S LRRK2 KI mice, elevated glutamate, and dopamine transmission and aberrant D2-receptor responses are detected independent of any change in the number of synapses or spine-like structures [25]. Glutamate terminals within the striatum are subject to active neuromodulation by other neurotransmitters released in the local area, including dopamine. Moreover, growing evidence underlines overlapping genes involved in both SV dynamics and autophagy, suggesting that vesicle trafficking has also an important function in the regulation of autophagic processes (for review see [26]).

In this context, the exocyst complex is an evolutionarily conserved multisubunit protein complex mainly implicated in tethering secretory vesicles to the plasma membrane. The exocyst complex is highly conserved in eukaryotic systems and is composed of eight single-copy subunits: Sec3, Sec5, Sec6, Sec8, Sec10, Sec15, Exo70, and Exo84 [27]. Genetic and biochemical studies in yeast indicate that the exocyst functions upstream of SNAREs. Different members of the exocyst complex interact with SNARE members or SNARE interacting proteins. In particular, yeast Sec6 can interact with the t-SNARE protein Sec9 (the SNAP-25 homolog) and with the Sec1/Munc18 family protein Sec1 [28]. These interactions are thought to precede vesicle priming, a process mediated by SNAREs (t-SNAREs on plasmatic membrane and v-SNARE on vesicle membrane) to dock the vesicles to the receiving membrane and finally to induce lipid fusion [29]. Importantly, mutations in the exocyst component Sec5 mainly alter the cell growth and membrane protein insertion without significant alteration in neurotransmitter release [30]. Axon and dendrite outgrowth relies on continuous membrane expansion and cytoskeletal remodeling and, in fact, neurite outgrowth is impaired in the absence of functional exocyst subunits in various biological systems such as primary neurons, PC12 cells, or multicellular model organisms [31–33] highlighting the prominent role played by the exocyst in the determination of neuronal cell polarity. Interestingly exocyst and Rabs (including Rab8 and Rab10, two LRRK2 phosphorylation targets) are part of the same protein complex that couples the generation of secretory vesicles at donor compartments to their docking and fusion [34].

The gene encoding for Sec8 is a 110-kDa multidomain protein containing 974 amino acids. Sec8 is expressed throughout the brain, and there is no significant regional variation

in the different brain areas. Knockout of the Sec8 gene in mice is early embryonic lethal; mutant embryos initiate gastrulation but are unable to progress beyond the primitive streak stage [35]. Interestingly, Sec8 binds to postsynaptic density protein 95 (PSD95) by the C-terminal region, which contains a PDZ binding domain. PSD95 is a synaptic scaffolding protein that plays a pivotal role in synaptic plasticity [36]. Moreover, Sec8 is essential for appropriate targeting to the cell membrane of the α -amino-3-hydroxy-5-methyl-4-isoxazole propionic acid receptor (AMPA) and the *N*-methyl-D-aspartate receptor (NMDAR) [37]. This last effect is mediated by the interaction of the Sec8 PDZ binding domain with the Synapse-associated protein (SAP) 102 [37]. Finally, exo70 and Sec8 subunits of the exocyst complex directly associate with the intracellular domain of NCAM140 [38]. NCAM promotes FGF receptor-mediated phosphorylation of two tyrosine residues in the Sec8 protein and is required for efficient recruitment of the exocyst complex to growth cones [38]. Sec8 is associated with various biological processes, such as cell migration, invadopodia formation, cytokinesis, glucose uptake, and neural development. It plays a crucial role in targeting intracellular vesicles to their sites of fusion with plasma membrane both during neurite outgrowth and synaptogenesis as well as in mature synapses [39]. In neurons, this process is crucial since both the regulated protein localization on the plasma membrane of axon or dendrites (e.g., neurotransmitter or neurotrophic factor receptors) and the correct release of proteins (e.g., neurotransmitters or neurotrophic factors) mediate neuronal communication and underlie virtually all functions of the nervous system.

In the present study, we show that LRRK2 associates Sec8 and modulates the exocyst complex assembly. Importantly, the LRRK2 effect is mediated by its kinase domain since it is significantly impaired by LRRK2 kinase inhibitor treatment or by the absence of the LRRK2 kinase domain itself. Finally, the over-expression of Sec8 can significantly rescue the LRRK2 G2019S pathological mutant phenotype in neuronal cellular systems.

2. Materials and Methods

2.1. Reagents and Solutions

Tween[®] 20 (Polyethylene glycol sorbitan monolaurate), protease inhibitor cocktails, IGEPAL[®] CA-630 (Octylphenoxy poly(ethyleneoxy)ethanol), LRRK2 inhibitors: CZC-25146 from Merck (Darmstadt, Germany) The phosphate-buffered saline (PBS) solution was made using NaCl (137 mM), KCl (2.7 mM), Na₂HPO₄ (8.1 mM), KH₂PO₄ (1.47 mM) from Merck (Darmstadt, Germany) and then adjusted to pH 7.4. Dulbecco's modified Eagle's medium (DMEM)-F12, Fetal Bovine Serum (FBS), Streptomycin/Penicillin, Geneticin-G418 were purchased from ThermoFisher Scientific (Waltham, MA, USA).

2.2. Plasmid Constructions

Plasmids coding WT or mutants LRRK2 were previously described in [22]. LRR, Kinase, and WD40 domains were cloned in frame with GST into pGEX plasmid after PCR amplification using the following forward and reverse oligos: LRR (aggatccgtgttcatttgagcatc and aggatcccaagaagatccata), Kinase (aggatcctggctgacctgcttagaa and aggatcctgcgtctcgcagacaga), WD40 (aggatccacagcaggaatgcaagca and aggatccgcacttcattgtggaagat). After PCR amplification both pGEX plasmid and PCR products were cut by BamHI and ligated.

Rat Sec8 cDNA was a generous gift from Dr. Lienhard [40]. Human Sec8 was PCR amplified and cloned in frame with Flag-tag in the *N*-terminal position into pcDNA3 plasmid. Sec8 deletion mutants were generated by PCR following the QuikChange II Site-Directed Mutagenesis Kit using the following forward and reverse oligonucleotides (Sec8- Δ 1: ggcaagacagcttatcaaatcgact and acatcaaatcgactcaagatgttctaca; Sec8- Δ 2: acatcaaatcgactcaagatgttctaca and tgtagaacatcttgagtcgattgatgt; Sec8- Δ 3: ccaagatgttcattcctcctacagag and ctctgtaggagaggtagaacatcttg; Sec8- Δ 4: ctctcctacagagctgctgtgctgtctt and aagacaagcaagcagctctgtaggag; Sec8- Δ 5: ctgctgtcttaaagaagataactac and gtgattatcttctaagacaagaag).

2.3. Cell Lines

Human neuroblastoma SH-SY5Y cells (ATCC number CRL-2266) were grown in DMEM-F12 (ThermoFisher Scientific, Waltham, MA, USA), 10% fetal calf serum (FCS) (ThermoFisher Scientific, Waltham, MA, USA) at 37 °C. The PC12-TET-ON (Takara Bio Inc, Shiga, Japan) and PC12-TET-ON-G2019S cell lines were cultivated in DMEM-F12 supplemented with 10% Tetracycline-free FCS (Lonza, Milano, Italy) at 37 °C. HEK 293T (ATCC number CRL-3216) were grown in DMEM-F12 (Thermo Fisher Scientific), 10% fetal calf serum (FCS, Thermo Fisher Scientific) at 37 °C.

2.4. GST Pull-Down Assay

GST-pull down was previously described [41]. Briefly, GST-LRR, Kinase, or WD40 fusion domains were expressed in *E. coli* BL21. After induction with 0.5 mM IPTG for 3 h at 30 °C, bacteria were collected, washed twice in PBS1X and lysed by sonication (5'' at 100 W for 3 times) in lysis buffer (50 mM Tris HCl pH 8.0, 1 mM EDTA, 150 mM NaCl, 1% Triton X100, 1 mM PMSF, protease inhibitor cocktail 1X, 200 µg/mL lysozyme). GST-fused proteins were purified on glutathione-Sepharose 4 fast flow resin (GE Healthcare, Buckinghamshire, UK). Aliquots (500 ng) of the three GST-LRRK2 domains or GST alone were used for GST-pull down experiments. 5 mg of mouse brain protein extracts, obtained by homogenization in lysis buffer (50 mM Tris-HCl pH 8.0, 150 mM NaCl, 1% NP-40, 1 mM PMSF, protease inhibitor cocktail 1X) were incubated with GST-LRRK2 domains at 4° O/N. After five washes in lysis buffer, the beads were boiled in Laemmli Buffer 1X and loaded on SDS/PAGE acrylamide gel. Finally, the gels were stained with Mass Compatible Super Blue Stain Kit (Nurex Srl, Sassari, Italy).

2.5. In-Gel Digestion and Matrix-Assisted Laser Desorption/Ionization (MALDI) Mass Spectrometry (MS) Analysis

The mass spectrometry analysis was performed as described [41]. Briefly, the protein of interest was excised with a sterile scalpel and destained with 100 µL of 5 mM NH₄HCO₃/50% acetonitrile. Gel pieces were treated with 10 µL of 5 mM NH₄HCO₃ containing 10 ng/µL trypsin for 40 min on ice. Subsequently, excess digestion buffer was removed and substituted with an equal volume of 5 mM NH₄HCO₃. Tryptic digestion was conducted overnight at 37 °C. The MS spectra acquired were submitted to MASCOT (Matrix Science, London, UK).

2.6. Subcellular Fractionation of HEK293 Cells

Subcellular fractionation was performed as previously described in [42]. Briefly, the cells were homogenized in ice-cold homogenization-buffer (320 mM sucrose, 4 mM HEPES, pH 7.4, protease inhibitor cocktail (Sigma)). An aliquot of cell lysate was used as a total fraction in the western blot. The homogenates were centrifuged at 1000× *g* for 10 min to produce a pellet containing nuclei and large debris fraction that was discarded. The supernatant was further fractionated into a pellet (containing the membrane fraction) and supernatant by centrifugation at 10,000× *g* for 20 min. The membrane fraction was further washed by ice-cold homogenization-buffer to eliminate any cytoplasmic protein. The supernatant was ultra-centrifuged at 60,000× *g* for 60 min to obtain the pellet (containing the vesicle fraction) and the supernatant containing the cytoplasmic fraction. The vesicle fraction was further washed by ice-cold homogenization-buffer to obtain pure vesicles. Protein content was determined using the Bradford protein assay. An equal amount of protein extracts was loaded into the SDS-PAGE.

2.7. Immunoprecipitation

HEK293 cells were transfected with the indicated plasmids in 6 cm cell culture plates. The LRRK2 inhibitor CZC25146 (Merck, Darmstadt, Germany) was added 3 h before cell lysis at a final concentration of 1 µM. After 48 h the cells were washed twice in PBS 1X and lysed by 1 mL of NP40 lysis buffer (150 mM NaCl, 1% NP40, 20 mM Tris-HCl pH 7.5,

protease inhibitor cocktail). Cellular debris were removed by centrifugation at $13,000\times g$ and cell lysates were pre-cleared by incubation with protein A-agarose beads for 1 h at $4\text{ }^{\circ}\text{C}$. Then the samples were incubated by the indicated antibodies (anti-Flag, F3165, 1:2000 Merck, Darmstadt, Germany) or anti-Myc, M4439, 1:2000, Merck, Darmstadt, Germany) overnight at $4\text{ }^{\circ}\text{C}$. After incubation with protein A-agarose for 1 h at $4\text{ }^{\circ}\text{C}$, the beads were washed 4 times by lysis buffer. Samples were then resolved by SDS-PAGE.

2.8. Western Blot Analysis

Western blot analysis was performed as previously described [22]. Briefly, protein extracts were prepared by direct lysis in Laemmli buffer or NP40 1% buffer when protein content was determined using the Bradford protein assay. Equal amounts of protein extracts were resolved by standard sodium dodecyl sulfate-polyacrylamide gel electrophoresis and subsequently electroblotted into nitrocellulose membrane (Thermo Fisher Scientific). Membranes were incubated with 3% low-fat milk in 1X PBS-Tween 0.05% solution with the indicated antibody: anti-LRRK2 (1:5000 MJFF2 c41-2 ABCAM, Cambridge, UK), anti-Myc (1:5000 M4439 Sigma-Aldrich), anti-Flag (1:2500 F3165 Sigma-Aldrich), anti-beta-actin (A5441 1:5000 Sigma-Aldrich), anti-Sec8 (1:1000 610659 BD Biosciences, San Jose, CA, USA), anti-Exo70 (1:1000 HPA022840 Sigma-Aldrich), anti-Sec6 (1:1000 SAB2100729 Sigma-Aldrich) for 16 h at $4\text{ }^{\circ}\text{C}$. Goat anti-mouse immunoglobulin G (IgG) peroxidase-conjugated antibody (1:2500 Merck, Darmstadt, Germany) or goat anti-rabbit IgG peroxidase-conjugated antibody (1:5000 Millipore Corporation) were used to identify immunocomplexes by enhanced chemiluminescence (ECL start, Euroclone SpA, Milano, Italy).

2.9. Immunofluorescence

The cells were grown on a cover-glass, washed twice with PBS 1X, and then fixed with 4% paraformaldehyde/PBS for 10 min. Cells were permeabilized with 0.1% Triton X-100 diluted in PBS. Non-specific binding was blocked with 5% bovine serum albumin, 0.05% Tween-20 diluted in PBS for 1 h at room temperature. Cells were incubated with primary antibodies: anti-LRRK2 (1:500 Mjff2 c41-2 Eptomics), anti-Flag (F3165 1:2000 Sigma-Aldrich), anti-Myc (M4439 1:2000, Sigma-Aldrich) diluted in blocking solution, overnight at $4\text{ }^{\circ}\text{C}$. Cells were then washed with PBS, 0.05% Tween-20 diluted in PBS and incubated with secondary antibodies: Goat anti-Mouse IgG Secondary Antibody Alexa Fluor[®] 488 (ThermoFisher Scientific, Waltham, MA, USA) and Goat anti-Mouse IgG Secondary Antibody Alexa Fluor[®] 647 (Life Technologies) diluted 1:1000 in blocking solution for 1 h at room temperature. Before analysis, cells were mounted using Mowiol mounting medium, and fluorescence was revealed with a Leica TCS SP5 confocal microscope with LAS lite 170 image software.

2.10. Disuccinimidyl Suberate (DSS) Cross-Linking

The experiment was performed following the manufactory's instructions (21555 ThermoFisher Scientific, Waltham, MA, USA). Briefly, $\sim 2.5 \times 10^6$ cells in 6 cm plates were washed by PBS1X, collected in PBS1X using a scraper, and resuspended in 100 microliters of PBS1X. DSS solution to a final concentration of 2 mM was added and incubated for 30 min at room temperature. Finally, the cells were lysed by 1 mL of NP40 lysis buffer (150 mM NaCl, 1% NP40, 20 mM Tris-HCl pH 7.5, protease inhibitor cocktail (Roche, Basel, Switzerland)), and protein extracts were used for immunoprecipitation experiments as previously described.

2.11. Statistical Analysis

The results are presented as means \pm SEM. of independent experiments as indicated. Statistical evaluation was conducted by One-way ANOVA and Bonferroni's multiple comparison post-test. Values significantly different from the relative control are indicated with one, two, or three asterisks when $p < 0.05$, $p < 0.005$, and $p < 0.001$, respectively.

3. Results

3.1. LRRK2 Interacts with Sec8

To identify LRRK2 protein interactors we decided to realize a GST-pull down approach. We subcloned three different LRRK2 domains (LRR, kinase, or WD40 domain) in frame with GST to generate GST-LRR, GST-Kinase, or GST-WD40 constructs. All recombinant proteins were expressed in the BL21 strain of *E. coli* and purified by affinity chromatography. The purified proteins (GST-LRR, GST-WD40, or GST-Kinase) were used in GST pull-down experiments with 5 mg of mouse brain protein extracts. The mouse brain proteins interacting with the different GST-fused LRRK2 domains were separated by SDS-PAGE and identified by Mass Spectrometry. Interestingly we found that the GST-Kinase domain (but not the GST-LRR or GST-WD40) associates specifically with a protein of roughly 110 kD (Figure 1A). Mass spectrometry analysis permitted to identify this protein as Sec8, a member of the exocyst complex.

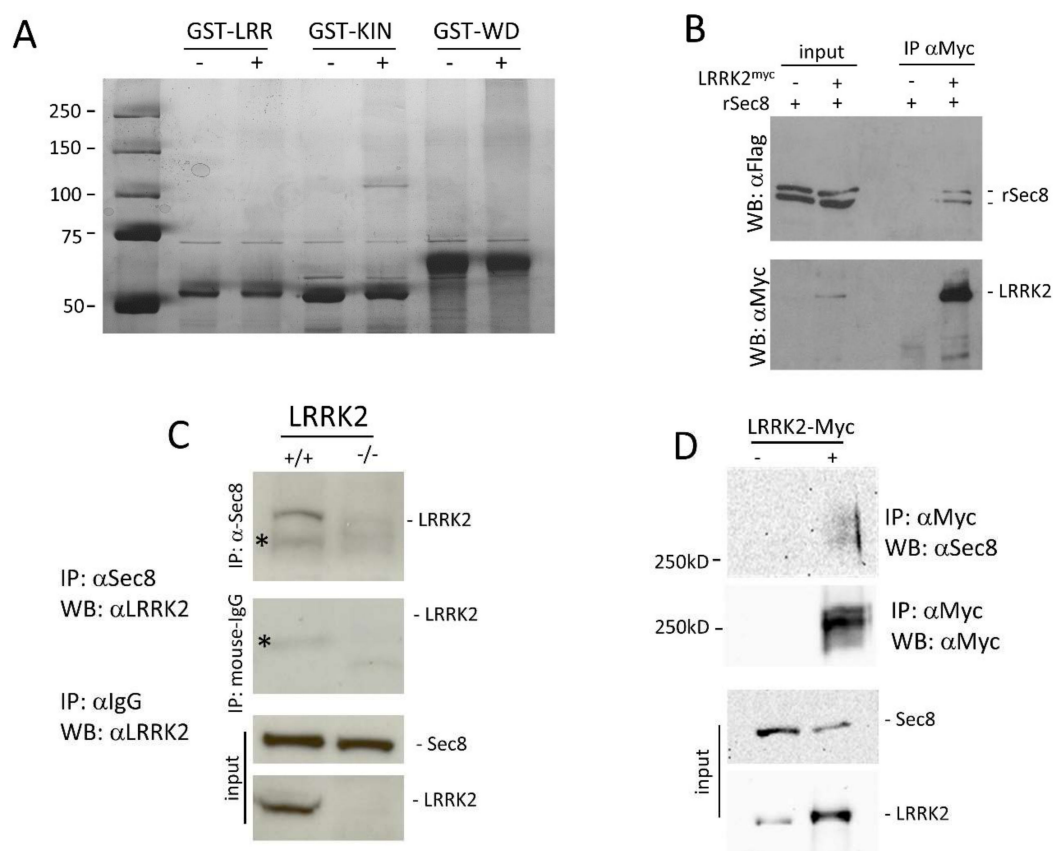


Figure 1. Analysis of LRRK2 and Sec8 physical interaction and colocalization. (A) 5 mg of mouse brain protein extracts were used for a GST pull-down experiment using three different LRRK2 domains: LRR, Kinase, and WD40. The protein complexes were separated by reducing SDS-PAGE and subjected to sensitive colloidal Coomassie Brilliant Blue staining. (B) HEK293 cells were transfected by ratSec8-Flag or co-transfected by Flag-ratSec8/Myc-LRRK2 WT for 48 h. The cells were lysed and the protein extracts were subjected to a co-immunoprecipitation experiment using an anti-Myc antibody. Total and immunoprecipitated proteins were visualized by western blot using an anti-Flag antibody to visualize ratSec8. Then the membrane was incubated by an anti-Myc to evaluate the immunoprecipitation efficacy. (C) Mouse brain protein extracts from WT or LRRK2 knock-out mice were subjected to a co-immunoprecipitation experiment using an anti-Sec8 or anti-IgG antibody and the immunocomplex were revealed by an anti-LRRK2 antibody. Anti-Sec8 and anti-LRRK2 were also used on the input fraction as the control for equal protein amount. * indicates a nonspecific band. (D) HEK293 cells were transfected or not by Myc-LRRK2 WT for 48 h. The cells were treated by DSS and protein extracts were subjected to a co-immunoprecipitation experiment using an anti-Myc antibody. Immunoprecipitated proteins were visualized by western blot using an anti-sec8 antibody to visualise endogenous Sec8. Then the membrane was incubated by an anti-Myc to evaluate the immunoprecipitation efficacy. The protein levels of endogenous Sec8 and endogenous or transfected LRRK2-Myc were visualized by anti-Sec8 and anti LRRK2 respectively.

The interaction between LRRK2 and Sec8 was validated through two different co-immunoprecipitation experiments. HEK293 cells were transfected by a plasmid construct coding Flag-ratSec8 or co-transfected by LRRK2-Myc and Flag-ratSec8. Using protein extracts prepared 48 h after transfection, we performed a co-immunoprecipitation experiment using an anti-Myc antibody for immunoprecipitation and anti-Flag antibody for the subsequent western blot analysis of the complexes. As illustrated in Figure 1B the immunoprecipitation by anti-Myc pulls down specifically Flag-ratSec8 (Figure 1B upper). Note that ratSec8 appears as a doublet band in a typical SDS-PAGE analysis [40]. The filter was then probed by an anti-Myc antibody to control the LRRK2 expression level and immunoprecipitation efficacy (Figure 1B lower).

To ensure that our results in HEK293 cells were physiologically relevant at protein endogenous levels, we performed a second co-immunoprecipitation experiment using striatal brain tissues using commercially available antibodies against LRRK2 or Sec8. The Sec8 immunoprecipitation pulls down LRRK2 in WT (+/+) but not in the LRRK2 knock-out (−/−) mouse brain (Figure 1C). To further confirm the LRRK2/Sec8 interaction we performed a cross-linking experiment using the membrane-permeable compound disuccinimidyl suberate (DSS). HEK293 cells were transfected by LRRK2-Myc for 48 h. Before lysis, the cells were treated with DSS, and then the protein extracts were used for a co-IP experiment using an anti-Myc antibody. As shown in Figure 1D endogenous Sec8 appears as a protein smear of molecular weight higher than 250 kD. All these findings clearly indicate the spatial proximity of LRRK2 and Sec8 strongly suggesting that they are part of a common protein complex.

Human Sec8 is a protein of roughly 110 kD (974aa) with not well-defined functional domains. To identify the Sec8 protein region interacting with LRRK2 we decided to create five different Flag-hSec8 deletion mutants. Each mutant is devoid of roughly 200 amino acids (Figure 2A). All Sec8 deletion mutants are stable when expressed in HEK293 cells (Figure 2B) with no gross alteration in the cytoplasmic localization (Figure 2C).

Then we performed a co-immunoprecipitation experiment co-transfecting HEK293 cells by Myc-LRRK2 with one of the different Sec8 deletion mutants. As shown in Figure 2D the lack of the C-terminal part of Sec8 protein ($\Delta 5$) leads to the loss of LRRK2 protein interaction. We repeated a similar experiment using LRRK2 deletion mutants [43]. The absence of the kinase domain of LRRK2 strongly reduces the Sec8 binding (Figure 2E and Figure S1A) although this interaction still slightly occurs suggesting a more intricate LRRK2/Sec8 interaction involving other LRRK2 protein domains.

Once validated the LRRK2/Sec8 protein interaction, we have analyzed the potential role of LRRK2 in modulating Sec8 phosphorylation. Sec8 has been identified as an interactor using the kinase domain of LRRK2, therefore it was reasonable to suppose that Sec8 could be a direct substrate of LRRK2 kinase activity. Although we used different experimental approaches including a phosphorylation site identification by a Mass Spectrometry covering roughly 75% of the Sec8 protein, we were not able to highlight any significant change in Sec8 phosphorylation level due to the presence of LRRK2 WT or G2019S pathological mutant (data not shown).

3.2. LRRK2 Modulates the Exocyst Complex Assembly

To explore the consequence of LRRK2 expression on Sec8 function, we have evaluated the LRRK2 effect on Sec8 sub-cellular localization, using a biochemical approach. Sec8 is a cytoplasmic protein distributed in the cytosol or associated with cytoplasmic membrane or vesicles [44]. To investigate any possible alteration in Sec8 subcellular distribution mediated by LRRK2, we transfected HEK293 cells with Sec8-Flag alone or in combination with LRRK2WT or G2019S mutant. 48 h after transfection the cells were lysed and four different cellular fractions were purified: total, cytosolic, membrane, or vesicle. As illustrated in Figure 3A neither the expression of LRRK2 WT nor G2019S could significantly alter the Sec8 subcellular distribution compared to the cells expressing Sec8 alone. Some apparent differences in Sec8 subcellular distribution are only due to differences in transfection

efficacy as pointed out by the analysis of total fractions and by the statistical analysis (Figure S1B).

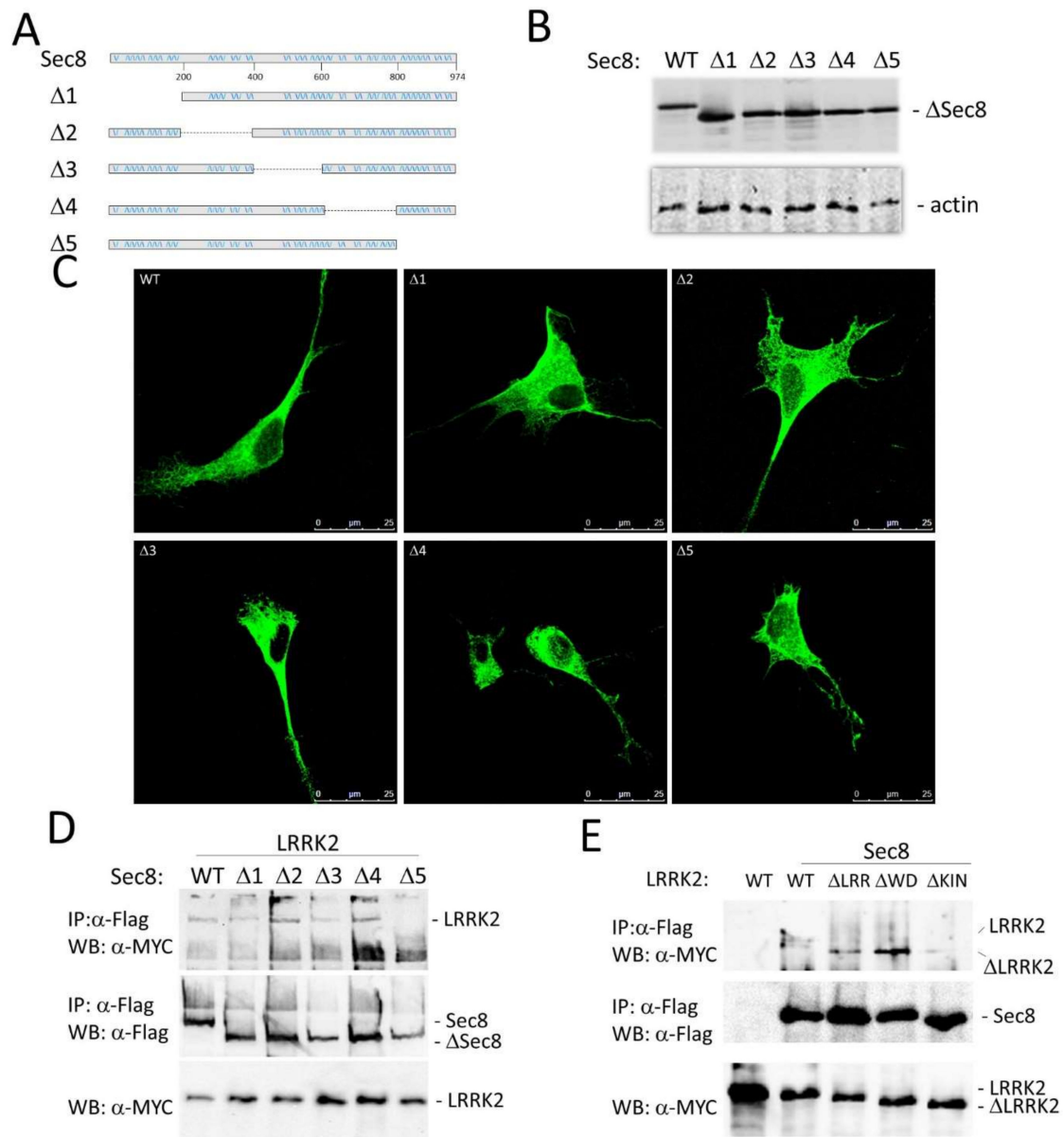


Figure 2. Identification of Sec8 protein region interacting with LRRK2. (A) Schematic representation of the Sec8 five deletion mutants generated. (B) HEK293 cells were transfected by the different Sec8 deletion mutants. 48 h after transfection, the protein extracts were analyzed by western blot using an antibody against Flag epitope to detect Sec8. (C) HEK293 cells were transfected with the five different Flag-Sec8 deletion mutants for 48 h. After fixation, the cells were incubated with anti-Flag primary antibody and with Alexa488-conjugated secondary antibody (green). (D) HEK293 cells were co-transfected by Flag-Sec8 WT or the Sec8 deletion mutants and Myc-LRRK2 WT for 48 h. The cells were lysed and the protein extracts were subjected to a co-immunoprecipitation experiment using an anti-Flag antibody. Total and immunoprecipitated proteins were visualized by western blot using an anti-Myc antibody to visualize LRRK2. Then the membrane was incubated by an anti-Flag to evaluate the immunoprecipitation efficacy. (E) HEK293 cells were transfected with Myc-LRRK2 WT or co-transfected with Myc-LRRK2 WT or LRR (ΔLRR) or Kinase (ΔKin) or WD40 (ΔWD40) deletion mutants and Flag-Sec8 for 48 h. The cells were lysed and the protein extracts were subjected to a co-immunoprecipitation experiment using an anti-Flag antibody. The co-immunoprecipitated proteins were visualized by western blot using an anti-Myc antibody to visualize LRRK2. Then the membrane was incubated by an anti-Flag to evaluate the immunoprecipitation efficacy. The input fraction was incubated by anti-Myc as the control for equal transfection efficacy of the different samples.

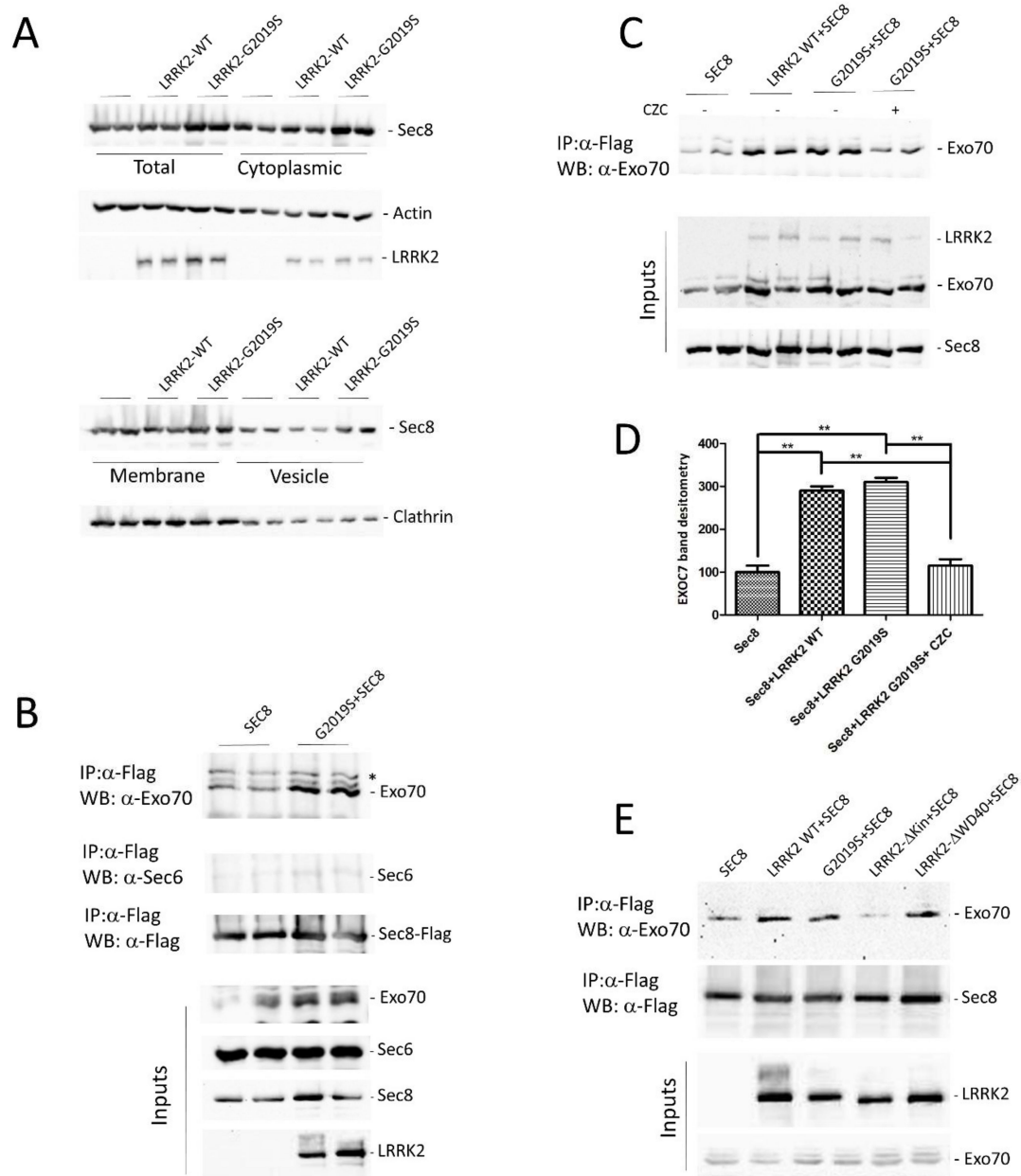


Figure 3. Evaluation of LRRK2 effect on Sec8 sub-cellular localization and exocyst assembly. **(A)** HEK 293 cells were transfected or co-transfected by the indicated plasmids. 48 h after transfection, different subcellular fractions (total, cytoplasm, membranes, and vesicles) were separated by differential centrifugation and analyzed by western blot using an antibody against Flag epitope to detect Sec8. Anti-β-actin and clathrin antibodies were used as loading control while anti-Myc was used to detect transfected LRRK2. **(B)** HEK293 cells were transfected or co-transfected for 48 h with Flag-Sec8 WT or Myc-LRRK2 G2019S as indicated. The cells were lysed and the protein extracts were subjected to a co-immunoprecipitation experiment using an anti-Flag antibody to isolate Sec8. The co-immunoprecipitated proteins were visualized by western blot using anti-Exo70 or Sec6 antibodies. Then the membrane was incubated by an anti-Flag to evaluate the Sec8 immunoprecipitation efficacy. The input fraction was incubated by anti-Exo70, Sec6 as a loading control, and anti-Flag or Myc as control of transfection efficacy. * indicates a nonspecific band **(C)** Co-immunoprecipitation experiment as in **(A)**. The LRRK2 kinase inhibitor (CZC 25146) was added 3 h before cell lysis. **(D)** Relative band densitometry for Exo70 of data obtained in **(C)** normalized to cells transfected by Sec8 alone. The data represent the mean ± SEM of three independent experiments. ** $p < 0.01$. One-way ANOVA and Bonferroni post-test were used. **(E)** Co-immunoprecipitation experiment as in **(A)** in the presence of two different LRRK2 deletion mutants: Kinase (ΔKin) or WD40 (ΔWD40) domains.

Then we have analyzed the association of exocyst complex in the presence of LRRK2. Sec8 associates in co-immunoprecipitation experiments with both Exo70 [45] and Sec6 [46], the other two members of the exocyst complex. In a preliminary experiment, we transfected HEK293 cells by Sec8-Flag alone or in the presence of LRRK2 G2019S. 48 h later, Sec8 was immunoprecipitated from protein extracts and the immuno-complexes were analyzed for the presence of Exo70 or Sec6. As shown in Figure 3B, in the presence of LRRK2 G2019S there is a significant increase in Sec8 association with Exo70 and to a less extent with Sec6. Then we repeated a similar experiment to evaluate any difference in Sec8-Exo70 association between LRRK2 WT or G2019S or in the presence of LRRK2 kinase inhibitor (CZC-25146). We confirmed that the presence of LRRK2 leads to an increase in Sec8/Exo70 interaction, with no significant differences between LRRK2 WT and G2019S mutant, and importantly this association is strongly reduced upon LRRK2 kinase inhibitor treatment (Figure 3C,D). Finally, to further explore the importance of the LRRK2 kinase domain in the exocyst complex assembly, we performed the same co-immunoprecipitation experiment using two different LRRK2 deletion mutants: delta-kinase and delta-WD40 domain. The lack of LRRK2 kinase domain significantly impairs the LRRK2 effect on SEC8/Exo70 association while no effect was detectable by the LRRK2 WD40 deletion mutant (Figure 3E and Figure S1C).

Taken together, our results underline a prominent role of LRRK2 in the modulation of exocyst complex association mainly mediated by LRRK2 kinase domain or activity.

3.3. Functional Role of LRRK2/Sec8 Interaction

We reasoned that Sec8, when overexpressed, could strongly interact with LRRK2, likely blocking the LRRK2 physio-pathological effect on endogenous Sec8 or, in the alternative, Sec8 overexpression could overcome the LRRK2 effect on endogenous exocyst complex. The most common and easily detectable phenotype of LRRK2 pathological mutant expression is the impairment in neurite outgrowth in neuronal cells in different experimental models [17,47,48]. Therefore, we decided to analyze the effect of Sec8 overexpression on PC12 differentiation in the presence of LRRK2 G2019S pathological mutant. As previously published, PC12-ON cells stably expressing a doxycycline-inducible form of LRRK2 G2019S showed a significant impairment in neurite outgrowth due to Nerve Growth Factor (NGF) treatment [48]. After transfection with Sec8-Flag, we started the differentiation by NGF treatment for 6 days in the presence or absence of doxycycline to induce the LRRK2 G2019S expression. The differentiated cells were analyzed by immunofluorescence using antibodies against LRRK2 and Flag (for Sec8). The results confirmed that PC12-ON expressing LRRK2 G2019S (treated by doxycycline) show the typical round cellular phenotype of PC12 cells (Figure 4A upper panel), whereas those cells co-expressing Sec8 showed a significant change in cell body morphology with elongated/branched cytoplasm shape, a typical differentiation sign (Figure 4A lower panel). The PC12 cells expressing only Sec8 appeared well elongated (Figure 4A intermediate panel) without any significant difference with PC12-ON untransfected cells (data not shown). The data presented in Figure 4 were quantified in the bar graph of Figure 4B by analyzing a high number of cells.

The percentage of differentiated cells in the presence of LRRK2 G2019S (treated by doxycycline) was lower than 11% while the Sec8 over-expression led to a significant rescue (roughly 50% compared to 75% of cells expressing only Sec8). Similar results were obtained in another experimental system, the neuroblastoma SH-SY5Y cells differentiated by retinoic acid treatment (data not shown). The results strongly suggest that the over-expression of Sec8 may interfere with the LRRK2 G2019S pathological phenotype. To further highlight the change in PC12 cell morphology we acquired some images by phase-contrast microscopy (Figure S1D).

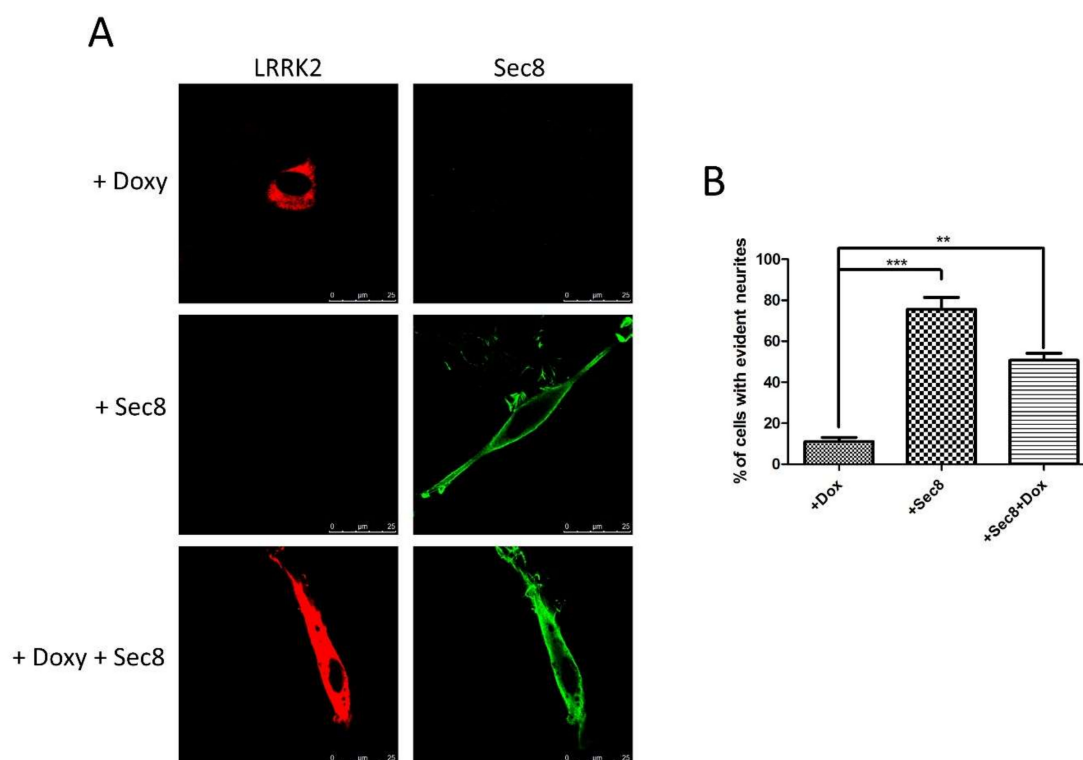


Figure 4. Analysis of Sec8 over-expression on neurite branching in PC12 or SH-SY5Y cells expressing LRRK2 G2019S. (A) PC12 cells stably expressing dox-inducible LRRK2 G2019S were transfected by Flag-Sec8 for 48 h and then treated for 6 days by NGF in the presence or absence of dox. (B) Quantification of data obtained in (A). The data represent the numbers of cells showing evident elongated cytoplasm in three independent experiments and are represented as mean \pm SEM. At least 20 cells have been analyzed for each biological replicate. ** $p < 0.01$; *** $p < 0.001$. One-way ANOVA and Bonferroni post-test were used.

4. Discussion

Dominant variants of LRRK2 are considered the main genetic cause of hereditary parkinsonism, ranging from 1–6% of cases including many sporadic cases [4]. Different experimental results suggest an important role of LRRK2 in the control of vesicle trafficking, and alteration in synaptic vesicle trafficking seems a common pathogenetic mechanism in PD [6]. Interestingly, we describe a specific protein interaction between LRRK2 and Sec8, a member of the exocyst complex. LRRK2 and Sec8 protein complex was analyzed in transfected cell cultures and, most importantly, in the mouse brain at physiological protein levels (Figure 1C). Moreover, a cross-linking experiment further supports the LRRK2-Sec8 protein proximity (Figure 1D). The exocyst complex plays a crucial role in vesicle dynamics involved in a wide range of cellular functions. This octameric complex has been mainly implicated in the vesicular transport and recruitment to regions of rapid membrane growth, a process followed by SNARE-mediated vesicle fusion. In neurons, members of the exocyst are engaged in neurite outgrowth, and in cooperation with multidomain scaffolding proteins controls receptor transport to the synapse [39,45,49].

As mentioned in the introduction, exocyst and Rabs (including Rab8 and Rab10, two LRRK2 phosphorylation targets) are part of the same protein complex [34]. In their GTP-bound form, Rab proteins interact with downstream effectors, including exocyst members, controlling various steps of vesicle trafficking. For instance, Rab10 colocalizes and interacts with exocyst proteins, in particular Sec8, at the base of nascent cilia in renal epithelial cells [50]; Sec8 loss of function mutations cause proximal dendritic arborization defects and lead to the accumulation of intracellular Rab10 vesicles [51]; furthermore, Sec15, another member of the exocyst complex, interacts with Rab11 and affects Rab11 localization in vivo [52]. Therefore, we favor the hypothesis that the interaction between LRRK2 and

Sec8 may explain different physio-pathological effects ascribed to LRRK2s including the cellular outcomes due to the LRRK2 modulation of Rab activity. We have identified the C-terminal region of Sec8 as the putative interaction region with LRRK2. Unfortunately, we could not use the Sec8 $\Delta 5$ deletion mutant for further experiments, since this mutant, although does not manifest gross alterations in the cellular localization (Figure 2C) shows a significant impairment in basal exocytosis (data not shown). This result is not surprising since Sec8 sequence analysis has shown that the Sec8 C-terminal region contains a type-1 PDZ-binding domain (TXV) that plays an important role in protein-protein interaction. For instance, this region regulates the interaction with two specific neuronal proteins: PSD-95 [36] and SAP102 [37], both concentrated at the post-synaptic density (PSD) of excitatory synapses and acting to assemble synaptic-signaling complexes.

Preliminary studies, mainly in yeast, had suggested that the exocyst complex can exist in two different sub-complexes: one contains Sec3, Sec5, Sec6, and Sec8 on vesicles, and the other contains Sec10, Sec15, Exo70, and Exo84 on the cell membrane [27]. The Sec3 and Exo70 localization at the plasma membrane seems dependent on the interaction with a phosphatidylinositol (4,5)-bisphosphate (PIP2) [53–55]. However, accumulating evidence questioned the existence of these two sub-complexes prior to the formation of the full complex since, for instance, the endogenous Sec3 protein shows a similar cellular distribution of the other exocyst subunits [56]. Furthermore, no sub-complexes could be isolated from *S. cerevisiae*, by more advanced biochemical studies [57]. In fact, Sec8 can interact with both Exo70 [45] and Sec6 [46] in co-immunoprecipitation experiments. Moreover, the Exo70 and Sec8 subunits are both associated with the intracellular domain of the neural cell adhesion molecule (NCAM) [38]. Based on these specific Sec8 interactions we decided to evaluate whether LRRK2 may affect the Sec8 association with Exo70 and Sec6. Interestingly, our experimental approach shows an increase in Sec8/Exo70 association in the presence of LRRK2. Furthermore, the LRRK2 effect is mediated by the LRRK2 kinase domain since it is significantly reduced either in the presence of LRRK2 kinase deletion mutant or by LRRK2 kinase inhibitor treatment. The effect of LRRK2 on Sec8/Sec 6 interaction in the co-immunoprecipitation experiment is less evident. The Sec6 co-IP is producing a very faint band although the antibody is well working in immunoblotting experiments. The result may be easily explained by the presence of Flag epitope or by the binding of the anti-Flag antibody both in the N-terminal position of Sec8. This Sec8 region is very relevant for Sec6 interaction since the deletion of the N-terminal domain of the Sec8 protein decreases its interaction with Sec6 while only slightly reduces its interaction with Exo70 [45]. The particular relevance of the LRRK2 kinase domain in modulating the Sec8/Exo70 interaction pushed us to evaluate any change in the phosphorylation level of Sec8 in the presence or absence of LRRK2 G2019S. Unfortunately, we were not able to identify any change in Sec8 phosphorylation either by in vitro kinase assay or by the analysis of Sec8 phospho-sites by Mass Spectrometry approach (data not shown).

Finally, we have explored the idea that Sec8, when over-expressed, could interact/sequester LRRK2 and eventually impair the LRRK2 G2019S pathological effect. Interestingly, Sec8 over-expression can significantly rescue the inhibition in differentiation due to LRRK2 G2019S expression (Figure 4). Future experiments are required to fully identify the molecular mechanism by which the LRRK2 kinase domain regulates exocyst complex assembly and function. However, our results agree with the suggested role of LRRK2 in the regulation of vesicle trafficking. Pharmaceutical compounds able to modulate vesicle trafficking may be a possible therapeutic option for PD treatment as recently suggested by the ability of Levetiracetam to rescue the LRRK2 G2019S pathological effect [48]. Levetiracetam acts by binding the SV2A protein located on synaptic vesicles and modulating the vesicle trafficking although by an unclear molecular mechanism. Recently, a new small molecule able to interfere with the exocyst complex has been identified: Endosidin2 (ES2) [58]. ES2 binds specifically to the Exo70 resulting in inhibition of exocytosis and endosomal recycling in both plant and human cells [58]. Could be worth designing specific

experiments exploring the possible use of subliminal doses of ES2 compound in reducing the LRRK2 mediated toxicity in cellular and animal models.

Supplementary Materials: The following are available online at <https://www.mdpi.com/2073-4409/10/2/203/s1>.

Author Contributions: Conceived and designed the experiments: C.I., C.C., F.T., V.L.D., and T.M.D.; Performed the experiments: M.F., Y.X., F.C., T.T.D.N., M.U.T.T., G.S., and C.I. Analysed the data: M.F., C.C., and C.I. Contributed reagents/materials/analysis tools: M.G. and P.S. Wrote the paper: C.I. and C.C. Edit the paper: C.I. and C.C. All authors have read and agreed to the published version of the manuscript.

Funding: This research was supported in part by Michael J. Fox Foundation (LRRK2 Challenge 2014 ID9550), Fondazione Banco di Sardegna (grant number 2014.0489), and Regione Sardegna (grant number CRP-78083) to C.I. and in part by grants from the NIH P50 NS38377 to T.M.D. T.M.D. is the Leonard and Madlyn Abramson Professor in Neurodegenerative Diseases. P.S. and M.F. were supported by Ph.D. fellowships granted by PON 2014–2020 (CCI2014IT16M2OP005).

Institutional Review Board Statement: The study was conducted according to the guidelines of the Declaration of Helsinki, and approved by the Johns Hopkins University Animal Care and Use Committee (protocol number M020M262 approved on 17 September 2020).

Informed Consent Statement: Not applicable.

Data Availability Statement: The data presented in this study are available on request from the corresponding author.

Acknowledgments: This paper is dedicated to the memory of our friend and colleague Maria Teresa Carri. We would like to acknowledge all the people from the laboratory that critically read the manuscript.

Conflicts of Interest: The authors declare no conflict of interest.

References

1. Healy, D.G.; Falchi, M.; O’Sullivan, S.S.; Bonifati, V.; Durr, A.; Bressman, S.; Brice, A.; Aasly, J.; Zabetian, C.P.; Goldwurm, S.; et al. Phenotype, genotype, and worldwide genetic penetrance of LRRK2-associated Parkinson’s disease: A case-control study. *Lancet Neurol.* **2008**, *7*, 583–590. [[CrossRef](#)]
2. Zimprich, A.; Biskup, S.; Leitner, P.; Lichtner, P.; Farrer, M.; Lincoln, S.; Kachergus, J.; Hulihan, M.; Uitti, R.J.; Calne, D.B.; et al. Mutations in LRRK2 cause autosomal-dominant parkinsonism with pleomorphic pathology. *Neuron* **2004**, *44*, 601–607. [[CrossRef](#)] [[PubMed](#)]
3. Paisan-Ruiz, C.; Jain, S.; Evans, E.W.; Gilks, W.P.; Simon, J.; van der Brug, M.; Lopez de Munain, A.; Aparicio, S.; Gil, A.M.; Khan, N.; et al. Cloning of the gene containing mutations that cause PARK8-linked Parkinson’s disease. *Neuron* **2004**, *44*, 595–600. [[CrossRef](#)] [[PubMed](#)]
4. Cookson, M.R. The role of leucine-rich repeat kinase 2 (LRRK2) in Parkinson’s disease. *Nat. Rev. Neurosci.* **2010**, *11*, 791–797. [[CrossRef](#)] [[PubMed](#)]
5. Sanna, G.; Del Giudice, M.G.; Crosio, C.; Iaccarino, C. LRRK2 and vesicle trafficking. *Biochem. Soc. Trans.* **2012**, *40*, 1117–1122. [[CrossRef](#)] [[PubMed](#)]
6. Esposito, G.; Ana Clara, F.; Verstreken, P. Synaptic vesicle trafficking and Parkinson’s disease. *Dev. Neurobiol.* **2012**, *72*, 134–144. [[CrossRef](#)] [[PubMed](#)]
7. Yun, H.J.; Kim, H.; Ga, I.; Oh, H.; Ho, D.H.; Kim, J.; Seo, H.; Son, I.; Seol, W. An early endosome regulator, Rab5b, is an LRRK2 kinase substrate. *J. Biochem.* **2015**, *157*, 485–495. [[CrossRef](#)]
8. Dodson, M.W.; Zhang, T.; Jiang, C.; Chen, S.; Guo, M. Roles of the Drosophila LRRK2 homolog in Rab7-dependent lysosomal positioning. *Hum. Mol. Genet.* **2012**, *21*, 1350–1363. [[CrossRef](#)]
9. MacLeod, D.A.; Rhinn, H.; Kuwahara, T.; Zolin, A.; Di Paolo, G.; McCabe, B.D.; Marder, K.S.; Honig, L.S.; Clark, L.N.; Small, S.A.; et al. RAB7L1 interacts with LRRK2 to modify intraneuronal protein sorting and Parkinson’s disease risk. *Neuron* **2013**, *77*, 425–439. [[CrossRef](#)]
10. Beilina, A.; Rudenko, I.N.; Kaganovich, A.; Civiero, L.; Chau, H.; Kalia, S.K.; Kalia, L.V.; Lobbstaël, E.; Chia, R.; Ndukwe, K.; et al. Unbiased screen for interactors of leucine-rich repeat kinase 2 supports a common pathway for sporadic and familial Parkinson disease. *Proc. Natl. Acad. Sci. USA* **2014**, *111*, 2626–2631. [[CrossRef](#)]
11. Cho, H.J.; Yu, J.; Xie, C.; Rudrabhatla, P.; Chen, X.; Wu, J.; Parisiadou, L.; Liu, G.; Sun, L.; Ma, B.; et al. Leucine-rich repeat kinase 2 regulates Sec16A at ER exit sites to allow ER-Golgi export. *EMBO J.* **2014**, *33*, 2314–2331. [[CrossRef](#)] [[PubMed](#)]

12. Steger, M.; Tonelli, F.; Ito, G.; Davies, P.; Trost, M.; Vetter, M.; Wachter, S.; Lorentzen, E.; Duddy, G.; Wilson, S.; et al. Phosphoproteomics reveals that Parkinson's disease kinase LRRK2 regulates a subset of Rab GTPases. *eLife* **2016**, *5*, e12813. [[CrossRef](#)] [[PubMed](#)]
13. Matta, S.; Van Kolen, K.; da Cunha, R.; van den Bogaart, G.; Mandemakers, W.; Miskiewicz, K.; De Bock, P.J.; Morais, V.A.; Vilain, S.; Haddad, D.; et al. LRRK2 controls an EndoA phosphorylation cycle in synaptic endocytosis. *Neuron* **2012**, *75*, 1008–1021. [[CrossRef](#)] [[PubMed](#)]
14. Parisiadou, L.; Yu, J.; Sgobio, C.; Xie, C.; Liu, G.; Sun, L.; Gu, X.L.; Lin, X.; Crowley, N.A.; Lovinger, D.M.; et al. LRRK2 regulates synaptogenesis and dopamine receptor activation through modulation of PKA activity. *Nat. Neurosci.* **2014**, *17*, 367–376. [[CrossRef](#)] [[PubMed](#)]
15. Jaleel, M.; Nichols, R.J.; Deak, M.; Campbell, D.G.; Gillardon, F.; Knebel, A.; Alessi, D.R. LRRK2 phosphorylates moesin at threonine-558: Characterization of how Parkinson's disease mutants affect kinase activity. *Biochem. J.* **2007**, *405*, 307–317. [[CrossRef](#)]
16. Godena, V.K.; Brookes-Hocking, N.; Moller, A.; Shaw, G.; Oswald, M.; Sancho, R.M.; Miller, C.C.; Whitworth, A.J.; De Vos, K.J. Increasing microtubule acetylation rescues axonal transport and locomotor deficits caused by LRRK2 Roc-COR domain mutations. *Nat. Commun.* **2014**, *5*, 5245. [[CrossRef](#)]
17. Law, B.M.; Spain, V.A.; Leinster, V.H.; Chia, R.; Beilina, A.; Cho, H.J.; Taymans, J.M.; Urban, M.K.; Sancho, R.M.; Blanca Ramirez, M.; et al. A direct interaction between leucine-rich repeat kinase 2 and specific beta-tubulin isoforms regulates tubulin acetylation. *J. Biol. Chem.* **2014**, *289*, 895–908. [[CrossRef](#)]
18. Piccoli, G.; Condliffe, S.B.; Bauer, M.; Giesert, F.; Boldt, K.; De Astis, S.; Meixner, A.; Sarioglu, H.; Vogt-Weisenhorn, D.M.; Wurst, W.; et al. LRRK2 controls synaptic vesicle storage and mobilization within the recycling pool. *J. Neurosci.* **2011**, *31*, 2225–2237. [[CrossRef](#)]
19. Pan, P.Y.; Li, X.; Wang, J.; Powell, J.; Wang, Q.; Zhang, Y.; Chen, Z.; Wicinski, B.; Hof, P.; Ryan, T.A.; et al. Parkinson's disease associated LRRK2 hyperactive kinase mutant disrupts synaptic vesicle trafficking in ventral midbrain neurons. *J. Neurosci.* **2017**, *37*, 11366–11376. [[CrossRef](#)]
20. Belluzzi, E.; Gonnelli, A.; Cinaru, M.D.; Marte, A.; Plotegher, N.; Russo, I.; Civiero, L.; Cogo, S.; Carrion, M.P.; Franchin, C.; et al. LRRK2 phosphorylates pre-synaptic N-ethylmaleimide sensitive fusion (NSF) protein enhancing its ATPase activity and SNARE complex disassembling rate. *Mol. Neurodegener.* **2016**, *11*, 1. [[CrossRef](#)]
21. Xiong, Y.; Neifert, S.; Karuppagounder, S.S.; Liu, Q.; Stankowski, J.N.; Lee, B.D.; Ko, H.S.; Lee, Y.; Grima, J.C.; Mao, X.; et al. Robust kinase- and age-dependent dopaminergic and norepinephrine neurodegeneration in LRRK2 G2019S transgenic mice. *Proc. Natl. Acad. Sci. USA* **2018**, *115*, 1635–1640. [[CrossRef](#)] [[PubMed](#)]
22. Rattu, M.; Del Giudice, M.G.; Sanna, S.; Taymans, J.M.; Morari, M.; Brugnoli, A.; Frassinetti, M.; Masala, A.; Esposito, S.; Galioto, M.; et al. Role of LRRK2 in the regulation of dopamine receptor trafficking. *PLoS ONE* **2017**, *12*, e0179082. [[CrossRef](#)] [[PubMed](#)]
23. Beccano-Kelly, D.A.; Volta, M.; Munsie, L.N.; Paschall, S.A.; Tatarnikov, I.; Co, K.; Chou, P.; Cao, L.P.; Bergeron, S.; Mitchell, E.; et al. LRRK2 overexpression alters glutamatergic presynaptic plasticity, striatal dopamine tone, postsynaptic signal transduction, motor activity and memory. *Hum. Mol. Genet.* **2015**, *24*, 1336–1349. [[CrossRef](#)] [[PubMed](#)]
24. Matikainen-Ankney, B.A.; Kezunovic, N.; Mesias, R.E.; Tian, Y.; Williams, F.M.; Huntley, G.W.; Benson, D.L. Altered Development of Synapse Structure and Function in Striatum Caused by Parkinson's Disease-Linked LRRK2-G2019S Mutation. *J. Neurosci.* **2016**, *36*, 7128–7141. [[CrossRef](#)]
25. Volta, M.; Beccano-Kelly, D.A.; Paschall, S.A.; Cataldi, S.; MacIsaac, S.E.; Kuhlmann, N.; Kadgien, C.A.; Tatarnikov, I.; Fox, J.; Khinda, J.; et al. Initial elevations in glutamate and dopamine neurotransmission decline with age, as does exploratory behavior, in LRRK2 G2019S knock-in mice. *eLife* **2017**, *6*, e28377. [[CrossRef](#)]
26. Sheehan, P.; Yue, Z. Deregulation of autophagy and vesicle trafficking in Parkinson's disease. *Neurosci. Lett.* **2019**, *697*, 59–65. [[CrossRef](#)]
27. Wu, B.; Guo, W. The Exocyst at a Glance. *J. Cell Sci.* **2015**, *128*, 2957–2964. [[CrossRef](#)]
28. Morgera, F.; Sallah, M.R.; Dubuke, M.L.; Gandhi, P.; Brewer, D.N.; Carr, C.M.; Munson, M. Regulation of exocytosis by the exocyst subunit Sec6 and the SM protein Sec1. *Mol. Biol. Cell* **2012**, *23*, 337–346. [[CrossRef](#)]
29. Martin-Urdiroz, M.; Deeks, M.J.; Horton, C.G.; Dawe, H.R.; Jourdain, I. The Exocyst Complex in Health and Disease. *Front. Cell Dev. Biol.* **2016**, *4*, 24. [[CrossRef](#)]
30. Murthy, M.; Garza, D.; Scheller, R.H.; Schwarz, T.L. Mutations in the exocyst component Sec5 disrupt neuronal membrane traffic, but neurotransmitter release persists. *Neuron* **2003**, *37*, 433–447. [[CrossRef](#)]
31. Pommereit, D.; Wouters, F.S. An NGF-induced Exo70-TC10 complex locally antagonises Cdc42-mediated activation of N-WASP to modulate neurite outgrowth. *J. Cell Sci.* **2007**, *120*, 2694–2705. [[CrossRef](#)] [[PubMed](#)]
32. Koon, A.C.; Chen, Z.S.; Peng, S.; Fung, J.M.S.; Zhang, X.; Lembke, K.M.; Chow, H.K.; Frank, C.A.; Jiang, L.; Lau, K.F.; et al. Drosophila Exo70 Is Essential for Neurite Extension and Survival under Thermal Stress. *J. Neurosci.* **2018**, *38*, 8071–8086. [[CrossRef](#)] [[PubMed](#)]
33. Lira, M.; Arancibia, D.; Orrego, P.R.; Montenegro-Venegas, C.; Cruz, Y.; Garcia, J.; Leal-Ortiz, S.; Godoy, J.A.; Gundelfinger, E.D.; Inestrosa, N.C.; et al. The Exocyst Component Exo70 Modulates Dendrite Arbor Formation, Synapse Density, and Spine Maturation in Primary Hippocampal Neurons. *Mol. Neurobiol.* **2019**, *56*, 4620–4638. [[CrossRef](#)] [[PubMed](#)]
34. Das, A.; Guo, W. Rabs and the exocyst in ciliogenesis, tubulogenesis and beyond. *Trends Cell Biol.* **2011**, *21*, 383–386. [[CrossRef](#)]

35. Friedrich, G.A.; Hildebrand, J.D.; Soriano, P. The secretory protein Sec8 is required for paraxial mesoderm formation in the mouse. *Dev. Biol.* **1997**, *192*, 364–374. [[CrossRef](#)]
36. Riefler, G.M.; Balasingam, G.; Lucas, K.G.; Wang, S.; Hsu, S.C.; Firestein, B.L. Exocyst complex subunit sec8 binds to postsynaptic density protein-95 (PSD-95): A novel interaction regulated by cypin (cytosolic PSD-95 interactor). *Biochem. J.* **2003**, *373*, 49–55. [[CrossRef](#)]
37. Sans, N.; Prybylowski, K.; Petralia, R.S.; Chang, K.; Wang, Y.X.; Racca, C.; Vicini, S.; Wenthold, R.J. NMDA receptor trafficking through an interaction between PDZ proteins and the exocyst complex. *Nat. Cell Biol.* **2003**, *5*, 520–530. [[CrossRef](#)]
38. Chernyshova, Y.; Leshchyn'ska, I.; Hsu, S.C.; Schachner, M.; Sytnyk, V. The neural cell adhesion molecule promotes FGFR-dependent phosphorylation and membrane targeting of the exocyst complex to induce exocytosis in growth cones. *J. Neurosci.* **2011**, *31*, 3522–3535. [[CrossRef](#)]
39. Tanaka, T.; Goto, K.; Iino, M. Diverse Functions and Signal Transduction of the Exocyst Complex in Tumor Cells. *J. Cell. Physiol.* **2017**, *232*, 939–957. [[CrossRef](#)]
40. Lyons, P.D.; Peck, G.R.; Kettenbach, A.N.; Gerber, S.A.; Roudaia, L.; Lienhard, G.E. Insulin stimulates the phosphorylation of the exocyst protein Sec8 in adipocytes. *Biosci. Rep.* **2009**, *29*, 229–235. [[CrossRef](#)]
41. Iaccarino, C.; Mura, M.E.; Esposito, S.; Carta, F.; Sanna, G.; Turrini, F.; Carri, M.T.; Crosio, C. Bcl2-A1 interacts with pro-caspase-3: Implications for amyotrophic lateral sclerosis. *Neurobiol. Dis.* **2011**, *43*, 642–650. [[CrossRef](#)] [[PubMed](#)]
42. Migheli, R.; Del Giudice, M.G.; Spissu, Y.; Sanna, G.; Xiong, Y.; Dawson, T.M.; Dawson, V.L.; Galioto, M.; Rocchitta, G.; Biosa, A.; et al. LRRK2 affects vesicle trafficking, neurotransmitter extracellular level and membrane receptor localization. *PLoS ONE* **2013**, *8*, e77198. [[CrossRef](#)] [[PubMed](#)]
43. Iaccarino, C.; Crosio, C.; Vitale, C.; Sanna, G.; Carri, M.T.; Barone, P. Apoptotic mechanisms in mutant LRRK2-mediated cell death. *Hum. Mol. Genet.* **2007**, *16*, 1319–1326. [[CrossRef](#)] [[PubMed](#)]
44. Yeaman, C.; Grindstaff, K.K.; Wright, J.R.; Nelson, W.J. Sec6/8 complexes on trans-Golgi network and plasma membrane regulate late stages of exocytosis in mammalian cells. *J. Cell Biol.* **2001**, *155*, 593–604. [[CrossRef](#)]
45. Vega, I.E.; Hsu, S.C. The exocyst complex associates with microtubules to mediate vesicle targeting and neurite outgrowth. *J. Neurosci.* **2001**, *21*, 3839–3848. [[CrossRef](#)]
46. Hsu, S.C.; Ting, A.E.; Hazuka, C.D.; Davanger, S.; Kenny, J.W.; Kee, Y.; Scheller, R.H. The mammalian brain rsec6/8 complex. *Neuron* **1996**, *17*, 1209–1219. [[CrossRef](#)]
47. Civiero, L.; Cirnaru, M.D.; Beilina, A.; Rodella, U.; Russo, I.; Belluzzi, E.; Lobbstaël, E.; Reyniers, L.; Hondhamuni, G.; Lewis, P.A.; et al. Leucine-rich repeat kinase 2 interacts with p21-activated kinase 6 to control neurite complexity in mammalian brain. *J. Neurochem.* **2015**, *135*, 1242–1256. [[CrossRef](#)]
48. Rassa, M.; Biosa, A.; Galioto, M.; Fais, M.; Sini, P.; Greggio, E.; Piccoli, G.; Crosio, C.; Iaccarino, C. Levetiracetam treatment ameliorates LRRK2 pathological mutant phenotype. *J. Cell. Mol. Med.* **2019**, *23*, 8505–8510. [[CrossRef](#)]
49. Anitei, M.; Ifrim, M.; Ewart, M.A.; Cowan, A.E.; Carson, J.H.; Bansal, R.; Pfeiffer, S.E. A role for Sec8 in oligodendrocyte morphological differentiation. *J. Cell Sci.* **2006**, *119*, 807–818. [[CrossRef](#)]
50. Babbey, C.M.; Bacallao, R.L.; Dunn, K.W. Rab10 associates with primary cilia and the exocyst complex in renal epithelial cells. *American journal of physiology. Ren. Physiol.* **2010**, *299*, F495–F506. [[CrossRef](#)]
51. Zou, W.; Yadav, S.; DeVault, L.; Nung Jan, Y.; Sherwood, D.R. RAB-10-Dependent Membrane Transport Is Required for Dendrite Arborization. *PLoS Genet.* **2015**, *11*, e1005484. [[CrossRef](#)] [[PubMed](#)]
52. Wu, S.; Mehta, S.Q.; Pichaud, F.; Bellen, H.J.; Quijcho, F.A. Sec15 interacts with Rab11 via a novel domain and affects Rab11 localization in vivo. *Nat. Struct. Mol. Biol.* **2005**, *12*, 879–885. [[CrossRef](#)] [[PubMed](#)]
53. He, B.; Xi, F.; Zhang, X.; Zhang, J.; Guo, W. Exo70 interacts with phospholipids and mediates the targeting of the exocyst to the plasma membrane. *EMBO J.* **2007**, *26*, 4053–4065. [[CrossRef](#)] [[PubMed](#)]
54. Liu, J.; Zuo, X.; Yue, P.; Guo, W. Phosphatidylinositol 4,5-bisphosphate mediates the targeting of the exocyst to the plasma membrane for exocytosis in mammalian cells. *Mol. Biol. Cell* **2007**, *18*, 4483–4492. [[CrossRef](#)] [[PubMed](#)]
55. Pleskot, R.; Cwiklik, L.; Jungwirth, P.; Zarsky, V.; Potocky, M. Membrane targeting of the yeast exocyst complex. *Biochim. Biophys. Acta* **2015**, *1848*, 1481–1489. [[CrossRef](#)]
56. Roumanie, O.; Wu, H.; Molk, J.N.; Rossi, G.; Bloom, K.; Brennwald, P. Rho GTPase regulation of exocytosis in yeast is independent of GTP hydrolysis and polarization of the exocyst complex. *J. Cell Biol.* **2005**, *170*, 583–594. [[CrossRef](#)]
57. Heider, M.R.; Gu, M.; Duffy, C.M.; Mirza, A.M.; Marcotte, L.L.; Walls, A.C.; Farrall, N.; Hakhverdyan, Z.; Field, M.C.; Rout, M.P.; et al. Subunit connectivity, assembly determinants and architecture of the yeast exocyst complex. *Nat. Struct. Mol. Biol.* **2016**, *23*, 59–66. [[CrossRef](#)]
58. Zhang, C.; Brown, M.Q.; van de Ven, W.; Zhang, Z.M.; Wu, B.; Young, M.C.; Synek, L.; Borchardt, D.; Harrison, R.; Pan, S.; et al. Endosidin2 targets conserved exocyst complex subunit EXO70 to inhibit exocytosis. *Proc. Natl. Acad. Sci. USA* **2016**, *113*, E41–E50. [[CrossRef](#)]

2.4

Result 4: Parkinson's disease-related genes and lipid alteration

Finally, during my PhD I focused my attention on lipid alteration in relation to Parkinson's disease. We wrote a review article analysing the specific lipid alterations described both in PD patients and PD experimental models.

Changes in membrane lipids have been observed in both affected and unaffected regions of the brain of patients with PD, and in several experimental models expressing genes causative or risk factors for PD, indicating that altered lipid metabolism may precede disease development.

Both localization and aggregation of α -synuclein depend on the specific composition of membrane lipids, and LRRK2 may regulate lipid metabolism directly or, more likely, indirectly through control of vesicle trafficking by phosphorylation of RABs.

In addition, the synthesis and delivery of endogenous lipids is of particular relevance in neurons because some circulating plasma lipids cannot reach these cells due to the presence of the blood-brain barrier. Different PD causative genes are directly or indirectly involved in the control of lipid metabolism and trafficking. For instance, SYNJ1 and PLA2G6 are directly involved in the control of lipid metabolism; they are both localized on neuronal mitochondria, endosomal and lysosomal membranes, and the plasma membrane and could play an essential role in the remodelling of membrane phospholipids in cell organelles or axons and synapses. GBA is clearly and directly implicated in lipid metabolism.

Pathological GBA mutations result in reduced glucocerebrosidase activity and a significant alteration in lipid composition.



Review

Parkinson's Disease-Related Genes and Lipid Alteration

Milena Fais ¹, Antonio Dore ², Manuela Galioto ¹, Grazia Galleri ³, Claudia Crosio ¹ and Ciro Iaccarino ^{1,*}

¹ Department of Biomedical Sciences, University of Sassari, 07100 Sassari, Italy; faismilena@gmail.com (M.F.); galioto@uniss.it (M.G.); ccrosio@uniss.it (C.C.)

² Istituto di Scienza delle Produzioni Alimentari, CNR, 07040 Sassari, Italy; antonio.dore@cnr.it

³ Department of Medical, Surgical and Experimental Sciences, University of Sassari, 07100 Sassari, Italy; galleri@uniss.it

* Correspondence: ciaccarino@uniss.it; Tel.: +39-079-228610

Abstract: Parkinson's disease (PD) is a complex and progressive neurodegenerative disorder with a prevalence of approximately 0.5–1% among those aged 65–70 years. Although most of its clinical manifestations are due to a loss of dopaminergic neurons, the PD etiology is largely unknown. PD is caused by a combination of genetic and environmental factors, and the exact interplay between genes and the environment is still debated. Several biological processes have been implicated in PD, including mitochondrial or lysosomal dysfunctions, alteration in protein clearance, and neuroinflammation, but a common molecular mechanism connecting the different cellular alterations remains incompletely understood. Accumulating evidence underlines a significant role of lipids in the pathological pathways leading to PD. Beside the well-described lipid alteration in idiopathic PD, this review summarizes the several lipid alterations observed in experimental models expressing PD-related genes and suggests a possible scenario in relationship to the molecular mechanisms of neuronal toxicity. PD could be considered a lipid-induced proteinopathy, where alteration in lipid composition or metabolism could induce protein alteration—for instance, alpha-synuclein accumulation—and finally neuronal death.

Keywords: Parkinson's disease; lipid metabolism; alpha-synuclein; GBA; LRRK2



Citation: Fais, M.; Dore, A.; Galioto, M.; Galleri, G.; Crosio, C.; Iaccarino, C. Parkinson's Disease-Related Genes and Lipid Alteration. *Int. J. Mol. Sci.* **2021**, *22*, 7630. <https://doi.org/10.3390/ijms22147630>

Academic Editors: Ornit Chiba-Falek and Boris Kantor

Received: 4 June 2021

Accepted: 14 July 2021

Published: 16 July 2021

Publisher's Note: MDPI stays neutral with regard to jurisdictional claims in published maps and institutional affiliations.



Copyright: © 2021 by the authors. Licensee MDPI, Basel, Switzerland. This article is an open access article distributed under the terms and conditions of the Creative Commons Attribution (CC BY) license (<https://creativecommons.org/licenses/by/4.0/>).

1. Introduction

Parkinson's Disease (PD) is the second most common neurodegenerative disorder characterized mainly by the progressive loss of dopaminergic neurons of the substantia nigra pars compacta and other monoaminergic cell groups in the brainstem [1]. The depletion of the neurotransmitter dopamine in the nigrostriatal system leads to the hallmark motor symptoms of PD, such as bradykinesia, rigidity, resting tremor, and postural and gait impairment. More than 6 million people worldwide are living with PD and this number is estimated to double by the year 2040. Importantly, PD symptoms appear when more than 50–70% of nigrostriatal dopaminergic neurons have been lost; thus, the human population of undiagnosed asymptomatic patients is probably large. Up to now, no treatment can slow the dopaminergic neuronal death and PD progression of PD; the main pharmacological treatments (levodopa and dopamine agonists) only relieve motor symptoms. Neuropathologically, PD is characterized by the presence of proteinaceous inclusions termed Lewy bodies (LBs), primarily composed of alpha-synuclein (α -syn) aggregates. The etiology of PD is unknown, although older age and neurotoxins are established risk factors, and smoking appears to be protective [1]. Although the pathogenesis of PD remains incompletely understood, both genetic susceptibility and environmental factors appear to be involved [2]. The identification of rare familial forms of parkinsonism and the subsequent cloning of causal genetic mutations has had a significant impact on our understanding of the molecular mechanisms underlying idiopathic PD. Genes whose mutations have been associated with parkinsonism include autosomal dominantly (α -synuclein, LRRK2, VPS35, EIF4G1) as

well as recessively (PARK2, PINK1, DJ-1, SYNJ1, and PLA2G6) inherited mutations [3,4]. Moreover, heterozygous mutations in the gene encoding β -glucocerebrosidase (GBA) are considered the greatest genetic risk factor for developing PD [5].

The similarities in the pathological and clinical phenotypes between sporadic and familiar PD forms in humans suggest that different causes may lead to a common neuropathological cascade of events. In this context, lipids are implicated in many aspects of PD pathology, ranging from specific cytotoxic interactions with PD-causative genes, lipid pathways or metabolism alterations in PD patients or experimental models to mutations in enzymes involved in lipid metabolism that significantly enhance PD risk. Different reviews exploring lipid alteration in idiopathic PD have already been published [6,7], while an extensive analysis of significant alteration on either lipid pathways or metabolism in familial PD patients or in experimental models expressing different PD-causative or -susceptibility genes is largely lacking.

2. Lipid Alteration in the Different PD-Related Genes

2.1. Alpha-Synuclein (PARK1-4)

Different lines of evidence underline an important role of lipids in α -syn physiology and pathology. Likewise, α -syn possibly regulates lipid metabolism. Alpha-syn has a disordered conformation in solution, while it can assume an α -helical structure upon membrane lipid binding [8]. The lipid composition strongly affects α -syn binding to membranes as well as α -syn aggregation and propagation. Initially, Davidson and colleagues showed that α -syn preferentially binds to vesicles containing acidic phospholipids [8], then the results were confirmed by other independent groups [9,10]. Moreover, either lipid composition, for instance the presence of 1-O-hexadecyl-2-acetyl-sn-glycero-3-phosphocholine (C16:0 PAF) [11] or arachidonoyl and docosahexaenoyl polyunsaturated fatty acids [12] or changes in chemical properties of the lipids [13] are likely to be key factors in regulating the balance between functional and deleterious interactions of α -syn with membranes. Docosahexaenoic acid (DHA), an abundant fatty acid of neuronal membranes, readily promotes α -syn aggregation and the morphology of aggregates is dependent on the ratio between the protein content and DHA [14]. Physiologically, α -syn was first shown to co-localize with synaptic vesicles [15] and afterwards, it was identified around different membrane structures [16] and brain lipids [17]. For instance, α -syn is associated to phospholipid monolayers, mainly containing high levels of triacylglycerols (TAGs), around lipid droplets (LD), and, interestingly, the pathological synuclein mutant seems to affect the TAGs hydrolysis compared with WT α -syn [18]. Moreover, α -syn is associated to mitochondria and this interaction requires cardiolipin, a mitochondria-specific lipid, and the anionic charge of the diphosphatidyl glycerol headgroup in particular [10]. Cole et al. demonstrated that cytosolic acidification rapidly induces α -syn translocation to mitochondrial surface, likely by low pH-induced exposure of cardiolipin on the mitochondrial membrane [19].

An interesting recent study, mostly based on correlative light and electron microscopy, postulated that LBs are largely composed of lipids, membrane fragments, and membranous organelles, such as vesicles [20]. This would be consistent with the idea that α -syn-membrane interaction could be the nucleation event in the aggregation of the α -syn protein [21]. Importantly, the prospect that at least some LBs may be largely composed of vesicle clusters, lipid droplets, membranes, and mitochondria rather than solely fibrillar α -syn offers a potential important change in the way we conceptualize PD pathogenesis.

As mentioned above, α -syn also plays an important role in lipid metabolism and homeostasis. Alpha-syn expression regulates the acyl-CoA synthetase activity, likely modulating the acyl-CoA synthetase localization to endoplasmic reticulum leading to an alteration in arachidonate (20:4n-6) turnover in brain phospholipids in α -syn KO mice [22]. Likewise, activation of Acyl-CoA synthetase leading to an increase in TAG content was obtained by A53T α -syn overexpression in N27 dopaminergic neuronal cells [23]. Controversial results have been accumulated related to alpha-synuclein inhibition of phospholipase D activity. Although initial studies have identified alpha and beta-synucleins as potent

and specific inhibitors of phospholipase D2 activity [24], subsequent studies, using either purified proteins in cell-free assays or different cell line experimental models, have not confirmed a significant inhibitory effect of α -syn on the PLD activity [25]. However, many experimental results strongly suggest a functional interaction between α -syn and phospholipase D. For instance, *pld2* overexpression in rat Substantia Nigra pars compacta causes the loss of dopaminergic neurons due to excess of lipase activity, and, interestingly, α -syn co-expression suppressed the PLD2 toxicity [26]. Moreover, phospholipase D1 regulates the autophagic flux and clearance of alpha-synuclein aggregates [27], while the overexpression of wild-type α -syn in human neuroblastoma cells inhibits the PLD1 expression [28].

The analysis of brain phospholipids in alpha-syn knockout mice has shown different alteration in lipid metabolism with an increase in docosahexaenoic acid incorporation and turnover [29] or an increase in cholesteryl esters and cholesterol mass [30,31] and a reduction in both cardiolipin and its precursor phosphatidylglycerol concentration [32].

2.2. Glucocerebrosidase (GBA)

Heterozygous mutations in the *gba* gene, encoding lysosomal enzyme glucocerebrosidase (GCase), represent the most common genetic risk factor for PD. GBA deficiency, first discovered in patients suffering from Gaucher Disease (GD), results in the accumulation of glycolipids in macrophages residing in liver, lung and spleen and importantly, type 2 and type 3 GD also exhibit deficits involving the central nervous system [33]. GBA mutations occur in 7–15% of PD cases [5,34], and the PD risk increase is between 3-fold for carriers of mild GBA mutation (N370S) and 15-fold for carriers of more severe GBA mutation (L444P or 84GG) [35]. Between the different genes related to PD, GBA is clearly and directly implicated in lipid metabolism. Up to now, different heterozygous GBA mutations associated with PD have been identified: N370S, L444P, and E326K. Pathological GBA mutations result in reduced glucocerebrosidase activity [36], and, importantly, PD patients without GBA mutations also exhibit lower levels of GCase activity in the central nervous system, further confirming the contribution of the *gba* gene to the disease pathogenesis [37,38].

The exact mechanism of GBA mutation toxicity is still debated; both loss- and gain-of-function hypotheses are supported by experimental evidence, and these hypotheses are not mutually exclusive. Generation of GBA animal models has permitted a more extensive analysis of GBA-related molecular mechanisms leading to cell toxicity. In mice, the presence of pathological point mutations in homozygotes leads to strong decrease in GCase activity in liver, lung, and spleen, with a residual activity between 2% and 25% compared with WT [39], while heterozygous mice bearing the L444P mutation show a 40% reduction in GCase activity [40]. In the serum of PD patients carrying pathological GBA mutations, a significant modification in lipid composition has been described: monohexosylceramide, ceramide, and sphingomyelin were elevated, while phosphatidic acid, phosphatidylethanolamine, plasmalogen phosphatidylethanolamine, and acyl phosphatidylglycerol were decreased [41]. The exact mechanism by which GCase dysfunction increases the risk of PD remains elusive, although a number of different pathological mechanisms have been proposed. Different experimental evidence suggests that the loss of the GCase function in patient neurons, as well as in cellular or animal GBA models, compromises lysosomal protein degradation that in turn leads to an α -syn accumulation (for review, see [42]). In addition to their primary consequence—the lysosomal dysfunction—GBA1 mutations and abnormal GCase activity have also been linked to mitochondrial dysfunction [43,44]. Recently, a dysregulation of mitochondria–lysosome contacts in PD patient-derived dopaminergic neurons in the presence of reduced lysosomal GCase enzymatic activity was found, resulting in misregulated axonal distribution of mitochondria and decreased ATP levels [45]. Another suggested hypothesis is that GBA activity could modulate the cell-to-cell transmission/propagation of α -syn aggregates [46]. In this context, it is also noteworthy that GBA overexpression *in vitro* results in a significant decrease in exosome secretion of synuclein, while either the virus-mediated expression of mutant GBA

in the mouse striatum or chronic inhibition of GCCase activity in vivo result in an increase in exosome-associated synuclein oligomers [47].

Recently, another genetic link between aberrant lipid metabolism and PD has been identified. Mutations in the *smpd1* gene, which encodes the lysosomal enzyme acid sphingomyelinase (ASMase), have been associated with an increased risk of PD [48–51]. Interestingly, ASMases with the L302P or fsP330 mutations compared with WT or A487V variant failed to reach the lysosomal compartment and were retained in the ER in transfected HeLa cells [51]. Moreover, in silico analysis suggests that mutations in SMPD1 disrupt either enzymatic domain fold or lipid-binding site [51]. Regardless of the SMPD1 molecular mechanism of toxicity, a reduction in ASMase activity by RNA interference approach or CRISPR/Cas9-mediated knockout both in HeLa cells and in the BE(2)-M17 dopaminergic cell line leads to an increase in α -syn levels likely due to an impairment in α -syn degradation by the lysosomal compartment [51].

2.3. Leucine-Rich Repeat Kinase 2 (LRRK2/PARK8)

Lrrk2 gene is the most frequently mutated gene in both sporadic and familial Parkinson's disease (PD) cases, reaching up to 40% in some ethnic groups, Ashkenazi Jewish and North African Arab Berbers [52,53]. LRRK2 consists of four protein–protein interaction domains (armadillo repeats, ankyrin repeats, leucine-rich repeats and WD40 domain) and two catalytic domains (Ras of complex (Roc) domain associated with C-terminal of Roc (COR) domain and the kinase domain) [53]. Pathological LRRK2 mutations are autosomal dominant and are all distributed in the two catalytic domains including the most common mutation associated with LRRK2 (G2019S). Increased LRRK2 kinase activity has been proposed to strongly contribute to pathogenesis, suggesting the potential therapeutic use of LRRK2 kinase inhibitors in the treatment of PD [54]. However, LRRK2 pathological mechanisms of toxicity are still debated. The most prominent hypothesis is a direct LRRK2 involvement in the control of vesicle trafficking, strongly supported by LRRK2 association with intracellular membranes of different compartments, such as the Golgi complex, late endosomes, lysosomes, and synaptic vesicles and by the fact that many putative LRRK2 interactors belong to protein families involved in the regulation of vesicle trafficking or in cytoskeleton dynamics that in turn may modulate vesicle trafficking [53]. In neurons, the vesicle trafficking controls fundamental physiological functions, such as neurotransmitter or protein release and uptake, localization of membrane receptors, organelle biogenesis, and also changes in lipid membrane composition. Although an extensive analysis of lipidome profile in LRRK2 cellular or animal models is still missing, different lines of evidence suggest a potential role of LRRK2 in lipid metabolism and/or lipid signaling pathway(s). For instance, LRRK2 knockout mice show increased number and density of lipid droplets in both hepatocytes and stellate cells, compared with WT animals [55], and distinct lipid profile alterations [56]. In the same animal model, higher level of cholesterol was observed [55]. LRRK2 involvement in lipid metabolism was further confirmed in HepG2 cells, where the overexpression of LRRK2 promotes the β -oxidation by positively regulating carnitine palmitoyltransferase 1A, whereas LRRK2 knockdown inhibited β -oxidation [57]. Using a targeted lipidomic approach, Ferrazza and colleagues reported an altered sphingolipid composition in LRRK2 KO mice. In particular, ceramide content is significantly higher in KO compared with WT mice, suggesting that the absence of LRRK2 has an impact on ceramide metabolism [58]. Interestingly, ceramide is a component of all major sphingolipid species, and several studies have provided evidence that sphingolipid levels are often altered in neurodegenerative diseases, including PD [59,60].

LRRK2 may also play a role in the phosphoinositide metabolism. LRRK2 and synaptotagmin1 (SYNJ1) loss of function share a similar pathogenic pathway in deregulating SV endocytosis in the dopaminergic neurons [58]. In particular, the SV endocytosis impairment seems to be mediated by direct LRRK2-mediated phosphorylation of SYNJ1, at least in vitro [61]. Interestingly, the results were further confirmed in drosophila models, where LRRK2 R1441C expression induces an enhanced phosphorylation of different SV pro-

teins, including SYNJ1, in the brain [62]. SYNJ1 is a phosphoinositide phosphatase highly expressed in nerve terminals and able to dephosphorylate phosphatidylinositol bis- or trisphosphates, localized on plasma membranes. Inositol lipids are essential components of eukaryotic membranes and important intracellular second messengers activating different downstream pathways.

Numerous experimental results link LRRK2 and its phosphorylation substrates Rabs to lipids. Phosphoinositides and Rab GTPases regulate each other's localization, and, importantly, membrane trafficking relies on dynamic changes in membrane identities that are determined by the regulation of distinct RAB GTPases and phosphoinositides. In fact, phosphoinositides mediate the recruitment of different Rab GTPases regulators, and Rab GTPases affect the recruitment of phosphoinositide regulators (for extensive review, see [63]). In some cases, the Rab binding to the membrane, in addition to prenylation, is dependent on a specific protein–protein interaction or on the presence of particular phosphoinositides [64]. For instance, the plasma membrane localization of Rab35 involves direct binding to the negatively charged phosphoinositides PtdIns(4,5)P2 and PtdIns(3,4,5)P3. Moreover, the molecular mechanism by which Rab35, a specific LRRK2 substrate [65], regulates different cellular functions, including endosomal trafficking, phagocytosis, cell migration and neurite outgrowth, probably involves regulation of phosphoinositides and F-actin, both on endosomes and at the plasma membrane [66]. Rab35 also controls the lipid turnover by myotubularins to repress mTORC1 activity and to control myelin growth [67]. Interestingly, the Rab proteins (including specific LRRK2 substrates) are also involved in lipid droplet (LD) formation and mobilization [68], and in fact, mutant LRRK2 Y1699C, by Rab8a phosphorylation on serine residue 72, regulates the fusion and enlargement of lipid droplets [69]. LDs consist of an organic core comprising neutral lipids (mainly triacylglycerols and sterol esters) bounded by a monolayer of phospholipids. Neutral lipids in LDs are mobilized by lipases to provide metabolic energy (through the oxidation of fatty acids) and lipids for membrane synthesis. Rab5 is associated to LD and modulates LD formation [64]. Rab10 is involved in the selective targeting of LDs to autophagic machinery by a Rab10/Dynamin-2 complex formation [70]. As previously mentioned, phosphorylation of Rab8A by LRRK2 promotes the formation of large lipid droplets [69] and Rab8A is required for muscle lipid uptake and storage [71]. Finally, Rab18 (although not specifically investigated as a LRRK2 substrate but showing a phosphorylation sequence similar to the other Rab members [54]) is a key regulator of LD formation and mobilization [72]. Interestingly, increasing evidence indicates that LDs dynamically interact with different cellular organelles, including mitochondria, endosomes, peroxisomes, and the plasma membrane and that this association might facilitate the exchange of lipids, either for anabolic growth of LDs or for their catabolic breakdown.

2.4. PTEN-Induced Kinase 1 (PINK-1/PARK6) and PARKIN (PARK2)

Although PINK-1 and PARKIN are considered key factors in mitochondrial quality control by promoting the removal of damaged mitochondria [73], different lines of evidence have implicated these two genes in the control of lipid and lipoprotein metabolism. Interestingly, lipid biology and mitochondrial homeostasis are tightly connected. Mitochondrial membrane lipids are essential for mitochondrial function. The biogenesis and the mitochondrial architecture, activity of respiratory protein, and transport of proteins into mitochondria are largely dependent on the mitochondrial lipid composition [74,75]. Valadas and colleagues, using both hypothalamic neurons differentiated from patient induced pluripotent stem cells (iPSCs) and fruit fly models lacking the parkin or pink-1 gene, found an excess of endoplasmic reticulum–mitochondria contacts [76]. These excessive contact sites cause abnormal lipid trafficking that depletes phosphatidylserine from the endoplasmic reticulum (ER) and disrupts the production of neuropeptide-containing vesicles without major defects in the mitochondria of mutant neuropeptidergic neurons. Importantly feeding mutant flies with phosphatidylserine rescues neuropeptidergic vesicle production and acutely restores normal sleep patterns [76]. Moreover, independent

research groups have observed specific lipidomic alterations in mitochondria of aged PARKIN knock-out mice. For instance, Gaudio et al. observed an enrichment in less unsaturated forms of CL, lower phosphatidylglycerol and phosphatidylinositol levels, and higher levels of some forms of hydroxylated ceramides [77]. Finally, a genome-wide RNAi screen performed in a PD cellular model to identify genes involved in PARKIN-mediated mitophagy identified the sterol regulatory element binding transcription factor 1 (SREBF1), a master regulator of lipid synthesis [78]. In SREBF1 knockdown, both Parkin translocation and mitophagy are altered [78]. Besides, the toxicity induced by PINK1 deficiency in different animal and cellular models was significantly reduced by the partial genetic or pharmacological inhibition of fatty acid synthase (FASN) [79]. Lower FASN activity in PINK1 mutants decreases palmitate levels and increases the levels of cardiolipin, a mitochondrial inner membrane-specific lipid. Furthermore, cardiolipin supplementation to isolated mitochondria rescues the PINK1-induced complex I defects and the inefficient electron transfer between complex I and ubiquinone [79]. The role of CL in mitochondrial physiology is of particular relevance because CL exposure to the outer membrane not only regulates mitophagy and the electron transport, but, relevantly for PD, also affects the α -synuclein aggregation [80]. Interestingly, in rotenone-treated rats, a reduction of polyunsaturated fatty acid (PUFA) cardiolipin and accumulation of mono-oxygenated cardiolipin species in the substantia nigra was observed, with an increase in PUFA-containing cardiolipins in the plasma [81].

Recently a new and specific role of parkin in fat intake and lipid metabolism has been described [82]. Parkin KO mice resisted weight gain, steatohepatitis, and insulin resistance when exposed to high-fat and -cholesterol diet [83]. The molecular mechanism of PARKIN effect seems to be the mono-ubiquitination of the class B scavenger receptor CD36 (also known as FA translocase, FAT), a transmembrane protein that binds with high affinity to a number of lipid ligands, including long chain FAs, anionic phospholipids, and native or modified lipoproteins [83].

2.5. *Synaptojanin1 (SYNJ1/PARK20)*

Synj1 has been recently identified independently by two research groups as the gene responsible of autosomal recessive, early-onset atypical parkinsonism (PARK20) [84,85]. Two main SYNJ1 isoforms, generated by alternative splicing, have been discovered of, respectively, 145 kDa (short isoform) and 170 kDa (long isoform). The short isoform was the first to be identified and it is highly expressed in the brain with a significant localization in the presynaptic nerve terminals [86]. SYNJ1 is a polyphosphoinositide phosphatase acting on various phosphoinositides, including phosphatidylinositol 4-phosphate, phosphatidylinositol (4,5)-bisphosphate (PI(4,5)P₂), and phosphatidylinositol (3,4,5)-trisphosphate. Phosphoinositides are key regulators of cell physiology. In particular, PI(4,5)P₂ plays a major regulatory role at the cell surface, both as a precursor of important signaling molecules, as well as via interactions with cytosolic and membrane proteins. The SYNJ1 protein contains two different phosphatase domains (N-terminal Sac1-like inositol domain and a central 5'-phosphatase domain) followed by a C-terminal proline-rich domain. The long isoform contains an additional proline-rich domain. Interestingly, most of the pathological SYNJ1 mutations are located in one of the two phosphatase domains, although recently, a new pathological SYNJ1 mutation was reported in the C-terminal domain of the longer isoform in a Tunisian family with juvenile Parkinson's disease associated with epilepsy [87]. Up to now, by regulating phospholipid signaling, SYNJ1 seems to be mainly involved in the regulation of vesicle trafficking. For instance, synapses of knock-in mice carrying the homozygous R258Q mutation display endocytic defects and a striking accumulation of clathrin-coated intermediates [88]. Moreover, the pathological SYNJ1 mutation in the C-terminal domain, reported in the Tunisian family, is located in the clathrin adaptor protein 2 (AP2) binding domain, further supporting the SYNJ1 role the regulation of endocytic vesicle recycling in neurons [87]. Interestingly, as previously mentioned, LRRK2 directly phosphorylates synaptojanin1 in vitro, resulting in the disruption of endophilin-

synaptojanin1 interaction required for SV endocytosis. Moreover, midbrain neurons from mice carrying both LRRK2 G2019S and SYNJ1+/- show a significant impairment in the exocytosis processes, strongly suggesting that LRRK2 and SYNJ1 control vesicle trafficking via a common pathological pathway [61]. The LRRK2–SYNJ1 physiological interaction was further confirmed in drosophila models, where the pathological LRRK2 R1441C mutant expression induces an enhanced phosphorylation of SYNJ1, both in vivo and in vitro [62].

2.6. Phospholipase A2 Group VI (PLA2G6/PARK14)

Mutations in PLA2G6 were first associated to neurodegenerative disease in the 2006. In particular, mutations in PLA2G6 were identified in a locus for infantile neuroaxonal dystrophy (INAD) and neurodegeneration with brain iron accumulation (NBIA) [89]. Independently, the genetic association was validated by Khateeb et al. in two consanguineous Israeli Bedouin kindreds with INAD [90]. They identified a 3 bp deletion in the homozygous PLA2G6 gene, leading to a valine deletion in position 691. Neurodegenerative disorders with high brain iron include Parkinson disease, Alzheimer disease, and several childhood genetic disorders categorized as neuroaxonal dystrophies. PLA2G6 was first associated to PD in 2009 by mutational analysis in three individuals from two unrelated families with adult-onset dystonia-parkinsonism (PARK14), and, surprisingly, none of the affected patients showed brain iron accumulation [91]. To date, different types of pathological mutations have been identified, including nonsense and missense mutations, small exons deletions, splicing sites. Patients with homozygous mutations in PLA2G6 show young onset, progressive cognitive decline, and dopa-responsive dystonia-parkinsonism.

The phospholipase A2 (PLA2) superfamily consists of many different groups of enzymes that catalyze the hydrolysis of the sn-2 ester bond in a variety of different phospholipids, leading to the release of arachidonic acid and other fatty acids [92]. PLA2 plays a key role in both phospholipid remodeling and signal transduction as the PLA2 products are important second messengers that play relevant roles in different signal transduction pathways. PLA2G6 encodes a calcium-independent group VI phospholipase A2, which localizes to the neuronal mitochondria and endosomal and lysosomal membranes. In the nervous system, PLA2G6 could be essential for the remodeling of membrane phospholipids in axons and synapses; however, the exact molecular mechanism by which PLA2G6 contributes to neurodegeneration has not yet been fully elucidated. For instance, in contrast to INAD mutations, it remains debated whether PD-associated mutations in PLA2G6 protein affect its catalytic activity [93].

Different PLA2G6 knock-out mice have been generated [94,95]. Malik et al. show age-dependent accumulation of distinctive spheroids in distal axons that contain membranes accumulated due to an impairment in axonal membrane homeostasis and in protein degradation pathways [96]. In old PLA2G6 knock-out mice, a significant neuroaxonal dystrophy was visible, likely due to insufficient remodeling and degeneration of mitochondrial inner membranes and presynaptic membranes [97]. The insufficient membrane remodeling was further confirmed by imaging mass spectrometry showing a significant increase in docosahexaenoic acid-containing phosphatidylcholine in the gray matter of the spinal cord of PLA2G6 KO mice, especially in the posterior horn [97]. Moreover, PLA2G6 KO mice showed decreased rates of incorporation of unesterified docosahexaenoic acid (DHA) from plasma into brain phospholipids, reduced concentrations of several fatty acids (including DHA) esterified in ethanolamine- and serine-glycerophospholipids, and increased lysophospholipid fatty acid concentrations [98].

In drosophila, PLA2G6 loss results in acyl-chain shortening in phospholipids, which affects ER homeostasis and neurotransmission and promotes α -synuclein aggregation. Interestingly, administration of linoleic acid or the overexpression of C19orf12, another NBIA-causative gene, rescues the acyl-chain shortening due to PLA2G6 loss [99].

3. Conclusions

There is a growing body of evidence linking dysfunctional lipid metabolism to PD pathogenesis. Changes in membrane lipids have been observed in both affected and unaffected regions of brains from PD patients, and in different experimental models expressing PD-causative or -risk genes, indicating that alteration in lipid metabolism/pathways may precede PD development. In Figure 1, some molecular pathways altered by PD-related gene expression leading to alteration in lipid metabolism, composition, or signal transduction are schematized.

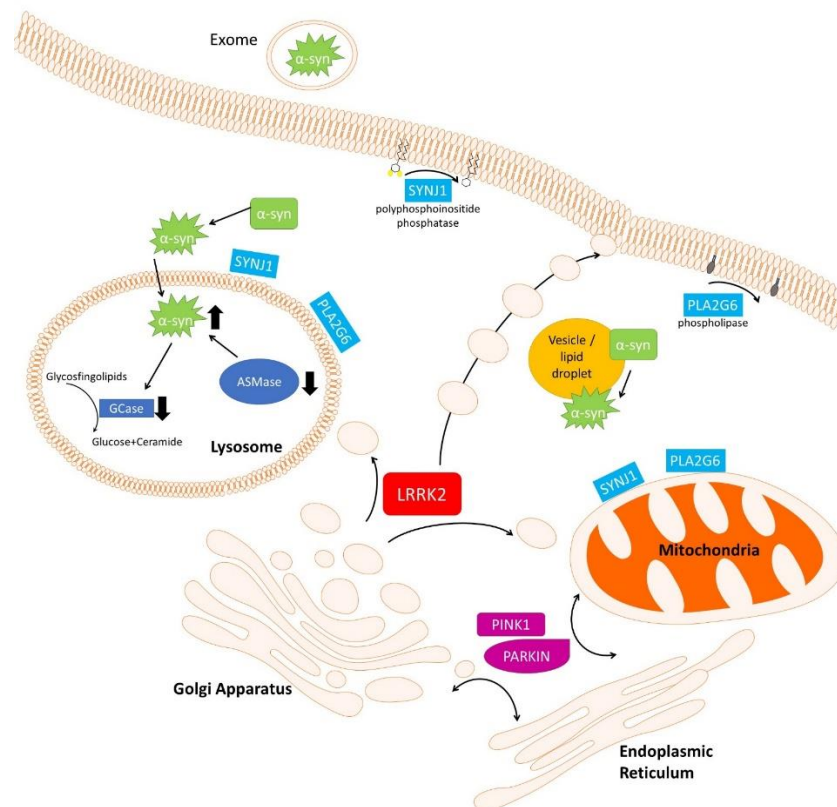


Figure 1. Cell biological processes impacted by PD-related genes leading to lipid alteration. As described in the main text, different PD-causative or -risk genes (GBA, SMPD1, SYNJ1, and PLA2G6) directly control lipid metabolism in neuronal cells. PD-causative genes (LRRK2, PINK-1, and PARKIN) may indirectly control lipid metabolism, localization or signaling by controlling vesicle trafficking and/or lipid exchange between various organelles inside the cells. Finally, α -synuclein physiology is tightly related to lipid: α -synuclein controls lipid metabolism, α -synuclein localization and aggregation are strongly dependent on a specific membrane lipid composition, and, lastly, LBs are largely composed of α -synuclein tightly associated to lipids and membrane fragments. Aggregated α -synuclein is represented as green stars.

Both α -synuclein localization and aggregation are dependent on specific membrane lipid composition. Moreover, lipid metabolism alteration in lysosomes for instance by GBA or SMPD1 mutants may affect the α -synuclein clearance. LRRK2 may regulate lipid metabolism either directly or, more likely, indirectly through the control of vesicle trafficking by the phosphorylation of different RAB family proteins. Eukaryotic cells rely on a complex and regulated network of vesicular transport to ensure efficient delivery of lipids to target organelles. Moreover, the endogenous lipid synthesis and delivery is of particular relevance in neurons because some circulating plasma lipids (e.g., cholesterol) cannot reach these cells due to the inability of different lipoproteins to traverse the blood–brain barrier. SYNJ1 is a polyphosphoinositide phosphatase acting on various phosphoinositides, and

PLA2G6 is a calcium-independent group VI phospholipase A2; therefore, both are directly involved in the control of lipid metabolism. SYNJ1 and PLA2G6 are both localized on neuronal mitochondria, endosomal and lysosomal membranes, and plasma membrane and could play an essential role in remodeling membrane phospholipids either in cellular organelles or in axons and synapses. Importantly, the biogenesis and architecture of different cell structures (mitochondria, lysosomes, vesicles or lipid droplets, cell membranes) are largely dependent on the lipid composition. Furthermore, products generated by SYNJ1 or PLA2G6 are important second messengers that play relevant roles in different signal transduction pathways in neurons. Recent evidence has highlighted specific alteration in mitochondria due to abnormal lipid trafficking from the endoplasmic reticulum in both human hypothalamic neurons and fruit fly models lacking parkin or pink-1 genes. These data are further corroborated by specific alterations in lipid metabolism/composition in different PARKIN or PINK1 experimental models. Finally, experimental results indicating that LBs are largely composed of lipids, membrane fragments, and membranous organelles, such as vesicles, further confirm the importance of lipid composition in PD pathology.

Author Contributions: Reading of the literature and original draft preparation: M.F., A.D., M.G., G.G., C.C. and C.I. Editing the paper: C.C. and C.I. All authors have read and agreed to the published version of the manuscript.

Funding: Fondazione Banco di Sardegna (Bando-2017-Iaccarino). Fondo di Ateneo per la ricerca 2019 Iaccarino and Fondo di Ateneo per la ricerca 2019 Crosio. M.F. was supported by PhD fellowships granted by PON 2014-2020 (CCI2014IT16M2OP005).

Institutional Review Board Statement: Not applicable.

Informed Consent Statement: Not applicable.

Data Availability Statement: Not applicable.

Acknowledgments: We would like to acknowledge all the people from the laboratory that critically read the manuscript.

Conflicts of Interest: The authors declare no conflict of interest.

References

1. Obeso, J.A.; Stamelou, M.; Goetz, C.G.; Poewe, W.; Lang, A.E.; Weintraub, D.; Burn, D.; Halliday, G.M.; Bezard, E.; Przedborski, S.; et al. Past, Present, and Future of Parkinson's Disease: A Special Essay on the 200th Anniversary of the Shaking Palsy. *Mov. Disord.* **2017**, *32*, 1264–1310. [[CrossRef](#)]
2. Bonifati, V. The Pleomorphic Pathology of Inherited Parkinson's Disease: Lessons from LRRK2. *Curr. Neurol. Neurosci. Rep.* **2006**, *6*, 355–357. [[CrossRef](#)]
3. Bandres-Ciga, S.; Diez-Fairen, M.; Kim, J.J.; Singleton, A.B. Genetics of Parkinson's Disease: An Introspection of Its Journey towards Precision Medicine. *Neurobiol. Dis.* **2020**, *137*, 104782. [[CrossRef](#)]
4. Bandres-Ciga, S.; Blauwendraat, C.; Singleton, A.B. Assessment of Genetic Association Between Parkinson Disease and Bipolar Disorder. *JAMA Neurol.* **2020**, *77*, 1034–1035. [[CrossRef](#)]
5. Blandini, F.; Cilia, R.; Cerri, S.; Pezzoli, G.; Schapira, A.H.V.; Mullin, S.; Lanciego, J.L. Glucocerebrosidase Mutations and Synucleinopathies: Toward a Model of Precision Medicine. *Mov. Disord.* **2019**, *34*, 9–21. [[CrossRef](#)]
6. Xicoy, H.; Wieringa, B.; Martens, G.J.M. The Role of Lipids in Parkinson's Disease. *Cells* **2019**, *8*, 27. [[CrossRef](#)] [[PubMed](#)]
7. Fanning, S.; Selkoe, D.; Dettmer, U. Parkinson's Disease: Proteinopathy or Lipidopathy? *NPJ Park. Dis.* **2020**, *6*, 3. [[CrossRef](#)] [[PubMed](#)]
8. Davidson, W.S.; Jonas, A.; Clayton, D.F.; George, J.M. Stabilization of Alpha-Synuclein Secondary Structure upon Binding to Synthetic Membranes. *J. Biol. Chem.* **1998**, *273*, 9443–9449. [[CrossRef](#)]
9. Jo, E.; McLaurin, J.; Yip, C.M.; St George-Hyslop, P.; Fraser, P.E. Alpha-Synuclein Membrane Interactions and Lipid Specificity. *J. Biol. Chem.* **2000**, *275*, 34328–34334. [[CrossRef](#)]
10. Nakamura, K.; Nemani, V.M.; Azarbal, F.; Skibinski, G.; Levy, J.M.; Egami, K.; Munishkina, L.; Zhang, J.; Gardner, B.; Wakabayashi, J.; et al. Direct Membrane Association Drives Mitochondrial Fission by the Parkinson Disease-Associated Protein Alpha-Synuclein. *J. Biol. Chem.* **2011**, *286*, 20710–20726. [[CrossRef](#)] [[PubMed](#)]
11. Wislet-Gendebien, S.; Visanji, N.P.; Whitehead, S.N.; Marsilio, D.; Hou, W.; Figeys, D.; Fraser, P.E.; Bennett, S.A.; Tandon, A. Differential Regulation of Wild-Type and Mutant Alpha-Synuclein Binding to Synaptic Membranes by Cytosolic Factors. *BMC Neurosci.* **2008**, *9*, 92. [[CrossRef](#)]

12. Perrin, R.J.; Woods, W.S.; Clayton, D.F.; George, J.M. Exposure to Long Chain Polyunsaturated Fatty Acids Triggers Rapid Multimerization of Synucleins. *J. Biol. Chem.* **2001**, *276*, 41958–41962. [[CrossRef](#)]
13. Galvagnion, C.; Brown, J.W.; Ouberai, M.M.; Flagmeier, P.; Vendruscolo, M.; Buell, A.K.; Sparr, E.; Dobson, C.M. Chemical Properties of Lipids Strongly Affect the Kinetics of the Membrane-Induced Aggregation of Alpha-Synuclein. *Proc. Natl. Acad. Sci. USA* **2016**, *113*, 7065–7070. [[CrossRef](#)]
14. De Franceschi, G.; Frare, E.; Pivato, M.; Relini, A.; Penco, A.; Greggio, E.; Bubacco, L.; Fontana, A.; de Laureto, P.P. Structural and Morphological Characterization of Aggregated Species of Alpha-Synuclein Induced by Docosahexaenoic Acid. *J. Biol. Chem.* **2011**, *286*, 22262–22274. [[CrossRef](#)]
15. Maroteaux, L.; Campanelli, J.T.; Scheller, R.H. Synuclein: A Neuron-Specific Protein Localized to the Nucleus and Presynaptic Nerve Terminal. *J. Neurosci.* **1988**, *8*, 2804–2815. [[CrossRef](#)] [[PubMed](#)]
16. Auluck, P.K.; Caraveo, G.; Lindquist, S. Alpha-Synuclein: Membrane Interactions and Toxicity in Parkinson's Disease. *Annu. Rev. Cell Dev. Biol.* **2010**, *26*, 211–233. [[CrossRef](#)] [[PubMed](#)]
17. Ruiperez, V.; Darios, F.; Davletov, B. Alpha-Synuclein, Lipids and Parkinson's Disease. *Prog. Lipid Res.* **2010**, *49*, 420–428. [[CrossRef](#)] [[PubMed](#)]
18. Cole, N.B.; Murphy, D.D.; Grider, T.; Rueter, S.; Brasaemle, D.; Nussbaum, R.L. Lipid Droplet Binding and Oligomerization Properties of the Parkinson's Disease Protein Alpha-Synuclein. *J. Biol. Chem.* **2002**, *277*, 6344–6352. [[CrossRef](#)] [[PubMed](#)]
19. Cole, N.B.; Dieuliis, D.; Leo, P.; Mitchell, D.C.; Nussbaum, R.L. Mitochondrial Translocation of Alpha-Synuclein Is Promoted by Intracellular Acidification. *Exp. Cell Res.* **2008**, *314*, 2076–2089. [[CrossRef](#)]
20. Shahmoradian, S.H.; Lewis, A.J.; Genoud, C.; Hench, J.; Moors, T.E.; Navarro, P.P.; Castano-Diez, D.; Schweighauser, G.; Graff-Meyer, A.; Goldie, K.N.; et al. Lewy Pathology in Parkinson's Disease Consists of Crowded Organelles and Lipid Membranes. *Nat. Neurosci.* **2019**, *22*, 1099–1109. [[CrossRef](#)] [[PubMed](#)]
21. Galvagnion, C.; Buell, A.K.; Meisl, G.; Michaels, T.C.; Vendruscolo, M.; Knowles, T.P.; Dobson, C.M. Lipid Vesicles Trigger Alpha-Synuclein Aggregation by Stimulating Primary Nucleation. *Nat. Chem. Biol.* **2015**, *11*, 229–234. [[CrossRef](#)]
22. Golovko, M.Y.; Rosenberger, T.A.; Faergeman, N.J.; Feddersen, S.; Cole, N.B.; Pribill, I.; Berger, J.; Nussbaum, R.L.; Murphy, E.J. Acyl-CoA Synthetase Activity Links Wild-Type but Not Mutant Alpha-Synuclein to Brain Arachidonate Metabolism. *Biochemistry* **2006**, *45*, 6956–6966. [[CrossRef](#)]
23. Sanchez Campos, S.; Alza, N.P.; Salvador, G.A. Lipid Metabolism Alterations in the Neuronal Response to A53T Alpha-Synuclein and Fe-Induced Injury. *Arch. Biochem. Biophys.* **2018**, *655*, 43–54. [[CrossRef](#)]
24. Jenco, J.M.; Rawlingson, A.; Daniels, B.; Morris, A.J. Regulation of Phospholipase D2: Selective Inhibition of Mammalian Phospholipase D Isoenzymes by Alpha- and Beta-Synucleins. *Biochemistry* **1998**, *37*, 4901–4909. [[CrossRef](#)]
25. Rappley, I.; Gitler, A.D.; Selvy, P.E.; LaVoie, M.J.; Levy, B.D.; Brown, H.A.; Lindquist, S.; Selkoe, D.J. Evidence That Alpha-Synuclein Does Not Inhibit Phospholipase D. *Biochemistry* **2009**, *48*, 1077–1083. [[CrossRef](#)] [[PubMed](#)]
26. Mendez-Gomez, H.R.; Singh, J.; Meyers, C.; Chen, W.; Gorbatyuk, O.S.; Muzyczka, N. The Lipase Activity of Phospholipase D2 Is Responsible for Nigral Neurodegeneration in a Rat Model of Parkinson's Disease. *Neuroscience* **2018**, *377*, 174–183. [[CrossRef](#)] [[PubMed](#)]
27. Bae, E.J.; Lee, H.J.; Jang, Y.H.; Michael, S.; Masliah, E.; Min, D.S.; Lee, S.J. Phospholipase D1 Regulates Autophagic Flux and Clearance of Alpha-Synuclein Aggregates. *Cell Death Differ.* **2014**, *21*, 1132–1141. [[CrossRef](#)] [[PubMed](#)]
28. Conde, M.A.; Alza, N.P.; Iglesias Gonzalez, P.A.; Scodelaro Bilbao, P.G.; Sanchez Campos, S.; Uranga, R.M.; Salvador, G.A. Phospholipase D1 Downregulation by Alpha-Synuclein: Implications for Neurodegeneration in Parkinson's Disease. *Biochim. Biophys. Acta Mol. Cell Biol. Lipids* **2018**, *1863*, 639–650. [[CrossRef](#)] [[PubMed](#)]
29. Golovko, M.Y.; Rosenberger, T.A.; Feddersen, S.; Faergeman, N.J.; Murphy, E.J. Alpha-Synuclein Gene Ablation Increases Docosahexaenoic Acid Incorporation and Turnover in Brain Phospholipids. *J. Neurochem.* **2007**, *101*, 201–211. [[CrossRef](#)] [[PubMed](#)]
30. Castagnet, P.I.; Golovko, M.Y.; Barcelo-Coblijn, G.C.; Nussbaum, R.L.; Murphy, E.J. Fatty Acid Incorporation Is Decreased in Astrocytes Cultured from Alpha-Synuclein Gene-Ablated Mice. *J. Neurochem.* **2005**, *94*, 839–849. [[CrossRef](#)]
31. Barcelo-Coblijn, G.; Golovko, M.Y.; Weinhofer, I.; Berger, J.; Murphy, E.J. Brain Neutral Lipids Mass Is Increased in Alpha-Synuclein Gene-Ablated Mice. *J. Neurochem.* **2007**, *101*, 132–141. [[CrossRef](#)] [[PubMed](#)]
32. Ellis, C.E.; Murphy, E.J.; Mitchell, D.C.; Golovko, M.Y.; Scaglia, F.; Barcelo-Coblijn, G.C.; Nussbaum, R.L. Mitochondrial Lipid Abnormality and Electron Transport Chain Impairment in Mice Lacking Alpha-Synuclein. *Mol. Cell. Biol.* **2005**, *25*, 10190–10201. [[CrossRef](#)] [[PubMed](#)]
33. Riboldi, G.M.; Di Fonzo, A.B. GBA, Gaucher Disease, and Parkinson's Disease: From Genetic to Clinic to New Therapeutic Approaches. *Cells* **2019**, *8*, 364. [[CrossRef](#)] [[PubMed](#)]
34. Sidransky, E.; Nalls, M.A.; Aasly, J.O.; Aharon-Peretz, J.; Annesi, G.; Barbosa, E.R.; Bar-Shira, A.; Berg, D.; Bras, J.; Brice, A.; et al. Multicenter Analysis of Glucocerebrosidase Mutations in Parkinson's Disease. *N. Engl. J. Med.* **2009**, *361*, 1651–1661. [[CrossRef](#)] [[PubMed](#)]
35. Gan-Or, Z.; Amshalom, I.; Kilarski, L.L.; Bar-Shira, A.; Gana-Weisz, M.; Mirelman, A.; Marder, K.; Bressman, S.; Giladi, N.; Orr-Urtreger, A. Differential Effects of Severe vs Mild GBA Mutations on Parkinson Disease. *Neurology* **2015**, *84*, 880–887. [[CrossRef](#)]

36. Alcalay, R.N.; Levy, O.A.; Waters, C.C.; Fahn, S.; Ford, B.; Kuo, S.H.; Mazzoni, P.; Pauciulo, M.W.; Nichols, W.C.; Gan-Or, Z.; et al. Glucocerebrosidase Activity in Parkinson's Disease with and without GBA Mutations. *Brain* **2015**, *138*, 2648–2658. [[CrossRef](#)] [[PubMed](#)]
37. Balducci, C.; Pierguidi, L.; Persichetti, E.; Parnetti, L.; Sbaragli, M.; Tassi, C.; Orlacchio, A.; Calabresi, P.; Beccari, T.; Rossi, A. Lysosomal Hydrolases in Cerebrospinal Fluid from Subjects with Parkinson's Disease. *Mov. Disord.* **2007**, *22*, 1481–1484. [[CrossRef](#)]
38. Parnetti, L.; Chiasserini, D.; Persichetti, E.; Eusebi, P.; Varghese, S.; Qureshi, M.M.; Dardis, A.; Deganuto, M.; De Carlo, C.; Castrioto, A.; et al. Cerebrospinal Fluid Lysosomal Enzymes and Alpha-Synuclein in Parkinson's Disease. *Mov. Disord.* **2014**, *29*, 1019–1027. [[CrossRef](#)]
39. Xu, Y.H.; Quinn, B.; Witte, D.; Grabowski, G.A. Viable Mouse Models of Acid Beta-Glucosidase Deficiency: The Defect in Gaucher Disease. *Am. J. Pathol.* **2003**, *163*, 2093–2101. [[CrossRef](#)]
40. Fishbein, I.; Kuo, Y.M.; Giasson, B.I.; Nussbaum, R.L. Augmentation of Phenotype in a Transgenic Parkinson Mouse Heterozygous for a Gaucher Mutation. *Brain* **2014**, *137*, 3235–3247. [[CrossRef](#)]
41. Guedes, L.C.; Chan, R.B.; Gomes, M.A.; Conceicao, V.A.; Machado, R.B.; Soares, T.; Xu, Y.; Gaspar, P.; Carrico, J.A.; Alcalay, R.N.; et al. Serum Lipid Alterations in GBA-Associated Parkinson's Disease. *Park. Relat. Disord.* **2017**, *44*, 58–65. [[CrossRef](#)] [[PubMed](#)]
42. Paciotti, S.; Albi, E.; Parnetti, L.; Beccari, T. Lysosomal Ceramide Metabolism Disorders: Implications in Parkinson's Disease. *J. Clin. Med.* **2020**, *9*, 594. [[CrossRef](#)]
43. Cleeter, M.W.; Chau, K.Y.; Gluck, C.; Mehta, A.; Hughes, D.A.; Duchen, M.; Wood, N.W.; Hardy, J.; Mark Cooper, J.; Schapira, A.H. Glucocerebrosidase Inhibition Causes Mitochondrial Dysfunction and Free Radical Damage. *Neurochem. Int.* **2013**, *62*, 1–7. [[CrossRef](#)] [[PubMed](#)]
44. Li, H.; Ham, A.; Ma, T.C.; Kuo, S.H.; Kanter, E.; Kim, D.; Ko, H.S.; Quan, Y.; Sardi, S.P.; Li, A.; et al. Mitochondrial Dysfunction and Mitophagy Defect Triggered by Heterozygous GBA Mutations. *Autophagy* **2019**, *15*, 113–130. [[CrossRef](#)]
45. Kim, S.; Wong, Y.C.; Gao, F.; Krainc, D. Dysregulation of Mitochondria-Lysosome Contacts by GBA1 Dysfunction in Dopaminergic Neuronal Models of Parkinson's Disease. *Nat. Commun.* **2021**, *12*, 1807. [[CrossRef](#)]
46. Bae, E.J.; Yang, N.Y.; Song, M.; Lee, C.S.; Lee, J.S.; Jung, B.C.; Lee, H.J.; Kim, S.; Masliah, E.; Sardi, S.P.; et al. Glucocerebrosidase Depletion Enhances Cell-to-Cell Transmission of Alpha-Synuclein. *Nat. Commun.* **2014**, *5*, 4755. [[CrossRef](#)]
47. Papadopoulos, V.E.; Nikolopoulou, G.; Antoniadou, I.; Karachaliou, A.; Arianoglou, G.; Emmanouilidou, E.; Sardi, S.P.; Stefanis, L.; Vekrellis, K. Modulation of Beta-Glucocerebrosidase Increases Alpha-Synuclein Secretion and Exosome Release in Mouse Models of Parkinson's Disease. *Hum. Mol. Genet.* **2018**, *27*, 1696–1710. [[CrossRef](#)]
48. Foo, J.N.; Liang, H.; Bei, J.X.; Yu, X.Q.; Liu, J.; Au, W.L.; Prakash, K.M.; Tan, L.C.; Tan, E.K. Rare Lysosomal Enzyme Gene SMPD1 Variant (p.R591C) Associates with Parkinson's Disease. *Neurobiol. Aging* **2013**, *34*, 2890.e13–2890.e15. [[CrossRef](#)]
49. Dagan, E.; Schlesinger, I.; Ayoub, M.; Mory, A.; Nassar, M.; Kurolap, A.; Peretz-Aharon, J.; Gershoni-Baruch, R. The Contribution of Niemann-Pick SMPD1 Mutations to Parkinson Disease in Ashkenazi Jews. *Park. Relat. Disord.* **2015**, *21*, 1067–1071. [[CrossRef](#)]
50. Gan-Or, Z.; Ozelius, L.J.; Bar-Shira, A.; Saunders-Pullman, R.; Mirelman, A.; Kornreich, R.; Gana-Weisz, M.; Raymond, D.; Rozenkrantz, L.; Deik, A.; et al. The p.L302P Mutation in the Lysosomal Enzyme Gene SMPD1 Is a Risk Factor for Parkinson Disease. *Neurology* **2013**, *80*, 1606–1610. [[CrossRef](#)] [[PubMed](#)]
51. Alcalay, R.N.; Mallett, V.; Vanderperre, B.; Tavassoly, O.; Dauvilliers, Y.; Wu, R.Y.J.; Ruskey, J.A.; Leblond, C.S.; Ambalavanan, A.; Laurent, S.B.; et al. SMPD1 Mutations, Activity, and Alpha-Synuclein Accumulation in Parkinson's Disease. *Mov. Disord.* **2019**, *34*, 526–535. [[CrossRef](#)]
52. Correia Guedes, L.; Ferreira, J.J.; Rosa, M.M.; Coelho, M.; Bonifati, V.; Sampaio, C. Worldwide Frequency of G2019S LRRK2 Mutation in Parkinson's Disease: A Systematic Review. *Park. Relat Disord.* **2010**, *16*, 237–242. [[CrossRef](#)] [[PubMed](#)]
53. Kluss, J.H.; Mamais, A.; Cookson, M.R. LRRK2 Links Genetic and Sporadic Parkinson's Disease. *Biochem. Soc. Trans.* **2019**, *47*, 651–661. [[CrossRef](#)] [[PubMed](#)]
54. Steger, M.; Tonelli, F.; Ito, G.; Davies, P.; Trost, M.; Vetter, M.; Wachter, S.; Lorentzen, E.; Duddy, G.; Wilson, S.; et al. Phosphoproteomics Reveals That Parkinson's Disease Kinase LRRK2 Regulates a Subset of Rab GTPases. *eLife* **2016**, *5*, e12813. [[CrossRef](#)]
55. Baptista, M.A.S.; Dave, K.D.; Frasier, M.A.; Sherer, T.B.; Greeley, M.; Beck, M.J.; Varsho, J.S.; Parker, G.A.; Moore, C.; Churchill, M.J.; et al. Loss of Leucine-Rich Repeat Kinase 2 (LRRK2) in Rats Leads to Progressive Abnormal Phenotypes in Peripheral Organs. *PLoS ONE* **2013**, *8*, e80705. [[CrossRef](#)]
56. Boddu, R.; Hull, T.D.; Bolisetty, S.; Hu, X.; Moehle, M.S.; Daher, J.P.L.; Kamal, A.I.; Joseph, R.; George, J.F.; Agarwal, A.; et al. Leucine-Rich Repeat Kinase 2 Deficiency Is Protective in Rhabdomyolysis-Induced Kidney Injury. *Hum. Mol. Genet.* **2015**, *24*, 4078–4093. [[CrossRef](#)] [[PubMed](#)]
57. Lin, C.-W.; Peng, Y.-J.; Lin, Y.-Y.; Mersmann, H.J.; Ding, S.-T. LRRK2 Regulates CPT1A to Promote β -Oxidation in HepG2 Cells. *Molecules* **2020**, *25*, 4122. [[CrossRef](#)]
58. Ferrazza, R.; Cogo, S.; Melrose, H.; Bubacco, L.; Greggio, E.; Guella, G.; Civiero, L.; Plotegher, N. LRRK2 Deficiency Impacts Ceramide Metabolism in Brain. *Biochem. Biophys. Res. Commun.* **2016**, *478*, 1141–1146. [[CrossRef](#)]
59. Czubowicz, K.; Jesko, H.; Wencel, P.; Lukiw, W.J.; Strosznajder, R.P. The Role of Ceramide and Sphingosine-1-Phosphate in Alzheimer's Disease and Other Neurodegenerative Disorders. *Mol. Neurobiol.* **2019**, *56*, 5436–5455. [[CrossRef](#)]

60. Huebeker, M.; Moloney, E.B.; van der Spoel, A.C.; Priestman, D.A.; Isacson, O.; Hallett, P.J.; Platt, F.M. Reduced Sphingolipid Hydrolase Activities, Substrate Accumulation and Ganglioside Decline in Parkinson's Disease. *Mol. Neurodegener.* **2019**, *14*, 40. [[CrossRef](#)]
61. Pan, P.Y.; Li, X.; Wang, J.; Powell, J.; Wang, Q.; Zhang, Y.; Chen, Z.; Wicinski, B.; Hof, P.; Ryan, T.A.; et al. Parkinson's Disease Associated LRRK2 Hyperactive Kinase Mutant Disrupts Synaptic Vesicle Trafficking in Ventral Midbrain Neurons. *J. Neurosci.* **2017**, *37*, 11366–11376. [[CrossRef](#)]
62. Islam, M.S.; Nolte, H.; Jacob, W.; Ziegler, A.B.; Pütz, S.; Grosjean, Y.; Szczepanowska, K.; Trifunovic, A.; Braun, T.; Heumann, H.; et al. Human R1441C LRRK2 Regulates the Synaptic Vesicle Proteome and Phosphoproteome in a Drosophila Model of Parkinson's Disease. *Hum. Mol. Genet.* **2016**, *25*, 5365–5382. [[CrossRef](#)] [[PubMed](#)]
63. Jean, S.; Kiger, A.A. Coordination between RAB GTPase and Phosphoinositide Regulation and Functions. *Nat. Rev. Mol. Cell Biol.* **2012**, *13*, 463–470. [[CrossRef](#)] [[PubMed](#)]
64. Li, F.; Yi, L.; Zhao, L.; Itzen, A.; Goody, R.S.; Wu, Y.W. The Role of the Hypervariable C-Terminal Domain in Rab GTPases Membrane Targeting. *Proc. Natl. Acad. Sci. USA* **2014**, *111*, 2572–2577. [[CrossRef](#)]
65. Steger, M.; Diez, F.; Dhekne, H.S.; Lis, P.; Nirujogi, R.S.; Karayel, O.; Tonelli, F.; Martinez, T.N.; Lorentzen, E.; Pfeffer, S.R.; et al. Systematic Proteomic Analysis of LRRK2-Mediated Rab GTPase Phosphorylation Establishes a Connection to Ciliogenesis. *eLife* **2017**, *6*, e31012. [[CrossRef](#)] [[PubMed](#)]
66. Klinkert, K.; Echard, A. Rab35 GTPase: A Central Regulator of Phosphoinositides and F-Actin in Endocytic Recycling and Beyond. *Traffic* **2016**, *17*, 1063–1077. [[CrossRef](#)] [[PubMed](#)]
67. Sawade, L.; Grandi, F.; Mignanelli, M.; Patino-Lopez, G.; Klinkert, K.; Langa-Vives, F.; Di Guardo, R.; Echard, A.; Bolino, A.; Haucke, V. Rab35-Regulated Lipid Turnover by Myotubularins Represses MTORC1 Activity and Controls Myelin Growth. *Nat. Commun.* **2020**, *11*, 2835. [[CrossRef](#)] [[PubMed](#)]
68. Li, C.; Yu, S.S. Rab Proteins as Regulators of Lipid Droplet Formation and Lipolysis. *Cell Biol. Int.* **2016**, *40*, 1026–1032. [[CrossRef](#)]
69. Yu, M.; Arshad, M.; Wang, W.; Zhao, D.; Xu, L.; Zhou, L. LRRK2 Mediated Rab8a Phosphorylation Promotes Lipid Storage. *Lipids Health Dis.* **2018**, *17*, 34. [[CrossRef](#)] [[PubMed](#)]
70. Li, Z.; Weller, S.G.; Drizyte-Miller, K.; Chen, J.; Krueger, E.W.; Mehall, B.; Casey, C.A.; Cao, H.; McNiven, M.A. Maturation of Lipophagic Organelles in Hepatocytes Is Dependent Upon a Rab10/Dynamin-2 Complex. *Hepatology* **2020**, *72*, 486–502. [[CrossRef](#)]
71. Chen, Q.; Rong, P.; Xu, D.; Zhu, S.; Chen, L.; Xie, B.; Du, Q.; Quan, C.; Sheng, Y.; Zhao, T.J.; et al. Rab8a Deficiency in Skeletal Muscle Causes Hyperlipidemia and Hepatosteatosis by Impairing Muscle Lipid Uptake and Storage. *Diabetes* **2017**, *66*, 2387–2399. [[CrossRef](#)]
72. Dejgaard, S.Y.; Presley, J.F. Rab18: New Insights into the Function of an Essential Protein. *Cell. Mol. Life Sci.* **2019**, *76*, 1935–1945. [[CrossRef](#)]
73. Pickrell, A.M.; Youle, R.J. The Roles of PINK1, Parkin, and Mitochondrial Fidelity in Parkinson's Disease. *Neuron* **2015**, *85*, 257–273. [[CrossRef](#)] [[PubMed](#)]
74. Bottinger, L.; Ellenrieder, L.; Becker, T. How Lipids Modulate Mitochondrial Protein Import. *J. Bioenerg. Biomembr.* **2016**, *48*, 125–135. [[CrossRef](#)] [[PubMed](#)]
75. Aufschnaiter, A.; Kohler, V.; Diessl, J.; Peselj, C.; Carmona-Gutierrez, D.; Keller, W.; Buttner, S. Mitochondrial Lipids in Neurodegeneration. *Cell Tissue Res.* **2017**, *367*, 125–140. [[CrossRef](#)] [[PubMed](#)]
76. Valadas, J.S.; Esposito, G.; Vandekerckhove, D.; Miskiewicz, K.; Deaulmerie, L.; Raitano, S.; Seibler, P.; Klein, C.; Verstreken, P. ER Lipid Defects in Neuropeptidergic Neurons Impair Sleep Patterns in Parkinson's Disease. *Neuron* **2018**, *98*, 1155–1169.e6. [[CrossRef](#)] [[PubMed](#)]
77. Gaudioso, A.; Garcia-Rozas, P.; Casarejos, M.J.; Pastor, O.; Rodriguez-Navarro, J.A. Lipidomic Alterations in the Mitochondria of Aged Parkin Null Mice Relevant to Autophagy. *Front. Neurosci.* **2019**, *13*, 329. [[CrossRef](#)]
78. Ivatt, R.M.; Sanchez-Martinez, A.; Godena, V.K.; Brown, S.; Ziviani, E.; Whitworth, A.J. Genome-Wide RNAi Screen Identifies the Parkinson Disease GWAS Risk Locus SREBF1 as a Regulator of Mitophagy. *Proc. Natl. Acad. Sci. USA* **2014**, *111*, 8494–8499. [[CrossRef](#)]
79. Vos, M.; Geens, A.; Bohm, C.; Deaulmerie, L.; Swerts, J.; Rossi, M.; Craessaerts, K.; Leites, E.P.; Seibler, P.; Rakovic, A.; et al. Cardiolipin Promotes Electron Transport between Ubiquinone and Complex I to Rescue PINK1 Deficiency. *J. Cell Biol.* **2017**, *216*, 695–708. [[CrossRef](#)] [[PubMed](#)]
80. Ryan, T.; Bamm, V.V.; Stykel, M.G.; Coackley, C.L.; Humphries, K.M.; Jamieson-Williams, R.; Ambasudhan, R.; Mosser, D.D.; Lipton, S.A.; Harauz, G.; et al. Cardiolipin Exposure on the Outer Mitochondrial Membrane Modulates Alpha-Synuclein. *Nat. Commun.* **2018**, *9*, 817. [[CrossRef](#)]
81. Tyurina, Y.Y.; Polimova, A.M.; Maciel, E.; Tyurin, V.A.; Kapralova, V.I.; Winnica, D.E.; Vikulina, A.S.; Domingues, M.R.; McCoy, J.; Sanders, L.H.; et al. LC/MS Analysis of Cardiolipins in Substantia Nigra and Plasma of Rotenone-Treated Rats: Implication for Mitochondrial Dysfunction in Parkinson's Disease. *Free Radic. Res.* **2015**, *49*, 681–691. [[CrossRef](#)]
82. Abumrad, N.A.; Moore, D.J. Parkin Reinvents Itself to Regulate Fatty Acid Metabolism by Tagging CD36. *J. Clin. Investig.* **2011**, *121*, 3389–3392. [[CrossRef](#)]

83. Kim, K.Y.; Stevens, M.V.; Akter, M.H.; Rusk, S.E.; Huang, R.J.; Cohen, A.; Noguchi, A.; Springer, D.; Bocharov, A.V.; Eggerman, T.L.; et al. Parkin Is a Lipid-Responsive Regulator of Fat Uptake in Mice and Mutant Human Cells. *J. Clin. Investig.* **2011**, *121*, 3701–3712. [[CrossRef](#)]
84. Krebs, C.E.; Karkheiran, S.; Powell, J.C.; Cao, M.; Makarov, V.; Darvish, H.; Di Paolo, G.; Walker, R.H.; Shahidi, G.A.; Buxbaum, J.D.; et al. The Sac1 Domain of SYNJ1 Identified Mutated in a Family with Early-Onset Progressive Parkinsonism with Generalized Seizures. *Hum. Mutat.* **2013**, *34*, 1200–1207. [[CrossRef](#)] [[PubMed](#)]
85. Quadri, M.; Fang, M.; Picillo, M.; Olgiati, S.; Breedveld, G.J.; Graafland, J.; Wu, B.; Xu, F.; Erro, R.; Amboni, M.; et al. Mutation in the SYNJ1 Gene Associated with Autosomal Recessive, Early-Onset Parkinsonism. *Hum. Mutat.* **2013**, *34*, 1208–1215. [[CrossRef](#)] [[PubMed](#)]
86. McPherson, P.S.; Garcia, E.P.; Slepnev, V.I.; David, C.; Zhang, X.; Grabs, D.; Sossin, W.S.; Bauerfeind, R.; Nemoto, Y.; De Camilli, P. A Presynaptic Inositol-5-Phosphatase. *Nature* **1996**, *379*, 353–357. [[CrossRef](#)] [[PubMed](#)]
87. Ben Romdhan, S.; Sakka, S.; Farhat, N.; Triki, S.; Dammak, M.; Mhiri, C. A Novel SYNJ1 Mutation in a Tunisian Family with Juvenile Parkinson's Disease Associated with Epilepsy. *J. Mol. Neurosci.* **2018**, *66*, 273–278. [[CrossRef](#)]
88. Cao, M.; Wu, Y.; Ashrafi, G.; McCartney, A.J.; Wheeler, H.; Bushong, E.A.; Boassa, D.; Ellisman, M.H.; Ryan, T.A.; De Camilli, P. Parkinson Sac Domain Mutation in Synaptojanin 1 Impairs Clathrin Uncoating at Synapses and Triggers Dystrophic Changes in Dopaminergic Axons. *Neuron* **2017**, *93*, 882–896.e5. [[CrossRef](#)]
89. Morgan, N.V.; Westaway, S.K.; Morton, J.E.; Gregory, A.; Gissen, P.; Sonek, S.; Cangul, H.; Coryell, J.; Canham, N.; Nardocci, N.; et al. PLA2G6, Encoding a Phospholipase A2, Is Mutated in Neurodegenerative Disorders with High Brain Iron. *Nat. Genet.* **2006**, *38*, 752–754. [[CrossRef](#)]
90. Khateeb, S.; Flusser, H.; Ofir, R.; Shelef, I.; Narkis, G.; Vardi, G.; Shorer, Z.; Levy, R.; Galil, A.; Elbedour, K.; et al. PLA2G6 Mutation Underlies Infantile Neuroaxonal Dystrophy. *Am. J. Hum. Genet.* **2006**, *79*, 942–948. [[CrossRef](#)]
91. Paisan-Ruiz, C.; Bhatia, K.P.; Li, A.; Hernandez, D.; Davis, M.; Wood, N.W.; Hardy, J.; Houlden, H.; Singleton, A.; Schneider, S.A. Characterization of PLA2G6 as a Locus for Dystonia-Parkinsonism. *Ann. Neurol.* **2009**, *65*, 19–23. [[CrossRef](#)] [[PubMed](#)]
92. Burke, J.E.; Dennis, E.A. Phospholipase A2 Structure/Function, Mechanism, and Signaling. *J. Lipid Res.* **2009**, *50*, S237–S242. [[CrossRef](#)] [[PubMed](#)]
93. Engel, L.A.; Jing, Z.; O'Brien, D.E.; Sun, M.; Kotzbauer, P.T. Catalytic Function of PLA2G6 Is Impaired by Mutations Associated with Infantile Neuroaxonal Dystrophy but Not Dystonia-Parkinsonism. *PLoS ONE* **2010**, *5*, e12897. [[CrossRef](#)]
94. Shinzawa, K.; Sumi, H.; Ikawa, M.; Matsuoka, Y.; Okabe, M.; Sakoda, S.; Tsujimoto, Y. Neuroaxonal Dystrophy Caused by Group VIA Phospholipase A2 Deficiency in Mice: A Model of Human Neurodegenerative Disease. *J. Neurosci.* **2008**, *28*, 2212–2220. [[CrossRef](#)]
95. Zhou, Q.; Yen, A.; Rymarczyk, G.; Asai, H.; Trengrove, C.; Aziz, N.; Kirber, M.T.; Mostoslavsky, G.; Ikezu, T.; Wolozin, B.; et al. Impairment of PARK14-Dependent Ca(2+) Signalling Is a Novel Determinant of Parkinson's Disease. *Nat. Commun.* **2016**, *7*, 10332. [[CrossRef](#)]
96. Malik, I.; Turk, J.; Mancuso, D.J.; Montier, L.; Wohltmann, M.; Wozniak, D.F.; Schmidt, R.E.; Gross, R.W.; Kotzbauer, P.T. Disrupted Membrane Homeostasis and Accumulation of Ubiquitinated Proteins in a Mouse Model of Infantile Neuroaxonal Dystrophy Caused by PLA2G6 Mutations. *Am. J. Pathol.* **2008**, *172*, 406–416. [[CrossRef](#)]
97. Beck, G.; Sugiura, Y.; Shinzawa, K.; Kato, S.; Setou, M.; Tsujimoto, Y.; Sakoda, S.; Sumi-Akamaru, H. Neuroaxonal Dystrophy in Calcium-Independent Phospholipase A2beta Deficiency Results from Insufficient Remodeling and Degeneration of Mitochondrial and Presynaptic Membranes. *J. Neurosci.* **2011**, *31*, 11411–11420. [[CrossRef](#)]
98. Cheon, Y.; Kim, H.W.; Igarashi, M.; Modi, H.R.; Chang, L.; Ma, K.; Greenstein, D.; Wohltmann, M.; Turk, J.; Rapoport, S.I.; et al. Disturbed Brain Phospholipid and Docosahexaenoic Acid Metabolism in Calcium-Independent Phospholipase A(2)-VIA (IPLA(2)Beta)-Knockout Mice. *Biochim. Biophys. Acta* **2012**, *1821*, 1278–1286. [[CrossRef](#)] [[PubMed](#)]
99. Mori, A.; Hatano, T.; Inoshita, T.; Shiba-Fukushima, K.; Koinuma, T.; Meng, H.; Kubo, S.I.; Spratt, S.; Cui, C.; Yamashita, C.; et al. Parkinson's Disease-Associated IPLA2-VIA/PLA2G6 Regulates Neuronal Functions and Alpha-Synuclein Stability through Membrane Remodeling. *Proc. Natl. Acad. Sci. USA* **2019**, *116*, 20689–20699. [[CrossRef](#)] [[PubMed](#)]

3. CONCLUSIONS

Parkinson's disease (PD) is an age-dependent neurodegenerative disorder that presents with disabling motor symptoms, and to date no drug treatment is able to act on the cause of the disease but only on motor symptoms.

The causes leading to the disease onset are related to both environmental and genetic factors. In recent years genetic studies have discovered different pathways that are involved in both genetic and sporadic forms of PD leading to oxidative stress, abnormal protein homeostasis, mitochondrial dysfunction and lysosomal defects.

Much emphasis has been placed on the involvement of certain genes, in particular α -synuclein and LRRK2, likely implicated in intracellular vesicle trafficking and their functional consequences. In neurons, vesicle trafficking underlies almost every functions of the nervous system, in fact it mediates the release and uptake of neurotransmitters or the release and uptake of proteins, the localization of membrane receptors, changes in the composition of the plasma membrane at the cell surface and, not least, the biogenesis of organelles.

Vesicular trafficking is tightly regulated and its dysregulation has been extensively implicated in PD and other neurological disorders⁸².

During the years of my PhD thesis I was mainly involved in deciphering the molecular mechanisms involved in the toxicity LRRK2 pathological mutant expression.

Considerable experimental evidence obtained by the analysis of LRRK2 cellular localization and LRRK2-interacting proteins suggests a significant involvement in the pathways regulating vesicle trafficking. LRRK2 is likely a scaffold protein keeping together and modulating a protein complex involved in vesicle dynamics. Interestingly SV2A, an integral transmembrane protein localized on neuronal vesicles, is part of this

complex. SV2A is the molecular target of a widely used drug for the treatment of epilepsy, the Levetiracetam (LEV)⁹⁴. Experimental evidence suggests that LEV may be considered not only an antiepileptic drug but also neuroprotective and analgesic compound⁹⁵. The absence of SV2A protein in knockout animals results in the development of frequent seizures, suggesting an agonistic rather than antagonistic effect of LEV on SV2A⁹¹ although the mechanism of action is far to be elucidated.

We demonstrated using different experimental models that LEV is able to reverse the pathological effects associated with LRRK2 G2019S expression.

In primary neurons from WT or LRRK2 G2019S BAC transgenic mice, G2019S expression results in a significant reduction in neurite outgrowth compared with primary WT neurons. LEV treatment significantly improves the shortening phenotype of G2019S neurons.

The same treatment was performed on PC12 cells expressing the dox-inducible LRRK2 G2019S mutant. After 6 days of NGF treatment, the expression of mutant G2019S, induced by doxycycline treatment, results in a strong reduction in neurite outgrowth. Addition of LEV significantly increased neurite outgrowth. Moreover, LEV treatment rescues the LRRK2 effect on DRD2 intracellular trafficking.

Our data strongly suggest that LEV treatment may represent a valuable neuroprotective compound for PD.

To further investigate the involvement of LRRK2 in vesicle trafficking, we developed a GST-pulldown approach to identify possible LRRK2 protein interactors. We identified the protein Sec8 as a specific LRRK2 interactor. The LRRK2 and Sec8 protein interaction was confirmed in transfected cell cultures and, most importantly, in mouse brain at physiological protein levels.

Sec8 is a member of the exocyst complex, an evolutionarily conserved multisubunit protein, primarily implicated in binding secretory vesicles to the plasma membrane. The exocyst complex is composed of eight single-copy subunits: Sec3, Sec5, Sec6, Sec8, Sec10, Sec15, Exo70, and Exo84.

Several members of the exocyst complex interact with SNARE members. These interactions are thought to precede vesicle priming, a process mediated by SNAREs to dock vesicles to the membrane and ultimately to induce lipid fusion.

We have shown that LRRK2 not only associates with Sec8, but, importantly, modulates the association of Sec8 with Exo70 and Sec6, two other members of the exocyst complex, strongly suggesting that LRRK2 may mediate the complex assembly. Interestingly, the LRRK2 effect is mediated by the kinase domain since it is significantly reduced either in the presence of LRRK2 kinase deletion mutant or by treatment with an LRRK2 kinase inhibitor.

Finally, we evidenced that overexpression of Sec8 can significantly impair the inhibition of SH-SY5Y differentiation due to LRRK2 G2019S expression.

Our data strongly support the role of LRRK2 in the control of vesicle trafficking. Since one of the first analysis by Piccoli et al. in 2011 demonstrating that LRRK2 may control the storage and mobilization of synaptic vesicles within the recycling pool, hundreds of different publications have highlight the role of LRRK2 in vesicle trafficking: LRRK2 mutants alter endocytosis through phosphorylation of DNAJC6 (auxilin), synaptojanin1, endoA, or Rab5b and modulate vesicle dynamics through aberrant phosphorylation of NSF or several Rab family proteins (see Introduction).

Alteration in vesicle trafficking may determine not only changes in the release and uptake of neurotransmitters, or the release and uptake of proteins, or the localization of membrane receptors, but also changes in the lipid composition of plasma membrane and organelles.

Indeed, changes in membrane lipids have been observed in both affected and unaffected regions of the brain of patients with PD, and in several experimental models expressing genes causative of or at risk for PD, indicating that altered lipid metabolism may precede disease development.

We extensively analyzed the changes in lipid composition in both PD patients and PD experimental models published in literature and we wrote a review article on this research topic.

During my doctoral years, I also partially contributed to two other research papers.



Review

Cyanobacteria, Cyanotoxins, and Neurodegenerative Diseases: Dangerous Liaisons

Paola Sini ¹, Thi Bang Chau Dang ^{1,2}, Milena Fais ¹, Manuela Galioto ¹, Bachisio Mario Padedda ³, Antonella Lugliè ³, Ciro Iaccarino ¹ and Claudia Crosio ^{1,*}

- ¹ Department of Biomedical Sciences, University of Sassari, 07100 Sassari, Italy; sinipaoladrop@gmail.com (P.S.); bangchaykt@gmail.com (T.B.C.D.); faismilena@gmail.com (M.F.); galioto@uniss.it (M.G.); ciaccarino@uniss.it (C.I.)
- ² Department of Biochemistry, Hue University, Hue City 7474, Vietnam
- ³ Laboratory of Aquatic Ecology, Department of Architecture, Design and Urban Planning, University of Sassari, 07100 Sassari, Italy; bmpadedda@uniss.it (B.M.P.); luglie@uniss.it (A.L.)
- * Correspondence: ccrosio@uniss.it; Tel.: +39-079228653

Abstract: The prevalence of neurodegenerative disease (ND) is increasing, partly owing to extensions in lifespan, with a larger percentage of members living to an older age, but the ND aetiology and pathogenesis are not fully understood, and effective treatments are still lacking. Neurodegenerative diseases such as Alzheimer's disease, Parkinson's disease, and amyotrophic lateral sclerosis are generally thought to progress as a consequence of genetic susceptibility and environmental influences. Up to now, several environmental triggers have been associated with NDs, and recent studies suggest that some cyanotoxins, produced by cyanobacteria and acting through a variety of molecular mechanisms, are highly neurotoxic, although their roles in neuropathy and particularly in NDs are still controversial. In this review, we summarize the most relevant and recent evidence that points at cyanotoxins as environmental triggers in NDs development.

Keywords: cyanobacteria; cyanotoxins; neurodegenerative diseases; ALS; Amyotrophic Lateral Sclerosis; PD; Parkinson's Disease; AD; Alzheimer Disease; L-BMAA



Citation: Sini, P.; Dang, T.B.C.; Fais, M.; Galioto, M.; Padedda, B.M.; Lugliè, A.; Iaccarino, C.; Crosio, C. Cyanobacteria, Cyanotoxins, and Neurodegenerative Diseases: *Dangerous Liaisons*. *Int. J. Mol. Sci.* **2021**, *22*, 8726. <https://doi.org/10.3390/ijms22168726>

Academic Editors: Masaru Tanaka and László Vécsei

Received: 12 July 2021
Accepted: 5 August 2021
Published: 13 August 2021

Publisher's Note: MDPI stays neutral with regard to jurisdictional claims in published maps and institutional affiliations.



Copyright: © 2021 by the authors. Licensee MDPI, Basel, Switzerland. This article is an open access article distributed under the terms and conditions of the Creative Commons Attribution (CC BY) license (<https://creativecommons.org/licenses/by/4.0/>).

1. Introduction

The aetiology and pathogenesis of neurodegenerative diseases (NDs) such as Alzheimer's disease (AD), Parkinson's disease (PD), and amyotrophic lateral sclerosis (ALS) are not fully understood. All these neurodegenerative disorders have a significant genetic contribution, although mendelian forms of NDs, attributed to rare gene mutations, may account only for up to 5–10% of the cases, and the remaining 90–95% are due to idiopathic mechanisms. Recent high-throughput genomic technologies have demonstrated that the NDs share common genetic factors, and microarrays and next-generation RNA-sequencing point to shared gene expression signatures, such as neuroinflammation genes [1], with further overlaps identified in genes related to RNA splicing and protein turnover between ALS and PD and mitochondrial dysfunction genes as a common theme between PD and AD. Moreover, a recent meta-analysis study on -omic data obtained at all gene expression levels reveals significant overlaps between the different diseases [2].

Patients affected by NDs share common genetic patterns, although a consistent percentage of sporadic cases may have causes other than or in addition to human hereditary factors. The non-genetic factors may include the involvement of a variety of environmental factors, such as toxins, produced naturally by microorganisms. Table 1 summarizes some of the most representative epidemiological data, verified by meta-analysis, linking NDs to environmental factors.

Table 1. Environmental factors in neurodegenerative diseases.

Environmental Factors	Effects	Diseases	Reference
Heavy metals	Lead (crosses the blood–brain barrier and accumulates in neuronal and glial cells)	ALS ¹	[3,4]
	Aluminium	AD ²	[5,6]
	Manganese	PD ³	[6,7]
Pesticide	Pentachlorobenzene	ALS	[8]
	Rotenone and paraquat	ALS, PD	[9,10]
	Organophosphate pesticides	ALS, PD, AD	[11]
Electromagnetic fields	Contradictory results	ALS, AD	[12–14]
Smoking	Protective	PD	[15,16]
	Risk factor	AD, ALS	[17,18]
Physical activity	Protective	PD	[19]
Body mass index and nutritional state	Lower nutritional parameters	AD	[20]
Microbiota structure and dysfunction of the gut–brain axis	<i>Akkermansia muciniphila</i> reduces symptoms; <i>Ruminococcus torques</i> and <i>Parabacteroides distasonis</i>	ALS	[21,22]
	Suppression of <i>Prevotellaceae</i> and anti-inflammatory genera; blooming of pro-inflammatory <i>Proteobacteria</i> , <i>Enterococcaceae</i> , and <i>Enterobacteriaceae</i>	PD	[23–25]
	Suppression of anti-inflammatory taxa such as <i>Eubacterium rectale</i> and a profusion of pro-inflammatory taxa such as <i>Escherichia</i> and <i>Shigella</i>	AD	[24,26]
Cyanobacteria and cyanotoxins	Risk factors	ALS, PD, AD	[27,28]

¹ ALS, Amyotrophic Lateral Sclerosis, ² AD, Alzheimer's Disease, ³ PD, Parkinson's Disease.

Cyanobacteria and microalgae synthesize significant quantities of toxins that can act via multiple molecular mechanisms [29,30]. Recent studies showing the presence of the neurotoxin β -N-methylamino-L-alanine (L-BMAA), produced by cyanobacteria and algal species, in the brain and cerebro-spinal fluid samples from patients with AD and ALS suggest that exposure to cyanotoxins may contribute to the development of human neurodegenerative diseases [27,31,32]. However, understanding the neurotoxic effects of L-BMAA and other microalgal neurotoxins and identification of pharmacological strategies to attenuate these harmful effects is needed.

Harmful algal blooms (HABs) represent a natural phenomenon caused by the growth of single or more species of phytoplankton at the same time. The harmful algal species (HAS) may belong to two different kingdoms of life, prokaryotic cyanobacteria and eukaryotic microalgae in waterbodies. In the last decades, HABs have had an evident increase in connection to human impacts such as eutrophication, aquaculture, hydrodynamic modifications in coastal systems, and global climate change [33]. Part of this observed HAB expansion reflects a better assessment of the current and past scale of the phenomenon, long obscured by scarce monitoring [34].

Over recent decades, it has been demonstrated that increasing anthropogenic activities, such as intensive agriculture and farming, industrialization, and urbanization, have led to the widespread eutrophication of inland and coastal ecosystems, resulting in a range of environmental, social, and economic issues due to the degradation of water resources [35,36]. Eutrophication causes shifts in the aquatic ecosystem's state, leading to a loss of ecosystem goods and services [37]. In fact, the quantity and quality of nutrient inputs to a water body can have profound effects upon its ecosystem processes and structure, e.g., acting on its biogeochemistry and biodiversity and altering the water quality. Eutrophication has many negative effects, among which one of the most worrying is the increased growth of microalgae [38] and cyanobacteria [39,40] that interfere with the use of waters [41]. Their blooms contribute to a range of problems, including fish kills, foul odors, unpalatability of drinking water, and hazards for human health [40].

The nutrient supplies to water bodies originate from different sources, such as external inputs, including catchment drainage, groundwater, and the atmosphere, and internal inputs, such as release from sediments. Strong relationships have been demonstrated between total phosphorus inputs and phytoplankton production in freshwaters [42–44], where N₂-fixing cyanobacteria often dominate, compensating for any deficit in nitrogen [45,46], as well for the intake of total nitrogen in estuarine [47] and marine waters [48,49], on a worldwide scale. Changes in nutrient supply ratios, particularly for mineral (N:P or N:Si) and organic forms (DOC:DON), are responsible for the rearrangement of phytoplankton assemblages in favor of dominant species, which can lead to the formation of blooms [50–52]. Despite progress in our knowledge of the mechanisms by which nutrients are supplied to ecosystems and the pathways by which different species absorb them, the connections between nutrient supply and bloom growth, as well as their potential toxicity or damage, remain poorly understood [53]. The increase in the abundance of algal prey is also responsible for the widespread heterotrophic and mixotrophic species among HAB [54,55]. The ecological success of a microalgae or cyanobacteria species is influenced by biological factors, such as the presence and abundance of other species, grazers [56], and abiotic factors, such as the flushing rate or water residence time, weather conditions, water mixing, and stratification. The overall impact of nutrient overabundance on hazardous algal species is strongly species-specific. Control and reductions of nutrients have been demonstrated as the only effective and structural solution to preventing phytoplankton biomass or HAB incidence [57].

The HAS, mainly represented by dinoflagellates, diatoms, and cyanobacteria, produce significant environmental impacts due to high biomass and/or toxin production (Figure 1).

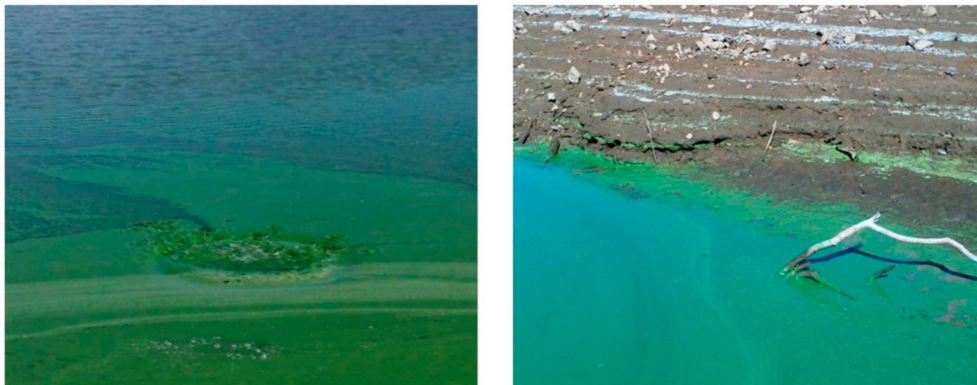


Figure 1. Evidence of intense cyano-HABs in Mediterranean artificial lakes (Sardinia; Lake Bidighinzu, on the left; Lake Posada, on the right). Cyanobacterial cell accumulation along shorelines, especially due to winds action, provokes blue-green colored waters.

Collectively, cyanotoxins and algal toxins have been implicated in an array of human diseases. In particular, the consumption of food contaminated by algal toxins results in various pathological conditions including seafood poisoning syndromes (diarrhetic shellfish poisoning—DSP, paralytic shellfish poisoning—PSP, neurotoxic shellfish poisoning—NSP, ciguatera fish poisoning—CFP, due to dinoflagellates; amnesic shellfish poisoning—ASP, due to diatoms). Human contact with aerosol or waterborne toxins can also have other minor deleterious impacts, such as dermatological or respiratory irritation [58]. Moreover, there is increasing epidemiological evidence of relationships between environmental toxins and neurodegenerative diseases, including ALS, AD, and PD [27,59,60].

Most of these pathological conditions are caused by neurotoxins, which show highly specific effects on the nervous system of animals, including humans, by interfering with nerve impulse transmission. Neurotoxins are a varied group of compounds, both chemically and pharmacologically. They vary in both chemical structure and mechanism of

action and produce very distinct biological effects, which provide a potential application of these toxins in pharmacology and toxicology.

Whereas dinoflagellates and diatoms are found primarily in marine environments, cyanobacteria are usually considered the major HAS in freshwater ecosystems. Actually, their impacts on transitional aquatic ecosystems may increase due to global climatic change [61]. Cyanobacteria produce an impressive range of toxic secondary metabolites, the cyanotoxins, whose presence and concentration in the waters is both a relevant threat to human health and the environment and a substantial economic cost [62,63]. Cyanobacteria are ancient, cosmopolitan inhabitants of terrestrial environments and fresh, transitional, and marine ecosystems; they are photosynthetic and prokaryotic organisms, classified in 150 genera, over 40 of which include species that produce cyanotoxins [64]. Cyanobacteria are fundamental components of phytoplankton, and their competitiveness, which depends on both biological traits and environmental conditions, allows them to dominate the phytoplankton of eutrophic and hypereutrophic water bodies. Interestingly, cyanobacteria have been globally growing due to the increase of the geographical distribution, including in the Mediterranean region, frequency, and extent of their harmful blooms (cyano-HABs), which are expected to further increase due to climate change [65,66]. Exposure to cyanotoxins, responsible for acute or (sub)chronic poisonings of wild/domestic animals and humans, can follow multiple routes: i) orally, via drinking water or via consumption of health food tablets or other organisms that have accumulated the cyanotoxins along the food chains; ii) in labour or recreational water environments dermally; or iii) by inhalation exposure [67].

Cyanotoxins are grouped, according to the physiological systems, organs, tissues, or cells that are primarily affected, in neurotoxins, hepatotoxins, cytotoxins, irritants, and gastrointestinal toxins. Many cyanotoxins are also tumor promoters, with carcinogenic activity, and are the causative agents of serious health threats for humans [68].

The purpose of this review is to summarize the scientific information on the relationship between neurodegenerative disorders and cyanobacterial/dinoflagellates neurotoxins, classified according to [69], focusing on the experimental models used to test CTX toxicity.

2. Cyanobacterial and Dinoflagellates Neurotoxins

According to [28,70], cyanobacterial and dinoflagellates neurotoxins can be divided in four main classes, based on their mode of action:

- saxitoxins (carbamate compounds, N-sulfocarbonyl compounds, decarbamyl compounds); ciguatoxins;
- anatoxins (anatoxin-a, homoanatoxin-a, guanitoxin);
- β -N-methylamino-L-alanine (L-BMAA) and its isomers (2,4-diaminobutyric acid, 2,4-DAB and aminoethylglycine, AEG);

3. Saxitoxins and the Paralytic Shellfish Poisoning

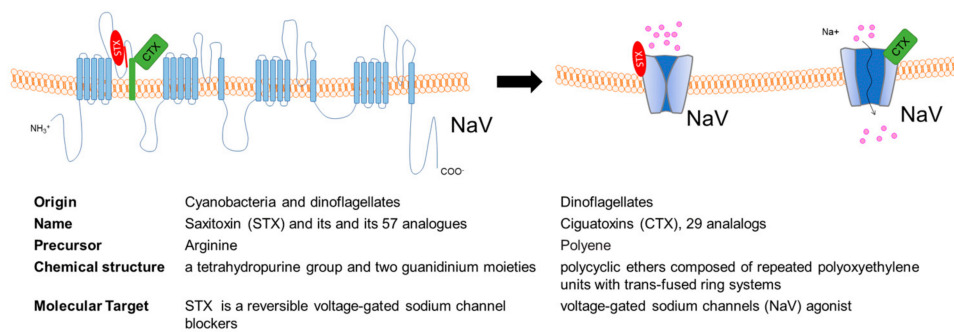
Saxitoxin (STX) and its 57 analogues, collectively indicated as paralytic shellfish toxins (PSTs), are a family of molecules consisting of a tetrahydropurine group and two guanidinium moieties, produced by both cyanobacteria and dinoflagellates [70,71].

The most well-known and researched source of the PSTs is marine dinoflagellates (e.g., *Alexandrium*), which are filtered by invertebrates such as shellfish, crustaceans, and molluscs without being affected by the toxins. The toxins become concentrated in the invertebrates and are then ingested by human consumers, causing paralytic shellfish poisoning (PSP). There are strict safety guidelines for commercially produced seafood that establish a shellfish harvesting prohibition if toxin levels exceed a maximum of 800 μ g STX eqv/1000 g edible tissue [72].

STX is one of the strongest natural neurotoxins, and it is also the most studied among PSTs [71]. STX is a reversible voltage-gated sodium channel blocker (Figure 2A) [73]. It crosses the blood–brain barrier and acts by blocking sodium channels in the central nervous system (CNS), therefore leading to paralytic effects [74]. A critical issue related to low-dose extended exposure of coastal communities who rely heavily on a seafood diet

is the study of the molecular mechanisms underlying STX toxicity. Exposure to STXs of cultured primary murine motoneurons as well neuronal cell lines (PC12 and SH-SY5Y cell lines) induces a reduction in axonal growth that is dependent on the presence of voltage-gated sodium channel isoform Nav1.9 [66,75]. Interestingly, the pharmacological activation to increase the opening probability of Nav1.9 could be a way to stimulate axon regeneration and maintenance in human neurodegenerative pathology such as spinal muscular atrophy (SMA), in which a defect in synapse maintenance appears as a central pathophysiological mechanism.

A. Saxitoxins and Ciguatoxins



B. Anatoxins

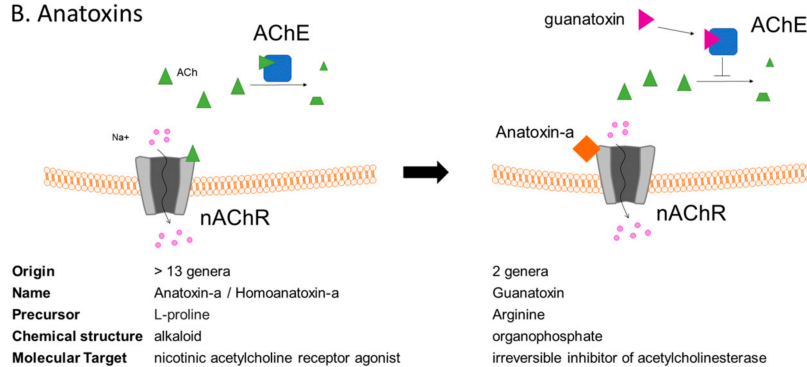


Figure 2. (A) Voltage-gated sodium channel (NaV) is the target of both saxitoxins (STXs) and ciguatoxins (CTXs). STX binding induces a block in Na⁺ conduction, while CTX binding slows down NaV inactivation. (B) Anatoxins act on the nicotinic acetylcholine receptor (nAChR): anatoxin-a is a nAChR receptor agonist, mimicking the binding of its natural ligand, acetylcholine (ACh), while guanatoxin inhibits acetylcholine esterase (AChE), inducing ACh accumulation at the neuromuscular junction.

A low dose of STXs induces an altered redox status that results in oxidative stress in different experimental paradigms, as reported in Table 2.

Recently, a proteomic study on murine neuroblastoma N2A cells identified different proteins altered upon low-dose saxitoxin exposure. The identified proteins are key regulators of cell apoptotic pathways, cell skeleton maintenance, membrane potentials, and mitochondrial functions [31]. Notably low doses of saxitoxins induce a decrease in voltage-dependent anion-selective channel 1 (VDAC1). VDAC1 is a multifunctional protein, expressed in the mitochondria and other cell compartments, that regulates the main metabolic and energetic functions of the cell (Ca²⁺ homeostasis, oxidative stress, and mitochondria-mediated apoptosis) [32]. Notably, VDAC1 represents the main mitochondrial docking site of many misfolded proteins, such as amyloid β and Tau in AD, α -synuclein in PD and several SOD1 mutants in ALS [33]. In AD post-mortem brains as well as in APP1 transgenic mouse models, VDAC1 was found to be over expressed in patients, and the possibility of decreasing it by using low doses of STX can be a fascinating therapeutic option [33].

Table 2. Saxitoxins treatment in different experimental models.

Experimental Model	Saxitoxins Exposure Protocol	Effects	Reference
primary neuron culture from tropical freshwater fish	0.3–3.0 mg L ⁻¹ 24h	oxidative stress, neurotoxicity, genotoxicity and apoptosis	[76]
murine neuroblastoma N2A	0–256 nM 24–48 h	high levels of ROS generation mild cytotoxic or apoptotic effects	[77]
rainbow trout fish cell line RTG-2	0–256 nM 24–48 h	mild cytotoxic or apoptotic effects	[77]
human primary astrocytes		high levels of ROS generation reduced cell survival	[78]
zebrafish embryos	0.05–0.1 µM	adverse effect on development of zebrafish embryos, oxidative stress-induced apoptosis	[79]
mouse neonate brain	single intraperitoneal 7.5 µg kg ⁻¹ body weight in pregnant mice	increased proliferation of OPCs, but not maturation process of these cells	[80]

4. Ciguatoxins

Ciguatoxins (CTXs) are polyether marine toxins known to activate voltage-gated sodium channels (NaV) and to cause one of the most widespread forms of nonbacterial food poisoning, named ciguatera. They are produced by dinoflagellates (i.e., *Gambierdiscus*) and reach humans via the food chain, with the consumption of fish that graze on reef macroalgae, including dinoflagellates that produce CTXs.

CTX-caused food poisoning was endemic only in tropical and subtropical areas, but it is spreading in Europe and Australia. Despite the high number of cases, estimated at around 50,000–500,000 cases per year, the prognosis is usually benign. In humans, more than 170 non-specific symptoms have been reported, although the most characteristic manifestations of ciguatera fish poisoning, found in all patients, are neurological symptoms, including paraesthesia and headache [81].

At present, more than 29 different CTX analogues have been identified, and they have been classified into three main groups that differ slightly in chemical structure according to the origin of the toxin: P for Pacific, C for the Caribbean, and I for Indian ciguatoxins [82] (Table 3).

Several lines of evidence suggest that chronic exposure to P-CTX-1 is associated with severe neurological manifestations in the peripheral nervous system (PNS) of some patients, suggesting that P-CTX-1 neurotoxicity, similar to other peripheral neuropathologies, primarily affects the PNS. In line with this hypothesis, it has been demonstrated, in mouse models, that the persistence of P-CTX-1 in peripheral nerves reduces the intrinsic growth capacity of peripheral neurons, resulting in delayed functional recovery after injury [83]. Moreover, P-CTX-1 has been shown to be a relatively non-selective activator of human NaVs subtypes (Figure 2A, displaying different functional effects on the different NaV subtypes, differentially expressed in peripheral sensory neurons [84]). It has been recently demonstrated that local application of 1 nM P-CTX-1 into the skin of human subjects induces a long-lasting, painful axon reflex flare and that CTXs are particularly effective in releasing calcitonin-gene related peptide (CGRP) from nerve terminals [85]. Significant alteration in CGRP expression has been also observed in the anterior horn of the spinal cord of familial ALS patients as well as in the transgenic mice expressing mutated human SOD1, one of the most-used ALS mice models [86]. In this ALS mouse model, the genetic deletion of CGRP accelerates muscle denervation and reduces cytotoxic neuroinflammation [87]. Interestingly, in the spinal cord of wobbler mice, a well-established model of motor neuron loss, an increase in mRNA of CGRP and its receptor, has been observed [88].

Additionally, CNS neuron physiology is altered upon CTXs exposure since synthetic ciguatoxin P-CTX-3C has been shown to have a profound effect on neuronal transmission

in mice primary cortical neurons [89]. The transcriptomic analysis of cortical neurons exposed for different time points to P-CTX-3C led to the identification of different signaling pathways activated downstream to the activating NaVs [90].

P-CTX-3C induces cytotoxicity in SHSY5Y human neuronal cells, only in the presence of the Na⁺ channel activator (veratridine) and of the inhibitor of the Na⁺/K⁺ ATPase (ouabain), mimicking a realistic human in vivo situation [91].

Interesting results were obtained using a tetracyclic analogue of ciguatoxin-like toxin, gambierol, in cellular and animal models for AD. In fact, although gambierol exhibits a potent acute lethal toxicity in mice (minimal lethal dose: 50 µg/kg, ip), its tetracyclic truncated analogue in a mouse model for AD induces a decrease of amyloid β1–42 level, a reduction of tau phosphorylation, and a reduction in the N2A subunit of the N-methyl-D-aspartate (NMDA) receptor level [92].

Table 3. Ciguatoxins treatment in different experimental models.

Experimental Model	Ciguatoxins Exposure Protocol	Molecular Target	effects	Reference
SH-SY5Y	25 pM–100 nM P-CTX-3C short-(4–24 h) and long-term exposure (10 days)		cytotoxic effect, alterations of the mitochondrial metabolism, cell morphology, and [Ca ²⁺] _i	[91]
primary cortical neurons	5 nM CTX3C 6-24-72 h		gene expression alteration mediated by voltage-gated sodium channel	[90]
C57BL/6 mice	shallow intraplantar (i.pl.) injection of P-CTX-1 (1–10 nM)	Nav 1.8 and TTXs Nav subtypes are effectors of ciguatoxin-induced cold allodynia	spontaneous pain	[93]
transgenic mice and rat	0.01–31 nM P-CTX-1 (>95% purity) isolated from moray eel (<i>Gymnothorax javanicus</i>) liver	Nav1.9	release of calcitonin-gene related peptide (CGRP) from nerve terminals	[85]
C57BL/6 mice	(0.26 ng/g body weight) intraperitoneally on day 0 followed by second exposure on day 3 P-CTX-1 (isolated and purified from moray eels)		irreversible motor deficit in 4-month pre-exposed mice following peripheral nerve injury astrogliosis and excitotoxic neuronal cell death via the activation of caspase 3 in motor cortex	[94]

5. Anatoxins

Anatoxins are water-soluble cyanotoxins (produced by different cyanobacterial genera, e.g., *Anabaena*, *Dolichospermum*, *Aphanizomenon*; Figure 3), lethal neurotoxins that can be classified into three main categories: anatoxin-a, its structural homologue homoanatoxin-a, and the unrelated guanitoxin, previously named anatoxin-a(s) [95].

Anatoxin-containing blooms have been found all over the world. As represented in Figure 2B, they have different physiological targets: (i) anatoxin-a is an alkaloid and an agonist of nicotine acetylcholine receptors (nAChRs), which are located both in the CNS as well as in the postsynaptic terminals of motor neurons, [96]; (ii) guanitoxin is an organophosphate that acts as an irreversible inhibitor of acetylcholinesterase (AChE, EC3.1.1.7) [28]. Notably, neuronal nAChRs are considered potential targets for the development of new therapeutic agents for the treatment of diverse disorders such as PD and AD [97,98], while AChE inhibitors have been demonstrated to be effective in slowing the clinical progression in AD patients [99].

Anatoxin-a was shown, at least in vitro, to induce inflammation and apoptosis in immune and brain cells [100], and it has been implicated in numerous animal poisonings worldwide. Up to date, there is no evidence of its toxic effects on the brain, and more detailed experiments are needed to find a link, if any, between anatoxin exposure and neurodegeneration.

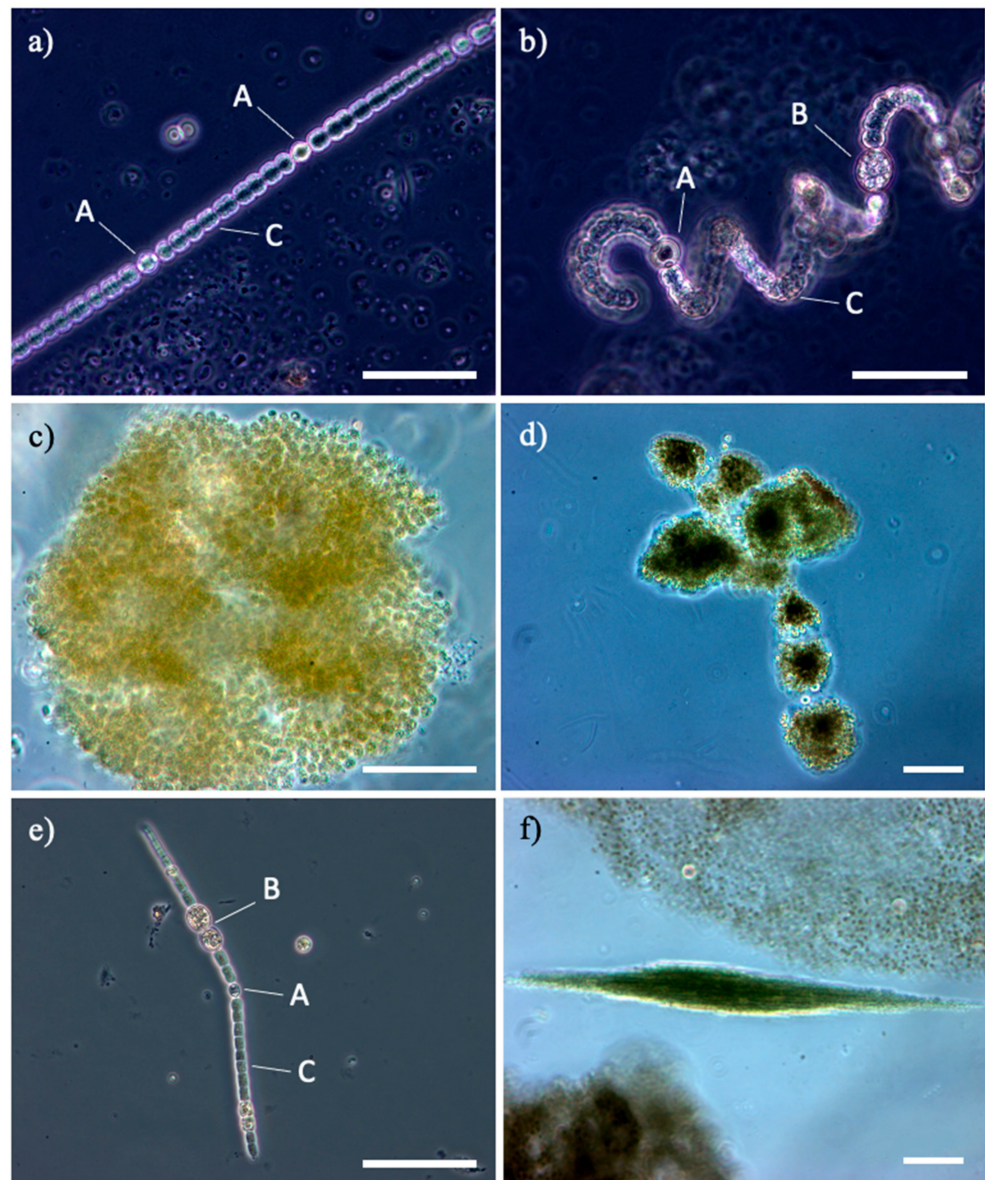


Figure 3. Cyanobacteria genera, potentially toxins producers in Mediterranean artificial lakes: (a,b): different species of *Dolichospermum* from Lake Bidighinzu; (c,d): different species of *Microcystis* from Lake Liscia and Lake Monte Lerno; (e,f): different species of *Aphanizomenon*, in single trichome from Lake Temo and in fascicle of trichomes from Lake Liscia. A: heterocyst, B: akinete; C: vegetative cells; bar 50 μm .

6. Role of L-BMAA in Neurodegenerative Diseases

L-BMAA was isolated for the first time from the seeds of *Cycas circinalis* L. [54]. L-BMAA is a non-protein neurotoxic amino acid produced almost from all known groups of cyanobacteria including cyanobacterial symbionts (e.g., *Nostoc*) and free-living cyanobacteria (e.g., *Anabaena*, *Microcystis*; Figure 3), marine diatoms (e.g., *Navicula*, *Skeletonema*), and dinoflagellates (e.g., *Gymnodinium*) in the most various ecosystems worldwide [101].

Despite some contradictory opinions [102], an increasingly large body of experimental outcomes provides significant evidence that L-BMAA plays an important role in slow-developing neurodegenerative diseases, including ALS/Parkinsonism Dementia Complex (ALS/PDC) found on Guam islands, ALS, AD, and PD (review [32,59]).

ALS/PDC, specific to Guam and certain other Marianas islands of the Western Pacific, with symptoms of all three diseases, came to the attention of the scientific community during and after World War II. In the 1950s, for Chamorro residents of Guam and Rota, ALS, ALS-like conditions, and their death rates were estimated to be 50–100 times higher than in the United States and in other developed countries. From the late 1960s to the early 1980s, the incidence of both disorders had decreased. The main causes responsible for the decreasing incidence appeared to be ethnographic, social, and ecological changes, brought about by the rapid westernization of Guam. This change suggests that the cause of the ALS/PDC was not genetic but rather environmental [103].

Since the indigenous Chamorro people consumed cycad seed flour in food and in traditional medicine, Spencer et al. [104] first proposed the connection between the etiopathogenesis of ALS/PDC and the neurotoxin L-BMAA produced by the cyanobacteria of the genus *Nostoc*, which are symbiont of coralloid roots cycads. In a preliminary study, Spencer et al. showed that repeated oral administration of L-BMAA (0–81 mmol/kg daily) to *Macaca fascicularis* monkeys was able to induce a degenerative motor-system disease with features of ALS and parkinsonism. Pyramidal dysfunction, limb weakness, atrophy, upper-extremity tremors and wrist drop, bradykinesia, behavioral changes, and degeneration of lower motor neurons were observed [104].

A significant finding in the primate study of Spencer et al. was that, while early signs of motor-neuron dysfunction were observed in animal models fed with high doses of L-BMAA, extrapyramidal damage developed slowly with lower doses of L-BMAA. This led the authors to propose that chronic toxicity might be separate from acute toxicity [60]. Interestingly, L-BMAA is then biomagnified up the food chain from symbiotic cyanobacteria to cycads to *flying fox* of the genus *Pteropus mariannus*. Cox et al. [105] observed a 10,000-fold biomagnification of free L-BMAA and 50-fold biomagnification in total L-BMAA. These data suggested a mechanism that could produce sufficiently high doses of toxins to induce neurological disease in humans [106–108].

Biomagnification of L-BMAA may not be unique to Guam; indeed, Cox and colleagues [109] detected L-BMAA not only in the brain tissue of Chamorros who died from ALS-PDC but also in Alzheimer's patients from Canada due to the capability of the neurotoxin to cross the blood–brain barrier through an active transport mechanism [110,111]. This finding suggests various ecological pathways for the bioaccumulation of L-BMAA in aquatic or terrestrial ecosystems.

L-BMAA is neurotoxic, and although different and multiple mechanisms of toxicity have been proposed (Figure 4), its involvement in neurotoxicity and neurodegeneration remains largely unidentified [112,113]. The neurotoxin is a non-lipophilic, non-essential amino acid that is present both in free and protein-bound forms. Weiss and Choi discovered that L-BMAA had activity in vitro only when a physiological concentration (10 mM and higher) of bicarbonate ions (HCO_3^-) was co-present in the cell culture media. L-BMAA's carbamate adduct, named β -carbamate, presents structural similarities to glutamate that may lead to neuronal degeneration via a mechanism regulated by the activation of excitatory amino acid (EAA) receptors and/or glutamate transporters through a three-fold mechanism [114,115]. At a glutamatergic synapse, β -carbamate binds to ionotropic (NMDA and AMPA/kainate receptors) receptors (iGluR) and metabotropic receptors (mGluR). Their activation induces a significant increase in intracellular Ca^{2+} , directly via iGluR and indirectly via mGluR (via phospholipase C signaling) [116], promoting mitochondrial reactive oxygen species (ROS) generation and endoplasmic reticulum (ER) stress [113]. This excitotoxicity of postsynaptic neurons typically leads to neuronal death. Besides being part of the pathogenic mechanism leading to ALS, excitotoxicity could be responsible for the selective vulnerability of motoneurons during the progression of the disease [117,118].

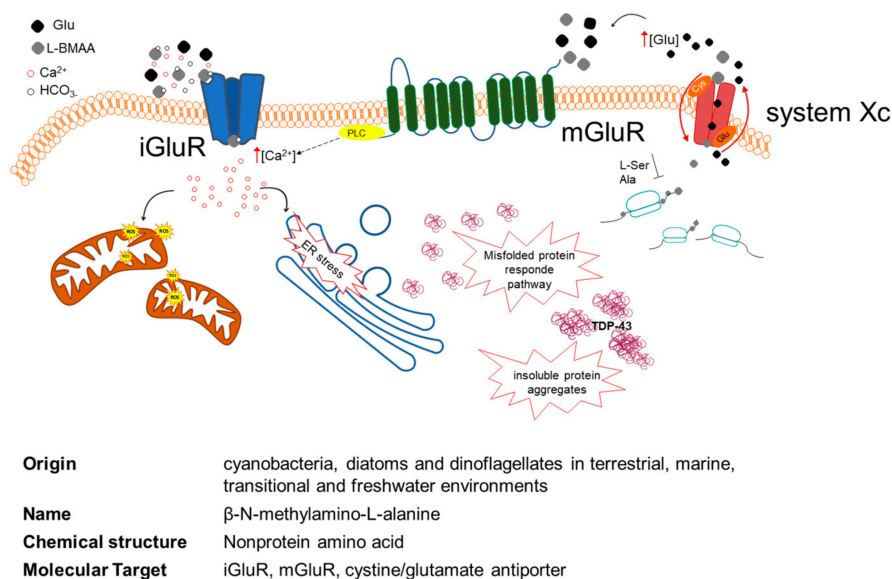


Figure 4. Multiple mechanisms of L-BMAA cellular toxicity. L-BMAA in the presence of bicarbonate ions (HCO₃⁻) forms L-BMAA's carbamate adduct, named β-carbamate, and binds to ionotropic (iGluR) and metabotropic (mGluR) receptors. The activation of iGluR and mGluR leads to a significant increase in intracellular Ca₂⁺, directly via iGluR and indirectly via mGluR (PLC signaling). This Ca₂⁺ increase promotes mitochondrial reactive oxygen species (ROS) generation and endoplasmic reticulum (ER) stress. L-BMAA inhibits the cystine/glutamate antiporter (system Xc)-mediated cystine uptake, which leads to glutathione depletion and increased oxidative stress. Once in the cytoplasm, the toxin is likely to be inserted into the neosynthesized cellular proteins and to prompt protein misfolding that often leads to the formation of insoluble aggregates, containing among other proteins TDP-43. iGluR: ionotropic glu receptors; mGluR: metabotropic glu receptors; PLC: phospholipase C; TDP-43: TAR DNA-binding protein 43.

Liu et al. in 2009 found that L-BMAA inhibits the cystine/glutamate antiporter (system Xc)-mediated cystine uptake, which leads to glutathione depletion and increased oxidative stress. In a cyclical system, L-BMAA seems to drive the release of glutamate through the Xc-system, which induces toxicity through the activation of the mGluR5 receptor. This transport may be the cause of L-BMAA accumulation in cells [118].

Once in the cytoplasm, the neurotoxin may probably be misincorporated in place of serine or alanine in neosynthesized cellular proteins. L-BMAA might also be associated with proteins through non-covalent bonds. The insertion of L-BMAA and other non-protein amino acids into proteins may generate protein dysfunction, misfolding, and/or aggregation. Although further research is required concerning L-BMAA incorporation into proteins, L-BMAA is incorporated into proteins in place of L-serine [119], and a large portion of L-BMAA is protein-bound (60- to 130-fold greater amount) compared to L-BMAA detected in the free [119,120].

This incorporated L-BMAA in brain tissues may function as an endogenous neurotoxic reservoir that can slowly release free L-BMAA, causing neurological damage over years or even decades, which may explicate the observed long-latency period for neurological disease onset among the Chamorro people [32].

Protein misfolding often leads to the formation of insoluble aggregates, and anomalous accumulation of aggregates in the affected tissues is one of the main pathological changes observed in neurodegenerative diseases. In ALS, this phenomenon involves biological markers including TDP-43 (TAR DNA-binding protein 43), a protein encoded by the TARDBP gene, located in the cell nucleus of most tissues. In physiological conditions, TDP-43 shuttles between the nucleus and cytoplasm, and it is involved in various steps of RNA biogenesis and processing such as alternative splicing [121,122]. In pathological conditions,

TDP-43 is hyperphosphorylated, ubiquitinated, and cleaved to generate C-terminal fragments, and it was identified as the main component of ubiquitinated inclusions in post-mortem tissues of ALS patients and patients with frontotemporal dementia [122,123].

Triggers with L-BMAA result in TDP-43 overexpression and aggregation in several *in vitro* and *in vivo* models: SH-SY5Y cell lines [124] and primary neurons (rats [124,125], mice [126,127], and zebrafish [128]). These specific forms of TDP-43 are present in patients with neurodegenerative diseases such as ALS and FTD.

The protein misincorporation of L-BMAA could affect protein-folding and successive accumulation of misfolded proteins into lysosomes [119]. This anomalous protein-synthesis is also supposed to lead to cell stress at the endoplasmic reticulum, independent of L-BMAA high concentration effects such as excitotoxicity and oxidative stress, deregulation of the reduction/oxidation systems, and an activation of some pro-apoptotic caspases like caspase-12 [129]. The resulting dysregulated protein homeostasis with low non-excitotoxic concentrations could be a contributing factor in the scenario of chronic L-BMAA exposure that may lead to late onset and slow progression of neurodegenerative diseases [129].

Moreover, L-BMAA leads to the activation of transcription factors known to be involved in the regulation of oxidative stress and cellular senescence such as X-box binding protein 1 and nuclear factor 2 erythroid like 2 [130]. Interestingly, the same high levels of these transcriptional regulators have been detected in the brains of patients with ALS, PD, AD, and front temporal dementia [131,132].

Numerous investigators used *in vitro* approaches to assess the potential role of L-BMAA on mammalian CNS models. It should be noted that most *in vitro* investigations needed high L-BMAA concentrations ($\geq 100 \mu\text{M}$) to produce cellular damage and toxicity (Table 4). These concentrations are not physiologically appropriate, and consequently the results are extremely difficult to interpret compared to *in vivo* responses. Therefore, numerous studies identified a possible mechanism of toxicity at a cellular level but are incomplete in relating the effects to L-BMAA environmental exposures.

Chiu and colleagues [114] reported NMDA receptor-mediated increases in intracellular calcium ions, ROS production, DNA damage, and neuronal death in primary human neuronal cells prepared from fetuses following exposure to L-BMAA, with the lowest toxic concentration in the presence of bicarbonate reported to be $400 \mu\text{M}$ [133]. The neuron-like cell lines are frequently chosen for their characteristics. SH-SY5Y, from human metastatic neuroblastoma, has dopaminergic, cholinergic, glutamatergic, and adenosinergic features; clonal rat pheochromocytoma cell line PC12, differentiated with nerve growth factor, is a recurrent model to study receptor-mediated excitotoxicity [134]. In order to investigate independent excitotoxic mechanisms, non-neuronal cells have also been used, but immortalized cells are significantly different from physiological characteristics in neurons; thus, numerous studies were made on primary neuronal cultures (Table 4).

Table 4. L-BMAA treatment in different experimental models.

Experimental Model	L-BMAA Exposure Protocol	Molecular Target	Reference
SH-SY5Y	3 mM plus antagonist for kainate/AMPA receptors 5 days	low neurotoxicity of BMAA and weak action at glutamatergic receptors	[135]
	0.1 mM 48h	Low non-excitotoxic BMAA concentrations induce effects on the ubiquitin/proteasome system not ROS-related	[129]
	3–10 mM 48h	decrease cell viability in a dose-response manner and evoke alterations in GSK3 β and TDP-43	[136]

Table 4. Cont.

Experimental Model	L-BMAA Exposure Protocol	Molecular Target	Reference
	0.5 mM 24h–48h–72h	Increased caspase-3 activity and cathepsins, ER stress	[137]
	0.05–0.25–1 mM 24 h	alterations in alanine, aspartate, and glutamate metabolism	[138]
	0.1–1 mM 24–48 h	autophagy	[139]
	3 mM 48h	disrupts mitochondrial metabolism	[140]
PC12	2 mM 6–12 h	apoptosis and mGluR1 increase	[141]
	0.4–1 mM 48h	promoted cell death and axon-like outgrowth	[142]
NSC-34	0.1–1 mM 72 h	exposure to BMAA causes protein misfolding, ER stress, induction of the UPR, disruption of the mitochondrial function	[130,141]
NIH/3T3	1–3 mM 48–96 h	L-BMAA causes arrest of cell cycle progression at the G1/S. No evidence of cell membrane damage, apoptosis, or ROS overproduction	[143]
primary cortical neurons	3 mM 1 h 20 mM HCO ₃ ⁻	L-BMAA activity is dependent on HCO ₃ ⁻ , resulting in a destruction of cortical neuronal population.	[115]
			[144]
primary cerebellar granule cells culture, rat	up to 3 mM 24–48h	L-BMAA induced both necrotic- and apoptotic-like cell death	[145]
primary neurons and astrocytes cortical cell cultures, fetal mouse	3–10 mM 3–24h 0.1 mM 48h	enhancement death of cortical neurons damaged by other insults; oxidative stress, Wallerian-Like Degeneration	[146–148]
neural stem cells	50 μM–3 mM 24 h	apoptosis, cellular differentiation, neurite outgrowth, and DNA methylation	[133]

The production of L-BMAA is not limited to cycad seeds, and the risk to exposure to this neurotoxin is not confined to Guam. In some locations, cyanobacteria are directly consumed by people. In the mountains of Peru, Cyanobacteria *Nostoc commune* Vaucher ex Bornet and Flahault (with a L-BMAA concentration of 10 μg/g) are collected in the highland lakes by the indigenous people, who call them llullucha [149]. Indigenous people eat them directly, sell them in markets, and add them to salads, soups, or meat dishes. Direct dietary intake is not the only possible mode of exposure to cyanobacterial neurotoxins. Inhalation as a systemic delivery route has been demonstrated for microcystins in nasal swabs and blood samples from people at risk of swallowing water or inhaling spray while swimming, water skiing, jet skiing, or boating during algal blooms [150]. In 2009, a causative link was hypothesized between the inhalation of L-BMAA, present in soil crusts dominated by cyanobacteria and detected in desert dust, and the higher incidence of ALS observed in the Gulf war veterans younger than 45 years old [151], but experiments in rat models observed significant biochemical responses to L-BMAA only at extremely high (non-physiological) concentrations [152].

Notably, L-BMAA misincorporation into neuroproteins produces protein misfolding and is inhibited by L-serine [108,139] that was proposed as a potential therapeutic option for ALS ([153] phase 2 [ClinicalTrials.gov](https://clinicaltrials.gov/ct2/show/study/NCT03580616) Identifier: NCT03580616), AD (Phase 2 [ClinicalTrials.gov](https://clinicaltrials.gov/ct2/show/study/NCT03062449) identifier: NCT03062449) and hereditary sensory autonomic neuropathy type I (HSAN1) [154]. The molecular mechanism underlying L-serine neuroprotection is not fully elucidated and can be independent of L-BMAA-mediated neurotoxicity [139].

7. Conclusion

An increasing cyanobacteria abundance is expected due to climate change and eutrophication, worsening the cyanotoxins issue and urging quick prevention and mitigation actions. Cyanobacteria detection in natural water samples with cyanotoxins (CTXs)-level determination should become a priority to prevent uncontrolled human exposure. Although pathophysiological mechanisms underlying ND is far from being completely understood, the link between CTX exposure and neurodegeneration is now widely accepted

by the scientific community. Apart from the well-described via of CTXs exposure (ingestion, dermal contact, biomagnification), it could be critical also to evaluate the presence of cyanobacteria in gut microbiota. In this respect, in the last 10 years, a growing recognition within the scientific and medical communities points at the “microbiota–gut–brain axis” as a key element in neurodegenerative process (Table 1 and [155] for a comprehensive review). Different lines of investigation have suggested that some species of cyanobacteria are present in small numbers in the gastrointestinal tract, and through the production of specific CTX, they could be considered potentially responsible for inducing neurodegeneration [155–157]. At present, only in PD patients, a specific decrease in cyanobacteria (Family Aphanizomenonaceae, Genus Dolichospermum) has been reported [158]. The lack of data for other neurodegenerative disorders can be linked to the low abundance of Cyanobacteria in biological samples tested. Nevertheless, human beings can be, via dietary sources, chronically exposed to cyanotoxins and/or other algal toxins, single or in combinations, which can alter different cellular processes and activate specific immune responses, chronic mild gut inflammation, and ultimately neurodegenerative processes [59].

The present review aims to emphasize the relationship between the increasing number of HABs and eutrophication with the molecular evidence linking CTXs to neurodegeneration. A multidisciplinary approach is required to mitigate the human health risks and to fill different scientific gaps. It is of particular interest to test the hypotheses whether CTXs in water samples are linked to their trophic state, to cyanobacteria abundance and/or species composition living there, and finally at the molecular level, to definitively establish the contribution of CTX chronic exposure to neurodegeneration.

Author Contributions: Read the literature and original draft preparation: P.S., M.F., T.B.C.D., M.G., B.M.P., A.L., C.I., and C.C. Edit the paper: C.I. and C.C. All authors have read and agreed to the published version of the manuscript.

Funding: Fondo di Ateneo per la Ricerca 2019 Crosio. Fondazione di Sardegna (Bando-2017-Iaccarino). Fondo di Ateneo per la Ricerca 2019 Iaccarino. P.S. and M.F. were supported by PhD fellowships granted by PON 2014–2020 (CCI2014IT16M2OP005). T.B.C.D. was supported by a Master Fellowship granted by Erasmus+—International Credit Mobility 2018-2019-Grant n° 2018-1-IT02-KA107-047494.

Acknowledgments: We would like to acknowledge all the people from the molecular biology laboratory that critically read the manuscript.

Conflicts of Interest: The authors declare no conflict of interest.

References

1. Tanaka, M.; Toldi, J.; Vécsei, L. Exploring the Etiological Links behind Neurodegenerative Diseases: Inflammatory Cytokines and Bioactive Kynurenines. *Int. J. Mol. Sci.* **2020**, *21*, 2431. [[CrossRef](#)]
2. Ruffini, N.; Klingenberg, S.; Schweiger, S.; Gerber, S. Common Factors in Neurodegeneration: A Meta-Study Revealing Shared Patterns on a Multi-Omics Scale. *Cells* **2020**, *9*, 2642. [[CrossRef](#)]
3. Gunnarsson, L.-G.; Bodin, L. Amyotrophic Lateral Sclerosis and Occupational Exposures: A Systematic Literature Review and Meta-Analyses. *Int. J. Environ. Res. Public Health* **2018**, *15*, 2371. [[CrossRef](#)]
4. Wang, H.; Yi, J.; Li, X.; Xiao, Y.; Dhakal, K.; Zhou, J. ALS-Associated Mutation SOD1(G93A) Leads to Abnormal Mitochondrial Dynamics in Osteocytes. *Bone* **2018**, *106*, 126–138. [[CrossRef](#)]
5. Killin, L.O.J.; Starr, J.M.; Shiue, I.J.; Russ, T.C. Environmental Risk Factors for Dementia: A Systematic Review. *BMC Geriatr.* **2016**, *16*, 175. [[CrossRef](#)] [[PubMed](#)]
6. Cicero, C.E.; Mostile, G.; Vasta, R.; Rapisarda, V.; Signorelli, S.S.; Ferrante, M.; Zappia, M.; Nicoletti, A. Metals and Neurodegenerative Diseases. A Systematic Review. *Environ. Res.* **2017**, *159*, 82–94. [[CrossRef](#)]
7. Racette, B.A.; Nielsen, S.S.; Criswell, S.R.; Sheppard, L.; Seixas, N.; Warden, M.N.; Checkoway, H. Dose-Dependent Progression of Parkinsonism in Manganese-Exposed Welders. *Neurology* **2017**, *88*, 344–351. [[CrossRef](#)] [[PubMed](#)]
8. Su, F.-C.; Goutman, S.A.; Chernay, S.; Mukherjee, B.; Callaghan, B.C.; Batterman, S.; Feldman, E.L. Association of Environmental Toxins With Amyotrophic Lateral Sclerosis. *JAMA Neurol.* **2016**, *73*, 803–811. [[CrossRef](#)] [[PubMed](#)]
9. Tanner, C.M.; Kamel, F.; Ross, G.W.; Hoppin, J.A.; Goldman, S.M.; Korell, M.; Marras, C.; Bhudhikanok, G.S.; Kasten, M.; Chade, A.R.; et al. Rotenone, Paraquat, and Parkinson’s Disease. *Environ. Health Perspect.* **2011**, *119*, 866–872. [[CrossRef](#)]

10. Ascherio, A.; Schwarzschild, M.A. The Epidemiology of Parkinson's Disease: Risk Factors and Prevention. *Lancet Neurol.* **2016**, *15*, 1257–1272. [[CrossRef](#)]
11. Sánchez-Santed, F.; Colomina, M.T.; Herrero Hernández, E. Organophosphate Pesticide Exposure and Neurodegeneration. *Cortex* **2016**, *74*, 417–426. [[CrossRef](#)] [[PubMed](#)]
12. Gunnarsson, L.-G.; Bodin, L. Occupational Exposures and Neurodegenerative Diseases-A Systematic Literature Review and Meta-Analyses. *Int. J. Environ. Res. Public Health* **2019**, *16*, 337. [[CrossRef](#)]
13. Gunnarsson, L.-G.; Bodin, L. Alzheimer's Disease and Occupational Exposures: A Systematic Literature Review and Meta-Analyses; 2015; Volume 17. In *Alzheimer's Disease & Treatment*. Available online: <http://openaccessbooks.com/alzheimers-disease-treatment/alzheimers-disease-and-occupational-exposures-a-systematic-literature-review-and-meta-analyses.pdf> (accessed on 2 August 2021).
14. Riancho, J.; Sanchez de la Torre, J.R.; Paz-Fajardo, L.; Limia, C.; Santurtun, A.; Cifra, M.; Kourtidis, K.; Fdez-Arroyabe, P. The Role of Magnetic Fields in Neurodegenerative Diseases. *Int. J. Biometeorol.* **2021**, *65*, 107–117. [[CrossRef](#)]
15. Jacobs, B.M.; Belete, D.; Bestwick, J.; Blauwendraat, C.; Bandres-Ciga, S.; Heilbron, K.; Dobson, R.; Nalls, M.A.; Singleton, A.; Hardy, J.; et al. Parkinson's Disease Determinants, Prediction and Gene–Environment Interactions in the UK Biobank. *J. Neurol. Neurosurg. Psychiatry* **2020**, *91*, 1046–1054. [[CrossRef](#)]
16. Noyce, A.J.; Bestwick, J.P.; Silveira-Moriyama, L.; Hawkes, C.H.; Giovannoni, G.; Lees, A.J.; Schrag, A. Meta-Analysis of Early Nonmotor Features and Risk Factors for Parkinson Disease. *Ann. Neurol.* **2012**, *72*, 893–901. [[CrossRef](#)] [[PubMed](#)]
17. Wallin, C.; Sholtz, S.B.; Österlund, N.; Luo, J.; Jarvet, J.; Roos, P.M.; Ilag, L.; Gräslund, A.; Wärmländer, S.K.T.S. Alzheimer's Disease and Cigarette Smoke Components: Effects of Nicotine, PAHs, and Cd(II), Cr(III), Pb(II), Pb(IV) Ions on Amyloid- β Peptide Aggregation. *Sci. Rep.* **2017**, *7*, 14423. [[CrossRef](#)]
18. Menounos, S.; Hansbro, P.M.; Diwan, A.D.; Das, A. Pathophysiological Correlation between Cigarette Smoking and Amyotrophic Lateral Sclerosis. *NeuroSci* **2021**, *2*, 120–134. [[CrossRef](#)]
19. Bellou, V.; Belbasis, L.; Tzoulaki, I.; Evangelou, E.; Ioannidis, J.P.A. Environmental Risk Factors and Parkinson's Disease: An Umbrella Review of Meta-Analyses. *Parkinsonism Relat. Disord.* **2016**, *23*, 1–9. [[CrossRef](#)] [[PubMed](#)]
20. Verhaar, B.J.H.; de Leeuw, F.A.; Doorduijn, A.S.; Fieldhouse, J.L.P.; van de Rest, O.; Teunissen, C.E.; van Berckel, B.N.M.; Barkhof, F.; Visser, M.; de van der Schueren, M.A.E.; et al. Nutritional Status and Structural Brain Changes in Alzheimer's Disease: The NUDAD Project. *Alzheimers Dement. Diagn. Assess. Dis. Monit.* **2020**, *12*, e12063. [[CrossRef](#)]
21. Depommier, C.; Everard, A.; Druart, C.; Plovier, H.; Van Hul, M.; Vieira-Silva, S.; Falony, G.; Raes, J.; Maiter, D.; Delzenne, N.M.; et al. Supplementation with Akkermansia Muciniphila in Overweight and Obese Human Volunteers: A Proof-of-Concept Exploratory Study. *Nat. Med.* **2019**, *25*, 1096–1103. [[CrossRef](#)]
22. Blacher, E.; Bashiardes, S.; Shapiro, H.; Rothschild, D.; Mor, U.; Dori-Bachash, M.; Kleimeyer, C.; Moresi, C.; Harnik, Y.; Zur, M.; et al. Potential Roles of Gut Microbiome and Metabolites in Modulating ALS in Mice. *Nature* **2019**, *572*, 474–480. [[CrossRef](#)]
23. Cryan, J.F.; O'Riordan, K.J.; Sandhu, K.; Peterson, V.; Dinan, T.G. The Gut Microbiome in Neurological Disorders. *Lancet Neurol.* **2020**, *19*, 179–194. [[CrossRef](#)]
24. Quigley, E.M.M. Microbiota-Brain-Gut Axis and Neurodegenerative Diseases. *Curr. Neurol. Neurosci. Rep.* **2017**, *17*, 94. [[CrossRef](#)]
25. Klingelhoefer, L.; Reichmann, H. Pathogenesis of Parkinson Disease—the Gut-Brain Axis and Environmental Factors. *Nat. Rev. Neurol.* **2015**, *11*, 625–636. [[CrossRef](#)] [[PubMed](#)]
26. Cattaneo, A.; Cattane, N.; Galluzzi, S.; Provasi, S.; Lopizzo, N.; Festari, C.; Ferrari, C.; Guerra, U.P.; Paghera, B.; Muscio, C.; et al. Association of Brain Amyloidosis with Pro-Inflammatory Gut Bacterial Taxa and Peripheral Inflammation Markers in Cognitively Impaired Elderly. *Neurobiol. Aging* **2017**, *49*, 60–68. [[CrossRef](#)]
27. Cox, P.A.; Kostrzewa, R.M.; Guillemin, G.J. BMAA and Neurodegenerative Illness. *Neurotox. Res.* **2018**, *3*, 178–183. [[CrossRef](#)] [[PubMed](#)]
28. Fiore, M.F.; de Lima, S.T.; Carmichael, W.W.; McKinnie, S.M.K.; Chekan, J.R.; Moore, B.S. Guanitoxin, Re-Naming a Cyanobacterial Organophosphate Toxin. *Harmful Algae* **2020**, *92*, 101737. [[CrossRef](#)]
29. Buratti, F.M.; Manganelli, M.; Vichi, S.; Stefanelli, M.; Scardala, S.; Testai, E.; Funari, E. Cyanotoxins: Producing Organisms, Occurrence, Toxicity, Mechanism of Action and Human Health Toxicological Risk Evaluation. *Arch Toxicol.* **2017**, *91*, 1049–1130. [[CrossRef](#)] [[PubMed](#)]
30. Plaas, H.E.; Paerl, H.W. Toxic Cyanobacteria: A Growing Threat to Water and Air Quality. *Environ. Sci. Technol.* **2021**, *55*, 44–64. [[CrossRef](#)]
31. Berntzon, L.; Ronnevi, L.O.; Bergman, B.; Eriksson, J. Detection of BMAA in the Human Central Nervous System. *Neuroscience* **2015**, *292*, 137–147. [[CrossRef](#)]
32. Dunlop, R.A.; Banack, S.A.; Bishop, E.S.; Metcalf, J.S.; Murch, S.J.; Davis, D.A.; Stommel, E.W.; Karlsson, A.; Bribetto, A.; Chatziefthimiou, A.; et al. Is Exposure to BMAA a Risk Factor for Neurodegenerative Diseases? A Response to a Critical Review of the BMAA Hypothesis. *Neurotox. Res.* **2021**, *39*, 81–106. [[CrossRef](#)]
33. Brooks, B.W.; Lazorchak, J.M.; Howard, M.D.; Johnson, M.V.; Morton, S.L.; Perkins, D.A.; Reavie, E.D.; Scott, G.I.; Smith, S.A.; Steevens, J.A. Are Harmful Algal Blooms Becoming the Greatest Inland Water Quality Threat to Public Health and Aquatic Ecosystems? *Environ. Toxicol. Chem.* **2016**, *35*, 6–13. [[CrossRef](#)]

34. Anderson, D.M.; Fensin, E.; Gobler, C.J.; Hoeglund, A.E.; Hubbard, K.A.; Kulis, D.M.; Landsberg, J.H.; Lefebvre, K.A.; Provoost, P.; Richlen, M.L.; et al. Marine Harmful Algal Blooms (HABs) in the United States: History, Current Status and Future Trends. *Harmful Algae* **2021**, *102*, 101975. [CrossRef]
35. Carpenter, S.R.; Caraco, N.F.; Correll, D.L.; Howarth, R.W.; Sharpley, A.N.; Smith, V.H. Nonpoint Pollution of Surface Waters with Phosphorus and Nitrogen. *Ecol. Appl.* **1998**, *8*, 559–568. [CrossRef]
36. Smith, V.H.; Tilman, G.D.; Nekola, J.C. Eutrophication: Impacts of Excess Nutrient Inputs on Freshwater, Marine, and Terrestrial Ecosystems. *Environ. Pollut.* **1999**, *100*, 179–196. [CrossRef]
37. Dodds, W.K.; Bouska, W.W.; Eitzmann, J.L.; Pilger, T.J.; Pitts, K.L.; Riley, A.J.; Schloesser, J.T.; Thornbrugh, D.J. Eutrophication of U.S. Freshwaters: Analysis of Potential Economic Damages. *Environ. Sci. Technol.* **2009**, *43*, 12–19. [CrossRef]
38. Assmy, P.; Smetacek, V. Algal Blooms. In *Encyclopedia of Microbiology*; Elsevier: New York, NY, USA, 2009; pp. 27–41. ISBN 978-0-12-373944-5.
39. Paerl, H.W.; Otten, T.G. Harmful Cyanobacterial Blooms: Causes, Consequences, and Controls. *Microb. Ecol.* **2013**, *65*, 995–1010. [CrossRef]
40. Merel, S.; Walker, D.; Chicana, R.; Snyder, S.; Baurès, E.; Thomas, O. State of Knowledge and Concerns on Cyanobacterial Blooms and Cyanotoxins. *Environ. Int.* **2013**, *59*, 303–327. [CrossRef] [PubMed]
41. Jørgensen, S.E.; International Lake Environment Committee and United Nations Environmental Programme. *Lakes and Reservoirs. Volume 3, Water Quality: The Impact of Eutrophication; UNEP-IETC/ILEC*. 2001. Available online: <https://www.ilec.or.jp/wp-content/uploads/pub/Vol.3.pdf> (accessed on 2 August 2021).
42. Padedda, B.M.; Sechi, N.; Lai, G.G.; Mariani, M.A.; Pulina, S.; Sarria, M.; Satta, C.T.; Viridis, T.; Buscarinu, P.; Lugliè, A. Consequences of Eutrophication in the Management of Water Resources in Mediterranean Reservoirs: A Case Study of Lake Cedrino (Sardinia, Italy). *Glob. Ecol. Conserv.* **2017**, *12*, 21–35. [CrossRef]
43. Mariani, M.A.; Padedda, B.M.; Kastovsky, J.; Buscarinu, P.; Sechi, N.; Viridis, T.; Lugliè, A. Effects of Trophic Status on Microcystin Production and the Dominance of Cyanobacteria in the Phytoplankton Assemblage of Mediterranean Reservoirs. *Sci. Rep.* **2015**, *5*, 17964. [CrossRef] [PubMed]
44. Mariani, M.A.; Lai, G.G.; Padedda, B.M.; Pulina, S.; Sechi, N.; Viridis, T.; Lugliè, A. Long-Term Ecological Studies on Phytoplankton in Mediterranean Reservoirs: A Case Study from Sardinia (Italy). *Inland Waters* **2015**, *5*, 339–354. [CrossRef]
45. Oliver, R.; Ganf, G. Freshwater blooms. In *The Ecology of Cyanobacteria*; Kluwer Academic Publishers: Dordrecht, The Netherlands, 2000; pp. 149–194.
46. Schindler, D.; Hecky, R.; Findlay, D.; Stainton, M.; Parker, B.; Paterson, M.; Beaty, K.; Lyng, M.; Kasian, S. Eutrophication of Lakes Cannot Be Controlled by Reducing Nitrogen Input: Results of a 37-Year Whole-Ecosystem Experiment | PNAS. Available online: <https://www.pnas.org/content/105/32/11254> (accessed on 29 July 2021).
47. Padedda, B.M.; Lugliè, A.; Ceccherelli, G.; Trebini, F.; Sechi, N. Nutrient-Flux Evaluation by the LOICZ Biogeochemical Model in Mediterranean Lagoons: The Case of Cabras Lagoon (Central-Western Sardinia). *Chem. Ecol.* **2010**, *26*, 147–162. [CrossRef]
48. Seitzinger, S.P.; Kroeze, C. Global Distribution of Nitrous Oxide Production and N Inputs in Freshwater and Coastal Marine Ecosystems. *Glob. Biogeochem. Cycles* **1998**, *12*, 93–113. [CrossRef]
49. Van Drecht, G.; Bouwman, A.F.; Knoop, J.M.; Beusen, A.H.W.; Meinardi, C.R. Global Modeling of the Fate of Nitrogen from Point and Nonpoint Sources in Soils, Groundwater, and Surface Water. *Glob. Biogeochem. Cycles* **2003**, *17*. [CrossRef]
50. Tilman, D. Resource Competition between Plankton Algae: An Experimental and Theoretical Approach. *Ecology* **1977**, *58*, 338–348. [CrossRef]
51. Smayda, T.J. Harmful Algal Blooms: Their Ecophysiology and General Relevance to Phytoplankton Blooms in the Sea. *Limnol. Oceanogr.* **1997**, *42*, 1137–1153. [CrossRef]
52. Smayda, T.; Graneli, E.; Sundstrom, B.; Edler, L.; Anderson, D.; Smayda, T. Novel and Nuisance Phytoplankton Blooms in the Sea: Evidence for a Global Epidemic. *Toxic Mar. Phytoplankton* **1990**, *1*, 29–40.
53. Anderson, D.M.; Glibert, P.M.; Burkholder, J.M. Harmful Algal Blooms and Eutrophication: Nutrient Sources, Composition, and Consequences. *Estuaries* **2002**, *25*, 704–726. [CrossRef]
54. Glibert, P.M.; Harrison, J.; Heil, C.; Seitzinger, S. Escalating Worldwide Use of Urea—A Global Change Contributing to Coastal Eutrophication. *Biogeochemistry* **2006**, *77*, 441–463. [CrossRef]
55. Burkholder, J.M.; Glibert, P.M.; Skelton, H.M. Mixotrophy, a Major Mode of Nutrition for Harmful Algal Species in Eutrophic Waters. *Harmful Algae* **2008**, *8*, 77–93. [CrossRef]
56. Fadda, A.; Marková, S.; Kotlík, P.; Lugliè, A.; Padedda, B.; Buscarinu, P.; Sechi, N.; Manca, M. First Record of Planktonic Crustaceans in Sardinian Reservoirs. *Biologia* **2011**, *66*, 856–865. [CrossRef]
57. Padedda, B.M.; Sechi, N.; Lai, G.G.; Mariani, M.A.; Pulina, S.; Satta, C.T.; Bazzoni, A.M.; Viridis, T.; Buscarinu, P.; Lugliè, A. A Fast-Response Methodological Approach to Assessing and Managing Nutrient Loads in Eutrophic Mediterranean Reservoirs. *Ecol. Eng.* **2015**, *85*, 47–55. [CrossRef]
58. Zingone, A.; Escalera, L.; Aligizaki, K.; Fernández-Tejedor, M.; Ismael, A.; Montresor, M.; Mozetič, P.; Taş, S.; Totti, C. Toxic Marine Microalgae and Noxious Blooms in the Mediterranean Sea: A Contribution to the Global HAB Status Report. *Harmful Algae* **2021**, *102*, 101843. [CrossRef] [PubMed]
59. Nunes-Costa, D.; Magalhães, J.D.; G-Fernandes, M.; Cardoso, S.M.; Empadinhas, N. Microbial BMAA and the Pathway for Parkinson’s Disease Neurodegeneration. *Front. Aging Neurosci.* **2020**, *12*, 26. [CrossRef] [PubMed]

60. Spencer, P.S.; Palmer, V.S.; Kisby, G.E. Cycad β -N-Methylamino-L-Alanine (BMAA), Methylazoxymethanol, Genotoxicity, and Neurodegeneration. *Toxicon* **2018**, *155*, 49–50. [[CrossRef](#)] [[PubMed](#)]
61. Luglie, A.; Pulina, S.; Bruno, M.; Padedda, B.M.; Satta, C.T.; Sechi, N. Marine Toxins and Climate Change: The Case of PSP from Cyanobacteria in Coastal Lagoons. In *Phycotoxins: Chemistry and Biochemistry*, 2nd ed.; Botana, L.M., Alfonso, A., Eds.; Wiley-Blackwell: Malden, MA, USA, 2015; ISBN 978-1-118-50033-0.
62. Rastogi, R.P.; Madamwar, D.; Incharoensakdi, A. Bloom Dynamics of Cyanobacteria and Their Toxins: Environmental Health Impacts and Mitigation Strategies. *Front. Microbiol.* **2015**, *6*, 1254. [[CrossRef](#)]
63. Sha, J.; Xiong, H.; Li, C.; Lu, Z.; Zhang, J.; Zhong, H.; Zhang, W.; Yan, B. Harmful Algal Blooms and Their Eco-Environmental Indication. *Chemosphere* **2021**, *274*, 129912. [[CrossRef](#)]
64. Moreira, C.; Vasconcelos, V.; Antunes, A. Phylogeny and Biogeography of Cyanobacteria and Their Produced Toxins. *Mar. Drugs* **2013**, *11*, 4350–4369. [[CrossRef](#)]
65. Paerl, H.W.; Huisman, J. Climate. Blooms like It Hot. *Science* **2008**, *320*, 57–58. [[CrossRef](#)]
66. O'Neill, K.; Musgrave, I.F.; Humpage, A. Extended Low-Dose Exposure to Saxitoxin Inhibits Neurite Outgrowth in Model Neuronal Cells. *Basic Clin. Pharmacol. Toxicol.* **2017**, *120*, 390–397. [[CrossRef](#)]
67. Drobac, D.; Tokodi, N.; Simeunovic, J.; Baltic, V.; Stanic, D.; Svircev, Z. Human Exposure to Cyanotoxins and Their Effects on Health. *Arh. Hig. Rada Toksikol.* **2013**, *64*, 119–130. [[CrossRef](#)]
68. Hernandez, B.Y.; Zhu, X.; Sotto, P.; Paulino, Y. Oral Exposure to Environmental Cyanobacteria Toxins: Implications for Cancer Risk. *Environ. Int.* **2021**, *148*, 106381. [[CrossRef](#)]
69. Rutkowska, M.; Plotka-Wasyłka, J.; Majchrzak, T.; Wojnowski, W.; Mazur-Marzec, H.; Namieśnik, J. Recent Trends in Determination of Neurotoxins in Aquatic Environmental Samples. *TrAC Trends Anal. Chem.* **2019**, *112*, 112–122. [[CrossRef](#)]
70. Wiese, M.; D'Agostino, P.M.; Mihali, T.K.; Moffitt, M.C.; Neilan, B.A. Neurotoxic Alkaloids: Saxitoxin and Its Analogs. *Mar. Drugs* **2010**, *8*, 2185–2211. [[CrossRef](#)]
71. Watanabe, R.; Kanamori, M.; Yoshida, H.; Okumura, Y.; Uchida, H.; Matsushima, R.; Oikawa, H.; Suzuki, T. Development of Ultra-Performance Liquid Chromatography with Post-Column Fluorescent Derivatization for the Rapid Detection of Saxitoxin Analogues and Analysis of Bivalve Monitoring Samples. *Toxins* **2019**, *11*, 573. [[CrossRef](#)] [[PubMed](#)]
72. Batoréu, M.C.C.; Dias, E.; Pereira, P.; Franca, S. Risk of Human Exposure to Paralytic Toxins of Algal Origin. *Environ. Toxicol. Pharmacol.* **2005**, *19*, 401–406. [[CrossRef](#)] [[PubMed](#)]
73. Shen, H.; Li, Z.; Jiang, Y.; Pan, X.; Wu, J.; Cristofori-Armstrong, B.; Smith, J.J.; Chin, Y.K.Y.; Lei, J.; Zhou, Q.; et al. Structural Basis for the Modulation of Voltage-Gated Sodium Channels by Animal Toxins. *Science* **2018**, *362*. [[CrossRef](#)]
74. Cervantes Cianca, R.C.; Pallares, M.A.; Durán Barbosa, R.; Vidal Adan, L.; Leão Martins, J.M.; Gago-Martínez, A. Application of Precolumn Oxidation HPLC Method with Fluorescence Detection to Evaluate Saxitoxin Levels in Discrete Brain Regions of Rats. *Toxic. Off. J. Int. Soc. Toxinol.* **2007**, *49*, 89–99. [[CrossRef](#)] [[PubMed](#)]
75. Subramanian, N.; Wetzel, A.; Dombert, B.; Yadav, P.; Havlicek, S.; Jablonka, S.; Nassar, M.A.; Blum, R.; Sendtner, M. Role of Na(v)1.9 in Activity-Dependent Axon Growth in Motoneurons. *Hum. Mol. Genet.* **2012**, *21*, 3655–3667. [[CrossRef](#)]
76. Da Silva, C.A.; de Moraes, E.C.P.; Costa, M.D.M.; Ribas, J.L.C.; Guiloski, I.C.; Ramsdorf, W.A.; Zanata, S.M.; Cestari, M.M.; Ribeiro, C.A.O.; Magalhães, V.F.; et al. Saxitoxins Induce Cytotoxicity, Genotoxicity and Oxidative Stress in Teleost Neurons in Vitro. *Toxic. Off. J. Int. Soc. Toxinol.* **2014**, *86*, 8–15. [[CrossRef](#)]
77. Zhou, Z.; Tang, X.; Chen, H.; Wang, Y. Comparative Studies of Saxitoxin (STX) -Induced Cytotoxicity in Neuro-2a and RTG-2 Cell Lines: An Explanation with Respect to Changes in ROS. *Chemosphere* **2018**, *192*, 66–74. [[CrossRef](#)]
78. D'Mello, F.; Braidy, N.; Marcal, H.; Guillemin, G.; Rossi, F.; Chinián, M.; Laurent, D.; Teo, C.; Neilan, B.A. Cytotoxic Effects of Environmental Toxins on Human Glial Cells. *Neurotox. Res.* **2017**, *31*, 245–258. [[CrossRef](#)]
79. Chen, G.; Jia, Z.; Wang, L.; Hu, T. Effect of Acute Exposure of Saxitoxin on Development of Zebrafish Embryos (Danio Rerio). *Environ. Res.* **2020**, *185*, 109432. [[CrossRef](#)] [[PubMed](#)]
80. Lima-Filho, C.M.; Nogaroli, L.; Hedin-Pereira, C.; Azevedo, S.M.F.O.; Soares, R.M. Effects of Saxitoxins Exposure on Oligodendrocyte Development in Mouse Neonates. *Toxicon* **2020**, *188*, 89–94. [[CrossRef](#)] [[PubMed](#)]
81. L'Herondelle, K.; Talagas, M.; Mignen, O.; Misery, L.; Le Garrec, R. Neurological Disturbances of Ciguatera Poisoning: Clinical Features and Pathophysiological Basis. *Cells* **2020**, *9*, 2291. [[CrossRef](#)] [[PubMed](#)]
82. Vilarino, N.; Louzao, M.C.; Abal, P.; Cagide, E.; Carrera, C.; Vieytes, M.R.; Botana, L.M. Human Poisoning from Marine Toxins: Unknowns for Optimal Consumer Protection. *Toxins* **2018**, *10*, 324. [[CrossRef](#)]
83. Au, N.P.; Kumar, G.; Asthana, P.; Tin, C.; Mak, Y.L.; Chan, L.L.; Lam, P.K.; Ma, C.H. Ciguatoxin Reduces Regenerative Capacity of Axotomized Peripheral Neurons and Delays Functional Recovery in Pre-Exposed Mice after Peripheral Nerve Injury. *Sci. Rep.* **2016**, *6*, 26809. [[CrossRef](#)]
84. Inserra, M.C.; Israel, M.R.; Caldwell, A.; Castro, J.; Deuis, J.R.; Harrington, A.M.; Keramidas, A.; Garcia-Caraballo, S.; Maddern, J.; Erickson, A.; et al. Multiple Sodium Channel Isoforms Mediate the Pathological Effects of Pacific Ciguatoxin-1. *Sci. Rep.* **2017**, *7*, 42810. [[CrossRef](#)] [[PubMed](#)]
85. Touska, F.; Sattler, S.; Malsch, P.; Lewis, R.J.; Reeh, P.W.; Zimmermann, K. Ciguatoxins Evoke Potent CGRP Release by Activation of Voltage-Gated Sodium Channel Subtypes NaV1.9, NaV1.7 and NaV1.1. *Mar. Drugs* **2017**, *15*, 269. [[CrossRef](#)]
86. Russell, F.A.; King, R.; Smillie, S.-J.; Kodji, X.; Brain, S.D. Calcitonin Gene-Related Peptide: Physiology and Pathophysiology. *Physiol. Rev.* **2014**, *94*, 1099–1142. [[CrossRef](#)] [[PubMed](#)]

87. Ringer, C.; Tune, S.; Bertoune, M.A.; Schwarzbach, H.; Tsujikawa, K.; Weihe, E.; Schütz, B. Disruption of Calcitonin Gene-Related Peptide Signaling Accelerates Muscle Denervation and Dampens Cytotoxic Neuroinflammation in SOD1 Mutant Mice. *Cell. Mol. Life Sci. CMLS* **2017**, *74*, 339–358. [[CrossRef](#)]
88. Ratliff, W.A.; Saykally, J.N.; Kane, M.J.; Citron, B.A. Neuromuscular Junction Morphology and Gene Dysregulation in the Wobbler Model of Spinal Neurodegeneration. *J. Mol. Neurosci. MN* **2018**, *66*, 114–120. [[CrossRef](#)]
89. Morabito, S.; Silvestro, S.; Faggio, C. How the Marine Biotoxins Affect Human Health. *Nat. Prod. Res.* **2018**, *32*, 621–631. [[CrossRef](#)]
90. Rubiolo, J.A.; Vale, C.; Boente-Juncal, A.; Hiram, M.; Yamashita, S.; Camiña, M.; Vieytes, M.R.; Botana, L.M. Transcriptomic Analysis of Ciguatoxin-Induced Changes in Gene Expression in Primary Cultures of Mice Cortical Neurons. *Toxins* **2018**, *10*, 192. [[CrossRef](#)]
91. Coccini, T.; Caloni, F.; De Simone, U. Human Neuronal Cell Based Assay: A New in Vitro Model for Toxicity Evaluation of Ciguatoxin. *Environ. Toxicol. Pharmacol.* **2017**, *52*, 200–213. [[CrossRef](#)]
92. Alonso, E.; Vieira, A.C.; Rodriguez, I.; Alvarino, R.; Gegunde, S.; Fuwa, H.; Suga, Y.; Sasaki, M.; Alfonso, A.; Cifuentes, J.M.; et al. Tetracyclic Truncated Analogue of the Marine Toxin Gambierol Modifies NMDA, Tau, and Amyloid β Expression in Mice Brains: Implications in AD Pathology. *ACS Chem. Neurosci.* **2017**, *8*, 1358–1367. [[CrossRef](#)] [[PubMed](#)]
93. Vetter, I.; Touska, F.; Hess, A.; Hinsbey, R.; Sattler, S.; Lampert, A.; Sergejeva, M.; Sharov, A.; Collins, L.S.; Eberhardt, M.; et al. Ciguatoxins Activate Specific Cold Pain Pathways to Elicit Burning Pain from Cooling. *EMBO J.* **2012**, *31*, 3795–3808. [[CrossRef](#)]
94. Asthana, P.; Zhang, N.; Kumar, G.; Chine, V.B.; Singh, K.K.; Mak, Y.L.; Chan, L.L.; Lam, P.K.S.; Ma, C.H.E. Pacific Ciguatoxin Induces Excitotoxicity and Neurodegeneration in the Motor Cortex Via Caspase 3 Activation: Implication for Irreversible Motor Deficit. *Mol. Neurobiol.* **2018**, *55*, 6769–6787. [[CrossRef](#)] [[PubMed](#)]
95. Du, X.; Liu, H.; Yuan, L.; Wang, Y.; Ma, Y.; Wang, R.; Chen, X.; Losiewicz, M.D.; Guo, H.; Zhang, H. The Diversity of Cyanobacterial Toxins on Structural Characterization, Distribution and Identification: A Systematic Review. *Toxins* **2019**, *11*, 530. [[CrossRef](#)] [[PubMed](#)]
96. Spivak, C.E.; Witkop, B.; Albuquerque, E.X. Anatoxin-a: A Novel, Potent Agonist at the Nicotinic Receptor. *Mol. Pharmacol.* **1980**, *18*, 384–394.
97. Posadas, I.; López-Hernández, B.; Ceña, V. Nicotinic Receptors in Neurodegeneration. *Curr. Neuropharmacol.* **2013**, *11*, 298–314. [[CrossRef](#)]
98. Koukoulis, F.; Changeux, J.-P. Do Nicotinic Receptors Modulate High-Order Cognitive Processing? *Trends Neurosci.* **2020**, *43*, 550–564. [[CrossRef](#)]
99. Moss, D.E. Improving Anti-Neurodegenerative Benefits of Acetylcholinesterase Inhibitors in Alzheimer’s Disease: Are Irreversible Inhibitors the Future? *Int. J. Mol. Sci.* **2020**, *21*, 3438. [[CrossRef](#)] [[PubMed](#)]
100. Takser, L.; Benachour, N.; Husk, B.; Cabana, H.; Gris, D. Cyanotoxins at Low Doses Induce Apoptosis and Inflammatory Effects in Murine Brain Cells: Potential Implications for Neurodegenerative Diseases. *Toxicol. Rep.* **2016**, *3*, 180–189. [[CrossRef](#)] [[PubMed](#)]
101. Nunn, P.B. 50 Years of Research on α -Amino- β -Methylaminopropionic Acid (β -Methylaminoalanine). *Phytochemistry* **2017**, *144*, 271–281. [[CrossRef](#)] [[PubMed](#)]
102. Chernoff, N.; Hill, D.J.; Diggs, D.L.; Faison, B.D.; Francis, B.M.; Lang, J.R.; Larue, M.M.; Le, T.-T.; Loftin, K.A.; Lugo, J.N.; et al. A Critical Review of the Postulated Role of the Non-Essential Amino Acid, β -N-Methylamino-L-Alanine, in Neurodegenerative Disease in Humans. *J. Toxicol. Environ. Health Part B* **2017**, *20*, 183–229. [[CrossRef](#)] [[PubMed](#)]
103. Pablo, J.; Banack, S.A.; Cox, P.A.; Johnson, T.E.; Papapetropoulos, S.; Bradley, W.G.; Buck, A.; Mash, D.C. Cyanobacterial Neurotoxin BMAA in ALS and Alzheimer’s Disease. *Acta Neurol. Scand.* **2009**, *120*, 216–225. [[CrossRef](#)]
104. Spencer, P.S.; Nunn, P.B.; Hugon, J.; Ludolph, A.C.; Robertson, R.C. Guam Amyotrophic Lateral Sclerosis-Parkinsonism- Dementia Linked to a Plant Excitant Neurotoxin. *Science* **1987**, *237*, 517–522. [[CrossRef](#)]
105. Cox, P.A.; Banack, S.A.; Murch, S.J.; Rasmussen, U.; Tien, G.; Bidigare, R.R.; Metcalf, J.S.; Morrison, L.F.; Codd, G.A.; Bergman, B. Diverse Taxa of Cyanobacteria Produce Beta-N-Methylamino-L-Alanine, a Neurotoxic Amino Acid. *Proc. Natl. Acad. Sci. USA* **2005**, *102*, 5074–5078. [[CrossRef](#)]
106. Cox, P.A.; Banack, S.A.; Murch, S.J. Biomagnification of Cyanobacterial Neurotoxins and Neurodegenerative Disease among the Chamorro People of Guam. *Proc. Natl. Acad. Sci. USA* **2003**, *100*, 13380–13383. [[CrossRef](#)]
107. Lage, S.; Annadotter, H.; Rasmussen, U.; Rydberg, S. Biotransfer of β -N-Methylamino-L-Alanine (BMAA) in a Eutrophicated Freshwater Lake. *Mar. Drugs* **2015**, *13*, 1185–1201. [[CrossRef](#)]
108. Samardzic, K.; Steele, J.R.; Violi, J.P.; Colville, A.; Mitrovic, S.M.; Rodgers, K.J. Toxicity and Bioaccumulation of Two Non-Protein Amino Acids Synthesised by Cyanobacteria, β -N-Methylamino-L-Alanine (BMAA) and 2,4-Diaminobutyric Acid (DAB), on a Crop Plant. *Ecotoxicol. Environ. Saf.* **2021**, *208*, 111515. [[CrossRef](#)] [[PubMed](#)]
109. Xie, X.; Basile, M.; Mash, D.C. Cerebral Uptake and Protein Incorporation of Cyanobacterial Toxin β -N-Methylamino-L-Alanine. *Neuroreport* **2013**, *24*, 779–784. [[CrossRef](#)] [[PubMed](#)]
110. Murch, S.J.; Cox, P.A.; Banack, S.A.; Steele, J.C.; Sacks, O.W. Occurrence of Beta-Methylamino-L-Alanine (BMAA) in ALS/PDC Patients from Guam. *Acta Neurol. Scand.* **2004**, *110*, 267–269. [[CrossRef](#)] [[PubMed](#)]
111. Bradley, W.G.; Mash, D.C. Beyond Guam: The Cyanobacteria/BMAA Hypothesis of the Cause of ALS and Other Neurodegenerative Diseases. *Amyotroph. Lateral Scler.* **2009**, *10* (Suppl. 2), 7–20. [[CrossRef](#)] [[PubMed](#)]


112. Dunlop, R.A.; Guillemin, G.J. The Cyanotoxin and Non-Protein Amino Acid β -Methylamino-L-Alanine (L-BMAA) in the Food Chain: Incorporation into Proteins and Its Impact on Human Health. *Neurotox. Res.* **2019**, *36*, 602–611. [[CrossRef](#)] [[PubMed](#)]
113. Lobner, D. Mechanisms of Beta-N-Methylamino-L-Alanine Induced Neurotoxicity. *Amyotroph. Lateral Scler.* **2009**, *10* (Suppl. 2), 56–60. [[CrossRef](#)]
114. Chiu, A.S.; Gehringer, M.M.; Braidy, N.; Guillemin, G.J.; Welch, J.H.; Neilan, B.A. Excitotoxic Potential of the Cyanotoxin β -Methyl-Amino-L-Alanine (BMAA) in Primary Human Neurons. *Toxicon* **2012**, *60*, 1159–1165. [[CrossRef](#)]
115. Weiss, J.H.; Choi, D.W. Beta-N-Methylamino-L-Alanine Neurotoxicity: Requirement for Bicarbonate as a Cofactor. *Sci. New Ser.* **1988**, *241*, 973–975. [[CrossRef](#)]
116. Delcourt, N.; Claudepierre, T.; Maignien, T.; Arnich, N.; Mattei, C. Cellular and Molecular Aspects of the β -N-Methylamino-L-Alanine (BMAA) Mode of Action within the Neurodegenerative Pathway: Facts and Controversy. *Toxins* **2017**, *10*, 6. [[CrossRef](#)]
117. Hardiman, O.; Al-Chalabi, A.; Chio, A.; Corr, E.M.; Logroscino, G.; Robberecht, W.; Shaw, P.J.; Simmons, Z.; van den Berg, L.H. Amyotrophic Lateral Sclerosis. *Nat. Rev. Primer* **2017**, *3*, 17071. [[CrossRef](#)]
118. Liu, X.; Rush, T.; Zapata, J.; Lobner, D. β -N-Methylamino-L-Alanine Induces Oxidative Stress and Glutamate Release through Action on System Xc⁻. *Exp. Neurol.* **2009**, *217*, 429–433. [[CrossRef](#)]
119. Dunlop, R.A.; Cox, P.A.; Banack, S.A.; Rodgers, K.J. The Non-Protein Amino Acid BMAA Is Misincorporated into Human Proteins in Place of L-Serine Causing Protein Misfolding and Aggregation. *PLoS ONE* **2013**, *8*, e75376. [[CrossRef](#)]
120. Glover, W.B.; Mash, D.C.; Murch, S.J. The Natural Non-Protein Amino Acid N- β -Methylamino-L-Alanine (BMAA) Is Incorporated into Protein during Synthesis. *Amino Acids* **2014**, *46*, 2553–2559. [[CrossRef](#)] [[PubMed](#)]
121. Sanna, S.; Esposito, S.; Masala, A.; Sini, P.; Nieddu, G.; Galioto, M.; Fais, M.; Iaccarino, C.; Cestra, G.; Crosio, C. HDAC1 Inhibition Ameliorates TDP-43-Induced Cell Death in Vitro and in Vivo. *Cell Death Dis.* **2020**, *11*, 369. [[CrossRef](#)]
122. Jo, M.; Lee, S.; Jeon, Y.-M.; Kim, S.; Kwon, Y.; Kim, H.-J. The Role of TDP-43 Propagation in Neurodegenerative Diseases: Integrating Insights from Clinical and Experimental Studies. *Exp. Mol. Med.* **2020**, *52*, 1652–1662. [[CrossRef](#)] [[PubMed](#)]
123. Prasad, A.; Bharathi, V.; Sivalingam, V.; Girdhar, A.; Patel, B.K. Molecular Mechanisms of TDP-43 Misfolding and Pathology in Amyotrophic Lateral Sclerosis. *Front. Mol. Neurosci.* **2019**, *12*, 25. [[CrossRef](#)]
124. De Munck, E.; Munoz-Saez, E.; Miguel, B.G.; Solas, M.T.; Ojeda, I.; Martinez, A.; Gil, C.; Arahuetes, R.M. Beta-N-Methylamino-L-Alanine Causes Neurological and Pathological Phenotypes Mimicking Amyotrophic Lateral Sclerosis (ALS): The First Step towards an Experimental Model for Sporadic ALS. *Environ. Toxicol. Pharmacol.* **2013**, *36*, 243–255. [[CrossRef](#)]
125. Scott, L.; Downing, T. Dose-Dependent Adult Neurodegeneration in a Rat Model After Neonatal Exposure to β -N-Methylamino-L-Alanine. *Neurotox. Res.* **2019**, *35*, 711–723. [[CrossRef](#)]
126. Yin, H.Z.; Yu, S.; Hsu, C.-I.; Liu, J.; Acab, A.; Wu, R.; Tao, A.; Chiang, B.J.; Weiss, J.H. Intrathecal Infusion of BMAA Induces Selective Motor Neuron Damage and Astrogliosis in the Ventral Horn of the Spinal Cord. *Exp. Neurol.* **2014**, *261*, 1–9. [[CrossRef](#)]
127. Ritson, G.P.; Custer, S.K.; Freibaum, B.D.; Guinto, J.B.; Geffel, D.; Moore, J.; Tang, W.; Winton, M.J.; Neumann, M.; Trojanowski, J.Q.; et al. TDP-43 Mediates Degeneration in a Novel Drosophila Model of Disease Caused by Mutations in VCP/P97. *J. Neurosci.* **2010**, *30*, 7729–7739. [[CrossRef](#)]
128. Martin, R.M.; Bereman, M.S.; Marsden, K.C. BMAA and MCLR Interact to Modulate Behavior and Exacerbate Molecular Changes Related to Neurodegeneration in Larval Zebrafish. *Toxicol. Sci. Off. J. Soc. Toxicol.* **2020**, *179*, 251–261. [[CrossRef](#)]
129. Okle, O.; Stemmer, K.; Deschl, U.; Dietrich, D.R. L-BMAA Induced ER Stress and Enhanced Caspase 12 Cleavage in Human Neuroblastoma SH-SY5Y Cells at Low Nonexcitotoxic Concentrations. *Toxicol. Sci.* **2013**, *131*, 217–224. [[CrossRef](#)]
130. Beri, J.; Nash, T.; Martin, R.M.; Bereman, M.S. Exposure to BMAA Mirrors Molecular Processes Linked to Neurodegenerative Disease. *PROTEOMICS* **2017**, *17*, 1700161. [[CrossRef](#)]
131. Ma, Q. Role of Nrf2 in Oxidative Stress and Toxicity. *Annu. Rev. Pharmacol. Toxicol.* **2013**, *53*, 401–426. [[CrossRef](#)] [[PubMed](#)]
132. Dunys, J.; Duplan, E.; Checler, F. The Transcription Factor X-Box Binding Protein-1 in Neurodegenerative Diseases. *Mol. Neurodegener.* **2014**, *9*, 35. [[CrossRef](#)] [[PubMed](#)]
133. Pierozan, P.; Cattani, D.; Karlsson, O. Hippocampal Neural Stem Cells Are More Susceptible to the Neurotoxin BMAA than Primary Neurons: Effects on Apoptosis, Cellular Differentiation, Neurite Outgrowth, and DNA Methylation. *Cell Death Dis.* **2020**, *11*, 910. [[CrossRef](#)]
134. Greene, L.A.; Tischler, A.S. Establishment of a Noradrenergic Clonal Line of Rat Adrenal Pheochromocytoma Cells Which Respond to Nerve Growth Factor. *Proc. Natl. Acad. Sci. USA* **1976**, *73*, 2424–2428. [[CrossRef](#)]
135. Lee, M.; McGeer, P.L. Weak BMAA Toxicity Compares with That of the Dietary Supplement Beta-Alanine. *Neurobiol. Aging* **2012**, *33*, 1440–1447. [[CrossRef](#)]
136. Munoz-Saez, E.; de Munck Garcia, E.; Arahuetes Portero, R.M.; Vicente, F.; Ortiz-Lopez, F.J.; Cantizani, J.; Gomez Miguel, B. Neuroprotective Role of Sphingosine-1-Phosphate in L-BMAA Treated Neuroblastoma Cells (SH-SY5Y). *Neurosci. Lett.* **2015**, *593*, 83–89. [[CrossRef](#)] [[PubMed](#)]
137. Main, B.J.; Dunlop, R.A.; Rodgers, K.J. The Use of L-Serine to Prevent Beta-Methylamino-L-Alanine (BMAA)-Induced Proteotoxic Stress in Vitro. *Toxicon* **2016**, *109*, 7–12. [[CrossRef](#)]
138. Engskog, M.K.R.; Ersson, L.; Haglöf, J.; Arvidsson, T.; Pettersson, C.; Brittebo, E. β -N-Methylamino-L-Alanine (BMAA) Perturbs Alanine, Aspartate and Glutamate Metabolism Pathways in Human Neuroblastoma Cells as Determined by Metabolic Profiling. *Amino Acids* **2017**, *49*, 905–919. [[CrossRef](#)] [[PubMed](#)]

139. Dunlop, R.A.; Carney, J.M. Mechanisms of L-Serine-Mediated Neuroprotection Include Selective Activation of Lysosomal Cathepsins B and L. *Neurotox. Res.* **2020**, *39*, 17–26. [[CrossRef](#)]
140. Silva, D.F.; Candeias, E.; Esteves, A.R.; Magalhães, J.D.; Ferreira, I.L.; Nunes-Costa, D.; Rego, A.C.; Empadinhas, N.; Cardoso, S.M. Microbial BMAA Elicits Mitochondrial Dysfunction, Innate Immunity Activation, and Alzheimer's Disease Features in Cortical Neurons. *J. Neuroinflamm.* **2020**, *17*, 332. [[CrossRef](#)]
141. Van Onselen, R.; Venables, L.; van de Venter, M.; Downing, T.G. β -N-Methylamino-L-Alanine Toxicity in PC12: Excitotoxicity vs. Misincorporation. *Neurotox. Res.* **2018**, *33*, 15–23. [[CrossRef](#)] [[PubMed](#)]
142. Soto, T.; Buzzi, E.D.; Rotstein, N.P.; German, O.L.; Politi, L.E. Damaging Effects of BMAA on Retina Neurons and Müller Glial Cells. *Exp. Eye Res.* **2021**, *202*, 108342. [[CrossRef](#)]
143. Okamoto, S.; Esumi, S.; Hamaguchi-Hamada, K.; Hamada, S. β -N-Methylamino-L-Alanine (BMAA) Suppresses Cell Cycle Progression of Non-Neuronal Cells. *Sci. Rep.* **2018**, *8*, 17995. [[CrossRef](#)]
144. Richter, K.E.; Mena, E.E. L- β -Methylaminoalanine Inhibits $[^3H]$ Glutamate Binding in the Presence of Bicarbonate Ions. *Brain Res.* **1989**, *492*, 385–388. [[CrossRef](#)]
145. Staton, P.C.; Bristow, D.R. The Dietary Excitotoxins β -N-Methylamino-L-Alanine and β -N-Oxalylamino-L-Alanine Induce Necrotic- and Apoptotic-Like Death of Rat Cerebellar Granule Cells. *J. Neurochem.* **1997**, *69*, 1508–1518. [[CrossRef](#)] [[PubMed](#)]
146. Lobner, D.; Piana, P.M.T.; Salous, A.K.; Peoples, R.W. β -N-Methylamino-L-Alanine Enhances Neurotoxicity through Multiple Mechanisms. *Neurobiol. Dis.* **2007**, *25*, 360–366. [[CrossRef](#)]
147. Tan, V.X.; Mazzocco, C.; Varney, B.; Bodet, D.; Guillemain, T.A.; Bessedé, A.; Guillemain, G.J. Detection of the Cyanotoxins L-BMAA Uptake and Accumulation in Primary Neurons and Astrocytes. *Neurotox. Res.* **2018**, *33*, 55–61. [[CrossRef](#)] [[PubMed](#)]
148. Tan, V.X.; Lassus, B.; Lim, C.K.; Tixador, P.; Courte, J.; Bessedé, A.; Guillemain, G.J.; Peyrin, J.-M. Neurotoxicity of the Cyanotoxin BMAA Through Axonal Degeneration and Intercellular Spreading. *Neurotox. Res.* **2018**, *33*, 62–75. [[CrossRef](#)] [[PubMed](#)]
149. Johnson, H.E.; King, S.R.; Banack, S.A.; Webster, C.; Callanaupa, W.J.; Cox, P.A. Cyanobacteria (Nostoc Commune) Used as a Dietary Item in the Peruvian Highlands Produce the Neurotoxic Amino Acid BMAA. *J. Ethnopharmacol.* **2008**, *118*, 159–165. [[CrossRef](#)]
150. Backer, L.C.; McNeel, S.V.; Barber, T.; Kirkpatrick, B.; Williams, C.; Irvin, M.; Zhou, Y.; Johnson, T.B.; Nierenberg, K.; Aubel, M.; et al. Recreational Exposure to Microcystins during Algal Blooms in Two California Lakes. *Toxic. Off. J. Int. Soc. Toxinol.* **2010**, *55*, 909–921. [[CrossRef](#)]
151. Cox, P.A. BMAA, Neurodegeneration, and Neuroprotection. *Neurotox. Res.* **2021**, *39*, 1–5. [[CrossRef](#)]
152. Scott, L.L.; Downing, S.; Downing, T.G. The Evaluation of BMAA Inhalation as a Potential Exposure Route Using a Rat Model. *Neurotox. Res.* **2018**, *33*, 6–14. [[CrossRef](#)] [[PubMed](#)]
153. Levine, T.D.; Miller, R.G.; Bradley, W.G.; Moore, D.H.; Saperstein, D.S.; Flynn, L.E.; Katz, J.S.; Forshe, D.A.; Metcalf, J.S.; Banack, S.A.; et al. Phase I Clinical Trial of Safety of L-Serine for ALS Patients. *Amyotroph. Lateral Scler. Front. Degener.* **2017**, *18*, 107–111. [[CrossRef](#)] [[PubMed](#)]
154. Fridman, V.; Suriyanarayanan, S.; Novak, P.; David, W.; Macklin, E.A.; McKenna-Yasek, D.; Walsh, K.; Aziz-Bose, R.; Oaklander, A.L.; Brown, R.; et al. Randomized Trial of L-Serine in Patients with Hereditary Sensory and Autonomic Neuropathy Type 1. *Neurology* **2019**, *92*, e359–e370. [[CrossRef](#)]
155. Brenner, S.R. Blue-Green Algae or Cyanobacteria in the Intestinal Micro-Flora May Produce Neurotoxins Such as Beta-N-Methylamino-L-Alanine (BMAA) Which May Be Related to Development of Amyotrophic Lateral Sclerosis, Alzheimer's Disease and Parkinson-Dementia-Complex in Humans and Equine Motor Neuron Disease in Horses. *Med. Hypotheses* **2013**, *80*, 103. [[CrossRef](#)]
156. Brenner, D.; Hiergeist, A.; Adis, C.; Mayer, B.; Gessner, A.; Ludolph, A.C.; Weishaupt, J.H. The Fecal Microbiome of ALS Patients. *Neurobiol. Aging* **2018**, *61*, 132–137. [[CrossRef](#)]
157. Ceppa, F.A.; Izzo, L.; Sardelli, L.; Raimondi, I.; Tunesi, M.; Albani, D.; Giordano, C. Human Gut-Microbiota Interaction in Neurodegenerative Disorders and Current Engineered Tools for Its Modeling. *Front. Cell. Infect. Microbiol.* **2020**, *10*, 297. [[CrossRef](#)] [[PubMed](#)]
158. Vascellari, S.; Palmas, V.; Melis, M.; Pisanu, S.; Cusano, R.; Uva, P.; Perra, D.; Madau, V.; Sarchioto, M.; Oppo, V.; et al. Gut Microbiota and Metabolome Alterations Associated with Parkinson's Disease. *Msystems* **2020**, *5*, e00561-20. [[CrossRef](#)] [[PubMed](#)]

ARTICLE

Open Access

HDAC1 inhibition ameliorates TDP-43-induced cell death in vitro and in vivo

Simona Sanna¹, Sonia Esposito¹, Alessandra Masala¹, Paola Sini¹, Gabriele Nieddu¹, Manuela Galioto¹, Milena Fais¹,
Ciro Iaccarino¹, Gianluca Cestra² and Claudia Crosio¹ 

ABSTRACT

TDP-43 pathology is a disease hallmark that characterizes both amyotrophic lateral sclerosis (ALS) and frontotemporal lobar degeneration (FTLD-TDP). TDP-43 undergoes several posttranslational modifications that can change its biological activities and its aggregative propensity, which is a common hallmark of different neurodegenerative conditions. New evidence is provided by the current study pointing at TDP-43 acetylation in ALS cellular models. Using both in vitro and in vivo approaches, we demonstrate that TDP-43 interacts with histone deacetylase 1 (HDAC1) via RRM1 and RRM2 domains, that are known to contain the two major TDP-43 acetylation sites, K142 and K192. Moreover, we show that TDP-43 is a direct transcriptional activator of CHOP promoter and this activity is regulated by acetylation. Finally and most importantly, we observe both in cell culture and in *Drosophila* that a HDCA1 reduced level (genomic inactivation or siRNA) or treatment with pan-HDAC inhibitors exert a protective role against WT or pathological mutant TDP-43 toxicity, suggesting TDP-43 acetylation as a new potential therapeutic target. HDAC inhibition efficacy in neurodegeneration has long been debated, but future investigations are warranted in this area. Selection of more specific HDAC inhibitors is still a promising option for neuronal protection especially as HDAC1 appears as a downstream target of both TDP-43 and FUS, another ALS-related gene.

Introduction

TDP-43 or TARDBP (TAR-DNA binding protein-43) is a 43 kDa ribonucleoprotein, originally identified as transcriptional repressor of HIV1 TAR-DNA, associated during the past decades with a spectrum of neurological diseases, namely TDP-43 proteinopathy¹. TDP-43 is a predominantly nuclear RNA/DNA-binding protein essential for the development of the central nervous system (CNS) from the earliest stages of embryonic life to adulthood². In the nucleus, TDP-43 is involved in transcriptional regulation, splicing and miRNA biogenesis, but upon stressing conditions it is partially relocated in the cytoplasm, becoming involved in mRNA stability control,

translation, and nucleocytoplasmic transport by forming stress granules³. TDP-43 undergoes several posttranslational modifications that can change its structure, localization, overall functions, its aggregative propensity and, importantly, TDP-43-positive aggregates are a common hallmark of different neurodegenerative conditions⁴. Ubiquitinated, phosphorylated, and acetylated-TDP-43 aggregates were, in fact, identified in 95–97% of patients affected by amyotrophic lateral sclerosis (ALS) and in about 50% of Frontotemporal Lobar Degeneration (FTLD)^{1,5,6}. Moreover, the direct role of TDP-43 in disease pathogenesis is underscored by the identification of more than 40 ALS-associated dominant missense mutations in the TDP-43 gene (*TARDBP*) in both familial and sporadic patients⁷. Several different pathological mutants display a propensity to form both nuclear and cytoplasmic aggregates indicating that loss of TDP-43 homeostasis and aggregation play a critical role in pathogenesis. In particular it has been demonstrated that acetylation

Correspondence: Claudia Crosio (ccrosio@uniss.it)

¹Department of Biomedical Sciences, University of Sassari, Via Muroni 25, I-07100 Sassari, Italy

²Institute of Molecular Biology and Pathology-National Research Council at Department of Biology and Biotechnology-Charles Darwin, Sapienza University of Rome, P.Le A.Moro 5, I-00185 Rome, Italy

Edited by B. Joseph

© The Author(s) 2020



Open Access This article is licensed under a Creative Commons Attribution 4.0 International License, which permits use, sharing, adaptation, distribution and reproduction in any medium or format, as long as you give appropriate credit to the original author(s) and the source, provide a link to the Creative Commons license, and indicate if changes were made. The images or other third party material in this article are included in the article's Creative Commons license, unless indicated otherwise in a credit line to the material. If material is not included in the article's Creative Commons license and your intended use is not permitted by statutory regulation or exceeds the permitted use, you will need to obtain permission directly from the copyright holder. To view a copy of this license, visit <http://creativecommons.org/licenses/by/4.0/>.

modifies both TDP-43 function and localization, by decreasing its ability to interact with nucleic acids^{5,8}. According to Choen et al.⁹ TDP-43 can be acetylated mainly on K154 and K192 by the HAT (histone acetyltransferase) activity of CBP (CREB binding-protein). Once acetylated, TDP-43 can be relocated in the cytoplasm where it can be deacetylated by the histone deacetylase 6 (HDAC6)^{9,10}. Given this experimental evidence, it is plausible that modulating TDP-43 acetylation might be a good strategy to prevent TDP-43 aggregation and cell damage.

HDACs are a complex family of proteins involved in many different cellular functions in CNS, including chromatin shaping to adjust transcriptional profiles during neuronal development and neuronal response to injury¹¹. HDAC substrates, which are implicated in neuronal development and survival, are not restricted to histones. As demonstrated, several different physiological functions are regulated by deacetylation^{12–14}. Among the different HDACs functionally associated with ALS onset and progression we focused our attention on HDAC1. HDAC1 is a Zn²⁺-dependent deacetylase of 482 amino acids, that can be found in large transcriptional repression complexes consisting of SIN3A, NuRD, and Co-REST¹⁵, which inactivate the expression of neuronal genes in non-neuronal tissues¹⁶. The role of HDAC1 in regulating neuronal viability is quite controversial ranging from neuronal protection from death to an increase in neurodegeneration and axonal death¹². The involvement of class I HDACs in the onset of ALS was first shown by Janssen et al.¹⁷. Different studies also suggest that some of these HDACs regulate vitality and mortality of nerve cells; first, HDAC1 assumes neurotoxic or neuroprotective function as it interacts with HDAC3 or HDAC9¹⁸. In fact, the role of HDAC1 in regulating neuronal vitality is quite controversial, since some studies show that such deacetylase is able to protect neurons from death, while other studies demonstrate that HDAC1 induces neurodegeneration and axonal death^{18,19}. Moreover, recent studies indicate that in degenerative neurons, HDAC1 moves to cytoplasm where it becomes implicated in axonal alteration and degeneration of the cell¹⁹.

Most relevant to ALS, HDAC1 interacts with FUS, another ALS-causative gene, on DNA double strand breaks and this interaction seems to be important for chromatin integrity; as a matter of fact, many FUS pathological mutations impair this interaction and lead to impaired DNA break repair^{20,21}. Notably, ALS patients show increased levels of ROS but also of 8-hydroxy-2'-deoxyguanosine (OH 8dG), a marker of DNA damage. In this context, the interaction between FUS (but also TDP-43) and HDAC1 could have an important role in preserving DNA stability and cell survival, and the alteration of this interaction in ALS patients could lead to

an imbalance in the delicate equilibrium between cell survival and cell death. Recently also TDP-43 has been shown to play a key role in DNA damage response (DDR), since its loss of function results in a faulty repair of DNA damage associated with a stopping in transcription and an inhibition of recruitment of critical components of the NHEJ repair system^{22,23}.

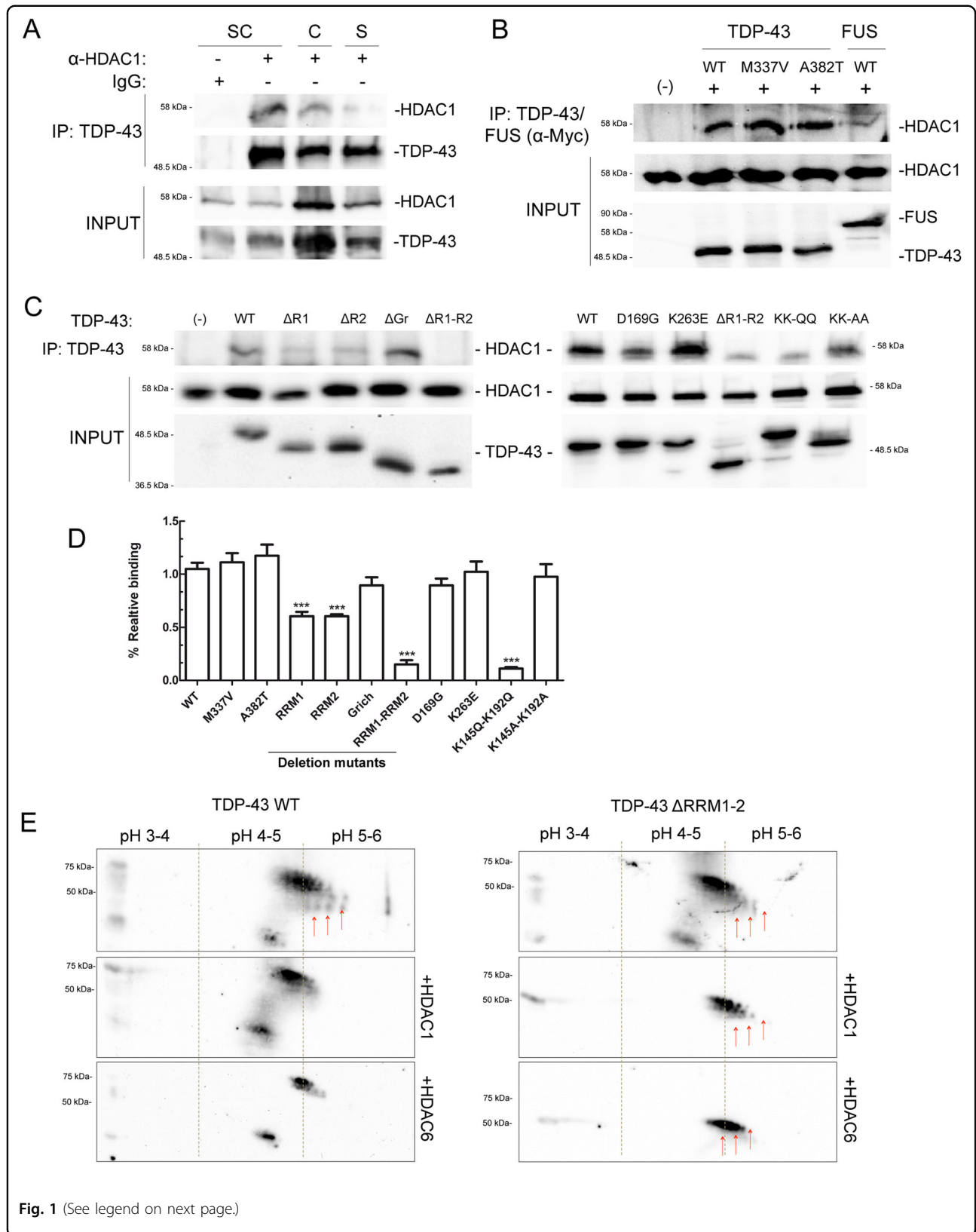
The striking functional and structural similarities between TDP-43 and FUS²⁴, as well as the observation that acetylation appears to promote aggregation and diminish TDP-43 functionality¹⁰, prompted us to investigate a possible interaction between HDAC1 and TDP-43. Since epigenetic drugs are at present one of the most promising strategies for ALS treatment, information on the physical, and functional interaction between TDP-43 and HDAC1 will provide the rationale for using the HDAC inhibitor (HDACi) in ALS therapy²⁵.

Results

TDP-43 interacts with HDAC1 in vitro and in vivo, via RNA binding domains

To assess the interaction between TDP-43 and HDAC1 a co-immunoprecipitation assay from mice neuronal tissues was performed, using an anti-TDP-43 antibody. As illustrated in Fig. 1a, a strong interaction between the two proteins in different neuronal tissues was observed, especially in the spinal cord. By transfection and co-immunoprecipitation this interaction was dissected and it was observed that TDP-43 binds to HDAC1 independently from the presence of the pathogenic point mutations M337V or A382T (Fig. 1b). Furthermore, this interaction was compared with the interaction between FUS and HDAC1 described elsewhere²⁰ showing a more prominent binding of HDAC1 to TDP-43 compared with FUS. Since HDAC1 and HDAC2 exhibit redundancies in various systems, a co-immunoprecipitation experiment was performed demonstrating no interaction between HDAC2 and TDP-43 (Fig. S1b).

To characterize TDP-43 domain(s) responsible for the interaction with HDAC1 a series of Myc-tagged TDP-43 fragments was generated, lacking the various putative functional domains of the protein (N-terminal, RRM1, RRM2, and G-rich domain). Since the N-terminal deletion causes the complete cytoplasmic re-localization of TDP-43 (Fig. S1), while HDAC1 is mainly nuclear, this mutant was excluded from further analysis. Co-immunoprecipitation experiments, performed on cell lysates from transfected cells, demonstrated that TDP-43 interacts with HDAC1 via both RRM1 and RRM2 domains, and that only in the double deletion mutant the interaction is abolished (Fig. 1c). Interestingly, RRM1 and RRM2 domains have been shown to be crucial in TDP-43 physiopathology^{9,26}. Two of the three TDP-43 pathological mutants that do not target the G-rich domain,



(see figure on previous page)

Fig. 1 TDP-43 interacts in vivo and in vitro via RRM1 and RRM2 domains, with HDAC1 that can modulate its acetylation. **a** Spinal cord, cerebellum, or striatum of BALB31c mice were used for co-immunoprecipitation experiments. After dissection tissues were lysed and protein extracts were immunoprecipitated, with specific antibodies. Proteins retained were separated on SDS-PAGE and visualized by western blot using specific antibodies (**b, c**) HEK 293T cells were transiently transfected with FLAG-tagged HDCA1 and Myc-tagged WT or mutant TDP-43. We tested pathological mutants M337V, A382T, D169G, K263E, acetylation null KK-AA or mimicking KK-QQ mutants, and the deletion mutants Δ RRM1, Δ RRM2, Δ G-rich, Δ RRM1/RRM2. Forty-eight hours after transfection, cells were lysed, protein extracts were immunoprecipitated and analysed as in (**a**). **d** Bar graph shows the relative binding of HDAC1 to mutant TDP-43, normalized to TDP-43 WT. The data were obtained from four independent experiments; * $p > 0.05$ and ** $p > 0.01$ versus WT binding, analysed by using one-way ANOVA with Bonferroni's Multiple comparison post-hoc test. **e** Representative 2-DE maps showing the change in TDP-43 acetylation status, upon HDAC1 or HDAC6 expression. SH-SY5Y were transfected by TDP-43 WT or deletion mutant Δ RRM1-2 and FLAG-tagged HDCA1 or HDAC6. Forty-eight hours after transduction, TDP-43 was immunoprecipitated and a visualized by western blot using an anti-acetyl lysine antibody.

ALS-linked mutation D169G²⁷, and FTLD-TDP linked mutation K263E²⁸ map in this region, as well as the two major TDP-43 acetylation sites, K145 and K192⁹. Thus, constructs coding for these pathogenic (D169G, K263E) or acetylation-mimic (KK-QQ) or acetylation-null (KK-AA) mutations were generated to assess whether they can affect the interaction with HDAC1. They were transiently expressed in SH-SY5Y cells and their localization was analysed by immunofluorescence (Fig. S1) demonstrating that all these variants are exclusively nuclear with the exception of TDP-43 D169G, which partially localizes in the cytoplasm. Moreover, according to previous published results, Δ RRM1-2 deletion mutant appeared more clustered in nuclear bodies, which were larger and more numerous compared with TDP-43 WT.

Interestingly, in the co-immunoprecipitation experiments performed the acetylation-mimic mutant (KK-QQ) displays a significant decrease in HDAC1 binding (Fig. 1c, d).

HDCA1 modulates TDP-43 acetylation

To study the interaction between TDP-43 and HDAC1, first their subcellular localization in SH-SY5Y cells was analysed. By immunofluorescence staining it was demonstrated that cellular stress induced by the overexpression of different TDP-43 mutants does not significantly affect HDAC1 localization (Fig. S2).

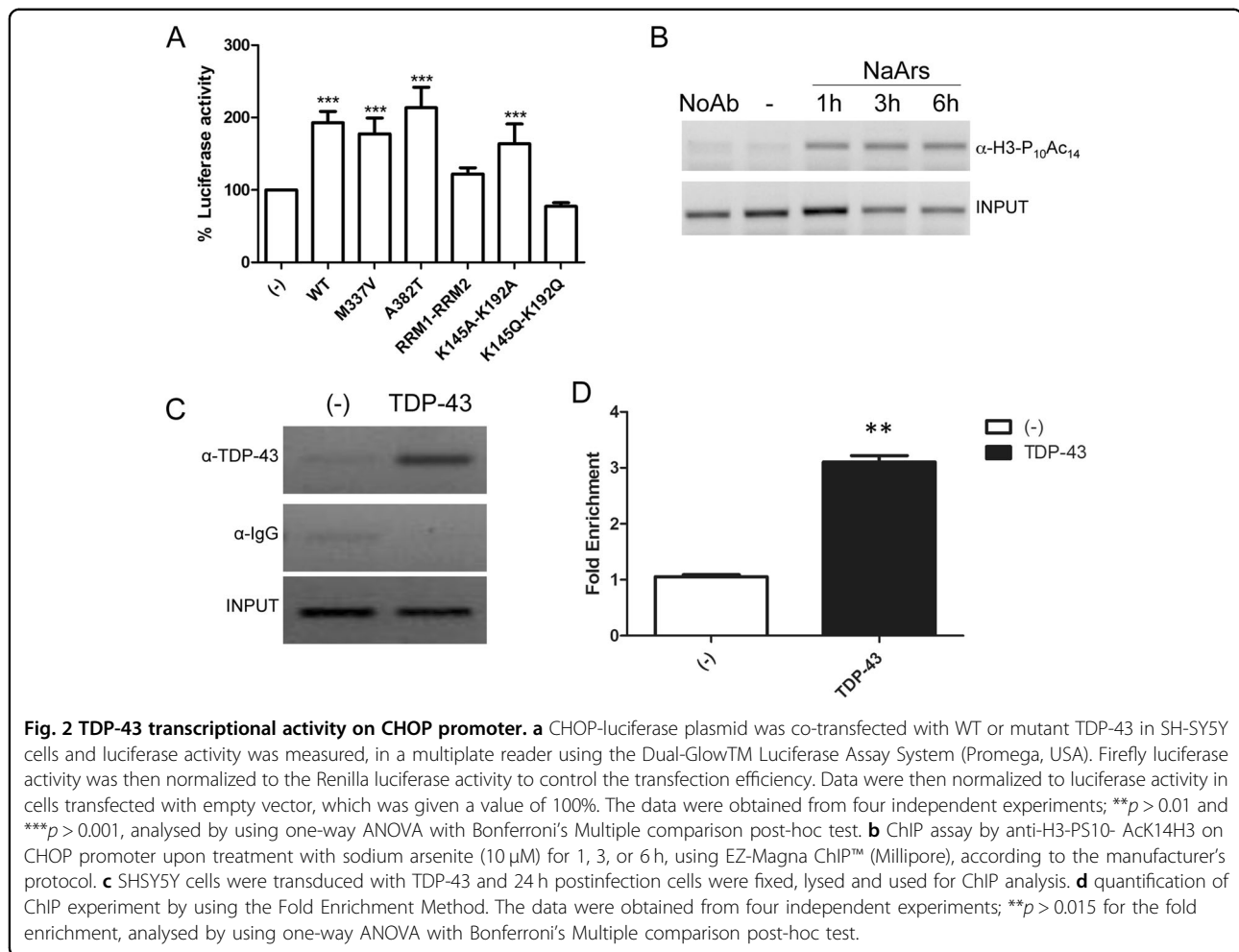
Up to now, acetylated-TDP-43 has been demonstrated to be only an HDAC6 substrate⁹. In order to investigate if HDAC1 alters TDP-43 acetylation, we performed a 2D gel-analysis of immunoprecipitated TDP-43 from SH-SY5Y cells transfected with TDP-43 alone or in combination with HDAC1. After immunoprecipitation TDP-43 was separated by isoelectrofocusing and SDS/PAGE. The level of TDP-43 acetylation was evaluated using anti-acetyl lysine antibody (Fig. 1e). The co-transfection with HDCA1, as well as the one with HDAC6, shifts the isoelectric point (pI) of immunoprecipitated TDP-43. This effect is partially prevented by deletion of RRM1-RRM2 domains, confirming that K145 and K192 are prominent

but nor exclusive acetylation sites⁹ and suggesting that also HDAC1 can modify TDP-43 pI, most likely by removing acetyl groups.

TDP-43 activates CHOP transcription and it is regulated by acetylation

TDP-43 was originally described as transcription factor for TAR DNA of HIV1²⁹, but at present the only direct other target is the testis specific mouse *acr1* (SP10) promoter^{30,31}. TDP-43 has been also shown to induce a transcriptional upregulation of C/EBP-homologous protein (CHOP) promoter and CHOP gene disruption markedly attenuates TDP-43-induced cell death³². Moreover, TDP-43-induced upregulation of CHOP expression is mediated by both reduction of CHOP degradation and by the increase of CHOP mRNA level. Thus, we decided to use CHOP promoter (from -954 to +91) to drive the expression of luciferase reporter and to test the ability of TDP-43 in regulating it. As shown in Fig. 2a, TDP-43 acts as a robust activator of CHOP promoter and the transcriptional activation on this promoter is slightly increased by the overexpression of the pathological mutation A382T, although it does not reach a statistical significance; notably, the transcriptional activation is abolished by RRM1-RRM2 deletion and particularly by the acetylation-mimic point mutations (KK-QQ).

This experimental evidence indicates a direct interaction between TDP-43 and CHOP promoter, which was confirmed by the ChIP approach. In a first attempt, the CHOP promoter activation was tested in response to sodium arsenite using the dual modification of histone H3, which is phosphorylated at serine 10 and acetylated at lysine 14 (H3-PS10/AcK14), as a marker of transcriptional activation. Accordingly, we observed that sodium arsenite treatment induces CHOP transcriptional activation demonstrated by histone H3 phospho-acetylation detection (Fig. 2b). Subsequently, chromatin was extracted and immunoprecipitated using anti-TDP-43 antibodies from SH-SY5Y cells transduced with adenoviral particles expressing 5xMyc-TDP-43³³. As shown in Fig. 2c, d, we



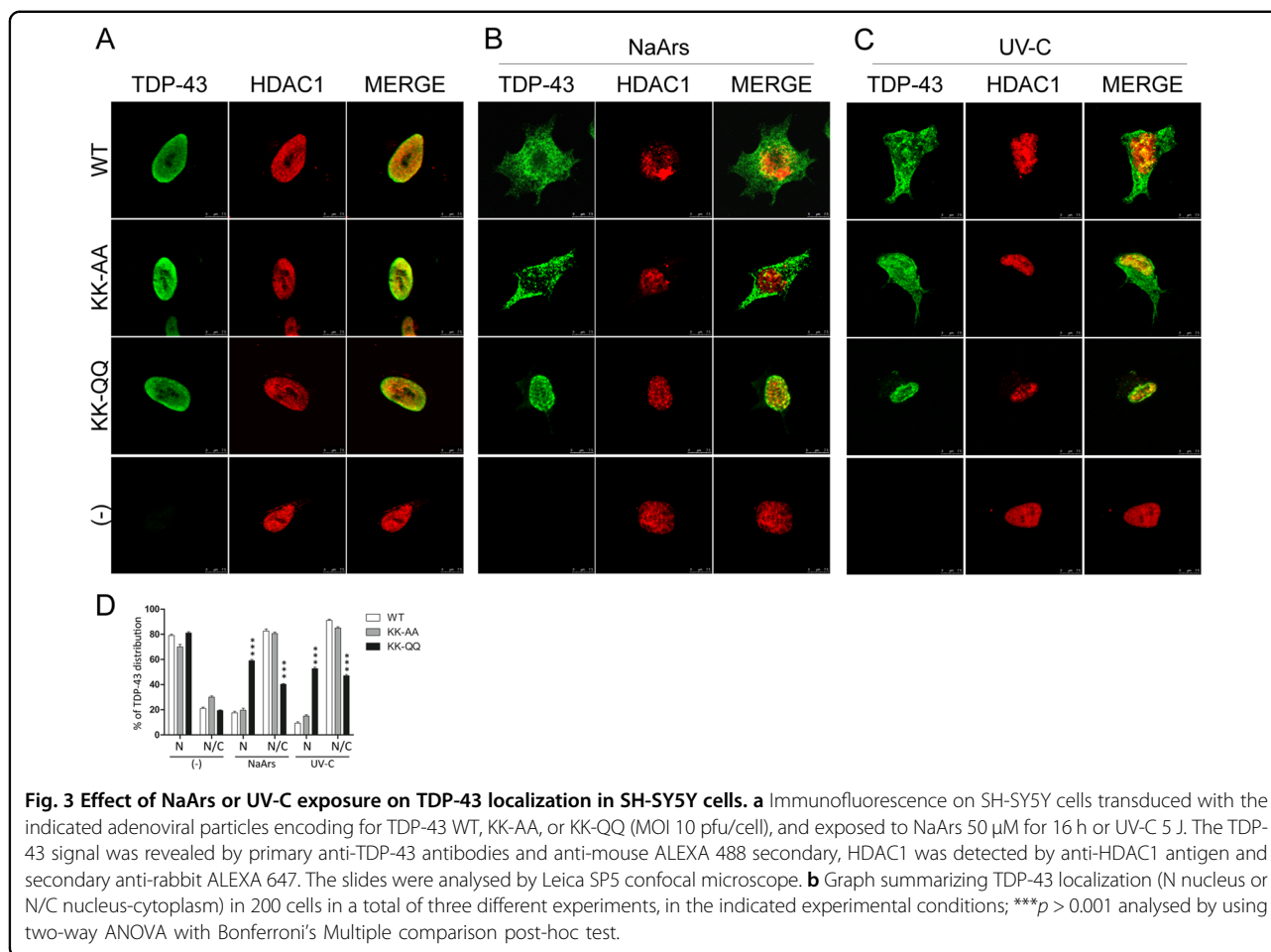
demonstrate that TDP-43 binds directly to the CHOP promoter, in a region comprised between -300 and -30 .

Acetylation affects TDP-43 re-localization under stressful conditions

TDP-43 acetylation status is suggested to be critical for TDP-43 toxicity, since the TDP-43 acetylation-mimic mutant K145Q induces TDP-43 pathology in muscle cells¹⁰. Starting from this observation the effects of double acetylation mimic or acetylation-null mutations on TDP-43 toxicity were assessed by measuring TDP-43 nuclear loss and cell death of SH-SY5Y cells³⁴. In particular, SH-SY5Y transduced with TDP-43 WT or bearing different mutations, were exposed to sodium arsenite, a classical agent used to induce stress granules formation, or UV-C to induce DDR^{35,36}. Although both treatments induce the re-localization of WT or acetylation-null mutations in the cytoplasm (Fig. 3), only the acetylation-mimicking KK-QQ mutant is completely unaffected and retained in the nucleus of treated and untreated cells.

TDP-43 and HDAC1 have a synergistic effect in decreasing cell vitality

The overexpression of either WT or pathological mutants of TDP-43 induces a reduction in cell survival, in different cellular, and animal systems³⁷, including SH-SY5Y cells³³. Thus, the effect of HDAC1 on TDP-43-induced cell toxicity was evaluated. Firstly, adenoviral particles expressing WT or mutant TDP-43 variants were generated and their effects on cell viability were measured. As shown in Fig. S4a, at MOI of 10 pfu/cell, the expression of WT or pathological mutant TDP-43 induces a decrease in cell viability. Notably, at the same MOI the expression of the KK-QQ mutant is less toxic, while the KK-AA mutant displays an intermediate effect. In this condition the ratio between endogenous and exogenous TDP-43 (corresponding to Myc-tagged TDP-43), measured by relative quantification of protein bands, is about 1:5 (Fig. S4b). To better characterize the molecular mechanisms underlying the reduction in cell viability that we observed by MTS assay upon TDP-43 overexpression



we evaluated the expression of apoptotic (caspase-3, PARP) or autophagic (LC3) markers, in SH-SY5Y and SH-SY5Y cells stably expressing CFP-DEVD-YFP reporter³⁸. As summarized in Fig. S4c, d, the reduction on cell viability likely does not involve the activation of apoptotic or autophagic pathways.

HDAC inhibition has been shown to be protective in a wide range of pathological conditions^{39,40}, including ALS. HDACis such as sodium butyrate (NaB), 4-phenylbutyrate (SPB), trichostatin A (TSA), and fatty acid derivatives, which inhibit most class I and II HDACs, have been used in SOD1-G93A mouse model. In fact, SPB treatment extends survival and motor performance in SOD1-G93A mice models and it has been demonstrated to be safe and well tolerated^{41,42} in a phase 2 clinical trial. TSA induces a modest improvement in motor function and survival as well as protection against motor neuron death⁴³. Furthermore, butyrate and valproic acid are also known to readily cross the BBB⁴⁴. Finally, the therapeutic potential of NaB has been also demonstrated in other neurodegenerative diseases such as Alzheimer disease, Parkinson's

and Huntington disease⁴⁰. Thus, the effects of these four HDACis on TDP-43-mediated cell death were assessed.

First, cellular toxicity of the different HDACis was evaluated by testing their dose-response effect on cell viability (Fig. S5) and two different nontoxic concentrations for each inhibitor to be used were defined. Afterwards, SH-SY5Y cells were transduced with recombinant adenovirus coding for WT or different mutants of TDP-43 (M337V, A382T, K145A-K192A, or K145Q-K192Q) and treated by HDACis. These experiments demonstrate an HDACi dose dependent increase in cell survival (Fig. 4). The positive effect of HDAC inhibition on TDP-43-induced cell toxicity was also confirmed in immunofluorescence experiments (Fig. 4g). HDCAi-treated cells display a diffuse staining of TDP-43 in the nuclei, which appear more spherical in respect to the ones of untreated cells. The expression of KK-AA and KK-QQ TDP-43 mutants is less toxic respect to WT TDP-43 and the treatment with HDACis induces a slight increase in cell viability, which does not reach statistical significance.

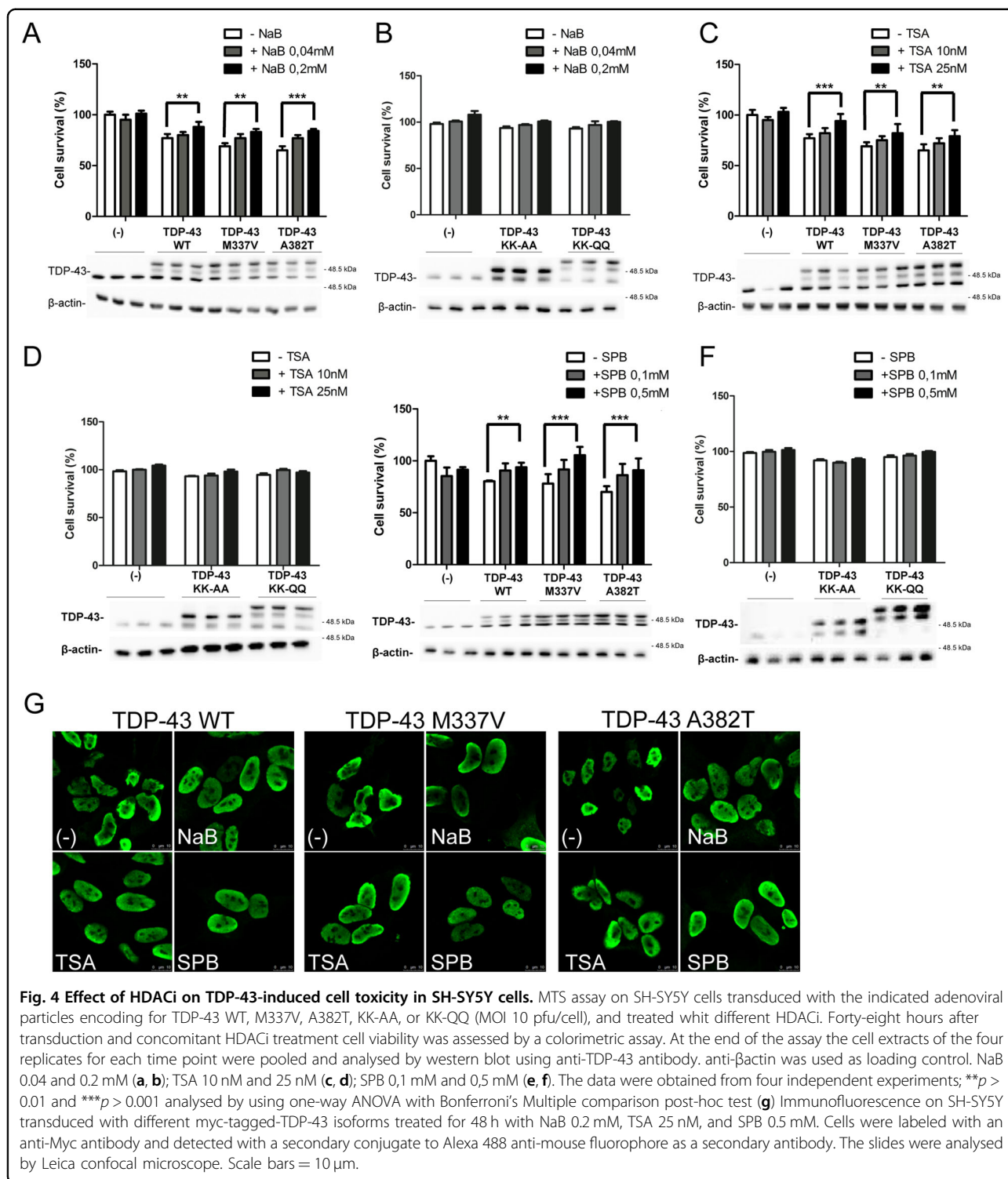
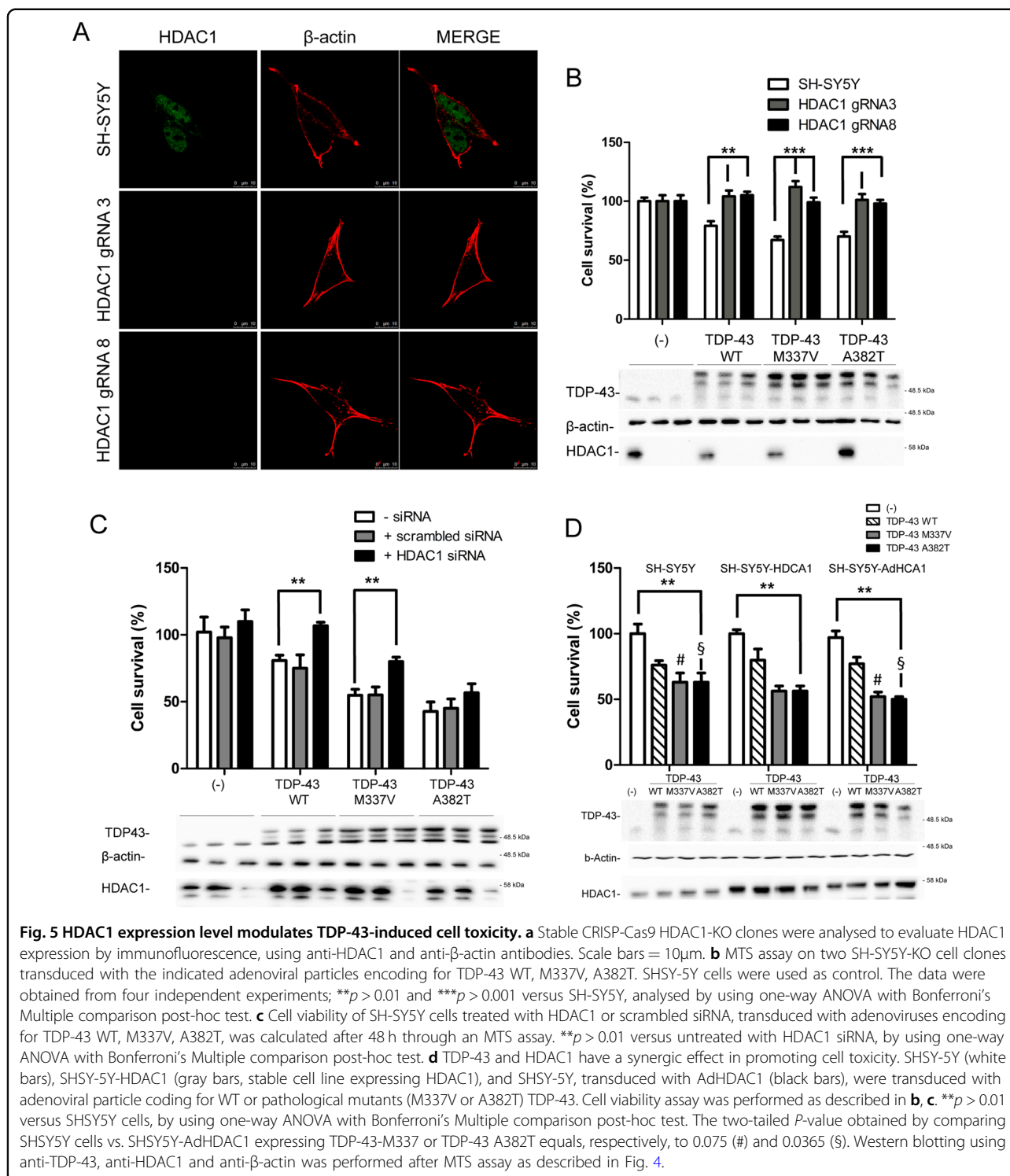


Fig. 4 Effect of HDACi on TDP-43-induced cell toxicity in SH-SY5Y cells. MTS assay on SH-SY5Y cells transduced with the indicated adenoviral particles encoding for TDP-43 WT, M337V, A382T, KK-AA, or KK-QQ (MOI 10 pfu/cell), and treated with different HDACi. Forty-eight hours after transduction and concomitant HDACi treatment cell viability was assessed by a colorimetric assay. At the end of the assay the cell extracts of the four replicates for each time point were pooled and analysed by western blot using anti-TDP-43 antibody. anti-βactin was used as loading control. NaB 0.04 and 0.2 mM (**a, b**); TSA 10 nM and 25 nM (**c, d**); SPB 0,1 mM and 0,5 mM (**e, f**). The data were obtained from four independent experiments; $**p > 0.01$ and $***p > 0.001$ analysed by using one-way ANOVA with Bonferroni's Multiple comparison post-hoc test (**g**) Immunofluorescence on SH-SY5Y transduced with different myc-tagged-TDP-43 isoforms treated for 48 h with NaB 0.2 mM, TSA 25 nM, and SPB 0.5 mM. Cells were labeled with an anti-Myc antibody and detected with a secondary conjugate to Alexa 488 anti-mouse fluorophore as a secondary antibody. The slides were analysed by Leica confocal microscope. Scale bars = 10 μm.

Then HDAC1 expression level was manipulated to assess its effect on TDP-43 toxicity. The CRISPR/Cas9 genome editing technique was used in SH-SY5Y cells to generate stable cell lines in which the expression of HDAC1 was ablated. SH-SY5Y were transfected with a

plasmid coding for the humanized Cas9 and different gRNA targeting the second exon of HDAC1 gene. After puromycin selection, single stable clones were isolated and analysed for HDAC1 expression leading to the identification of two lines in which HDAC1 protein



expression was absent as demonstrated by immunofluorescence experiment (Fig. 5a) and sequencing (data not shown).

These HDAC1-KO lines were used in cellular vitality tests, after being transduced with TDP-43 expressing adenoviruses. Interestingly, the ablation of HDAC1

expression significantly ameliorates TDP-43-mediated cell death (Fig. 5b).

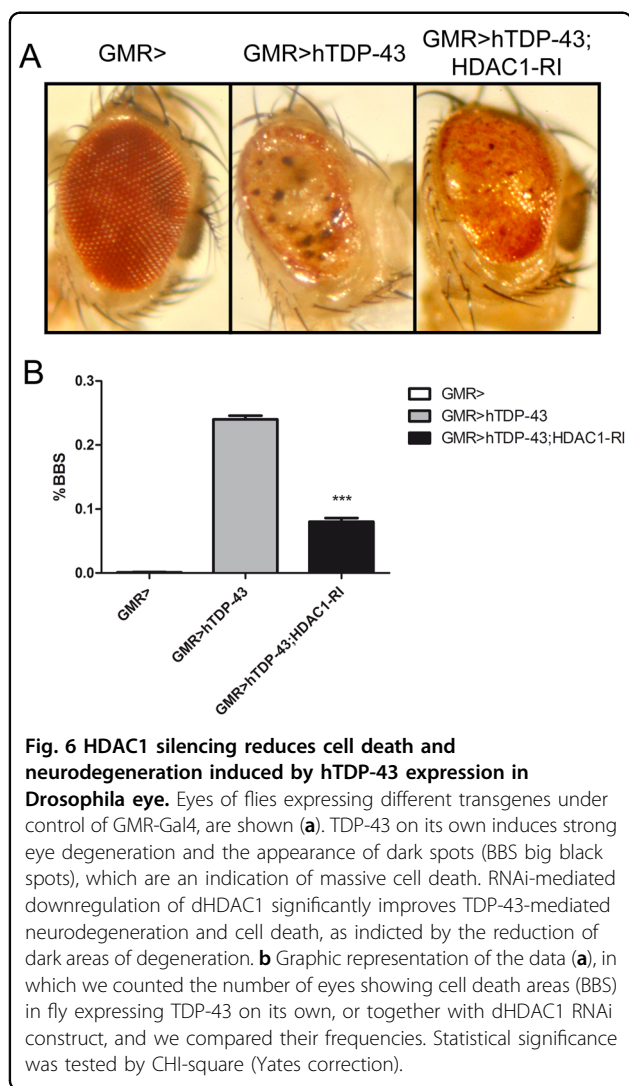
To confirm the evidence coming from HDCA1 genetic ablation, a commercial HDAC1 small interfering RNA (siRNA) to downregulate HDAC1 was used. Thus, we observed that the reduction of HDAC1 protein level by

70%, which causes a statistically significant decrease of TDP-43-induced cell toxicity, compared with the random sequence control (Fig. 5c).

Conversely, TDP-43 toxicity was exacerbated (Fig. 5d) when HDAC1 was transiently overexpressed via adenoviral transduction (Fig. S7) and at a less extent in SH-SY5Y stably expressing HDAC1 (Fig. S6).

Expression of human TDP-43 in fly eyes leads to progressive eye degeneration partially suppressed by HDAC1 silencing

The present study demonstrated that in three different experimental paradigms (genomic inactivation, siRNA, and HDACi treatment) the reduction of HDAC1 activity significantly reduces TDP-43-mediated cell death. To confirm these results through an in vivo approach, *Drosophila* ALS models³⁷ were exploited.



As shown in Fig. 6, expression of human TDP-43 in *Drosophila* eye leads to a well described retinal degeneration⁴⁵, which is associated to a strong cell death phenotype characterized by depigmentation, roughness, and dark spots. When these flies were crossed with a line in which Rpd3, the HDAC1 and HDAC2 *Drosophila* ortholog, is inactivated by the expression of an RNAi specific construct^{46,47}, a reduction in retinal degeneration can be clearly observed. These eyes exhibit a significant reduction of the dark apoptotic areas (Fig. 6).

These data strongly demonstrate that HDAC1 silencing in *Drosophila*, as well in SH-SY5Y cells, is able to ameliorate the toxic effect induced by TDP-43 expression.

Discussion

By using cellular and animal models we were able to describe a specific interaction between HDAC1 and TDP-43, via RRM1 and RRM2 domains. Interestingly, our experimental results suggest that HDAC1 may play a pivotal role on the deacetylation of TDP-43 in the nucleus. In addition, we observed as the impairment of TDP-43 deacetylation, by TDP-43 mutagenesis or by genetic/pharmacological HDAC1 inhibition, has a positive effect on TDP-43-induced cell death. Notably, through ChIP analysis and luciferase assays, evidence is provided that TDP-43 is a direct activator of CHOP (*C/EBP*-homologous protein) transcription, expanding what previously reported³². CHOP is a mediator of cell death, caused by the activation of the unfolded protein response, a key event in the ALS-linked proteinopathies⁴⁸. TDP-43 acetylation-mimicking mutant (TDP-43 QQ) loses its ability to induce CHOP transcription, indicating that TDP-43 acetylation can affect TDP-43-mediated pathways downstream ER stress, as well as further promote the nuclear retention of TDP-43 upon exposition to stressful signals.

The phenotype described is in line with the multiple crossroads between epigenome, epigenetic machinery, and ALS, described in the past 10 years^{14,49}.

We had previously demonstrated that TDP-43 M337V expression induces a decrease in global histone H3 phospho-acetylation³³, that can affect TDP-43-induced cell toxicity at multiple levels, since changes in acetylation of both histone and nonhistone proteins have been reported to affect cell physiology spanning from transcription, to DNA repair signal transduction, and protein aggregation⁵⁰.

HDACs are key modulators of the acetylome and they have been demonstrated to be deregulated in ALS experimental models and patients¹³. In fact, the levels of HDAC1, HDAC2, and sirtuins (a family of class III HDACs) are impaired in post-mortem ALS tissues¹⁷. In yeast Set-3, a component of the histone deacetylation complex, is a modulator of TDP-43 toxicity⁵¹. HDAC1,

like most HDACs, is a nuclear enzyme that can be re-localized in the cytosol in damaged axons of demyelinating models, such as in patients affected by multiple sclerosis and in cultured neurons exposed to glutamate or TNF- α ^{52,53}. More recently, during development of the *Xenopus* brain, HDAC1 was observed in the mitochondria of developing neurons⁵⁴. In addition, in a *FUS* knock-in mouse model HDAC1 is mislocalized to the cytoplasm⁵⁵, probably following dephosphorylation on serine 421 and 423⁵³. Despite this evidence we were not able to highlight HDAC1 re-localization in our cellular models.

HDACis were originally applied to cancer therapy and some of them, such as panobinostat, have been approved from FDA for multiple myeloma treatment, while others, like VPA and SPB, are in phase II or III clinical trials, respectively, for hematological and solid malignancies⁴⁰. At present more than 350 clinical trials involving HDACi have been carried out or are on-going not only as single therapeutic but also in combination with other targeted agents against various human diseases, including neurodegenerative diseases. VPA was approved by FDA in 1978 as an anticonvulsant drug for the treatment of seizure disorders, even if the molecular target of this drug it is not known yet. The possibility of using HDACi for neurodegenerative treatment originates in 2008, when Hahnen identified two major HDACi neuroprotective mechanisms, including the transcriptional activation of disease-modifying genes and the rectification of destabilization in histone acetylation homeostasis⁵⁶. Several pan-HDACis reduced ALS development in mice^{43,57,58}. SPB was shown to extend survival and motor performance in transgenic ALS SOD1 animal model, and these effects were attributed to an upregulation in the expression of nuclear factor κ B (NF- κ B) and bcl-2 proteins⁴¹, although the genetic inhibition of NF- κ B in SOD1 mice does not ameliorate disease onset and progression⁵⁹. Unfortunately, even if VPA and SPB are safe, tolerable, and efficient in improving histone acetylation levels, they failed to ameliorate clinical parameters in ALS patients^{42,60}. In line with this observation the work by Pigna et al. identified HDAC4, a class IIa HDAC, as having a crucial role in preserving the innervations and skeletal muscle in SOD1 ALS mouse model⁶¹. HDAC4 genetic ablation in skeletal muscle accelerates ALS pathological features, indicating a possible risk for using HDACs pan-inhibitors in ALS treatment. On the other hand, HDAC6 inhibition in motor neuron cultures derived from iPSCs, originated from fibroblasts of ALS patients carrying different *FUS* mutations, reverses axonal transport defects⁶². Treatment of *FUS* transgenic mice with ACY-738, a potent class I HDAC brain penetrable inhibitor, largely restores global histone acetylation, and metabolic gene expression in the spinal cord⁶³. ACY-738 inhibits HDAC6 with low nanomolar potency and a selectivity of 60- to 1500-fold over

class I HDACs, but its effect in *FUS* mouse model is independent from HDAC6 itself, indicating that other members of the family, including HDAC1, can be the key element mediating the observed therapeutic effects⁶³. Moreover HDAC1 appears as a downstream target of both *FUS* and TDP-43 related ALS in mediating double strand-breaks repair^{20,22,23,64,65}.

Although HDACi translational failure underlies ALS complexity and can be related to the lack of selectivity for different HDACs, more specific drugs would be very useful. Particularly, evidence provided indicates that HDAC1 inhibition can be a precious therapeutic option in ALS therapy.

Material and methods

Antibodies and reagents

The following primary antibodies were used in this study: Myc monoclonal antibody (M4439, Sigma-Aldrich), β -actin (A5441, Sigma-Aldrich), Flag (F3165, Sigma-Aldrich), HDAC1 (10197-1-AP, Proteintech), TARDBP (190782-2-AP, Proteintech), Acetylated-Lysine antibody (9441, Cell Signaling), GFP (33-260, ThermoFisher Scientific), caspase-3 (#9662, Cell Signaling Technology), PARP (#9542, Cell Signaling Technology), LC3B (#2775, 2Cell Signaling Technology), anti-rabbit peroxidase-conjugated secondary antibody (AP132P EMD Millipore) and anti-mouse peroxidase-conjugated secondary antibody (AP124P EMD Millipore); anti-rabbit, anti-mouse Alexa 488 (A-11001, Life Technologies) or 647-conjugated secondary antibody (A-21244, Life Technologies). All antibodies were used at the dilution recommended by the manufacturer's instructions.

The following HDACis were used in this study: Sodium phenil butyrate (SML0309, Sigma-Aldrich), Trichostatin A (T8552, Sigma-Aldrich), Sodium butyrate (B5887, Sigma-Aldrich), Valproic acid sodium salt (P4543, Sigma-Aldrich).

Mice tissue

Mice tissues were dissected from BALB31c mice housed at the *Istituto Zooprofilattico della Sardegna (Sassari, Italy)*. All animal procedures have been performed according to the European Guidelines for the use of animals in research (86/609/CEE) and the requirements of Italian laws (D.L. 116/92, Directive 2010/63/EU). The ethical procedure has been approved by the Animal welfare office, Department of Public Health and Veterinary, Nutrition and Food Safety, General Management of Animal Care and Veterinary Drugs of the Italian Ministry of Health (Application number 32/08 of 7 July 2008; Approval number 744 of 9 January 2009). Authorized investigators performed all the experiments. Dissected tissue was immediately frozen in liquid nitrogen and stored at -80°C .

Drosophila model

Flies expressing insect codon-optimized version of human wild-type TDP-43 (gl-TDP-43CO)⁶⁶ under UAS promoter during fly eye development, driven by GMR-Gal4, were crossed at 25 °C with flies expressing a unique dsRNA that targets *Drosophila* HDAC1. In particular, GMR-GAL4 on X-chromosome was originally placed in trans to generate a GMR-GAL4;gl-TDP-165 43CO/CyO transgenic fly, which was obtained from Bloomington Stock Center⁶⁷. RNAi line to target HDAC1 (v30599) (also named Rpd3 in *Drosophila*), which was previously utilized to downregulated Rpd3 according to^{46,47}, was obtained by Vienna *Drosophila* Research Center. Eye neurodegeneration was evaluated according to⁶⁸. A minimum of 60 flies were randomly choosed, with investigators blind to the genotypes, during the analysis.

Plasmids construction and oligonucleotides

Sequence coding for human TDP-43 (NM_007375.3) or human HDAC1 (NM_004964.2) were cloned in different expression vectors (pCS2-MTK, pCMV-3xFlag or pShuttle2) and used for site-directed mutagenesis (QuickChange site-directed mutagenesis kit, Agilent). Mutants were obtained by mutagenesis starting from hTDP-43, by site-directed mutagenesis. Positive clones were screened by sequencing. Human HDAC6 (NC_000023.11) and HDAC2 (NM_001527) were cloned in expression vector pCMV-3xFlag.

Adenoviral particle production

All adenoviral vectors (*pAdenoX-hTDP-43WT/Q331K/M337V/A382T/ΔRRM1-2/K145A-K192A/K145Q-K192Q* and *pAdenoX-hHDAC1*) were generated using the Adeno-X Expression System 1 (Clontech) and partially described. All constructions were verified by automated sequencing. Adenoviral particles were produced and titrated using the Adenoviral-X Expression System 1 (Clontech) according to manufacturer's instruction. Cells were transduced by adenoviral particles (5–30 pfu/cell) in DMEM-F12 and incubated at 37°C for 1 h. The transduced cells (usually more than 90% expressing TDP-43) were analysed 48 h transduction.

Cell lines and culture

Human neuroblastoma SH-SY5Y cells (CRL-2266, ATCC, Rockville, MD) and SH-SY5Y-CFP-DEVD-YFP³⁸ cells were grown in DMEM-F12, 10% Fetal Bovine Serum (FBS) at 37 °C. The plasmid pcDNA3 containing cDNA coding for 3 × Flag-HDAC1 was transfected using Lipofectamine[®] LTX Reagent (Life Technologies) according to the manufacturer's protocol. The different SH-SY5Y clones were maintained under selection by 400 µg/mL of G418. Individual clones were picked after 14 days of selection, moved in a 96 well plate, and maintained under

selective medium until confluence growth. Different individual clones were analysed for HDAC1 expression by western blot and immunofluorescence.

To expose cells to stressful conditions after transduction with the indicated adenoviral particle, cells were either exposed to NaArs 50 µM for 16 h or for UV irradiation: cells were treated with UV-C (254 nm) using a low pressure mercury lamp, and the cells were subjected to global (2.5 J/m²). After microirradiation, cells were incubated for 4 h at 37 °C in a humidified atmosphere containing 5% CO₂. All slides were processed by assaying the previously mentioned immunofluorescence protocol and analysed by confocal microscopy.

Adeno-X 293 cell line

Adenovirus 5-transformed Human Embryonic Kidney 293 cell line (CRL 1573 HEK 293; ATCC, Rockville, MD,) was used to package and propagate the recombinant adenoviral- based vectors produced with the BD Adeno-X Expression System.

SH-SY5Y cells (ATCC number CRL-2266) were grown in DMEM-F12, 10% FBS at 37 °C whereas, *Adeno-X 293 cell line* were grown in DMEM, 10% FBS at 37 °C. Transient expression of each vector (2,5 µg DNA/1 × 10⁶ cells) was obtained with Lipofectamine Plus reagent (Thermo-Fisher) according to manufacturer's instructions. After an incubation of 4 h with transfection reagents, the cells were cultured in normal growth medium for 24 or 48 h. Transduction with adenoviral particle with a MOI of 5–10 pfu/cell was performed according to⁶⁹.

Co-immunoprecipitation

Briefly, cultured cells were lysed with lysis buffer (120 mM NaCl, 50 mM Tris pH 7.5, 5 mM EDTA, 0.5% NP-40, and 1 mM freshly prepared PMSF), containing protease inhibitors (SIGMA P 8340). Cell lysates were immunoprecipitated overnight at 4 °C with specific antibodies; immunocomplexes were then captured by incubating for 16 h at 4 °C with continuous gentle shaking, with protein-A sepharose from *Staphylococcus aureus* (Sigma-Aldrich P3391). Subsequently, immunocomplexes were analysed by means of western blotting, using specific antibodies.

SDS-PAGE and western immunoblotting

Protein content was determined using Bradford protein assay (27813 SIGMA). Equal amounts of protein extracts were resolved by standard SDS/PAGE. Samples were then electroblotted onto Protan nitrocellulose membranes (GE Healthcare Life Science). Afterwards, membranes were incubated in 3% low-fat milk, diluted in 1 × PBS-Tween 0.05% solution with the indicated antibody for 16 h at 4 °C. Anti-Rabbit IgG (whole molecule)- and Anti-Mouse IgG (whole molecule)-peroxidase antibody (EMD

Millipore) were used to reveal immunocomplexes by enhanced chemiluminescence (ThermoFischer). The apparent molecular weight of proteins was determined by calibrating the blots with prestained molecular weight markers (Bio-Rad, Hercules, CA). Where indicated, the relative signal intensity acquired by using the ChemiDoc XRS+ (Bio-Rad, Hercules, CA) was quantified using QuantityOne Software.

Two-dimensional electrophoresis analysis

Two-dimensional electrophoresis (2-DE) was used to separate proteins according to their isoelectric point (1st dimension) and, orthogonally, to their molecular weight (2nd dimension).

2-DE was performed as reported elsewhere^{70,71}. Briefly, samples were applied to 70 mm IPG strips (pH 4-7, Bio-Rad, Hercules, CA), by overnight rehydration loading at 20 °C, and then isoelectrofocussed at 50 μ A/IPG strip for 22 kWh at 20 °C. Once isoelectric focusing was completed, proteins were in-gel reduced by incubating IPG strips with 50 mM Tris buffer containing 6 M urea, 30% glycerol v/v, 3% SDS w/v, and 1% DTT w/v, followed by in-gel alkylation with the same solution containing 2.5% iodoacetamide w/v, in place of DTT. Each step was performed keeping strips under continuous shaking for 15 min. IPG strips were then sealed with 0.5% low melting point agarose w/v, in SDS running buffer, at top of second dimension gels (8 \times 7 cm \times 0.1 cm). SDS-PAGE was carried out using 15% T, 3% C polyacrylamide gels at the following conditions: 50 V for 15 min and subsequently at 150 V until the Bromophenol dye front reached the lower limit of the gel, in a Mini-Protean Tetra Cell (Bio-Rad, Hercules, CA). Later gels were subjected to western blot analysis, as described above.

Immunofluorescence

Cells were grown on a cover-glass, were washed twice with PBS 1X and then fixed with 4% paraformaldehyde in 1 \times PBS and permeabilized with 0.2% Triton X-100 in 1 \times PBS. After a blocking step for 1 h in 5% BSA, diluted in 1 \times PBS-0.05% Tween-20, cells were incubated with the primary antibody mouse anti-Myc (Sigma-Aldrich), diluted 1:10000 in blocking solution, overnight at 4 °C, and then incubated with a secondary antibody Alexa Fluor[®]488 goat anti-mouse IgG (Life Technologies), diluted 1:1000 in blocking solution, for 1 h at the room temperature. Cells were then analysed with a Leica TCS SP5 confocal microscopy, with LAS lite 170 image software.

Chromatin immunoprecipitation (ChIP)

SH-SY5Y cells (4×10^6) were plated 24 h before transduction, and infected by using viruses encoding for TDP WT at a multiplicity of 30 pfu/cell. After 24 h, cells were

harvested and chromatin immunoprecipitation was performed using EZ-Magna ChIP[™] (Millipore), according to the manufacturer's protocol.

Each immunoprecipitated (IP) reaction was performed using about 1×10^6 cells equivalents of chromatin. The antibodies used for immunoprecipitation were the following: TARDBP Polyclonal Antibody (Proteintech_10782-2-AP) and Normal Rabbit Ig (reagent supplied) as negative control. Purified chromatin was eluted and DNA fragments were used for qPCR (S2). The results were normalized using the Fold Enrichment Method (ChIP signals were divided by the no-antibody signals, representing the ChIP signal as the fold increase in signal relative to the background signal). ** $p < 0,01$ Student's *t* test.

Luciferase activity assay

The DNA-damage-inducible transcript 3 (gene-synonym CEBPZ, CHOP, GADD153⁷²) promoter from -954 to +91 was cloned between the *XhoI* and *HindIII* sites in the pGLE-Basic Vector. All constructions were verified by automated sequencing. SH-SY5Y cells were seeded in 24-well plates and cultured for 16 h. Cells were then transfected by wild-type or mutant of TDP-43, HDAC1 and luciferase constructs, in addition to a Renilla vector, used as an internal control for luciferase activity; transfected cells were further cultured for 48 h. Luciferase assays were conducted using dual luciferase assay system (Promega). Each experiment was performed in triplicate.

siRNA on HDAC1 mRNA

SH-SY5Y cells (1×10^5) were seeded 24 h before the first transfection with the siRNA oligonucleotide specific for HDAC1 gene. Lipofectamine 3000 reagent (Lipofectamine[®] 3000, ThermoFisher) was combined with Optimem medium (Promega) (reaction 1); meanwhile, in a different tube, 148 pmol of HDAC1 siRNA and 500 ng of TDP, WT or mutant, were mixed with Optimem (reaction 2). Both reactions were mixed and left for 5 min at the room temperature. Afterwards, the mixture was added to the cells and incubated at 37 °C and 5% of CO₂. After 48 h the transfection procedure was repeated only for HDAC1 siRNA, and cells were incubated at 37 °C and 5% of CO₂ for other 24 h. After 72 h a MTS assay was performed, and cells were finally washed two times with PBS; subsequently, cell lysates were subjected to western blot analysis with anti-HDAC1 antibodies to evaluate expression level.

Design of targeting components and the use of the CRISPR Design Tool

The web interface of CRISPR Design Tool (<http://tools.genome-engineering.org>) was used to develop gRNAs. Off-target activity was evaluated additionally with Blastn

(<https://blast.ncbi.nlm.nih.gov/Blast.cgi>). The pSpCas9 (BB)-2A-Puro (Addgene # 48139) that expresses the *Streptococcus pyogenes* Cas9 (including an NLS and a FLAG tag) from a CAG promoter and has a U6 promoter driven gRNA, was used as cloning backbone according to⁷³. Briefly, phosphorylation and annealing were performed with the three pairs of oligos, mentioned above, harboring a BbsI overhang. Afterwards, BbsI (#FD1014, ThermoFisher) mediated digestion and T4 DNA ligase (#M0318L, NEB) directed ligation in the linearized pSpCas9(BB)-2A-Puro was performed. After the transformation, cloning was verified with a control PCR with the primers in the table. Plasmids were purified and sequenced. After transfection of the indicated combinations of pSpCas9(BB)-2A-Puro-gRNAs (Addgene #62988), positive cells were selected using puromycin ($2 \mu\text{g mL}^{-1}$) for 5 days prior to clonal expansion. Empty pSpCas9(BB)-2A-Puro was used as negative control.

MTS assay

Cell viability was assessed by a colorimetric assay using 3-(4,5-dimethylthiazol-2-yl)-5-(3-carboxymethoxyphenyl)-2-(4-sulfophenyl)-2H-tetrazolium (MTS) assay (Cell Titer 96 Aqueous One Solution Assay, Promega), according to manufacturer's instructions. Absorbance at 490 nm was measured in a multilabel counter (Victor X5, PerkinElmer) 72 h post transduction.

Statistical analysis

The results are presented as means \pm S.D. of $n \geq 3$ independent experiments. Statistical evaluation was conducted by one-way or two-way ANOVA and Bonferroni post test. Values significantly different from the relative control are indicated with a symbol: * $p < 0.05$; ** $p < 0.01$; *** $p < 0.001$ or $^{\$}p < 0.05$; $^{\$\$}p < 0.01$; $^{\$ \$ \$}p < 0.001$.

Acknowledgements

This paper is dedicated to the memory of our friend and colleague Prof Maria Teresa Carri. We would like to acknowledge all the people from the laboratory that critically read the manuscript. Thanks are due to Giustina Casu for proofreading the manuscript for English language. This study was supported by AriSLA (Pilot Grant Project ALSHDAC1) and PRIN 2015 (Grant 2015LFPNMN_005). SE and GN were supported by an AriSLA fellowship, PS and MF by PhD fellowships granted by PON 2014-2020 (CCI2014IT16M2OP005).

Conflict of interest

All authors disclose any financial and personal relationships with other people or organisations that could inappropriately influence our work.

Publisher's note

Springer Nature remains neutral with regard to jurisdictional claims in published maps and institutional affiliations.

Supplementary Information accompanies this paper at (<https://doi.org/10.1038/s41419-020-2580-3>).

Received: 6 September 2019 Revised: 22 April 2020 Accepted: 22 April 2020
Published online: 14 May 2020

References

- Berning, B. A. & Walker, A. K. The pathobiology of TDP-43 C-terminal fragments in ALS and FTL. *Front Neurosci.* **13**, 335 (2019).
- Sephton, C. F., Cenik, B., Cenik, B. K., Herz, J. & Yu, G. TDP-43 in central nervous system development and function: clues to TDP-43-associated neurodegeneration. *Biol. Chem.* **393**, 589–594 (2012).
- Ederle, H. & Dormann, D. TDP-43 and FUS en route from the nucleus to the cytoplasm. *FEBS Lett.* **591**, 1489–1507 (2017).
- Buratti, E. TDP-43 post-translational modifications in health and disease. *Expert Opin. Ther. Targets* **22**, 279–293 (2018).
- Neumann, M. et al. Ubiquitinated TDP-43 in frontotemporal lobar degeneration and amyotrophic lateral sclerosis. *Science* **314**, 130–133 (2006).
- van Es, M. A. et al. Amyotrophic lateral sclerosis. *Lancet* **390**, 2084–2098 (2017).
- Gendron, T. F., Rademakers, R. & Petrucelli, L. TARDBP mutation analysis in TDP-43 proteinopathies and deciphering the toxicity of mutant TDP-43. *J. Alzheimer's Dis.* **33**(Suppl 1), S35–S45 (2013).
- French, R. L. et al. Detection of TAR DNA-binding protein 43 (TDP-43) oligomers as initial intermediate species during aggregate formation. *J. Biol. Chem.* **294**, 6696–6709 (2019).
- Cohen, T. J. et al. An acetylation switch controls TDP-43 function and aggregation propensity. *Nat. Commun.* **6**, 5845 (2015).
- Wang, P., Wander, C. M., Yuan, C. X., Bereman, M. S. & Cohen, T. J. Acetylation-induced TDP-43 pathology is suppressed by an HSF1-dependent chaperone program. *Nat. Commun.* **8**, 82 (2017).
- Cho, Y. & Cavalli, V. HDAC signaling in neuronal development and axon regeneration. *Curr. Opin. Neurobiol.* **27**, 118–126 (2014).
- Chuang, D. M., Leng, Y., Marinova, Z., Kim, H. J. & Chiu, C. T. Multiple roles of HDAC inhibition in neurodegenerative conditions. *Trends Neurosci.* **32**, 591–601 (2009).
- Valle, C. et al. Tissue-specific deregulation of selected HDACs characterizes ALS progression in mouse models: pharmacological characterization of SIRT1 and SIRT2 pathways. *Cell Death Dis.* **5**, e1296 (2014).
- Bennett, S. A., Tanaz, R., Cobos, S. N. & Torrente, M. P. Epigenetics in amyotrophic lateral sclerosis: a role for histone post-translational modifications in neurodegenerative disease. *Transl. Res.* **204**, 19–30 (2019).
- Yang, X. J. & Seto, E. Collaborative spirit of histone deacetylases in regulating chromatin structure and gene expression. *Curr. Opin. Genet. Dev.* **13**, 143–153 (2003).
- Huang, Y., Myers, S. J. & Dingledine, R. Transcriptional repression by REST: recruitment of Sin3A and histone deacetylase to neuronal genes. *Nat. Neurosci.* **2**, 867–872 (1999).
- Janssen, C. et al. Differential histone deacetylase mRNA expression patterns in amyotrophic lateral sclerosis. *J. Neuropathol. Exp. Neurol.* **69**, 573–581 (2010).
- Bardai, F. H., Price, V., Zaayman, M., Wang, L. & D'Mello, S. R. Histone deacetylase-1 (HDAC1) is a molecular switch between neuronal survival and death. *J. Biol. Chem.* **287**, 35444–35453 (2012).
- Kim, J. Y. et al. HDAC1 nuclear export induced by pathological conditions is essential for the onset of axonal damage. *Nat. Neurosci.* **13**, 180–189 (2010).
- Wang, W. Y. et al. Interaction of FUS and HDAC1 regulates DNA damage response and repair in neurons. *Nat. Neurosci.* **16**, 1383–1391 (2013).
- Qiu, H. et al. ALS-associated mutation FUS-R521C causes DNA damage and RNA splicing defects. *J. Clin. Invest.* **124**, 981–999 (2014).
- Hill, S. J. et al. Two familial ALS proteins function in prevention/repair of transcription-associated DNA damage. *Proc. Natl Acad. Sci. USA* **113**, E7701–E7709 (2016).
- Mitra, J. et al. Motor neuron disease-associated loss of nuclear TDP-43 is linked to DNA double-strand break repair defects. *Proc Natl Acad Sci USA*, <https://doi.org/10.1073/pnas.1818415116>. (2019).
- Lagier-Tourenne, C. & Cleveland, D. W. Rethinking ALS: the FUS about TDP-43. *Cell* **136**, 1001–1004 (2009).
- Garbes, L., Riessland, M. & Wirth, B. Histone acetylation as a potential therapeutic target in motor neuron degenerative diseases. *Curr. Pharm. Des.* **19**, 5093–5104 (2013).
- Ayala, Y. M., Misteli, T. & Baralle, F. E. TDP-43 regulates retinoblastoma protein phosphorylation through the repression of cyclin-dependent kinase 6 expression. *Proc. Natl Acad. Sci. USA* **105**, 3785–3789 (2008).

27. Kabashi, E. et al. TARDBP mutations in individuals with sporadic and familial amyotrophic lateral sclerosis. *Nat. Genet.* **40**, 572–574 (2008).
28. Kovacs, G. et al. TARDBP variation associated with frontotemporal dementia, supranuclear gaze palsy, and chorea. *Mov. Disord.* **24**, 1843–1847 (2009).
29. Ou, S. H., Wu, F., Harrich, D., Garcia-Martinez, L. F. & Gaynor, R. B. Cloning and characterization of a novel cellular protein, TDP-43, that binds to human immunodeficiency virus type 1 TAR DNA sequence motifs. *J. Virol.* **69**, 3584–3596 (1995).
30. Lalmanasingh, A. S., Urekar, C. J. & Reddi, P. P. TDP-43 is a transcriptional repressor: the testis-specific mouse *acr1* gene is a TDP-43 target in vivo. *J. Biol. Chem.* **286**, 10970–10982 (2011).
31. Reddi, P. P. Transcription and splicing factor TDP-43: role in regulation of gene expression in testis. *Semin Reprod. Med.* **35**, 167–172 (2017).
32. Suzuki, H. & Matsuoka, M. TDP-43 toxicity is mediated by the unfolded protein response-unrelated induction of C/EBP homologous protein expression. *J. Neurosci. Res.* **90**, 641–647 (2012).
33. Masala, A. et al. Epigenetic changes associated with the expression of amyotrophic lateral sclerosis (ALS) causing genes. *Neuroscience* **390**, 1–11 (2018).
34. Liu-Yesucevitz, L. et al. Tar DNA binding protein-43 (TDP-43) associates with stress granules: analysis of cultured cells and pathological brain tissue. *PLoS ONE* **5**, e13250 (2010).
35. Gasset-Rosa, F. et al. Cytoplasmic TDP-43 de-mixing independent of stress granules drives inhibition of nuclear import, loss of nuclear TDP-43, and cell death. *Neuron* **102**, 339–357 e337 (2019).
36. Mann, J. R. et al. RNA binding antagonizes neurotoxic phase transitions of TDP-43. *Neuron* **102**, 321–338 e328 (2019).
37. Van Damme, P., Robberecht, W. & Van Den Bosch, L. Modelling amyotrophic lateral sclerosis: progress and possibilities. *Dis. Model Mech.* **10**, 537–549 (2017).
38. Sanna, V. et al. Single-step green synthesis and characterization of gold-conjugated polyphenol nanoparticles with antioxidant and biological activities. *Int J. Nanomed.* **9**, 4935–4951 (2014).
39. Petri, S. et al. Additive neuroprotective effects of a histone deacetylase inhibitor and a catalytic antioxidant in a transgenic mouse model of amyotrophic lateral sclerosis. *Neurobiol. Dis.* **22**, 40–49 (2006).
40. Falkenberg, K. J. & Johnstone, R. W. Histone deacetylases and their inhibitors in cancer, neurological diseases and immune disorders. *Nat. Rev. Drug Discov.* **13**, 673–691 (2014).
41. Ryu, H. et al. Sodium phenylbutyrate prolongs survival and regulates expression of anti-apoptotic genes in transgenic amyotrophic lateral sclerosis mice. *J. Neurochem.* **93**, 1087–1098 (2005).
42. Cudkovic, M. E. et al. Phase 2 study of sodium phenylbutyrate in ALS. *Amyotroph. Lateral Scler.* **10**, 99–106 (2009).
43. Yoo, Y. E. & Ko, C. P. Treatment with trichostatin A initiated after disease onset delays disease progression and increases survival in a mouse model of amyotrophic lateral sclerosis. *Exp. Neurol.* **231**, 147–159 (2011).
44. Butler, R. & Bates, G. P. Histone deacetylase inhibitors as therapeutics for polyglutamine disorders. *Nat. Rev. Neurosci.* **7**, 784–796 (2006).
45. Li, Y. et al. A Drosophila model for TDP-43 proteinopathy. *Proc. Natl Acad. Sci. USA* **107**, 3169–3174 (2010).
46. Burgio, G., Cipressa, F., Ingrassia, A. M., Cenci, G. & Corona, D. F. The histone deacetylase Rpd3 regulates the heterochromatin structure of Drosophila telomeres. *J. Cell Sci.* **124**, 2041–2048 (2011).
47. Zhang, Z. et al. Atrophin-Rpd3 complex represses Hedgehog signaling by acting as a corepressor of CiR. *J. Cell Biol.* **203**, 575–583 (2013).
48. Hu, Y. Axon injury induced endoplasmic reticulum stress and neurodegeneration. *Neural Regen. Res.* **11**, 1557–1559 (2016).
49. Paez-Colasante, X., Figueroa-Romero, C., Sakowski, S. A., Goutman, S. A. & Feldman, E. L. Amyotrophic lateral sclerosis: mechanisms and therapeutics in the epigenomic era. *Nat. Rev. Neurol.* **11**, 266–279 (2015).
50. Narita, T., Weinert, B. T. & Choudhary, C. Functions and mechanisms of non-histone protein acetylation. *Nat. Rev. Mol. Cell Biol.* **20**, 156–174 (2019).
51. Armakola, M. et al. Inhibition of RNA lariat debranching enzyme suppresses TDP-43 toxicity in ALS disease models. *Nat. Genet.* **44**, 1302–1309 (2012).
52. Vashisht Gopal, Y. N., Arora, T. S. & Van Dyke, M. W. Tumour necrosis factor- α depletes histone deacetylase 1 protein through IKK2. *EMBO Rep.* **7**, 291–296 (2006).
53. Zhu, Y. et al. Subcellular distribution of HDAC1 in neurotoxic conditions is dependent on serine phosphorylation. *J. Neurosci.* **37**, 7547–7559 (2017).
54. Guo, X. et al. Subcellular localization of class I histone deacetylases in the developing xenopus tectum. *Front Cell Neurosci.* **9**, 510 (2015).
55. Scekic-Zahirovic, J. et al. Toxic gain of function from mutant FUS protein is crucial to trigger cell autonomous motor neuron loss. *EMBO J.* **35**, 1077–1097 (2016).
56. Hahnen, E. et al. Histone deacetylase inhibitors: possible implications for neurodegenerative disorders. *Expert Opin. Investig. Drugs* **17**, 169–184 (2008).
57. Rouaux, C. et al. Sodium valproate exerts neuroprotective effects in vivo through CREB-binding protein-dependent mechanisms but does not improve survival in an amyotrophic lateral sclerosis mouse model. *J. Neurosci.* **27**, 5535–5545 (2007).
58. Iannitti, T. & Palmieri, B. Clinical and experimental applications of sodium phenylbutyrate. *Drugs R. D.* **11**, 227–249 (2011).
59. Crosio, C., Valle, C., Casciati, A., Iaccarino, C. & Carri, M. T. Astroglial inhibition of NF- κ B does not ameliorate disease onset and progression in a mouse model for amyotrophic lateral sclerosis (ALS). *PLoS ONE* **6**, e17187 (2011).
60. Piepers, S. et al. Randomized sequential trial of valproic acid in amyotrophic lateral sclerosis. *Ann. Neurol.* **66**, 227–234 (2009).
61. Pigna, E. et al. Histone deacetylase 4 protects from denervation and skeletal muscle atrophy in a murine model of amyotrophic lateral sclerosis. *EBioMedicine* **40**, 717–732 (2019).
62. Guo, W. et al. HDAC6 inhibition reverses axonal transport defects in motor neurons derived from FUS-ALS patients. *Nat. Commun.* **8**, 861 (2017).
63. Rossaert, E. et al. Restoration of histone acetylation ameliorates disease and metabolic abnormalities in a FUS mouse model. *Acta Neuropathol. Commun.* **7**, 107 (2019).
64. Gong, J. et al. RBM45 competes with HDAC1 for binding to FUS in response to DNA damage. *Nucleic Acids Res.* **45**, 12862–12876 (2017).
65. Boutillier, A.-L., Tzeplaeff, L. & Dupuis, L. The dark side of HDAC inhibition in ALS. *EBioMedicine* **40**, 38–39 (2019).
66. Yusuff, T. et al. Drosophila models of pathogenic copy-number variant genes show global and 1 non-neuronal defects during development. *BioRxiv*. <https://doi.org/10.1101/855338> (2019).
67. Yusuff, T., Chatterjee, S., Chang, Y.-C., Sang, T.-K. & Jackson, G. R. Codon-optimized TDP-43-mediated neurodegeneration in a Drosophila model for ALS/FTLD. *bioRxiv*. 696963, <https://doi.org/10.1101/696963> (2019).
68. Di Salvio, M. et al. Pur- α functionally interacts with FUS carrying ALS-associated mutations. *Cell Death Dis.* **6**, e1943 (2015).
69. Esposito, S. et al. Redox-sensitive GFP to monitor oxidative stress in neurodegenerative diseases. *Rev. Neurosci.* **28**, 133–144 (2017).
70. Lepedda, A. J. et al. Identification of differentially expressed plasma proteins in atherosclerotic patients with type 2 diabetes. *J. Diabetes Complications* **30**, 880–886 (2016).
71. Lepedda, A. J. et al. Proteomic analysis of plasma-purified VLDL, LDL, and HDL fractions from atherosclerotic patients undergoing carotid endarterectomy: identification of serum amyloid A as a potential marker. *Oxid. Med Cell Longev.* **2013**, 385214 (2013).
72. Bruhat, A. et al. Amino acids control mammalian gene transcription: activating transcription factor 2 is essential for the amino acid responsiveness of the CHOP promoter. *Mol. Cell Biol.* **20**, 7192–7204 (2000).
73. Ran, F. A. et al. Genome engineering using the CRISPR-Cas9 system. *Nat. Protoc.* **8**, 2281–2308 (2013).

4. REFERENCES

1. Dauer, W. & Przedborski, S. Parkinson's disease: mechanisms and models. *Neuron* **39**, 889–909 (2003).
2. Dorsey, E. R., Sherer, T., Okun, M. S. & Bloem, B. R. The Emerging Evidence of the Parkinson Pandemic. *JPD* **8**, S3–S8 (2018).
3. Collier, T. J., Kanaan, N. M. & Kordower, J. H. Aging and Parkinson's disease: Different sides of the same coin?: Aging and PD. *Mov Disord.* **32**, 983–990 (2017).
4. Sveinbjornsdottir, S. The clinical symptoms of Parkinson's disease. *J Neurochem* **139 Suppl 1**, 318–324 (2016).
5. Hughes, A. J., Daniel, S. E., Kilford, L. & Lees, A. J. Accuracy of clinical diagnosis of idiopathic Parkinson's disease: a clinico-pathological study of 100 cases. *J Neurol Neurosurg Psychiatry* **55**, 181–184 (1992).
6. Pereira, E. A. C. Surgical insights into Parkinson's disease. *Journal of the Royal Society of Medicine* **99**, 238–244 (2006).
7. Tambasco, N., Romoli, M. & Calabresi, P. Levodopa in Parkinson's Disease: Current Status and Future Developments. *CN* **16**, 1239–1252 (2018).
8. Nemade, D., Subramanian, T. & Shivkumar, V. An Update on Medical and Surgical Treatments of Parkinson's Disease. *Aging and disease* **12**, 1021 (2021).
9. Grosset, D. G., Macphee, G. J. A., Nairn, M., & on behalf of the Guideline Development Group. Diagnosis and pharmacological management of Parkinson's disease: summary of SIGN guidelines. *BMJ* **340**, b5614–b5614 (2010).
10. Dézsi, L. & Vécsei, L. Clinical implications of irregular ADMET properties with levodopa and other antiparkinson's drugs. *Expert Opinion on Drug Metabolism & Toxicology* **10**, 409–424 (2014).
11. Xie, C. *et al.* Levodopa/benserazide microsphere (LBM) prevents L-dopa induced dyskinesia by inactivation of the DR1/PKA/P-tau pathway in 6-OHDA-lesioned Parkinson's rats. *Sci Rep* **4**, 7506 (2015).
12. Dong, J., Cui, Y., Li, S. & Le, W. Current Pharmaceutical Treatments and Alternative Therapies of Parkinson's Disease. *CN* **14**, 339–355 (2016).
13. Palhagen, S. *et al.* Selegiline slows the progression of the symptoms of Parkinson disease. *Neurology* **66**, 1200–1206 (2006).
14. Moore, T. J., Glenmullen, J. & Mattison, D. R. Reports of Pathological Gambling, Hypersexuality, and Compulsive Shopping Associated With Dopamine Receptor Agonist Drugs. *JAMA Intern Med* **174**, 1930 (2014).
15. Lotan, I., Treves, T. A., Roditi, Y. & Djaldetti, R. Cannabis (Medical Marijuana) Treatment for Motor and Non–Motor Symptoms of Parkinson Disease: An Open-Label Observational Study. *Clinical*

Neuropharmacology **37**, 41–44 (2014).

16. Burns, R. S., LeWitt, P. A., Ebert, M. H., Pakkenberg, H. & Kopin, I. J. The Clinical Syndrome of Striatal Dopamine Deficiency: Parkinsonism Induced by 1-Methyl-4-Phenyl-1,2,3,6-Tetrahydropyridine (MPTP). *N Engl J Med* **312**, 1418–1421 (1985).

17. Stern, M. The Epidemiology of Parkinson's Disease: A Case-Control Study of Young-Onset and Old-Onset Patients. *Arch Neurol* **48**, 903 (1991).

18. Mat Taib, C. N. & Mustapha, M. MPTP-induced mouse model of Parkinson's disease: A promising direction of therapeutic strategies. *Bosn J of Basic Med Sci* (2020) doi:10.17305/bjbms.2020.5181.

19. Nandipati, S. & Litvan, I. Environmental Exposures and Parkinson's Disease. *IJERPH* **13**, 881 (2016).

20. Simon, D. K., Tanner, C. M. & Brundin, P. Parkinson Disease Epidemiology, Pathology, Genetics, and Pathophysiology. *Clin Geriatr Med* **36**, 1–12 (2020).

21. Saravanan, K. S., Sindhu, K. M. & Mohanakumar, K. P. Acute intranigral infusion of rotenone in rats causes progressive biochemical lesions in the striatum similar to Parkinson's disease. *Brain Research* **1049**, 147–155 (2005).

22. Betarbet, R. *et al.* Chronic systemic pesticide exposure reproduces features of Parkinson's disease. *Nat Neurosci* **3**, 1301–1306 (2000).

23. Manning-Bog, A. B. *et al.* The Herbicide Paraquat Causes Up-regulation and Aggregation of α -Synuclein in Mice. *Journal of Biological Chemistry* **277**, 1641–1644 (2002).

24. McCormack, A. L. *et al.* Environmental Risk Factors and Parkinson's Disease: Selective Degeneration of Nigral Dopaminergic Neurons Caused by the Herbicide Paraquat. *Neurobiology of Disease* **10**, 119–127 (2002).

25. Ansher, S. S., Cadet, J. L., Jakoby, W. B. & Baker, J. K. Role of N-methyltransferases in the neurotoxicity associated with the metabolites of 1-methyl-4-phenyl-1,2,3,6-tetrahydropyridine (MPTP) and other 4-substituted pyridines present in the environment. *Biochemical Pharmacology* **35**, 3359–3363 (1986).

26. Gillette, J. Differential up-regulation of striatal dopamine transporter and α -synuclein by the pyrethroid insecticide permethrin. *Toxicology and Applied Pharmacology* **192**, 287–293 (2003).

27. Elwan, M. A., Richardson, J. R., Guillot, T. S., Caudle, W. M. & Miller, G. W. Pyrethroid pesticide-induced alterations in dopamine transporter function. *Toxicology and Applied Pharmacology* **211**, 188–197 (2006).

28. Billingsley, K. J., Bandres-Ciga, S., Saez-Atienzar, S. & Singleton, A. B. Genetic risk factors in Parkinson's disease. *Cell Tissue Res* **373**, 9–20 (2018).
29. Kumar, K. R., Lohmann, K. & Klein, C. Genetics of Parkinson disease and other movement disorders: *Current Opinion in Neurology* **25**, 466–474 (2012).
30. Shibasaki, Y., Baillie, D. A. M., St. Clair, D. & Brookes, A. J. High-resolution mapping of SNCA encoding α -synuclein, the non-A β component of Alzheimer's disease amyloid precursor, to human chromosome 4q21.3 \rightarrow q22 by fluorescence in situ hybridization. *Cytogenet Genome Res* **71**, 54–55 (1995).
31. McLean, P. J. & Hyman, B. T. An alternatively spliced form of rodent α -synuclein forms intracellular inclusions in vitro: role of the carboxy-terminus in α -synuclein aggregation. *Neuroscience Letters* **323**, 219–223 (2002).
32. Polymeropoulos, M. H. *et al.* Mutation in the alpha-synuclein gene identified in families with Parkinson's disease. *Science* **276**, 2045–2047 (1997).
33. Spillantini, M. G. *et al.* α -Synuclein in Lewy bodies. *Nature* **388**, 839–840 (1997).
34. Pirkevi, C., Lesage, S., Brice, A. & Nazli Basıřak, A. From Genes to Proteins in Mendelian Parkinson's Disease: An Overview. *Anat Rec* **292**, 1893–1901 (2009).
35. Sarchione, A., Marchand, A., Taymans, J.-M. & Chartier-Harlin, M.-C. Alpha-Synuclein and Lipids: The Elephant in the Room? *Cells* **10**, 2452 (2021).
36. Lashuel, H. A., Overk, C. R., Oueslati, A. & Masliah, E. The many faces of α -synuclein: from structure and toxicity to therapeutic target. *Nat Rev Neurosci* **14**, 38–48 (2013).
37. Atik, A., Stewart, T. & Zhang, J. Alpha-Synuclein as a Biomarker for Parkinson's Disease: Alpha-Synuclein as a Biomarker for PD. *Brain Pathology* **26**, 410–418 (2016).
38. Oueslati, A. Implication of Alpha-Synuclein Phosphorylation at S129 in Synucleinopathies: What Have We Learned in the Last Decade? *JPD* **6**, 39–51 (2016).
39. Kitada, T. *et al.* Mutations in the parkin gene cause autosomal recessive juvenile parkinsonism. *Nature* **392**, 605–608 (1998).
40. Seirafi, M., Kozlov, G. & Gehring, K. Parkin structure and function. *FEBS J* **282**, 2076–2088 (2015).
41. Hedrich, K. *et al.* Distribution, type, and origin of Parkin mutations: Review and case studies. *Mov Disord.* **19**, 1146–1157 (2004).
42. Madsen, D. A., Schmidt, S. I., Blaabjerg, M. & Meyer, M.

- Interaction between Parkin and α -Synuclein in PARK2-Mediated Parkinson's Disease. *Cells* **10**, 283 (2021).
43. Biskup, S. *et al.* Genes associated with Parkinson syndrome. *J Neurol* **255**, 8–17 (2008).
 44. Gandhi, S. & Wood, N. W. Molecular pathogenesis of Parkinson's disease. *Hum Mol Genet* **14 Spec No. 2**, 2749–2755 (2005).
 45. Arena, G. & Valente, E. M. PINK1 in the limelight: multiple functions of an eclectic protein in human health and disease: Functions of PINK1 in human pathology. *J. Pathol.* **241**, 251–263 (2017).
 46. Tanaka, K. The PINK1–Parkin axis: An Overview. *Neuroscience Research* **159**, 9–15 (2020).
 47. Fan, H.-C., Chen, S.-J., Harn, H.-J. & Lin, S.-Z. Parkinson's Disease: From Genetics to Treatments. *Cell Transplant* **22**, 639–652 (2013).
 48. Kluss, J. H., Mamais, A. & Cookson, M. R. LRRK2 links genetic and sporadic Parkinson's disease. *Biochem Soc Trans* **47**, 651–661 (2019).
 49. Paisán-Ruíz, C. *et al.* Cloning of the Gene Containing Mutations that Cause PARK8-Linked Parkinson's Disease. *Neuron* **44**, 595–600 (2004).
 50. Zimprich, A. *et al.* Mutations in LRRK2 Cause Autosomal-Dominant Parkinsonism with Pleomorphic Pathology. *Neuron* **44**, 601–607 (2004).
 51. Gasser, T. Molecular pathogenesis of Parkinson disease: insights from genetic studies. *Expert Rev. Mol. Med.* **11**, e22 (2009).
 52. Myasnikov, A. *et al.* Structural analysis of the full-length human LRRK2. *Cell* **184**, 3519–3527.e10 (2021).
 53. Tewari, R., Bailes, E., Bunting, K. A. & Coates, J. C. Armadillo-repeat protein functions: questions for little creatures. *Trends Cell Biol* **20**, 470–481 (2010).
 54. Mosavi, L. K., Cammett, T. J., Desrosiers, D. C. & Peng, Z.-Y. The ankyrin repeat as molecular architecture for protein recognition. *Protein Sci* **13**, 1435–1448 (2004).
 55. Mata, I. F., Wedemeyer, W. J., Farrer, M. J., Taylor, J. P. & Gallo, K. A. LRRK2 in Parkinson's disease: protein domains and functional insights. *Trends Neurosci* **29**, 286–293 (2006).
 56. Piccoli, G. *et al.* Leucine-Rich Repeat Kinase 2 Binds to Neuronal Vesicles through Protein Interactions Mediated by Its C-Terminal WD40 Domain. *Mol Cell Biol* **34**, 2147–2161 (2014).
 57. Deng, J. *et al.* Structure of the ROC domain from the Parkinson's disease-associated leucine-rich repeat kinase 2 reveals a dimeric GTPase. *Proc. Natl. Acad. Sci. U.S.A.* **105**, 1499–1504 (2008).
 58. Deniston, C. K. *et al.* Structure of LRRK2 in Parkinson's disease and model for microtubule interaction. *Nature* **588**, 344–349 (2020).

59. Berwick, D. C., Heaton, G. R., Azeggagh, S. & Harvey, K. LRRK2 Biology from structure to dysfunction: research progresses, but the themes remain the same. *Mol Neurodegeneration* **14**, 49 (2019).
60. Wang, X. *et al.* Understanding LRRK2 kinase activity in preclinical models and human subjects through quantitative analysis of LRRK2 and pT73 Rab10. *Sci Rep* **11**, 12900 (2021).
61. Rideout, H. J. & Stefanis, L. The Neurobiology of LRRK2 and its Role in the Pathogenesis of Parkinson's Disease. *Neurochem Res* **39**, 576–592 (2014).
62. Berger, Z., Smith, K. A. & Lavoie, M. J. Membrane localization of LRRK2 is associated with increased formation of the highly active LRRK2 dimer and changes in its phosphorylation. *Biochemistry* **49**, 5511–5523 (2010).
63. Li, X. *et al.* Phosphorylation-Dependent 14-3-3 Binding to LRRK2 Is Impaired by Common Mutations of Familial Parkinson's Disease. *PLoS ONE* **6**, e17153 (2011).
64. Marchand, A., Drouyer, M., Sarchione, A., Chartier-Harlin, M.-C. & Taymans, J.-M. LRRK2 Phosphorylation, More Than an Epiphenomenon. *Front. Neurosci.* **14**, 527 (2020).
65. Gloeckner, C. J. *et al.* Phosphopeptide Analysis Reveals Two Discrete Clusters of Phosphorylation in the N-Terminus and the Roc Domain of the Parkinson-Disease Associated Protein Kinase LRRK2. *J. Proteome Res.* **9**, 1738–1745 (2010).
66. Pungaliya, P. P. *et al.* Identification and Characterization of a Leucine-Rich Repeat Kinase 2 (LRRK2) Consensus Phosphorylation Motif. *PLoS ONE* **5**, e13672 (2010).
67. Muda, K. *et al.* Parkinson-related LRRK2 mutation R1441C/G/H impairs PKA phosphorylation of LRRK2 and disrupts its interaction with 14-3-3. *Proc. Natl. Acad. Sci. U.S.A.* **111**, (2014).
68. Seol, W., Nam, D. & Son, I. Rab GTPases as Physiological Substrates of LRRK2 Kinase. *Exp Neurobiol* **28**, 134–145 (2019).
69. Stenmark, H. & Olkkonen, V. M. [No title found]. *Genome Biol* **2**, reviews3007.1 (2001).
70. Bonet-Ponce, L. & Cookson, M. R. The role of Rab GTPases in the pathobiology of Parkinson' disease. *Current Opinion in Cell Biology* **59**, 73–80 (2019).
71. Li, G. & Marlin, M. C. Rab Family of GTPases. in *Rab GTPases* (ed. Li, G.) vol. 1298 1–15 (Springer New York, 2015).
72. Kiral, F. R., Kohrs, F. E., Jin, E. J. & Hiesinger, P. R. Rab GTPases and Membrane Trafficking in Neurodegeneration. *Current Biology* **28**, R471–R486 (2018).
73. Purlyte, E. *et al.* Rab29 activation of the Parkinson's disease-

- associated LRRK2 kinase. *EMBO J* **37**, 1–18 (2018).
74. Mir, R. *et al.* The Parkinson's disease VPS35[D620N] mutation enhances LRRK2-mediated Rab protein phosphorylation in mouse and human. *Biochemical Journal* **475**, 1861–1883 (2018).
75. Wu, B. & Guo, W. The Exocyst at a Glance. *Journal of Cell Science* jcs.156398 (2015) doi:10.1242/jcs.156398.
76. Mei, K. *et al.* Cryo-EM structure of the exocyst complex. *Nat Struct Mol Biol* **25**, 139–146 (2018).
77. Jourdain, I. The Exocyst Complex in Health and Disease. *Frontiers in Cell and Developmental Biology* **4**, 22 (2016).
78. Riefler, G. M. *et al.* Exocyst complex subunit sec8 binds to postsynaptic density protein-95 (PSD-95): a novel interaction regulated by cypin (cytosolic PSD-95 interactor). *J Biol Chem* **278**, 7 (2003).
79. Sans, N. *et al.* NMDA receptor trafficking through an interaction between PDZ proteins and the exocyst complex. *Nat Cell Biol* **5**, 520–530 (2003).
80. Chernyshova, Y., Leshchyn'ska, I., Hsu, S.-C., Schachner, M. & Sytnyk, V. The Neural Cell Adhesion Molecule Promotes FGFR-Dependent Phosphorylation and Membrane Targeting of the Exocyst Complex to Induce Exocytosis in Growth Cones. *Journal of Neuroscience* **31**, 3522–3535 (2011).
81. Zou, W., Yadav, S., DeVault, L., Jan, Y. N. & Sherwood, D. R. RAB-10-Dependent Membrane Transport Is Required for Dendrite Arborization. *PLoS Genet* **11**, e1005484 (2015).
82. Piccoli, G. *et al.* LRRK2 Controls Synaptic Vesicle Storage and Mobilization within the Recycling Pool. *J Biol Chem* **283**, 13 (2008).
83. Littleton, J. T. *et al.* SNARE-complex disassembly by NSF follows synaptic-vesicle fusion. *Proc. Natl. Acad. Sci. U.S.A.* **98**, 12233–12238 (2001).
84. Granseth, B., Odermatt, B., Royle, S. J. & Lagnado, L. Clathrin-Mediated Endocytosis Is the Dominant Mechanism of Vesicle Retrieval at Hippocampal Synapses. *Neuron* **51**, 773–786 (2006).
85. Martin, I., Kim, J. W., Dawson, V. L. & Dawson, T. M. LRRK2 pathobiology in Parkinson's disease. *J. Neurochem.* **131**, 554–565 (2014).
86. Migheli, R. *et al.* LRRK2 Affects Vesicle Trafficking, Neurotransmitter Extracellular Level and Membrane Receptor Localization. *PLoS ONE* **8**, e77198 (2013).
87. Beccano-Kelly, D. A. *et al.* LRRK2 overexpression alters glutamatergic presynaptic plasticity, striatal dopamine tone, postsynaptic signal transduction, motor activity and memory. *Human Molecular Genetics* **24**, 1336–1349 (2015).

88. Tozzi, A. *et al.* Dopamine D2 receptor activation potently inhibits striatal glutamatergic transmission in a G2019S LRRK2 genetic model of Parkinson's disease. *Neurobiology of Disease* **118**, 1–8 (2018).
89. Parisiadou, L. *et al.* LRRK2 regulates synaptogenesis and dopamine receptor activation through modulation of PKA activity. *Nat Neurosci* **17**, 367–376 (2014).
90. Gómez-Suaga, P. *et al.* LRRK2 delays degradative receptor trafficking by impeding late endosomal budding through decreasing Rab7 activity. *Human Molecular Genetics* **23**, 6779–6796 (2014).
91. Lynch, B. A. *et al.* The synaptic vesicle protein SV2A is the binding site for the antiepileptic drug levetiracetam. *6*.
92. Tokudome, K. *et al.* Synaptic vesicle glycoprotein 2A (SV2A) regulates kindling epileptogenesis via GABAergic neurotransmission. *Sci Rep* **6**, 27420 (2016).
93. Nowack, A. *et al.* Levetiracetam Reverses Synaptic Deficits Produced by Overexpression of SV2A. *PLoS ONE* **6**, e29560 (2011).
94. Steinhoff, B. J. & Staack, A. M. Levetiracetam and brivaracetam: a review of evidence from clinical trials and clinical experience. *Ther Adv Neurol Disord* **12**, 175628641987351 (2019).
95. Cortes-Altamirano, J. *et al.* Levetiracetam as an antiepileptic, neuroprotective, and hyperalgesic drug. *Neurol India* **64**, 1266 (2016).
96. Hanon, E. & Klitgaard, H. Neuroprotective properties of the novel antiepileptic drug levetiracetam in the rat middle cerebral artery occlusion model of focal cerebral ischemia. *Seizure* **10**, 287–293 (2001).
97. Wang, H. *et al.* Levetiracetam is Neuroprotective in Murine Models of Closed Head Injury and Subarachnoid Hemorrhage. *NCC* **5**, 71–78 (2006).
98. Kilicdag, H. *et al.* The effect of levetiracetam on neuronal apoptosis in neonatal rat model of hypoxic ischemic brain injury. *Early Human Development* **89**, 355–360 (2013).
99. Marcotulli, D., Fattorini, G., Bragina, L., Perugini, J. & Conti, F. Levetiracetam Affects Differentially Presynaptic Proteins in Rat Cerebral Cortex. *Front. Cell. Neurosci.* **11**, 389 (2017).
100. Hu, H., Tian, M., Ding, C. & Yu, S. The C/EBP Homologous Protein (CHOP) Transcription Factor Functions in Endoplasmic Reticulum Stress-Induced Apoptosis and Microbial Infection. *Front. Immunol.* **9**, 3083 (2019).

La borsa di dottorato è stata cofinanziata con risorse del
Programma Operativo Nazionale Ricerca e Innovazione 2014-2020 (CCI 2014IT16M2OP005),
Fondo Sociale Europeo, Azione I.1 "Dottorati Innovativi con caratterizzazione Industriale"



UNIONE EUROPEA
Fondo Sociale Europeo



